An Energy-based Blending of Classical Elasticity and Peridynamics

A Dissertation Presented for the

Doctor of Philosophy

Degree

The University of Tennessee, Knoxville

Kileen A. Berry

August 2019

© by Kileen A. Berry, 2019
All Rights Reserved.

Dedication

This dissertation is dedicated in loving memory to my mother, *Dawn Marie Berry*, who passed away halfway through my graduate career. Before her death, my mother had been my biggest supporter. She had confidence in me even when I had lost all confidence in myself. Though she did not understand much of the mathematics I talked with her about, she did her best to listen and try and help me through any and all struggles. My mother was my rock and without her love and support I would not be the person that I am today. Although she is not here to celebrate this accomplishment, I know that she would be very proud. *This is for you mom.*

Acknowledgments

Some of the material in this dissertation is based upon work supported by the U.S. Department of Energy, Office of Science, Office of Workforce Development for Teachers and Scientists, Office of Science Graduate Student Research (SCGSR) program. I participated in this program in the spring of 2018 at Oak Ridge National Lab. The SCGSR program is administered by the Oak Ridge Institute for Science and Education (ORISE) for the DOE. ORISE is managed by ORAU under contract number DE-SC0014664. I would like to thank the many people that are involved in this program for giving me this opportunity to spend six months working at this lab.

Some of the material presented in this dissertation is based on work that was supported by my one of my advisors' NSF award: DMS-1615726, "Mathematical Analysis on Peridynamic Models".

In particular, I would like to express my gratitude to many people without whom I would not have been able to complete the work presented here.

First, I would like to thank my two advisors, Drs. Tadele Mengesha and Steven Wise, for their continued support of my research. I would like to thank Dr. Wise for taking me on as a student and for suggesting that we meet with Dr. Mengesha to discuss some potential ideas. I would like to thank Dr. Mengesha for bringing your expertise to our group and helping me select an interesting and motivating topic for my research. Thank you both for teaching me what research is and helping me find a topic that I truly have enjoyed exploring. Thank you most of all for believing in me and instilling me with the confidence to complete this dissertation.

I would like to thank my advisors as well as Dr. Pablo Seleson for encouraging me to apply for the DOE Office of Science Graduate Student Research Program. I especially would like to thank Dr. Seleson for mentoring during my time in this program at ORNL. Thank you for helping me look at my research from a different angle and for encouraging me as I further explored the topics at hand. Thank you for continuing to collaborate with me when my time at the lab was up and for serving as a member of my committee.

I would also like to thank Dr. Abner Salgado for serving as a member of both my oral exam and my dissertation committee. In particular, thank you for throughly reading my entire dissertation and providing much needed and appreciated feedback.

I thank all four of my committee members for all the time, patience and knowledge that you have shared with me throughout these last few years. I also thank you for asking questions that helped me delve deeper into the research and for all of the comments and feedback you have provided on this dissertation.

I would like to thank Dr. Conrad Plaut, the Mathematics Department Head, for encouraging and supporting my time in the DOE SCGSR program. Particularly, I would like to thank you for helping me find the funding to remain a full-time student, so that I could take advantage of this opportunity.

I would like to thank all of the professors with whom I have taken classes: Dr. Steven Wise, Dr. Luis Finotti, Dr. Jim Conant, Dr. Morwen Thistlethwaite, Dr. Henry Simpson, Dr. Stefan Richter, Dr. Kenneth Stephenson, Dr. Jerzy Dydak, Dr. Shashikant Mulay, Dr. Alexandre Freire, Dr. Remus Nicoara, Dr. Michael Frazier, Dr. Ohannes Karakashian, and Dr. Tadele Mengesha. Thank you for sharing your time and your knowledge with me over the last six years.

I also would like to thank Mrs. Pam Armentrout and Dr. Xiaobing Feng for all that they do to support the graduate students at UTK.

I would like to thank my friends and family who have been there for me in the last six years. Without all of your love, encouragement, and sometimes necessary distractions I would not be completing this degree. Notably, I thank my husband, Terry Henderson, and my friend, Maggie Wieczorek, for continually encouraging and supporting me through all the ups and downs of graduate school.

Last but not least, I thank the doggos Hammer, Nala, and Luna whose cuddles have gotten me through some of the toughest times.

Abstract

The aim of this dissertation is to study both the analytical and numerical properties of the Energy-Based Blending Model. This model was proposed in [34] as a way to model material behavior and deformation under forces, that could capture discontinuous deformations accurately while remaining computationally cost effective.

Starting by looking through the lens of differential equations and functional analysis, properties analogous to ones that are well-known for the Laplace equation are established for the energy-based blended model. These properties include a weak formulation of the Dirichlet-type boundary value problem, a norm under which the function space is Hilbert, embeddings, a Poincaré-type inequality, and existence/uniqueness of solutions. In this dissertation, proofs of these properties are also included for the classical model, the bond-based peridynamic model for analogy.

Looking through the lens of numerical analysis, the blended model is solved using the finite element method. A Céa-type lemma and a best approximation theorem are shown. Further a discussion of the implementation of the finite element method for the model is included. In this discussion, the differences in the approaches are highlighted. Through L^2 and H^1 error analysis, it is shown that for smooth solutions the convergence rate agrees with both the classical and bond-based peridynamic models.

Although for both the classical and the PD models, zero force results in a linear solution, the same cannot be said for the blended model. The analysis shows that the size of this

ghost force is dependent on the smoothness of the blending function and the ratio of the length of the blending region to the material horizon, δ. As expected, increasing the length of the blending region, decreases the size of the ghost force. Although it was previously believed that a smoother blending function would cause a smaller ghost force, the included analysis has shown the optimal smoothness for the blending function depends on the ratio of length of the blending region to the horizon. Specifically, when this ratio is small, using the continuous piecewise linear rather than the continuously differentiable piecewise cubic blending function leads to a smaller ghost force.

Table of Contents

List of Tables

List of Figures

Part I

Introduction

Matter is made up of molecules, atoms, and subatomic particles. Therefore, physical matter is not continuous. Despite this fact, there are many large scale behaviors of materials that can be described by theories that ignore these small scale intricacies of matter. Continuum mechanics is a theory that analyzes the deformation of materials, modeled as continuous bodies rather than as a set of discrete particles, as a result of different loading conditions. Since continuum mechanics assumes that matter is indefinitely divisible, an infinitesimal volume of the material is considered a material point. Elasticity is a property that some materials have, in which the material returns to its original shape and size after all forces deforming it have been removed. The mathematical model that has traditionally been used in the study of elastic materials is called classical elasticity. In classical elasticity, partial differential equations are used to describe the motion of material points as well as the constitutive equations that the idealized body must follow. This classic model assumes that the deformation at a specific material point is only informed by the points in a very small neighborhood of the point, making classical elasticity a local model. The use of partial differential equations to describe the motion of the material points, makes the implicit assumption that the spatial deformation of the material is smooth. For more information on the theory of continuum mechanics and elasticity, the reader is referred to the following three textbooks [32, 9, 24].

While classical elasticity can be very useful in modeling and predicting some particular behaviors of materials, our everyday experience with materials informs us that materials can develop spatial discontinuities (such as cracks). Although there are techniques that have been developed that allow computational simulations to exhibit the same spatial discontinuities that are observed in experimentation, in order to implement these techniques one must know both the severity and location of the spatial discontinuities. In many applications, the goal of these computational simulations is to predict the material behavior, and thus prior knowledge of the spatial discontinuities is impractical.

Motivated by the numerous problems fundamental to solid mechanics in which the spatial deformation is discontinuous, in 2000 Sillling proposed an alternative mathematical model in the framework of continuum mechanics that describes the deformation of materials, called bond-based peridynamics [47]. This model uses spatial integration rather than spatial differentiation to describe the internal force density between material particles. The use of integration assumes particles that are separated by finite distances directly interact with each other, making this a nonlocal model. Since this formulation of continuum mechanics eliminates the use of spatial derivatives, the mathematical equations are equally valid both on and off spatial discontinuities. Thereby eliminating the need for the use of special techniques to handle any discontinuous spatial deformations. Although Silling was not the only to research nonlocal elasticity, [42, 31, 30, 29, 19], these nonlocal models still used spatial derivatives, making bond-based peridynamics the first nonlocal model that avoids the use of spatial derivatives.

Generalizations of the bond-based peridynamics proposed in [47] have also been presented in various places. In 2010, Silling introduced a generalization of the bond-based peridynamics called state-based peridynamics [3, 48]. This generalization allows for the response of the material at a point to depend collectively on the deformation of all bonds connected to that point, this allows for modeling things such as volume change or shear angles [49]. In 2017, Zhu and Ni proposed a generalization of bond-based peridynamics that allowed for bond rotation effects [53]. Connections between nonlocal continuum models and modelcular dynamics have been investigated [45, 46].

Applications of peridynamics include crack propagation and branching [25, 2, 6, 15], multi-scale material modeling [3, 50], and failure in composites [51, 4].

In addition to applications there has been a wealth of work done to fully develop function analytical foundations for peridynamics, which could allow for the development of more efficient and effective discretizations of the peridynamic model. In 2007 Emmrich and Weckner discussed the peridynamic equation's discretization and its convergence towards the Navier equation of linear elasticity. [17, 18]. In [38, 39, 40, 41] Du and Mengesha rigorously establish well-posedness of variational problems, convergence of the nonlocal energy to the local energy via Γ-convergence, Poincaré type inequalities, embeddings of the energy space into well-known spaces, completeness and regularity properties. Many of these proofs were aided by the development of nonlocal vector calculus in [23]. Other papers that involve the theoretical development of peridynamics include [1, 52, 12, 16]. The implementation of peridynamic models via finite element method are discussed in [13, 10, 28, 36, 50]

Another topic of interest is the coupling of nonlocal and local models. The goal of these couplings is to reduce computational cost of modeling with nonlocal models. There are two main classes of these couplings: force-based couplings and energy-based couplings. Of the energy-based couplings there are several methods that have been proposed including the Arlequin domain decomposition [26], the morphing method [34, 5], and quasinonlocal couplings [33, 14]. Force-based couplings are presented in [44, 43] which are nonconservative. Additionally an optimization based coupling is presented, which allows the models to operate independently of each other [11].

The coupling method that is the focus of this dissertation was proposed in [34]. This paper introduces the idea of a region over which the linearized peridynamic model morphs into the linearized classical model.

The first goal of this dissertation is to mathematically analyze this model and establish useful mathematical properties associated with it. Since this coupling is an energy-based blending, the space of functions for which the energy is finite is studied in detail. A norm is established on this space and the space is shown to be complete with respect to this norm. On a particular subspace properties such as a Poincaré-type inequality and the existence and uniqueness of solutions are also established. Before these properties are established for this blended model, all of the analogous properties are first established for the one-dimensional classical model (in Chapter 1) and the one-dimensional bond-based peridynamic model (in Chapter 2). In Chapter 3, the general blended model is motivated and compared to the general bond-based peridynamic model. The desired mathematical properties for the one-dimensional blended model are established in Chapter 4, with special attention given to converting this energy-based problem into the appropriate force-based problem with Dirchlet-type boundary conditions (see Sections 4.2 and 4.3) to complete the analogy between the three one-dimensional models.

One way in which the quality of a coupling method is evaluated is through an investigation of the ghost forces that arise from the coupling. The ghost force is the nonzero force required in the strong formulation of the problem to get a linear displacement $u(x) = Ax + B$ as the solution where $A, B \in \mathbb{R}$. This force is considered because in both the classical and the peridynamic models the force required to get a linear displacement as a solution is 0. Models in which this ghost force does not appear are said to be patch-test consistent. While some believe that this patch-test consistency is an essential test to determine the validity of this model, there is an other camp that allows for the ghost force to be nonzero. In the coupled model considered here, it makes sense that this ghost force would be nonzero, because the coupling is happening in the weak formulation of the problem (corresponding to the energy) rather than the strong formulation (corresponding to the force). In Chapter 5, the effects of choices made during the implementation of the model on the size of this ghost force are considered. Following this, in Chapter 6 there is a discussion of a basic implementation of the finite element method for solving these three one-dimensional problems. Although there is a discussion of the finite element method in general, particular attention is given to the differences that occur in the implementation of the three models in Section 6.2. Since the finite element method generates approximate solutions, the error between this approximate solution and the true solution are discussed in Chapter 7. In this chapter upper bounds are established in the L^2, H^1 and the energy norm for this error. In Chapter 8, the numerical results obtained from the implementations discussed in Chapter 6.2 are discussed and compared to the theoretical results given in Chapter 7. Many of the properties that were established for the one-dimensional blended model in Chapter 4 are extended to higher dimensions.

Since any mention of the strong formulation of the three problems assumes Dirichlet-type boundary conditions, a short discussion the form of Neumann-type boundary conditions is included in Appendix A. Specifically, because the region closest to the boundary in the blended model is actually the purely classical model, and the various possibilities for a nonlocal Neumann-type condition the goal of this Appendix is to propose one such possibility.

Chapter 1

The Classical Model

Most of the content in this section can be found in standard differential equations and/or functional analysis texts. The main sources for the discussion that is presented in this chapter are [22, 8, 27, 35, 20].

A general boundary value problem (BVP) in differential equations is given by a differential equation and a set of boundary conditions. Let Ω be a bounded subset in $\mathbb{R}^n$ with smooth enough boundary. Given f, g, α, β, find a u that satisfies

$$\begin{cases} \mathcal{L}u(x) = f(x), & x \in \Omega \\ \alpha(x)u(x) + \beta(x)\dfrac{\partial u}{\partial x}(x) = g(x), & x \in \partial\Omega \end{cases}$$

where $\mathcal{L}$ is some differential operator. A **solution**, u, is a function that satisfies the partial differential equation as well as the boundary conditions. Of course, the solution u to this problem will depend on the given functions as well as the differential operator $\mathcal{L}$.

In classical elasticity, the equation of motion is used to describe the deformation of a continuous body. In 1-dimension the stationary equilibrium equation is stated as

$$-\Delta u(x) = f(x)$$

where u is the deformation (i.e. expansion or compression), and f is the force that is applied to the body. For simplicity, we will restrict our attention to the one-dimensional case of this problem with Dirichlet-type boundary conditions:

Let $\Omega = (a, b)$ be an interval in $\mathbb{R}$. Given $f \in C(\Omega)$, find a u that satisfies

$$\begin{cases} -\Delta u(x) = f(x), & x \in \Omega \\ u(a) = g_a, \quad u(b) = g_b \end{cases} \tag{1.1}$$

In order to satisfy the differential equation in this boundary value problem (BVP) the expected solution is twice continuously differentiable. Since the given f is continuous, this BVP can often be solved through integration of the differential equation and the solution can be stated explicitly. It is often useful to rewrite this BVP in a different way before solving. To do this, define the following functions

$$g(x) = \frac{g_b - g_a}{b - a} x + \frac{b(g_a) - a(g_b)}{b - a} \tag{1.2}$$

and $w(x) = u(x) - g(x)$. The function g is the straight line connecting the two points given by the Dirichlet-type boundary conditions in 1.1. Since g is a differential function, the distributive property can be used to say that w satisfies the following differential equation

$$-\Delta w(x) = -\Delta(u(x) - g(x)) = -\Delta u(x) + \Delta g(x) = f(x) + 0 = f(x), \quad \forall x \in \Omega.$$

Since $u(a) = g_a$ and $u(b) = g_b$, w is a solution to the homogeneous Dirichlet-type boundary value problem (BVP):

Let $\Omega = (a, b)$ be an interval in $\mathbb{R}$. Given $f \in C(\Omega)$, find a w that satisfies

$$\begin{cases} -\triangle w(x) = f(x), & x \in \Omega \\ w(a) = 0, \; w(b) = 0 \end{cases} \tag{1.3}$$

Once the solution w to the homogeneous BVP has been found, adding g to it will return the solution u to the nonhomogeneous BVP 1.1. Thus, solving the homogeneous BVP 1.3 is equivalent to solving the original BVP 1.1. Therefore, the homogeneous Dirichlet-type BVP 1.3 will be studied.

In order to guarantee a solution to this BVP for a more general f, it will be necessary to weaken the statement of the problem.

To do so, we first multiply the partial differential equation in 1.3 by a test function $v \in C_0^\infty(\Omega)$. This results in the following differential equation

$$-\Delta w(x)v(x) = f(x)v(x), \quad \forall x \in \Omega.$$

Then integrate over Ω (the domain on which this equation holds) and obtain

$$\int_\Omega (-\triangle w)v\mathrm{d}x = \int_\Omega fv\mathrm{d}x, \quad \forall v \in C_0^\infty(\Omega).$$

Solving this equation, rather than the BVP, will result in a larger class of solutions. In particular, if $f \in C(\Omega)$, the set of solutions of this equation now not only includes $w \in C^2(\Omega)$ the solution to BVP 1.3, but also includes functions that are almost everywhere equal to w.

Taking this weakening one step further, we transfer one of the derivatives from w to v using integration by parts:

$$\int_\Omega w'v'\mathrm{d}x - w'v\,\big|_a^b = \int_\Omega fv\mathrm{d}x.$$

Since the test function v is in $C_0^\infty(\Omega)$, it implies that $v(a) = v(b) = 0$, this simplifies to

$$\int_\Omega w'v'\mathrm{d}x = \int_\Omega fv\mathrm{d}x, \quad \forall v \in C_0^\infty(\Omega). \tag{1.4}$$

It is clear to satisfy equation 1.4 for the same given function $f \in C(\Omega)$, the requirements on w are weaker than those needed to satisfy equation 1.3.

By weakening the definition of derivative as in Definition 1.1, we can further weaken this problem.

Definition 1.1. *We say h is a **weak derivative** of a function u, if*

$$\int_\Omega u'v'\mathrm{d}x = -\int_\Omega hv\mathrm{d}x \quad \forall v \in C_0^\infty(\Omega).$$

It is important to note that if u is a function with a strong derivative (or a pointwise derivative), u', then u' is also a weak derivative of u. For this reason the weak derivatives of u will be denoted in the same manner as the strong derivatives; u', $\frac{\partial u}{\partial x}, \nabla u$. Since the same notation is used, context will be important in determining whether a derivative is a strong derivative or a weak derivative.

Before we can begin solving equation 1.4, we want to explore a space of functions on which it makes sense to talk about weak derivatives.

1.1 The energy space $H^1(\Omega)$

Consider the function space $H^1(\Omega)$ given in Definition 1.2.

Definition 1.2.

$$H^1(\Omega) = \left\{u \in L^2(\Omega) : u' \in L^2(\Omega)\right\}.$$

This space is exactly the subspace of $L^2(\Omega)$ where the classical energy is finite, hence its name. Observe that if $u, v \in H^1(\Omega)$ it follows, through an application of Hölder's inequality that

$$\int_\Omega u'v'\mathrm{d}x \leq ||u'||_{L^2(\Omega)}||v'||_{L^2(\Omega)} < \infty$$

Definition 1.3. *We define the following functions on the space $H^1(\Omega)$: for $u \in H^1(\Omega)$*

$$|u|_{H^1(\Omega)} := ||\nabla u||_{L^2(\Omega)},$$

$$||u||_{H^1(\Omega)} := \sqrt{||u||^2_{L^2(\Omega)} + |u|^2_{H^1(\Omega)}}.$$

Proposition 1.4. *Let $u \in H^1(\Omega)$. If $|u|_{H^1(\Omega)} = 0$, then u is a constant a.e. in Ω.*

Proof. By definition,

$$|u|_{H^1(\Omega)} = ||\nabla u||_{L^2(\Omega)} = \left(\int_\Omega (u')^2 \mathrm{d}x \right)^{1/2}.$$

The facts $0^2 = 0$ and that the integrand is always nonnegative together imply that $(u'(x))^2 = 0$ almost everywhere (a.e.) in Ω. This implies that $u'(x) = 0$ for a.e. $x \in \Omega$, which in turn implies that u must be a constant a.e. in Ω. □

Proposition 1.5. $(H^1(\Omega), ||\cdot||_{H^1(\Omega)})$ *is a normed linear space.*

Proof. The fact that $||\cdot||_{H^1(\Omega)}$ is a norm on the space $H^1(\Omega)$, follows immediately from proposition 1.4 and the fact that $||\cdot||_{L^2(\Omega)}$ is a known norm. Therefore, we just need to show that $H^1(\Omega)$ is a linear space.

Let $u, v \in H^1(\Omega)$ and $\alpha \in \mathbb{R}$. By definition $u, v, u', v' \in L^2(\Omega)$. Since $L^2(\Omega)$ is a vector space it is clear that linear combinations of these functions are also in $L^2(\Omega)$. Therefore in order to show that $H^1(\Omega)$ is a linear space, all that must be shown is that $(u + v)' = u' + v'$. By the definition of weak derivative,

$$\int_\Omega u w' \mathrm{d}x = -\int_\Omega u' w \mathrm{d}x \quad \forall w \in C_c^\infty(\Omega)$$

$$\int_\Omega v w' \mathrm{d}x = -\int_\Omega v' w \mathrm{d}x \quad \forall w \in C_c^\infty(\Omega)$$

Therefore, using properties of the integral, for all $w \in C_c^\infty(\Omega)$ it follows

$$\begin{aligned}\int_\Omega (u+v)w'\mathrm{d}x &= \int_\Omega uw'\mathrm{d}x + \int_\Omega vw'\mathrm{d}x \\ &= -\int_\Omega u'w\mathrm{d}x - \int_\Omega v'w\mathrm{d}x \\ &= -\int_\Omega (u'+v')w\mathrm{d}x.\end{aligned}$$

Thus, $(u+v)' = (u'+v')$. Therefore, $(H^1(\Omega), ||\cdot||_{H^1(\Omega)})$ is a normed linear space. $\square$

Theorem 1.6. *$(H^1(\Omega), ||\cdot||_{H^1(\Omega)})$ is a Hilbert space.*

Proof. Let $\{u_n\} \subseteq H^1(\Omega)$ be a Cauchy sequence with respect to $||\cdot||_{H^1(\Omega)}$. Therefore, $\{u_n\}$ and $\{u_n'\}$ are Cauchy sequences in $L^2(\Omega)$. Since $L^2(\Omega)$ is a complete space, it follows that these sequences converge to some $u, h \in L^2(\Omega)$ respectively. Since $\{u_n\}$ is a subset of $H^1(\Omega)$, it follows that

$$\int_\Omega u_n v'\mathrm{d}x = -\int_\Omega u_n' v\mathrm{d}x, \ \forall v \in C_c^\infty(\Omega).$$

Through an application of Fatou's lemma it is clear that

$$\int_\Omega uv'\mathrm{d}x = -\int_\Omega hv\mathrm{d}x, \ \forall v \in C_c^\infty(\Omega).$$

Therefore $H^1(\Omega)$ is a Hilbert Space. $\square$

Theorem 1.7. *$H^1(\Omega)$ embeds continuously into $L^2(\Omega)$.*

Proof. Let $u \in H^1(\Omega)$. Recall that

$$||u||_{H^1(\Omega)} = \sqrt{||u||^2_{L^2(\Omega)} + |u|^2_{H^1(\Omega)}}.$$

But $|\cdot|_{H^1}$ is a semi-norm, and therefore $|u|_{H^1} \geq 0$ for all $u \in H^1(\Omega)$. Therefore,

$$\begin{aligned} ||u||_{L^2(\Omega)} =& \sqrt{||u||^2_{L^2(\Omega)}} \\ \leq& \sqrt{||u||^2_{L^2(\Omega)} + |u|^2_{H^1(\Omega)}} \\ =& ||u||_{H^1(\Omega)} \end{aligned}$$

Therefore, $H^1(\Omega)$ continuously embeds into $L^2(\Omega)$. □

The following is a fact that we will use, but the proof of which will be omitted as analogous propositions will not be needed in the subsequent chapters.

Proposition 1.8. *If I is an interval subset of $\mathbb{R}$, and $u \in H^1(I)$, then there exists a function $\bar{u} \in C(\bar{I})$ such that*

$$u = \bar{u} \quad a.e.. \text{ on } I$$

and

$$\bar{u}(x) - \bar{u}(y) = \int_y^x u'(t)\mathrm{d}t \quad \forall x, y, \in \bar{I}$$

This asserts that there is a continuous function $\bar{u}$ that is equal to u almost everywhere. Therefore, for each $u \in H^1(I)$ there is a continuous representative. This statement is exactly the statement of Theorem 8.2 in [8], and the proof can be found there. The following is a higher order result of this same concept.

Proposition 1.9. *If Ω is a n dimensional domain with a Lipshitz boundary and let k and m be positive integers satisfying $m < k$ and let p be a real number in the range $1 \leq p < \infty$ such that*

$$k - m \geq n \text{ when } p = 1$$

$$k - m > n/p \text{ when } p > 1.$$

Then there is a constant C such that for all $u \in W^{k,p}(\Omega)$

$$||u||_{W^{m,\infty}(\Omega)} \leq C||u||_{W^{k,p}(\Omega)}.$$

Moreover, there is a C^m function in the $L^p(\Omega)$ equivalence class of u.

This statement and its proof can be found in Corollary 1.4.7 of [7]. Although this fact is not used in this chapter the following version of this result is cited in Chapter 7.

Corollary 1.10. *If $u \in H^2(\Omega)$, then there exists a C^1 function in the $L^2(\Omega)$ equivalence class of u.*

Proof. In proposition 1.9 let $n = 1$, $k = 2$, $m = 1$ and $p = 2$. □

1.2 The subspace of the energy space corresponding to homogeneous Dirichlet-type boundary conditions

Definition 1.11. *Let $\mathbf{H_0^1(\Omega)}$ denote the closure of $C_0^\infty(\Omega)$ with respect to the $||\cdot||_{H^1(\Omega)}$. Since $\Omega = (a, b)$ is bounded, this means*

$$H_0^1(\Omega) = \big\{u \in H^1(\Omega) : \bar{u}(a) = \bar{u}(b) = 0\big\}$$

where $\bar{u}$ is the continuous representative of $u \in H^1(\Omega)$ extended to the boundary from Proposition 1.8.

Since any closed subspace of a Hilbert space is Hilbert, $(H_0^1(\Omega), ||\cdot||_{H^1(\Omega)})$ is a Hilbert space.

Proposition 1.12. *Let $u \in H_0^1(\Omega)$. If $|u|_{H^1(\Omega)} = 0$, then u is zero almost everywhere on Ω.*

Proof. Since $H_0^1(\Omega) \subset H^1(\Omega)$, by 1.4 this implies that $u = c$ almost everywhere on Ω. Any constant almost everywhere function, can be represented by its continuous representative by Proposition 1.8. The only constant function with continuous representative in $H_0^1(\Omega)$ is the function that is zero almost everywhere in Ω. □

Therefore, it follows that $|\cdot|_{H^1(\Omega)}$ is a norm on $H_0^1(\Omega)$. We will show that these norms are equivalent norms on this space. For any $u \in H_0^1(\Omega)$, one direction of this equivalency is clear by definition:

$$||u||_{H^1(\Omega)}^2 = |u|_{H^2(\Omega)}^2 + ||u||_{L^2(\Omega)}^2 \geq |u|_{H^1(\Omega)}^2.$$

The other direction requires more work. Therefore, the other direction will be stated as a corollary to the following theorem.

Theorem 1.13 (Poincaré inequality). *Let Ω be a bounded interval, and without loss of generality, assume that $0 \in \Omega$. There exists a $k > 0$ such that $||u||_{L^2(\Omega)} \leq k|u|_{H^1(\Omega)}$ for all $u \in H_0^1(\Omega)$.*

Proof. As $C_0^\infty(\Omega)$ is dense in $H_0^1(\Omega)$, we will prove this statement for $u \in C_0^\infty(\Omega)$ and the rest will follow by a density argument.

Let $u \in C_0^\infty(\Omega)$. By the Fundamental Theorem of Calculus, for all $x \in \Omega$

$$u(x) = u(x) - u(0) = \int_0^x u'(t)\mathrm{d}t.$$

Apply Hölder's inequality to get

$$u(x) = \int_0^x u'(t)\mathrm{d}t \ \leq \ \left(\int_0^x (u'(t))^2 \, \mathrm{d}t\right)^{1/2} \left(\int_\Omega 1\mathrm{d}t\right)^{1/2}.$$

Since $0, x \in \Omega$, a bounded interval, $\displaystyle\int_0^x 1\mathrm{d}t \leq \int_\Omega 1\mathrm{d}t = |\Omega|$. Thus,

$$u(x) \leq |\Omega|^{1/2} \left(\int_0^x (u'(t))^2 \, \mathrm{d}t\right)^{1/2}.$$

This implies that

$$u(x)^2 \leq |\Omega| \int_0^x (u'(t))^2 \, \mathrm{d}t \ \leq \ |\Omega| \int_\Omega (u'(t))^2 \, \mathrm{d}t.$$

Therefore,

$$\begin{aligned}\int_\Omega u(x)^2 \mathrm{d}x &\le \int_\Omega \left(|\Omega| \int_\Omega (u'(t))^2 \mathrm{d}t \right) \mathrm{d}x \\ &\le |\Omega| \left(\int_\Omega (u'(t))^2 \mathrm{d}t \right) \left(\int_\Omega \mathrm{d}x \right) \\ &= |\Omega|^2 \int_\Omega (u'(t))^2 \mathrm{d}t.\end{aligned}$$

We have shown that for $u \in C_0^\infty(\Omega)$ that $||u||^2_{L^2(\Omega)} \le |\Omega|^2 ||u'||^2_{L^2(\Omega)} = |\Omega|^2 |u|^2_{H^1(\Omega)}$. Taking the square root of both sides and using a density argument, we have the desired inequality. □

Corollary 1.14. *(to 1.13) For all $u \in H_0^1(\Omega)$, there exist a $C > 0$ such that*

$$|u|^2_{H^1(\Omega)} \ge C ||u||^2_{H^1(\Omega)}.$$

Proof. By Theorem 1.13,

$$||u||^2_{L^2(\Omega)} \quad = \quad \int_\Omega u(x)^2 \mathrm{d}x \quad \le \quad k^2 \int_\Omega (u'(t))^2 \mathrm{d}t \quad = \quad k^2 |u|^2_{H^1}$$

where $k = |\Omega|$. Adding $|u|^2_{H^1(\Omega)}$ to both sides of the equation, it follows that

$$||u||^2_{H^1(\Omega)} \quad = \quad ||u||^2_{L^2(\Omega)} + |u|^2_{H^1(\Omega)} \quad \le \quad k^2 |u|^2_{H^1(\Omega)} + |u|^2_{H^1(\Omega)} \quad = \quad (k^2+1)|u|^2_{H^1(\Omega)}.$$

□

Corollary 1.15. $||\cdot||_{H^1(\Omega)}$ *and* $|\cdot|_{H^1(\Omega)}$ *are equivalent norms on the function space* $H_0^1(\Omega)$*.*

Proof. We have shown

$$\frac{1}{k^2+1} ||u||_{H^1(\Omega)} \le |u|^2_{H^1(\Omega)} \le ||u||^2_{H^1(\Omega)}.$$

where $k = |\Omega|$. □

Corollary 1.16. $(H_0^1(\Omega), |\cdot|_{H^1(\Omega)})$ *is a Hilbert space.*

By the density of $C_0^\infty(\Omega)$ in $H_0^1(\Omega)$ with respect to $||\cdot||_{H^1(\Omega)}$, it follows that if

$$\int_\Omega w'v'\mathrm{d}x = -\int_\Omega fv\mathrm{d}x \quad \forall v \in C_0^\infty(\Omega),$$

then

$$\int_\Omega w'v'\mathrm{d}x = -\int_\Omega fv\mathrm{d}x \quad \forall v \in H_0^1(\Omega).$$

Definition 1.17. *Therefore, for $f \in C(\Omega)$, we say that w is a* ***weak solution*** *to the homogeneous boundary value problem 1.3, if $w \in H_0^1(\Omega)$ such that*

$$\int_\Omega w'v'\mathrm{d}x = \int_\Omega fv\mathrm{d}x \;\forall v \in H_0^1(\Omega).$$

Furthermore, through an application of Hölder's inequality it is clear that if $f \in L^2(\Omega)$ and $v \in H_0^1(\Omega)$, then $fv \in L^1(\Omega)$. Therefore, weakening the definition of solution, will allow us to consider finding weak solutions to a more general BVP (one with $f \in L^2(\Omega)$ rather than in $C(\Omega)$). In later sections, when we refer to the weak homogeneous BVP we will be referring to the following: Given $f \in L^2(\Omega)$. Find a $w \in H_0^1(\Omega)$ such that

$$\int_\Omega w'v'\mathrm{d}x = \int_\Omega fv\mathrm{d}x \quad \forall v \in H_0^1(\Omega). \tag{1.5}$$

With the goal of showing that this weak homogeneous BVP in fact has a solution, we prove Proposition 1.18.

Proposition 1.18. *The function $b(\cdot,\cdot)\colon H_0^1(\Omega) \times H_0^1(\Omega) \to \mathbb{R}$ given by*

$$b(u,v) = \int_\Omega u'v'\mathrm{d}x, \tag{1.6}$$

is a real symmetric positive definite bilinear form. Furthermore, it is a bounded bilinear form.

Proof. Let $u, v, w \in H_0^1(\Omega)$ and let $\alpha \in \mathbb{R}$. Clearly, b is symmetric. Bilinearity of this function follows from the linearity of integration. To prove that b is positive definite assume

$u \in H_0^1(\Omega)$ such that

$$b(u,u) = \int_\Omega \left(u'(x)\right)^2 \mathrm{d}x = 0.$$

By Corollary 1.12, this implies that $u = 0$ almost everywhere in Ω and therefore this bilinear form is positive definite on $H_0^1(\Omega)$. To show that b is bounded, use Hölder's inequality:

$$b(u,v) = \int_\Omega u'v'\mathrm{d}x \ \leq \ \left(\int_\Omega (u')^2 \mathrm{d}x\right)^{1/2} \left(\int_\Omega (v')^2 \mathrm{d}x\right)^{1/2}.$$

□

Observe that $b(u,u) = |u|^2_{H^1}$ for all $u \in H_0^1(\Omega)$. By combining the results of 1.13 and 1.18, we have shown that b is a coercive and bounded bilinear form.

The following is a well known result in functional analysis:

Theorem 1.19 (Lax-Millgram Theorem)**.** *Let ϕ be a bounded coercive bilinear form on a Hilbert space, A. If $\mathscr{L}$ is a bounded linear functional on A, then there exists a unique $u \in A$ such that*

$$\mathscr{L}(v) = \phi(v,u) \quad \forall v \in A$$

Proof of this result can be found in any functional analysis textbook, therefore we will use this result without justification to show the following:

Theorem 1.20. *If f is an element of $L^2(\Omega)$, then there exists a unique $u_f \in H_0^1(\Omega)$ such that*

$$b(u_f, v) = \int_\Omega f v \mathrm{d}x \quad \forall v \in H_0^1(\Omega).$$

Proof. Let $f \in L^2(\Omega)$ be given. Define $\mathscr{L} : H_0^1(\Omega) \to \mathbb{R}$ by

$$\mathscr{L}(v) = (f,v)_{L^2(\Omega)} \quad \forall v \in H_0^1(\Omega).$$

Through an application of Hölder's inequality, it can be shown that $\mathscr{L}$ is a bounded linear operator on $H_0^1(\Omega)$. We have already shown that $b(\cdot,\cdot)$ is a bounded coercive bilinear form on $H_0^1(\Omega)$. Therefore, by the Lax-Millgram Theorem 1.19, we know there exists a unique $u_f \in H_0^1(\Omega)$ such that

$$\mathscr{L}(v) = b(v, u_f) \;\; \forall v \in H_0^1(\Omega)$$

By definition $\mathscr{L}(v) = (v, f)_{L^2(\Omega)}$ and therefore we have a unique $u_f \in H_0^1(\Omega)$ such that

$$b(u_f, v) = (v, f)_{L^2(\Omega)} \;\; \forall v \in H_0^1(\Omega).$$

□

This means that for any function f in $L^2(\Omega)$, there is a unique weak solution $w \in H_0^1(\Omega)$ to the more general BVP 1.3 (but with $f \in L^2(\Omega)$). Thus, by adding the function g (defined in 1.2) to this solution w, we have a unique weak solution to the more general nonhomogeneous Dirichlet-type BVP 1.1 (with $f \in L^2(\Omega)$).

Chapter 2

The PD Model

Many of the results from this chapter can be found in either [47, 38]. The ones that are not specifically mentioned in those papers, are direct extensions of the corresponding local results.

The nonlocal model we will focus on is called **bond-based peridynamics** (PD) and was proposed in 2000 by Silling [47]. In bond-based peridynamics, on a *homogeneous material*, we assume that particles that are separated by a finite distance δ interact with each other through a *spring-like bond*. The distance δ is known as the material **horizon**. The strength of this bond is described by the **peridynamic kernel**, c^δ. We assume that c^δ is a nonnegative function of the distance between two material points [38]. Since we expect the strength of the bond to decrease as the distance between the material points increases, we assume that c^δ is a nonincreasing function with compact support. Specifically, to model our understanding of bonds, we will assume that c^δ has finite second moment. To agree with our experiences with spring-like bonds, we make the following assumptions about the function c^δ:

$$\begin{cases} \text{nonnegative, nonincreasing, radial,} \\ c^\delta \text{ has compact support in } B_\delta(0), \\ \text{and } \displaystyle\int_{-\delta}^{\delta} c^\delta(|\xi|)|\xi|^2 \mathrm{d}\xi = E^0 \end{cases} \tag{2.1}$$

where E^0 is the **Young's Modulus** of the material.

Restricting our focus to the one-dimensional nonlocal analogue of problem 1.3. Let Ω be a bounded interval in $\mathbb{R}$, (a,b). Let $\Gamma = (a-\delta, a] \cup [b, b+\delta)$. Define $\Omega^* = \Omega \cup \Gamma$. Given f and g, find a u that satisfies

$$\begin{cases} \mathcal{L}^\delta u(x) = f(x), & x \in \Omega \\ u(x) = g(x), & x \in \Gamma \end{cases} \tag{2.2}$$

where

$$\mathcal{L}^\delta u(x) = -2\int_{B_\delta(x)} c^\delta(|p-x|)\,[u(p)-u(x)]\,\mathrm{d}p.$$

As in the classical case, we want to weaken the definition of solution to this problem, which will allow us to chose f from a wider class of functions and still be able to get a solution.

Knowing that $u = g$ on Γ, define a function

$$\tilde{g}(x) = \begin{cases} \dfrac{g(b)-g(a)}{b-a}x + \dfrac{bg(a)-ag(b)}{b-a}, & x \in \Omega \\ g(x) & x \in \Gamma \end{cases} \tag{2.3}$$

If we let $w(x) = u(x) - \tilde{g}(x)$ for $x \in \Omega^*$,

$$\begin{aligned} \mathcal{L}^\delta w(x) &= \mathcal{L}^\delta (u-\tilde{g})(x) \\ &= f - \mathcal{L}^\delta \tilde{g}(x) \end{aligned}$$

Analogously to the approach used for the classical differential equation, $\mathcal{L}^\delta \tilde{g}(x) = 0$ for some $x \in \Omega$, but notice that for $x \in \Gamma \cup \{x \in \Omega \mid d(x,\Gamma) \le \delta\}$ this quantity (generally speaking) nonzero. This is an essential difference that accounts for the nonlocal interaction between material points that is assumed in bond-based peridynamics. We can see that w satisfies

$$\begin{cases} \mathcal{L}^\delta w(x) = f(x) - \mathcal{L}^\delta \tilde{g}(x), & x \in \Omega \\ w(x) = 0, & x \in \Gamma \end{cases} \tag{2.4}$$

where

$$\mathcal{L}^\delta w(x) = -2 \int_{B_\delta(x)} c^\delta(|p-x|)\,[w(p) - w(x)]\,\mathrm{d}p.$$

In order to derive the weak formulation of the problem, follow similar steps to those taken with the classical homogeneous BVP 1.3.

First, multiply the integral equation by a test function $v \in L^2(\Omega^*)$ such that $v = 0$ a.e. in Γ and integrate over the domain on which the integral equation is defined, Ω. Therefore,

$$\int_\Omega v(x)\mathcal{L}^\delta w(x)\mathrm{d}x = \int_\Omega f(x)v(x)\mathrm{d}x + \int_\Omega v(x)\mathcal{L}^\delta \tilde{g}(x)\mathrm{d}x.$$

which can equivalently be stated as

$$\begin{aligned} &\int_\Omega v(x)\bigg(-2\int_{B_\delta(x)} c^\delta(|p-x|)\,[w(p)-w(x)]\,\mathrm{d}p\bigg)\mathrm{d}x \\ &\qquad\qquad = \int_\Omega f(x)v(x)\mathrm{d}x + \int_\Omega v(x)\bigg(2\int_{B_\delta(x)} c^\delta(|p-x|)\,[\tilde{g}(p)-\tilde{g}(x)]\,\mathrm{d}p\bigg)\mathrm{d}x. \end{aligned}$$

Let

$$I := \int_\Omega v(x)\bigg(-2\int_{B_\delta(x)} c^\delta(|p-x|)\,[w(p)-w(x)]\,\mathrm{d}p\bigg)\mathrm{d}x.$$

In order to apply nonlocal integration by parts to I, the two-dimensional domain of integration must be symmetric. Since we have assumed that $c^\delta(z)$ has support contained in $B_\delta(0)$, we can extend the inner domain of integration on the left hand side to Ω^*:

$$I = \int_\Omega v(x)\left(-2\int_{\Omega^*} c^\delta(|p-x|)\,[w(p)-w(x)]\,\mathrm{d}p\right)\mathrm{d}x.$$

Since it was assumed that v vanishes on Γ, we also extend the outer domain of integration to Ω^*. Now that we have a symmetric two-dimensional domain of integration nonlocal integration by parts can be applied. Nonlocal integration by parts is done through the following steps [23]: Split the integral in half

$$
\begin{aligned}
I = &-\int_{\Omega^*} v(x) \left(\int_{\Omega^*} c^\delta(|p-x|) \left[w(p) - w(x)\right] \mathrm{d}p \right) \mathrm{d}x \\
&- \int_{\Omega^*} v(x) \left(\int_{\Omega^*} c^\delta(|p-x|) \left[w(p) - w(x)\right] \mathrm{d}p \right) \mathrm{d}x.
\end{aligned}
$$

Switch the roles of p and x in the second term, recalling that c^δ is an even function, and switching the order of integration through Fubini's Theorem, we have that

$$
\begin{aligned}
I = &-\int_{\Omega^*} v(x) \left(\int_{\Omega^*} c^\delta(|p-x|) \left[w(p) - w(x)\right] \mathrm{d}p \right) \mathrm{d}x \\
&- \int_{\Omega^*} v(p) \left(\int_{\Omega^*} c^\delta(x-p) \left[w(x) - w(p)\right] \mathrm{d}x \right) \mathrm{d}p
\end{aligned}
$$

Recall that c^δ is an even function, therefore

$$
\begin{aligned}
I = &-\int_{\Omega^*} v(x) \left(\int_{\Omega^*} c^\delta(|p-x|) \left[w(p) - w(x)\right] \mathrm{d}p \right) \mathrm{d}x \\
&+ \int_{\Omega^*} v(p) \left(\int_{\Omega^*} c^\delta(|p-x|) \left[w(p) - w(x)\right] \mathrm{d}x \right) \mathrm{d}p.
\end{aligned}
$$

Switch the order of integration through Fubini's Theorem

$$
\begin{aligned}
I = &-\int_{\Omega^*} v(x) \left(\int_{\Omega^*} c^\delta(|p-x|) \left[w(p) - w(x)\right] \mathrm{d}p \right) \mathrm{d}x \\
&+ \int_{\Omega^*} \left(\int_{\Omega^*} v(p) c^\delta(|p-x|) \left[w(p) - w(x)\right] \mathrm{d}p \right) \mathrm{d}x.
\end{aligned}
$$

Finally, recombine the two terms to obtain

$$
I = \int_{\Omega^*} \int_{\Omega^*} c^\delta(|p-x|)[w(p) - w(x)][v(p) - v(x)] \mathrm{d}p \mathrm{d}x.
$$

Definition 2.1. *Define the following collection of functions*

$$
\mathbb{S}(\Omega^*) = \left\{ u \in L^2(\Omega^*) : \int_{\Omega^*} \int_{\Omega^*} c^\delta(|p-x|)[u(p) - u(x)]^2 \mathrm{d}p \mathrm{d}x < \infty \right\}, \tag{2.5}
$$

as they are defined in [38].

The function space $\mathbb{S}(\Omega^*)$ is nonempty, because any constant function $u = c$ is in this space. This is the subspace of This collection of functions, $\mathbb{S}(\Omega^*)$ is the nonlocal analog $H^1(\Omega)$, and thus we want to establish any similar properties.

2.1 The energy space $\mathbb{S}(\Omega^*)$

Proposition 2.2. $|u|^2_{\mathbb{S}(\Omega^*)} = \int_{\Omega^*}\int_{\Omega^*} c^\delta(|p-x|)[u(p)-u(x)]^2 \mathrm{d}p$ *is a semi-norm on* $\mathbb{S}(\Omega^*)$ *[38].*

Proof. Let $u, v \in \mathbb{S}(\Omega^*)$ and $\alpha \in \mathbb{R}$.

i. *Scalability:*

$$\begin{aligned}
|\alpha u|^2_{\mathbb{S}(\Omega^*)} &= \int_{\Omega^*}\int_{\Omega^*} c^\delta(|p-x|)[\alpha u(p) - \alpha u(x)]^2 \mathrm{d}p\mathrm{d}x \\
&= \alpha^2 \int_{\Omega^*}\int_{\Omega^*} c^\delta(|p-x|)[u(p) - u(x)]^2 \mathrm{d}p\mathrm{d}x \\
&= \alpha^2 |u|^2_{\mathbb{S}(\Omega^*)} \\
&= \left(\alpha |u|_{\mathbb{S}(\Omega^*)}\right)^2
\end{aligned}$$

ii. *Nonnegativity:*

We only need to focus on the integrand, as $\Omega^* \times \Omega^*$ is a space with positive measure. Since c^δ and $(u(p) - u(x))^2$ are both nonnegative, the integrand is nonnegative.

iii. *Semi-definite:*

(note: this is the analogue to Proposition 1.4)

$$0 = |u|^2_{\mathbb{S}(\Omega^*)} = \int_{\Omega^*}\int_{\Omega^*} c^\delta(|p-x|)[u(p) - u(x)]^2 \mathrm{d}p\mathrm{d}x$$

This implies that for a.e. $x, p \in \Omega^*$

$$0 = c^{\delta}(|p-x|)[u(p)-u(x)]^2 \text{ for a.e. } x, p \in \Omega^*.$$

Since c^{δ} is nonnegative and supported on a ball radius δ,

$$[u(p)-u(x)]^2 = 0 \text{ for a.e. } x, p \in \Omega^*.$$

Square rooting both sides further implies that $u(x)$ is constant a.e. in Ω^*.

iv. *Triangle inequality:*

If $|u|_{\mathbb{S}(\Omega^*)} = 0$ or $|v|_{\mathbb{S}(\Omega^*)} = 0$, the triangle inequality holds. So assume that neither equal 0. Then we can write

$$\begin{aligned}
|u+v|^2_{\mathbb{S}(\Omega^*)} &= \int_{\Omega^*}\int_{\Omega^*} c^{\delta}(|p-x|)\Big[\big(u+v\big)(p) - \big(u+v\big)(x)\Big]^2 \mathrm{d}p\mathrm{d}x \\
&= \int_{\Omega^*}\int_{\Omega^*} c^{\delta}(|p-x|)\Big[\big(u(p)-u(x)\big)^2 + \big(v(p)-v(x)\big)^2\Big]\mathrm{d}p\mathrm{d}x \\
&\qquad + \int_{\Omega^*}\int_{\Omega^*} c^{\delta}(|p-x|)\Big[2\big(u(p)-u(x)\big)\big(v(p)-v(x)\big)\Big]\mathrm{d}p\mathrm{d}x.
\end{aligned}$$

By Hölder's inequality,

$$\begin{aligned}
&2\int_{\Omega^*}\int_{\Omega^*} c^{\delta}(|p-x|)[(u(p)-u(x))(v(p)-v(x))]\mathrm{d}p\mathrm{d}x \\
&\le 2\Big(\int_{\Omega^*}\int_{\Omega^*} c^{\delta}(|p-x|)[u(p)-u(x)]^2\mathrm{d}p\mathrm{d}x\Big)^{\frac{1}{2}}\Big(\int_{\Omega^*}\int_{\Omega^*} c^{\delta}(|p-x|)[v(p)-v(x)]^2\mathrm{d}p\mathrm{d}x\Big)^{\frac{1}{2}}.
\end{aligned}$$

Therefore,

$$\begin{aligned}
\big|u+v\big|^2_{\mathbb{S}(\Omega^*)} &\le \big|u\big|^2_{\mathbb{S}(\Omega^*)} + 2\big|u\big|_{\mathbb{S}(\Omega^*)}\big|v\big|_{\mathbb{S}(\Omega^*)} + \big|v\big|^2_{\mathbb{S}(\Omega^*)} \\
&\le \Big(\big|u\big|_{\mathbb{S}(\Omega^*)} + \big|v\big|_{\mathbb{S}(\Omega^*)}\Big)^2
\end{aligned}$$

which is equivalent to the triangle inequality.

$\square$

Proposition 2.3. $||\cdot||_{\mathbb{S}(\Omega^*)} := \sqrt{||\cdot||^2_{L^2(\Omega^*)} + |\cdot|^2_{\mathbb{S}(\Omega^*)}}$

is a norm on the space $\mathbb{S}(\Omega^*)$.

Proof. The proposition follows directly from the fact that $||\cdot||_{L^2(\Omega^*)}$ is a norm and Proposition 2.2. $\square$

Theorem 2.4. $(\mathbb{S}(\Omega^*), ||\cdot||_{\mathbb{S}(\Omega^*)})$ *is a Hilbert space.*

Proof. This proof is taken from Theorem 2.1 of [38].
Let $\{u_n\} \subseteq \mathbb{S}(\Omega^*)$ be a Cauchy sequence with respect to $||\cdot||_{\mathbb{S}(\Omega^*)}$. Therefore, $\{u_n\}$ are Cauchy sequences with respect to the L^2-norm and the $\mathbb{S}$-seminorm. Since $L^2(\Omega^*)$ is a complete space, it follows that $\{u_n\}$ converges to some $u \in L^2(\Omega^*)$ respectively. If there was a limit function in $\mathbb{S}(\Omega^*)$ it would necessarily have to be u. Therefore, we must show that $|u_n - u|_{\mathbb{S}(\Omega^*)} \to 0$ as n increases.

Since the sequence $\{u_n\}$ is Cauchy for all $n, m \geq N$ we have that :

$$\int_{\Omega^*}\int_{\Omega^*} c^\delta(|p-x|)[u_n(p) - u_m(p) - u_n(x) + u_m(x)]^2 \mathrm{d}p\mathrm{d}x < \epsilon$$

For $\tau > 0$, we introduce a modified operator with a truncated kernel,

$$c^\delta_\tau(|z|) := \chi_{|z|>\tau}(z)c^\delta(|z|).$$

It is important to notice that $c^\delta_\tau(|z|) \to c^\delta(|z|)$ pointwise as $\tau \to 0$. Therefore, for all $\tau > 0$ and $n, m > N$,

$$\begin{aligned}
&\int_{\Omega^*}\int_{\Omega^*} c^\delta_\tau(|p-x|)[u_n(p) - u_m(p) - u_n(x) + u_m(x)]^2 \mathrm{d}p\mathrm{d}x \\
&\qquad\qquad \leq \int_{\Omega^*}\int_{\Omega^*} c^\delta(|p-x|)[u_n(p) - u_m(p) - u_n(x) + u_m(x)]^2 \mathrm{d}p\mathrm{d}x \\
&\qquad\qquad \leq \epsilon
\end{aligned}$$

For fixed m and $\forall\ x, p$, there exists a subsequence u_{n_k} such that

$$\lim_{k\to\infty} c_\tau^\delta(|p-x|)[u_{n_k}(p)-u_m(p)-u_{n_k}(x)+u_m(x)]^2 = c_\tau^\delta(|p-x|)[u(p)-u_m(p)-u(x)+u_m(x)]^2.$$

Therefore, by the Dominated Convergence Theorem, for all $\tau > 0$ and for all $m \geq N$

$$\begin{aligned}\lim_{n\to\infty} \int_{\Omega^*}\int_{\Omega^*} & c_\tau^\delta(|p-x|)[u_n(p)-u_m(p)-u_n(x)+u_m(x)]^2 \mathrm{d}p\mathrm{d}x \\ &= \int_{\Omega^*}\int_{\Omega^*} c_\tau^\delta(|p-x|)[u(p)-u_m(p)-u(x)+u_m(x)]^2 \mathrm{d}p\mathrm{d}x.\end{aligned}$$

That is for all $\tau > 0$ and for $m \geq N$,

$$\int_{\Omega^*}\int_{\Omega^*} c_\tau^\delta(|p-x|)[u(p)-u_m(p)-u(x)+u_m(x)]^2 \mathrm{d}p\mathrm{d}x \leq \epsilon$$

Now apply Fatou's Lemma over τ, to obtain that

$$\int_{\Omega^*}\int_{\Omega^*} c_\tau^\delta(|p-x|)[u(p)-u_m(p)-u(x)+u_m(x)]^2 \mathrm{d}p\mathrm{d}x \leq \epsilon$$

for all $m > N$. Therefore, $(\mathbb{S}(\Omega^*), ||\cdot||_{\mathbb{S}(\Omega^*)})$ is a complete normed vector space. $\square$

Remark 2.5. $\mathbb{S}(\Omega^*)$ *embeds continuously into* $L^2(\Omega^*)$

Proof. Let $u \in \mathbb{S}(\Omega^*)$. By definition

$$||u||_{\mathbb{S}(\Omega^*)} = \sqrt{||u||^2_{L^2(\Omega^*)} + |u|^2_{\mathbb{S}(\Omega^*)}}$$

But $|\cdot|_{\mathbb{S}(\Omega^*)}$ is a seminorm so $|u|_{\mathbb{S}(\Omega^*)} \geq 0$ for all $u \in \mathbb{S}(\Omega^*)$. Therefore,

$$||u||_{L^2(\Omega^*)} = \sqrt{||u||^2_{L^2(\Omega^*)}} \ \leq \ \sqrt{||u||^2_{L^2(\Omega^*)} + |u|^2_{\mathbb{S}(\Omega^*)}} \ = \ ||u||_{\mathbb{S}(\Omega^*)}$$

Therefore, $\mathbb{S}(\Omega^*)$ continuously embeds into $L^2(\Omega^*)$. $\square$

2.2 The subspace of the energy space corresponding to homogeneous Dirichlet-type boundary conditions

The following is a general statement of the nonlocal Poincaré-type inequality. Although this is called the *Poincare-type inequality*, this result is a stronger statement than we need for the analogue of the Poincaré inequality from Chapter 1. The proof of this Theorem is taken from [38].

Theorem 2.6 (Nonlocal Poincaré-type Inequality)**.** *Suppose that V is a closed subspace of $L^2(\Omega^*)$ that intersects with $\mathbb{R}$ trivially. Then there exists an $\mathcal{C} > 0$, such that*

$$||u||^2_{L^2(\Omega^*)} \leq \mathcal{C} \int_{\Omega^*} \int_{\Omega^*} c^\delta(|p-x|)|p-x|^2(u(p)-u(x))^2 \mathrm{d}p\mathrm{d}x$$

for all $u \in V$.

Note 2.7. *Before beginning the proof of this theorem, notice that the integrand here contains $c^\delta(|p-x|)|p-x|^2$, but the semi-norm we have been discussing up until now only contains $c^\delta(|p-x|)$. Since we have only been requiring that c^δ is a function with finite second moment, the addition of $|p-x|^2$ tells us that $c^\delta(|p-x|)|p-x|^2$ is integrable.*

Theorem 2.6 is stated as Proposition 1 in [38], the proof included here is largely taken from this paper, but with some additional details.

Proof of Theorem 2.6. In order to do a proof by contradiction, suppose the conclusion of the theorem is false. Then there must exist a sequence $u_n \in V$ such that for all n, $||u_n||_{L^2(\Omega^*)} = 1$ and as $n \to \infty$

$$\int_{\Omega^*} \int_{\Omega^*} c^\delta(|p-x|)|p-x|^2(u_n(p)-u_n(x))^2 \mathrm{d}p\mathrm{d}x \to 0.$$

Since the sequence $\{u_n\}$ is a bounded sequence in $L^2(\Omega^*)$, it (has a subsequence that) converges weakly to some $u \in L^2(\Omega^*)$. Since V is a closed subspace of $L^2(\Omega^*)$, we have that $u \in V$. We claim that $u = 0$, but in order to show this, we first must show that u is a constant function on Ω^*.

Consider the operator $L : L^2(\Omega^*) \to L^2(\Omega^*)$ given by

$$L(v(x)) = -2\int_{\Omega^*} c^\delta(|p-x|)|p-x|^2(v(p)-v(x))\mathrm{d}p.$$

Let $\phi \in C_c^\infty(\Omega^*)$, and define the sequence

$$\begin{aligned}
J_n(\phi) &= \int_{\Omega^*} L(\phi(x))u_n(x)\mathrm{d}x. \\
&= -2\int_{\Omega^*}\int_{\Omega^*} c^\delta(|p-x|)|p-x|^2(\phi(p)-\phi(x))u_n(x)\mathrm{d}p\mathrm{d}x \\
&= \int_{\Omega^*}\int_{\Omega^*} c^\delta(|p-x|)|p-x|^2(\phi(p)-\phi(x))(u_n(p)-u_n(x))\mathrm{d}p\mathrm{d}x \qquad (2.6) \\
&= -2\int_{\Omega^*}\int_{\Omega^*} c^\delta(|p-x|)|p-x|^2(u_n(p)-u_n(x))\phi(p)\mathrm{d}x\mathrm{d}p \\
&= \int_{\Omega^*} L(u_n(p))\phi(p)\mathrm{d}p.
\end{aligned}$$

We used nonlocal integration by parts to go from the second line to the third and again from the third line to the fourth. In order to apply nonlocal integration by parts the first time we use Tonelli's Theorem to switch the order of the integration. Therefore, we need to justify its use. Since

$$\begin{aligned}
|c^\delta(|p-x|)|p-x|^2(\phi(p)-\phi(x))u_n(x)| &\leq c^\delta(|p-x|)|p-x|^2|\phi(p)-\phi(x)||u_n(x)| \\
&= c^\delta(|p-x|)|p-x|^2(|\phi(p)|+|\phi(x)|)|u_n(x)| \\
&= c^\delta(|p-x|)|p-x|^2|u_n(x)||\phi(p)| \\
&\quad + c^\delta(|p-x|)|p-x|^2|u_n(x)||\phi(x)|
\end{aligned}$$

and both of these terms are integrable, we are justified in using Tonelli's Theorem. Applying Holders inequality to the righthand side of Equation 2.6, we find

$$\begin{aligned}
J_n(\phi(x)) \leq 2&\left(\int_{\Omega^*}\int_{\Omega^*} c^\delta(|p-x|)|p-x|^2(u_n(p)-u_n(x))^2\mathrm{d}x\mathrm{d}p\right)^{1/2} \\
&\left(\int_{\Omega^*}\int_{\Omega^*} c^\delta(|p-x|)|p-x|^2|\phi(p)|^2\mathrm{d}x\mathrm{d}p\right)^{1/2}.
\end{aligned}$$

Since $\phi \in C_c^\infty(\Omega^*)$, can say that

$$\left(\int_{\Omega^*}\int_{\Omega^*} c^\delta(|p-x|)|p-x|^2|\phi(p)|^2\mathrm{d}x\mathrm{d}p\right)^{1/2} \leq (E^0)^{1/2}||\phi||_{L^2(\Omega^*)}.$$

Therefore,

$$J_n(\phi(x)) \leq 2(E^0)^{1/2}||\phi||_{L^2(\Omega^*)}\int_{\Omega^*}\int_{\Omega^*} c^\delta(|p-x|)|p-x|^2(u_n(p)-u_n(x))^2\mathrm{d}p\mathrm{d}x$$

which converges to 0 as $n \to \infty$. Therefore, for all $\phi \in C_c^\infty(\Omega^*)$ we have that $J_n(\phi) \to 0$ as $n \to 0$. On the other hand, since u is the weak limit of u_n in $L^2(\Omega^*)$, we know that

$$\lim_{n\to\infty} J_n(\phi) = \int_{\Omega^*} L(\phi(x))u(x)\mathrm{d}x.$$

Therefore, we have shown that $\displaystyle\int_{\Omega^*} L(\phi(x))u(x)\mathrm{d}x = 0$. If we again iterate integrals, we obtain that for all $\phi \in C_c^\infty(\Omega^*)$

$$0 = \int_{\Omega^*} L(\phi(x))u(x)\mathrm{d}x = \int_{\Omega^*} L(u(p))\phi(p)\mathrm{d}p.$$

This directly implies that $L(u(p)) = 0$ for almost every $p \in \Omega^*$. Multiplying both side of this by $u(x)$ and then integrating in x we get that

$$-2\int_{\Omega^*}\int_{\Omega^*} c^\delta(|p-x|)|p-x|^2(u(p)-u(x))\mathrm{d}p(u(x))\mathrm{d}x = 0$$

If we once again, apply nonlocal integration by parts, we obtain that

$$0 = \int_{\Omega^*}\int_{\Omega^*} c^\delta(|p-x|)|p-x|^2(u(p)-u(x))^2\mathrm{d}p\mathrm{d}x.$$

Therefore $u(p) = u(x)$ for a.e. $p, x \in \Omega^*$ where $|p-x| < \delta$. Since Ω^* is a compact and connected space, a covering argument shows that u is a constant function on Ω^*. Recalling that $u \in V$ and that the only constant function in V is the trivial function, we have that $u = 0$ a.e. on Ω^*.

Now we want to show that this weak limit u is in fact a strong limit in $L^2(\Omega^*)$

Let $\bar{u}_n$ be the zero extension of u_n to $\mathbb{R}$. Since L is an operator on $L^2(\Omega^*)$, we can define L as the sum of two operators.

$$L(u_n) = T(u_n) + A(u_n)$$

where

$$T(u_n) = K * \bar{u}_n = -2\int_{\mathbb{R}} c^\delta(|p-x|)|p-x|^2\bar{u}_n(p)\mathrm{d}p$$
$$A(u_n) = a(x)u_n(x) = 2\int_{\Omega^*} c^\delta(|p-x|)|p-x|^2\mathrm{d}p \;\; u_n(x)$$

Observe that $T, A : L^2(\Omega^*) \to L^2(\Omega^*)$:

$$||T(u_n)||_{L^2(\Omega^*)} = ||K * \bar{u}_n||_{L^2(\Omega^*)} \leq ||K||_{L^1(\Omega^*)}||\bar{u}_n||_{L^2(\mathbb{R})} = ||K||_{L^1(\Omega^*)}||u_n||_{L^2(\Omega^*)} < \infty$$

and

$$||A(u_n)||^2_{L^2} = \int_{\Omega^*}\left(2\int_{\Omega^*} c^\delta(|p-x|)|p-x|^2\mathrm{d}p u_n(x)\right)^2 \mathrm{d}x \leq 4\int_{\Omega^*}(E^0u_n(x))^2\mathrm{d}x < \infty.$$

We will show that $||T(u_n)||_{L^2(\Omega^*)} \to ||T(u)||_{L^2(\Omega^*)}$. Corollary 4.28 in [8] states and proves the following:

"*Let G be a fixed function in $L^1(\mathbb{R}^N)$ and let*

$$\mathcal{F} = G * \mathcal{B}$$

where $\mathcal{B}$ is a bounded set in $L^p(\mathbb{R}^N)$ with $1 \leq p < \infty$. Then $\mathcal{F}|_\Omega$ has compact closure in $L^p(\Omega)$ for any measurable set Ω with finite measure."

By assumption $\{\bar{u}_n\}_{i=1}^\infty$ is a bounded set in $L^2(\mathbb{R})$ and c^δ has a finite second moment. Therefore, $\{(K * \bar{u}_n)|_{\Omega^*}\}$ has compact closure in $L^2(\Omega^*)$. This means that $(K * \bar{u}_n)|_{\Omega^*}$ converges strongly to some function, f, in $L^2(\Omega^*)$.

Letting $\psi \in C_0^\infty(\Omega^*)$, we have

$$\begin{aligned}\left(\bar{\psi}, K * \bar{u}_n\right)_{L^2(\mathbb{R})} &= \int_{\mathbb{R}}\int_{\mathbb{R}} c^\delta(|p-x|)|p-x|^2\bar{\psi}(x)\bar{u}_n(p)\mathrm{d}p\mathrm{d}x \\ &= \int_{\mathbb{R}}\int_{\mathbb{R}} c^\delta(|p-x|)|p-x|^2\bar{\psi}(x)\bar{u}_n(p)\mathrm{d}x\mathrm{d}p \\ &= \left(\bar{u_n}, K * \bar{\psi}\right)_{L^2(\mathbb{R})}.\end{aligned} \tag{2.7}$$

But we know that u_n converges weakly in $L^2(\Omega*)$ to u and since $\bar{u}_n$ is just the zero extension of u_n, we have that $\bar{u}_n$ converges weakly to $\bar{u}$ in $L^2(\Omega)$. Therefore, we have

$$\lim_{n\to\infty}\left(\bar{\psi}, K * \bar{u}_n\right)_{L^2(\mathbb{R})} = \lim_{n\to\infty}\left(\bar{u_n}, K * \bar{\psi}\right)_{L^2(\mathbb{R})} = \left(\bar{u}, K * \bar{\psi}\right)_{L^2(\mathbb{R})} = \left(\bar{\psi}, K * \bar{u}\right)_{L^2(\mathbb{R})}$$

Since $K * \bar{u}$ is the weak limit of $K * \bar{u}_n$ it follows by the uniqueness of limits that $f = K * \bar{u}|_{\Omega^*}$. In equation 2.7, we apply Tonelli's theorem to interate the integrals. This is justified through the an application of Hölder's inequality.

Therefore, we have shown that

$$||Tu_n||_{L^2(\Omega^*)} \to ||Tu||_{L^2(\Omega^*)} = 0 \quad \text{as } n \to \infty.$$

By the assumptions on c^δ and the absolute continuity of the integral, $a(x)$ is a positive continuous function on Ω^*. Thus, there exists a positive constant c such that $a(x) \geq c > 0$ for all $x \in \Omega^*$. Since $T(u) = 0$, it follows that

$$0 = \lim_{n\to\infty}\left(Lu_n, u_n\right)_{L^2(\Omega^*)} = \lim_{n\to\infty}\left(Tu_n, u_n\right) + \int_{\Omega^*} a(x)|u_n(x)|^2\mathrm{d}x \geq c||u_n||^2_{L^2(\Omega^*)}$$

which is a contradiction to the assumed fact that $||u_n||_{L^2(\Omega^*)} = 1$ for all n. □

The following corollary is stated as Corollary 1 in [38].

Corollary 2.8. *Suppose that V is a closed subspace of $L^2(\Omega^*)$ that intersects with $\mathbb{R}$ trivially. There exists an $\mathcal{C} > 0$ such that*

$$||u||^2_{L^2(\Omega^*)} \leq \mathcal{C} \int_{\Omega^*} \int_{\Omega^*} c^\delta(|p-x|)(u(p)-u(x))^2 \mathrm{d}p\mathrm{d}x$$

for all $u \in V$.

Proof. Let $u \in V$. Then by the nonlocal Poincare' there exists $\mathcal{C} > 0$ such that

$$||u||^2_{L^2(\Omega^*)} \leq \mathcal{C} \int_{\Omega^*} \int_{\Omega^*} c^\delta(|p-x|)|p-x|^2(u(p)-u(x))^2 \mathrm{d}p\mathrm{d}x$$

Since the support of c^δ is contained in a $\delta-$ball,

$$\int_{\Omega^*} \int_{\Omega^*} c^\delta(|p-x|)(p-x)^2(u(p)-u(x))^2 \mathrm{d}p\mathrm{d}x \leq \delta^2 \int_{\Omega^*} \int_{\Omega^*} c^\delta(|p-x|)(u(p)-u(x))^2 \mathrm{d}p\mathrm{d}x$$

□

Note 2.9. *It is Corollary 2.8 it analogous to the classical Poincaré inequality, and that the nonlocal Poincaré inequality is a stronger result.*

Define

$$\mathbb{S}_0(\Omega^*) = \left\{u \in \mathbb{S}(\Omega^*) : u_{|\Gamma} = 0\right\}. \tag{2.8}$$

Consider the closure of $\mathbb{S}_0(\Omega^*)$ with respect to $||\cdot||_{L^2(\Omega^*)}$. Clearly, if $u_n \in \mathbb{S}_0(\Omega^*)$ and $u \in L^2(\Omega^*)$ such that $||u_n - u||_{L^2(\Omega^*)} \to 0$, then it follows that

$$\int_\Gamma |u_n(x) - u(x)|^2 \mathrm{d}x \leq \int_{\Omega^*} |u_n(x) - u(x)|^2 \mathrm{d}x$$

and therefore, u_n converges to u on Γ. But, $u_n \in \mathbb{S}_0(\Omega^*)$ and therefore $u_n|_\Gamma = 0$. Thus, it follows that $u|_\Gamma = 0$. From this, it is clear that the closure of $\mathbb{S}_0$ with respect to $L^2(\Omega^*)$ is a closed subspace of $L^2(\Omega^*)$ whose intersection with $\mathbb{R}$ is only the zero function. Therefore, it follows that the weak Poincaré inequality holds on the closure of $\mathbb{S}_0(\Omega^*)$. Thus, the weak Poincaré inequality holds on $\mathbb{S}_0(\Omega^*)$.

This space is the nonlocal analogue to the space $H^1_0(\Omega)$ in Chapter 1, we establish the analogous properties.

Remark 2.10. *$H^1_0(\Omega)$ embeds continuously into $\mathbb{S}_0(\Omega^*)$.*

Proof. Let $u \in H^1_0(\Omega)$ and let $\tilde{u}$ be the zero extension of u to all of $\mathbb{R}$. By definition

$$|\tilde{u}|^2_{\mathbb{S}(\Omega^*)} = \int_{\Omega^*}\int_{\Omega^*} c^\delta(|p-x|)\Big(\tilde{u}(p) - \tilde{u}(x)\Big)^2 \mathrm{d}p\mathrm{d}x.$$

By the integral MVT we know that

$$\tilde{u}(p) - \tilde{u}(x) = \int_x^p \tilde{u}'(t)\mathrm{d}t.$$

Therefore, through the parameterization $t(s) = x + s(p-x)$, we have that

$$|\tilde{u}|^2_{\mathbb{S}(\Omega^*)} = \int_{\Omega^*}\int_{\Omega^*} c^\delta(|p-x|)\left(\int_0^1 (p-x)\tilde{u}'(s)\mathrm{d}s\right)^2 \mathrm{d}p\mathrm{d}x.$$

Through an application of Hölder's inequality it follows that

$$|\tilde{u}|^2_{\mathbb{S}(\Omega^*)} \leq \int_{\Omega^*}\int_{\Omega^*} c^\delta(|p-x|)\left((p-x)^2\int_0^1 |\tilde{u}'(s)|^2\mathrm{d}s\right)\mathrm{d}p\mathrm{d}x.$$

Since $\tilde{u} \in H^1(\mathbb{R})$ and $|\tilde{u}|_{H^1(\mathbb{R})} = |u|_{H^1(\Omega)}$, we have that

$$|\tilde{u}|^2_{\mathbb{S}(\Omega^*)} \leq \int_{\Omega^*}\int_{\Omega^*} c^\delta(|p-x|)\Big((p-x)^2|u|_{H^1(\Omega)}\Big)\mathrm{d}p\mathrm{d}x.$$

Pulling the constant $|u|_{H^1(\Omega)}$ out of the integral and evaluating, we find that

$$|\tilde{u}|^2_{\mathbb{S}(\Omega^*)} \leq E^0\big|\Omega^*\big||u|^2_{H^1(\Omega)}$$

which proves this continuous embedding. $\square$

Proposition 2.11. *Let $u \in \mathbb{S}_0(\Omega^*)$. If $\left|u\right|_{\mathbb{S}(\Omega^*)} = 0$, then u is zero a.e. on Ω^*.*

Proof. By Proposition 2.2 part iii we know that u is constant a.e. The only function that is constant almost everywhere on Ω^* and vanishes on Γ is the zero function. Therefore, since $u \in \mathbb{S}_0(\Omega^*)$, it must be that $u = 0$ almost everywhere on Ω^*. □

Remark 2.12. $\mathbb{S}_0(\Omega^*)$ *is a closed linear subspace of* $\mathbb{S}(\Omega^*)$.

Proof. First we want to show $\mathbb{S}_0(\Omega^*)$ is a linear subspace. Let $u, v \in \mathbb{S}_0(\Omega^*)$ and $\alpha \in \mathbb{R}$. Since $u, v \in \mathbb{S}_0(\Omega^*) \subseteq \mathbb{S}(\Omega^*)$, we know that $u + v, \alpha u \in \mathbb{S}(\Omega^*)$. And since u, v vanish on Γ, adding them together or multiplying by a scalar will not change this property. Therefore, we have that $\mathbb{S}_0(\Omega^*)$ is a linear subspace of $\mathbb{S}(\Omega^*)$. If $u_n \in \mathbb{S}_0(\Omega^*)$ is a sequence that converges to $u \in \mathbb{S}(\Omega^*)$ with respect to the norm $||\cdot||_{\mathbb{S}(\Omega^*)}$, then it follows that u_n converges to u with respect to $||\cdot||_{L^2(\Omega^*)}$ and therefore it must vanish on Γ. Therefore $u \in \mathbb{S}_0(\Omega^*)$. □

Theorem 2.13. $\mathbb{S}_0(\Omega^*)$ *is complete with respect to the seminorm* $|\cdot|_{\mathbb{S}(\Omega^*)}$.

Proof. Assume that u_n is a Cauchy sequence in $\mathbb{S}_0(\Omega^*)$ with respect to the semi-norm. Since we have already shown that $\mathbb{S}(\Omega^*)$ is closed that there is a $u \in \mathbb{S}(\Omega^*)$ that is the limit with respect to the $||\cdot||_{\mathbb{S}(\Omega^*)}$. So we need to show that $u \in \mathbb{S}_0(\Omega^*)$. We know that u is the $L^2(\Omega^*)$ limit.

$$||u_n - u||_{L^2(\Gamma)} \leq ||u_n - u||_{L^2(\Omega')} \to 0 \quad \text{as } n \to \infty$$

which implies that $||u||_{L^2(\Gamma)} = 0$. This in turn implies that $u = 0$ in Γ. □

Therefore $(\mathbb{S}_0(\Omega^*), |\cdot|_{\mathbb{S}(\Omega^*)})$ is a **Hilbert space**.

Additionally, we would like to establish the analogous definition of weak solution and weak problem.

Definition 2.14. *The **weak formulation** of the BVP 2.2 is given by: find a* $u \in \mathbb{S}_0(\Omega^*)$ *such that*

$$\begin{aligned}\int_{\Omega^*}\int_{\Omega^*} & c^\delta(|p-x|)\big[w(p)-w(x)\big]\big[v(p)-v(x)\big]\mathrm{d}p\mathrm{d}x \\ &= \int_\Omega f(x)v(x)\mathrm{d}x + 2\int_\Omega v(x)\bigg(\int_{\Omega^*} c^\delta(|p-x|)\big[\tilde{g}(p)-\tilde{g}(x)\big]\mathrm{d}p\bigg)\mathrm{d}x\end{aligned} \tag{2.9}$$

holds for each $v \in \mathbb{S}_0(\Omega^*)$ *and* $\tilde{g}$ *is defined by equation 2.3 and* $w(x) = u(x) - \tilde{g}(x)$.

Definition 2.15. *We say that* $w \in \mathbb{S}_0(\Omega^*)$ *is a **weak solution** to the weak homogeneous problem 2.4 if*

$$\begin{aligned}\int_{\Omega^*}\int_{\Omega^*} & c^\delta(|p-x|)[w(p)-w(x)][v(p)-v(x)]\mathrm{d}p\mathrm{d}x \\ &= \int_\Omega f(x)v(x)\mathrm{d}x + 2\int_\Omega v(x)\int_{\Omega^*} c^\delta(|p-x|)[\tilde{g}(p)-\tilde{g}(x)]\mathrm{d}p\mathrm{d}x\end{aligned} \tag{2.10}$$

for all $v \in \mathbb{S}_0(\Omega^*)$, *where* $\tilde{g}$ *is defined by equation 2.3. We say that* $u(x) = w(x) + \tilde{g}(x)$ *is a **weak solution** to the nonhomogeneous weak BVP 2.2.*

Proposition 2.16. $b : \mathbb{S}_0(\Omega^*) \times \mathbb{S}_0(\Omega^*) \to \mathbb{R}$ *given by*

$$b(u,v) = \int_{\Omega^*}\int_{\Omega^*} c^\delta(|p-x|)[u(p)-u(x)][v(p)-v(x)]\mathrm{d}p\mathrm{d}x. \tag{2.11}$$

is a bounded bilinear form.

Proof. Billinear:

Let $u, v, w \in \mathbb{S}_0(\Omega^*)$ and $a \in \mathbb{R}$.

$$\begin{aligned} b(u+v, aw) &= \int_{\Omega^*}\int_{\Omega^*} c^\delta(|p-x|)[u(p)+v(p)-u(x)-v(x)][aw(p)-aw(x)]\mathrm{d}p\mathrm{d}x \\ &= a\int_{\Omega^*}\int_{\Omega^*} c^\delta(|p-x|)[u(p)+v(p)-u(x)-v(x)][w(p)-w(x)]\mathrm{d}p\mathrm{d}x \\ &= a\int_{\Omega^*}\int_{\Omega^*} c^\delta(|p-x|)[(u(p)-u(x))+(v(p)-v(x))][w(p)-w(x)]\mathrm{d}p\mathrm{d}x \\ &= ab(u,w) + ab(v,w). \end{aligned}$$

Boundedness: By Holders inequality

$$\begin{aligned} b(u,v) &= \int_{\Omega^*}\int_{\Omega^*} c^{\delta}(|p-x|)[u(p)-u(x)][v(p)-u(x)]\mathrm{d}p\mathrm{d}x \\ &\leq \left(\int_{\Omega^*}\int_{\Omega^*} c^{\delta}(|p-x|)[u(p)-u(x)]^2\mathrm{d}p\mathrm{d}x\right)^{1/2} \\ &\quad \left(\int_{\Omega^*}\int_{\Omega^*} c^{\delta}(|p-x|)[v(p)-v(x)]^2\mathrm{d}p\mathrm{d}x\right)^{1/2} \end{aligned}$$

□

Theorem 2.17. *If f is an element of $L^2(\Omega^*)$, then there exists a unique $u_f \in \mathbb{S}_0(\Omega^*)$ such that*

$$b(u_f, v) = (f, v)_{L^2(\Omega)} \quad \forall v \in \mathbb{S}_0(\Omega^*).$$

Proof. Let $F : \mathbb{S}_0(\Omega^*) \to \mathbb{R}$ be defined as

$$F(v) = \int_{\Omega} f(x)v(x)\mathrm{d}x \quad \forall v \in \mathbb{S}_0(\Omega^*)$$

Through an application of Hölder's inequality, it can be shown that F is a bounded linear operator. We have already shown that $b(\cdot,\cdot)$ is a bounded coercive bilinear form on $\mathbb{S}_0(\Omega^*) \times \mathbb{S}_0(\Omega^*)$. Therefore, by Lax-Millgram Theorem 1.19, we know there exists a unique $u_f \in \mathbb{S}_0(\Omega^*)$ such that

$$b(u_f, v) = (f, v)_{L^2(\Omega)} \; \forall v \in \mathbb{S}_0(\Omega^*).$$

. □

Part II

An Energy-based Blending Model

Chapter 3

Model Description

In 2012 [34], a model that blended the classical model and the peridynamic model at the energy density level was proposed and called the ‘morphing strategy’. This method was suggested to model material deformation where the material defect would occur away from the boundary of the material and deformation would be smooth near the boundary. Since the deformation would be smooth near the boundary, the authors decided that a classical model should be used there and the nonlocal model should only be used near the material defect. They decided, rather than a sharp transition between the two models, that the energy should morph from classical to peridynamic as you approached the defect. This means that there would be three distinct regions of the domain. There would be the region closest to the boundary, where the energy would be described using a classical differential equations model, a region (containing the material defect) where the energy would be described using a bond-based peridynamic model, and a morphing or blending region where the energy would be described as some combination of the two types of models. This is essentially the blended model that would would like to further analyze.

3.1 Motivating an energy-based blending model

Assume that we want to model a bounded homogeneous body that occupies reference configuration $\Omega \subset \mathbb{R}^n$ and that we know (through experimentation with this material) or expect that the deformation of this body will not be spatially smooth and that the region where this discontinuous spatial deformation occurs is away from the boundary of the material.

Using a nonlocal model, such as bond-based peridynamics, will allow the both continuous and discontinuous spatial deformation of the material to be accurately captured within the model. But knowing (or expecting) that the spatial deformation of the material is smooth near the boundary means that using a nonlocal model in that region is an unnecessary expense, and would require nonlocal boundary conditions. Therefore, a coupling of a nonlocal and a local model would be beneficial and could lead to lower computational expense. Thus, we motivate such a model, that blends classical elasticity and bond-based peridynamics, in the following section.

Knowing that the bond-based peridynamic model will effectively capture both discontinuous and continuous spatial deformations, we start with the pure bond-based peridynamic model. In this model we assume that material points can interact over a finite distance δ, which is called the material *horizon*. This length is chosen depending on the material that will be modeled and is fixed. The strength of the interaction between two material points will be dependent solely on the distance between the two points. This bond will not increase as the distance between the material points increases to δ, at which point the bond will break. Select a function $c^\delta : \mathbb{R}^n \to \mathbb{R}$ to represent this bond strength. For this function to be consistent with the desired properties of this bond, we assume

$$\begin{cases} c^\delta \text{ is a nonnegative, nonincreasing, radial function,} \\ supp(c^\delta) = B_\delta(\mathbf{0}), \\ \text{and } \displaystyle\int_{\mathbb{R}^n} c^\delta(|\mathbf{z}|)\mathbf{z}^2 \mathrm{d}\mathbf{z} = E^0. \end{cases} \tag{3.1}$$

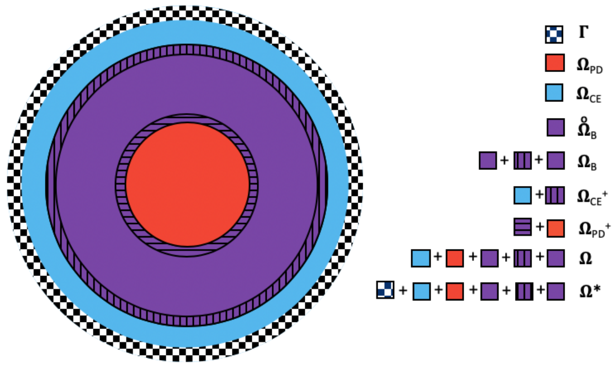

Figure 3.1: Simple Concentric Circular Subregions

Although this idea can be applied to more complicated domains, we will consider concentric circular regions. We will use the illustration in Figure 3.1 to help the reader keep track of the various subdomains that will be mentioned in this paper. We have three main regions to consider:

$\mathbf{\Omega_{PD}}$ - the region where the deformation is assumed to be discontinuous

$\mathbf{\Omega_{CE}}$ - the region where the deformation is assumed to be smooth but is away from Ω_{PD}

$\mathbf{\Omega_{B}}$ - the region between Ω_{CE} and Ω_{PD} where we will blend the two models.

Letting $\alpha : \mathbb{R}^n \to \mathbb{R}^n$ be the *blending function* (i.e. the function that describes how the transition from a purely CE model to a purely PD model will be accomplished), we require that α takes the value 1 throughout Ω_{PD}. In Ω_B, we will require the function to take values in $[0, 1]$ with the restrictions that: in the δ-layer closest to Ω_{CE} the blending function will take the value 0, in the δ-layer closest to Ω_{PD} the blending function takes the value one, and between those two regions in $\mathring{\Omega}_B$, $\alpha(x) \in (0, 1)$. Note that $\Omega^+_{PD} = \{x \in \Omega : d(x, \Omega_{PD}) < \delta\}$. Similarly $\Omega^+_{CE} = \{x \in \Omega : d(x, \Omega_{CE}) < \delta\}$. Therefore,

$$\alpha(\mathbf{x}) = \begin{cases} 1 & \mathbf{x} \in \Omega^+_{PD} \\ \in (0,1) & \mathbf{x} \in \mathring{\Omega}_B \\ 0 & \text{else.} \end{cases} \tag{3.2}$$

Notice that this implies for all material points $x \in \Omega^+_{CE}$, we have that $\alpha(x) = 0$. Starting with the PD strain energy density,

$$W^\delta_{PD}(\mathbf{u},\mathbf{x}) = \frac{1}{2}\int_\Omega c^\delta(|\mathbf{p}-\mathbf{x}|)\left[\big(\mathbf{u}(\mathbf{p})-\mathbf{u}(\mathbf{x})\big)\cdot\frac{\mathbf{p}-\mathbf{x}}{|\mathbf{p}-\mathbf{x}|}\right]^2 \mathrm{d}\mathbf{p}$$

we add and subtract

$$\frac{1}{2}\int_\Omega c^\delta(|\mathbf{p}-\mathbf{x}|)\left(\frac{\alpha(\mathbf{p})+\alpha(\mathbf{x})}{2}\right)\left[\big(\mathbf{u}(\mathbf{p})-\mathbf{u}(\mathbf{x})\big)\cdot\frac{\mathbf{p}-\mathbf{x}}{|\mathbf{p}-\mathbf{x}|}\right]^2 \mathrm{d}\mathbf{p}.$$

Next use the approximation

$$\big(\mathbf{u}(\mathbf{p})-\mathbf{u}(\mathbf{x})\big)\cdot\big(\mathbf{p}-\mathbf{x}\big) \approx \nabla\mathbf{u}(\mathbf{x})(\mathbf{p}-\mathbf{x})\cdot(\mathbf{p}-\mathbf{x}) \tag{3.3}$$

in the subtracted term to get the *first attempt* at strain energy density for the blended model

$$\begin{aligned} W^\delta_B(\mathbf{u},\mathbf{x}) =& \frac{1}{2}\int_\Omega c^\delta(|\mathbf{p}-\mathbf{x}|)\left(1-\frac{\alpha(\mathbf{p})+\alpha(\mathbf{x})}{2}\right)\frac{1}{|\mathbf{p}-\mathbf{x}|^2}\Big[\nabla\mathbf{u}(\mathbf{x})(\mathbf{p}-\mathbf{x})\cdot(\mathbf{p}-\mathbf{x})\Big]^2 \mathrm{d}\mathbf{p} \\ &+ \frac{1}{2}\int_\Omega c^\delta(|\mathbf{p}-\mathbf{x}|)\left(\frac{\alpha(\mathbf{p})+\alpha(\mathbf{x})}{2}\right)\left[\big(\mathbf{u}(\mathbf{p})-\mathbf{u}(\mathbf{x})\big)\cdot\frac{\mathbf{p}-\mathbf{x}}{|\mathbf{p}-\mathbf{x}|}\right]^2 \mathrm{d}\mathbf{p}. \end{aligned}$$

But recalling the goal of having the model be purely classical near the boundary, the strain energy density is modified so that the integration with respect to $\mathbf{p}$ in the local term is over an entire ball, $B_\delta(\mathbf{x})$. This yields

$$\begin{aligned} W^\delta_B(\mathbf{u},\mathbf{x}) =& \frac{1}{2}\int_{B_\delta(\mathbf{x})} c^\delta(|\mathbf{p}-\mathbf{x}|)\left(1-\frac{\alpha(\mathbf{p})+\alpha(\mathbf{x})}{2}\right)\frac{1}{|\mathbf{p}-\mathbf{x}|^2}\Big[\nabla\mathbf{u}(\mathbf{x})(\mathbf{p}-\mathbf{x})\cdot(\mathbf{p}-\mathbf{x})\Big]^2 \mathrm{d}\mathbf{p} \\ &+ \frac{1}{2}\int_\Omega c^\delta(|\mathbf{p}-\mathbf{x}|)\left(\frac{\alpha(\mathbf{p})+\alpha(\mathbf{x})}{2}\right)\left[\big(\mathbf{u}(\mathbf{p})-\mathbf{u}(\mathbf{x})\big)\cdot\frac{\mathbf{p}-\mathbf{x}}{|\mathbf{p}-\mathbf{x}|}\right]^2 \mathrm{d}\mathbf{p}. \end{aligned} \tag{3.4}$$

We define the strain energy density of the blended model to be equation 3.4, which can be equivalently stated, due to the nature of the blending function α,

$$\begin{aligned}W_B^\delta(\mathbf{u},\mathbf{x}) =&\frac{1}{2}\int_{B_\delta(\mathbf{x})} c^\delta(|\mathbf{p}-\mathbf{x}|)\left(1-\frac{\alpha(\mathbf{p})+\alpha(\mathbf{x})}{2}\right)\frac{1}{|\mathbf{p}-\mathbf{x}|^2}\Big[\nabla\mathbf{u}(\mathbf{x})(\mathbf{p}-\mathbf{x})\cdot(\mathbf{p}-\mathbf{x})\Big]^2 \mathrm{d}\mathbf{p}\\ &+\frac{1}{2}\int_{B_\delta(\mathbf{x})} c^\delta(|\mathbf{p}-\mathbf{x}|)\left(\frac{\alpha(\mathbf{p})+\alpha(\mathbf{x})}{2}\right)\left[\Big(\mathbf{u}(\mathbf{p})-\mathbf{u}(\mathbf{x})\Big)\cdot\frac{\mathbf{p}-\mathbf{x}}{|\mathbf{p}-\mathbf{x}|}\right]^2 \mathrm{d}\mathbf{p}.\end{aligned}$$

Observe that

1. if $\mathbf{x}\in\Omega_{CE}$, then $W_B^\delta(\mathbf{u},\mathbf{x})$ reduces the classical strain energy density

$$\begin{aligned}W_B^\delta(\mathbf{u},\mathbf{x}) &= \frac{1}{2}\int_{B_\delta(\mathbf{x})} c^\delta(|\mathbf{p}-\mathbf{x}|)\frac{1}{|\mathbf{p}-\mathbf{x}|^2}\Big[\nabla\mathbf{u}(\mathbf{x})(\mathbf{p}-\mathbf{x})\cdot(\mathbf{p}-\mathbf{x})\Big]^2 \mathrm{d}\mathbf{p}\\ &= \frac{E^0}{2}\left\{2|\mathcal{E}(\mathbf{u}(\mathbf{x}))|^2+|\mathrm{div}\mathbf{u}(\mathbf{x})|^2\right\}\end{aligned}$$

   where $\mathcal{E}(\mathbf{u}(\mathbf{x}))$ is the strain tensor $\mathcal{E}(\mathbf{u}(\mathbf{x}))=\frac{1}{2}(\nabla\mathbf{u}(\mathbf{x})+\nabla\mathbf{u}(\mathbf{x})^T)$.

2. if $\mathbf{x}\in\Omega_{PD}$, then $W_B^\delta(\mathbf{u},\mathbf{x})$ reduces to the peridynamic strain energy density

$$W_B^\delta(\mathbf{u},\mathbf{x}) = \frac{1}{2}\int_{\Omega} c^\delta(|\mathbf{p}-\mathbf{x}|)\left[\Big(\mathbf{u}(\mathbf{p})-\mathbf{u}(\mathbf{x})\Big)\cdot\frac{\mathbf{p}-\mathbf{x}}{|\mathbf{p}-\mathbf{x}|}\right]^2 \mathrm{d}\mathbf{p}.$$

Moreover, for smooth vector fields $\mathbf{u}$, in the event nonlocality vanishes the blended energy approaches the classical strain energy density.

Proposition 3.1. *Suppose that $c^\delta(|\mathbf{z}|)=\delta^{-n-2}c\left(\frac{|\mathbf{z}|}{\delta}\right)$, for a given function $c>0$ that is supported on the unit ball and with finite second moment. For a twice differentiable $\mathbf{u}$, the blended strain energy density converges to the classical strain energy density as δ approaches 0, i.e.*

$$\lim_{\delta\to 0} W_B^\delta(\mathbf{u},\mathbf{x}) = \frac{E^0}{2}\left\{2|\mathcal{E}(\mathbf{u}(\mathbf{x}))|^2+|\mathrm{div}\,\mathbf{u}(\mathbf{x})|^2\right\}.$$

where $\mathcal{E}(\mathbf{u}(\mathbf{x}))$ is the strain tensor $\mathcal{E}(\mathbf{u}(\mathbf{x}))=\frac{1}{2}(\nabla\mathbf{u}(\mathbf{x})+\nabla\mathbf{u}(\mathbf{x})^T)$.

Proof. For $\mathbf{x} \in \Omega$, we may rewrite $W_B^\delta(\mathbf{u}, \mathbf{x})$ in a slightly different form as

$$
\begin{aligned}
W_B^\delta(\mathbf{u}, \mathbf{x}) =& \frac{1}{2} \int_\Omega c^\delta(|\mathbf{p}-\mathbf{x}|) \frac{1}{|\mathbf{p}-\mathbf{x}|^2} \Big[\nabla \mathbf{u}(\mathbf{x})(\mathbf{p}-\mathbf{x}) \cdot (\mathbf{p}-\mathbf{x}) \Big]^2 \mathrm{d}\mathbf{p} \\
&- \frac{1}{2} \int_\Omega c^\delta(|\mathbf{p}-\mathbf{x}|) \left(\frac{\alpha(\mathbf{p}) + \alpha(\mathbf{x})}{2} \right) \frac{1}{|\mathbf{p}-\mathbf{x}|^2} \Big[\nabla \mathbf{u}(\mathbf{x})(\mathbf{p}-\mathbf{x}) \cdot (\mathbf{p}-\mathbf{x}) \Big]^2 \mathrm{d}\mathbf{p} \\
&+ \frac{1}{2} \int_\Omega c^\delta(|\mathbf{p}-\mathbf{x}|) \left(\frac{\alpha(\mathbf{p}) + \alpha(\mathbf{x})}{2} \right) \Big[\big(\mathbf{u}(\mathbf{p}) - \mathbf{u}(\mathbf{x})\big) \cdot \frac{\mathbf{p}-\mathbf{x}}{|\mathbf{p}-\mathbf{x}|} \Big]^2 \mathrm{d}\mathbf{p}.
\end{aligned}
$$

We now choose $\delta > 0$ sufficiency small so that $B_\delta(\mathbf{x}) \subset \Omega$. Then first term can be simplified as

$$
\begin{aligned}
&\frac{1}{2} \int_\Omega c^\delta(|\mathbf{p}-\mathbf{x}|) \frac{1}{|\mathbf{p}-\mathbf{x}|^2} \Big[\nabla \mathbf{u}(\mathbf{x})(\mathbf{p}-\mathbf{x}) \cdot (\mathbf{p}-\mathbf{x}) \Big]^2 \mathrm{d}\mathbf{p} \\
&= \frac{1}{2} \int_{B_\delta(\mathbf{0})} c^\delta(|\mathbf{p}|) \frac{1}{|\mathbf{p}|^2} |\nabla \mathbf{u}(\mathbf{x}) \mathbf{p} \cdot \mathbf{p}|^2 \mathrm{d}\mathbf{p} \\
&= \frac{E^0}{2} \left\{ 2|\mathcal{E}(\mathbf{u}(\mathbf{x}))|^2 + |\mathrm{div}(\mathbf{u}((\mathbf{x})|^2 \right\},
\end{aligned}
$$

where we used the second moment condition. What remain is to show that the remaining terms coverage to zero as $\delta \to 0$. To that end, since $\mathbf{u}$ is assumed to be differentiable, we may use Taylor expansion around $\mathbf{x}$ to obtain a continuous vector function $\mathbf{h}$ such that $\dfrac{\mathbf{h}(\mathbf{x}, \mathbf{z})}{|\mathbf{z}|}$ is a bounded function and

$$
\mathbf{u}(\mathbf{p}) = \mathbf{u}(\mathbf{x}) + \nabla \mathbf{u}(\mathbf{x})(\mathbf{p}-\mathbf{x}) + \mathbf{h}(\mathbf{x}, \mathbf{p}-\mathbf{x}), \quad \text{where } \lim_{\mathbf{p} \to \mathbf{x}} \frac{\mathbf{h}(\mathbf{x}, \mathbf{p}-\mathbf{x})}{|\mathbf{p}-\mathbf{x}|} = 0
$$

Therefore, for sufficiently small $\delta > 0$ we have

$$
\begin{aligned}
&|W_B^\delta(\mathbf{u}, \mathbf{x}) - \frac{E^0}{2} \left\{ 2|\mathcal{E}(\mathbf{u}(\mathbf{x}))|^2 + |\mathrm{div}\mathbf{u}(\mathbf{x})|^2 \right\} | \\
&\leq \frac{1}{2} \int_\Omega c^\delta(|\mathbf{p}-\mathbf{x}|) |\mathbf{p}-\mathbf{x}|^2 \left| \Big[\frac{\mathbf{u}(\mathbf{p}) - \mathbf{u}(\mathbf{x})}{|\mathbf{p}-\mathbf{x}|} \cdot \frac{\mathbf{p}-\mathbf{x}}{|\mathbf{p}-\mathbf{x}|} \Big]^2 - \Big[\nabla \mathbf{u}(\mathbf{x}) \frac{\mathbf{p}-\mathbf{x}}{|\mathbf{p}-\mathbf{x}|} \cdot \frac{\mathbf{p}-\mathbf{x}}{|\mathbf{p}-\mathbf{x}|} \Big]^2 \right| \mathrm{d}\mathbf{p} \\
&= \frac{1}{2} \int_\Omega c^\delta(|\mathbf{p}-\mathbf{x}|) |\mathbf{p}-\mathbf{x}|^2 \left(2|\nabla \mathbf{u}(\mathbf{x})| \frac{|\mathbf{h}(\mathbf{x}, \mathbf{p}-\mathbf{x})|}{|\mathbf{p}-\mathbf{x}|} + \frac{|\mathbf{h}(\mathbf{x}, \mathbf{p}-\mathbf{x})|^2}{|\mathbf{p}-\mathbf{x}|^2} \right) \mathrm{d}\mathbf{p} \\
&= \frac{1}{2} \int_{B_1(\mathbf{0})} c(|\mathbf{z}|) |\mathbf{z}|^2 \left(2|\nabla \mathbf{u}(\mathbf{x})| \frac{|\mathbf{h}(\mathbf{x}, \delta\mathbf{z})|}{|\delta \mathbf{z}|} + \frac{|\mathbf{h}(\mathbf{x}, \delta\mathbf{z})|^2}{|\delta \mathbf{z}|^2} \right) \mathrm{d}\mathbf{z}
\end{aligned}
$$

One can now use Lebesgue Dominated Convergence Theorem to conclude that as $\delta \to 0$, the last term approaches 0, completing the proof. $\square$

3.2 Bounding the difference between the PD and the blended strain energy densities

The proof of the following proposition was inspired by the analysis done in [44] on the force-based blended model.

Proposition 3.2. *For* $\mathbf{u}$ *that is three times differentiable, the quantity* $\left|W^\delta_{PD}(\mathbf{u},\mathbf{x}) - W^\delta_B(\mathbf{u},\mathbf{x})\right|$ *can be bounded by a function* $Q : \Omega \to \mathbb{R}$ *that depends on the dimension of the space* N*,* δ*,* α *and* E^0*.*

Proof. For $\mathbf{x} \in \Omega_{PD}$ we have that both $\alpha(\mathbf{x})$ and $\alpha(\mathbf{p})$ are 1. Therefore, for a given solution $\mathbf{u}$,

$$\left|W^\delta_{PD}(\mathbf{u},\mathbf{x}) - W^\delta_B(\mathbf{u},\mathbf{x})\right| = 0 \text{ when } \mathbf{x} \in \Omega_{PD}.$$

To determine the difference in $\big(\Omega \setminus \Omega_{PD}\big)$, recall that by assumption $\mathbf{u}$ is a three times differentiable spacial deformation, therefore in $\big(\Omega \setminus \Omega_{PD}\big)$ it is smooth enough to use a Taylor approximation. Use a Taylor expansion to represent the difference $\big(\mathbf{u}(\mathbf{p}) - \mathbf{u}(\mathbf{x})\big)$ in the peridynamic strain energy density.

The PD strain energy density can be written as

$$\begin{aligned} W^\delta_{PD}(\mathbf{u},\mathbf{x}) =& \frac{1}{2}\int_{B_\delta(\mathbf{x})} c^\delta(|\mathbf{p}-\mathbf{x}|)\left(1 - \frac{\alpha(\mathbf{p}) + \alpha(\mathbf{x})}{2}\right)\frac{1}{|\mathbf{p}-\mathbf{x}|^2}\Big[\big(\mathbf{u}(\mathbf{p}) - \mathbf{u}(\mathbf{x})\big)\cdot(\mathbf{p}-\mathbf{x})\Big]^2 \mathrm{d}\mathbf{p} \\ &+ \frac{1}{2}\int_{B_\delta(\mathbf{x})} c^\delta(|\mathbf{p}-\mathbf{x}|)\left(\frac{\alpha(\mathbf{p}) + \alpha(\mathbf{x})}{2}\right)\left[\big(\mathbf{u}(\mathbf{p}) - \mathbf{u}(\mathbf{x})\big)\cdot\frac{\mathbf{p}-\mathbf{x}}{|\mathbf{p}-\mathbf{x}|}\right]^2 \mathrm{d}\mathbf{p}. \end{aligned}$$

Let $\boldsymbol{\xi} = \mathbf{p} - \mathbf{x}$. Using Einstein's notation we expand

$$u_i(\mathbf{x}+\boldsymbol{\xi}) - u_i(\mathbf{x}) = \frac{\partial u_i}{\partial x_j}(\mathbf{x})\xi_j + \frac{\partial^2 u_i}{\partial x_j \partial x_k}(\mathbf{x})\frac{\xi_j\xi_k}{2} + \frac{\partial^3 u_i}{\partial x_j \partial x_k \partial x_l}(\mathbf{z})\frac{\xi_j\xi_k\xi_l}{6}$$

where $\mathbf{z}$ is on the line segment connection $\mathbf{x}$ and $\mathbf{x}+\boldsymbol{\xi}$. Therefore, through expanding the expression

$$\begin{aligned}
((u_i(\mathbf{x}+\boldsymbol{\xi}) - u_i(\mathbf{x}))\xi_i)^2 = &\Bigg(\left[\xi_k\frac{\partial u_i}{\partial x_k}(\mathbf{x}) + \frac{\xi_k\xi_m}{2}\frac{\partial^2 u_i}{\partial x_k\partial x_m}(\mathbf{x}) + \frac{\xi_m\xi_k\xi_n}{6}\frac{\partial^3 u_i}{\partial x_k\partial x_m\partial x_n}(\mathbf{z})\right]\xi_i \\
&\times\left[\xi_l\frac{\partial u_j}{\partial x_l}(\mathbf{x}) + \frac{\xi_l\xi_q}{2}\frac{\partial^2 u_j}{\partial x_l\partial x_q}(\mathbf{x}) + \frac{\xi_l\xi_q\xi_p}{6}\frac{\partial^3 u_j}{\partial x_l\partial x_q\partial x_p}(\mathbf{z})\right]\xi_j\Bigg) \\
=&(\xi_i\xi_j\xi_k\xi_l)\left[\frac{\partial u_i}{\partial x_k}(\mathbf{x})\frac{\partial u_j}{\partial x_l}(\mathbf{x}) + \xi_q\frac{\partial u_i}{\partial x_k}(\mathbf{x})\frac{\partial^2 u_j}{\partial x_l\partial x_q}(\mathbf{x})\right. \\
&+\frac{\xi_q\xi_p}{3}\frac{\partial u_i}{\partial x_k}(\mathbf{x})\frac{\partial^3 u_j}{\partial x_l\partial x_q\partial x_p}(\mathbf{z}) \\
&+\frac{\xi_m\xi_q}{4}\frac{\partial^2 u_i}{\partial x_k\partial x_m}(\mathbf{x})\frac{\partial^2 u_j}{\partial x_l\partial x_q}(\mathbf{x}) \\
&+\frac{\xi_m\xi_q\xi_p}{6}\frac{\partial^2 u_i}{\partial x_k\partial x_m}(\mathbf{x})\frac{\partial^3 u_j}{\partial x_l\partial x_q\partial x_p}(\mathbf{z}) \\
&\left.+\frac{\xi_m\xi_n\xi_q\xi_p}{36}\frac{\partial^3 u_i}{\partial x_k\partial x_m\partial x_n}(\mathbf{z})\frac{\partial^3 u_j}{\partial x_l\partial x_q\partial x_p}(\mathbf{z})\right].
\end{aligned}$$

Plugging this into the term of the peridynamic strain energy density that contains $\left(1 - \dfrac{\alpha(\mathbf{x}) + \alpha(\mathbf{x}+\boldsymbol{\xi})}{2}\right)$ and letting

$$E := E(\mathbf{x}) = \Big|W_{PD}(\mathbf{u},\mathbf{x}) - W_B(\mathbf{u},\mathbf{x})\Big|$$

we have

$$\begin{aligned}
E = \Bigg|\frac{1}{2}\int_{B_\delta(\mathbf{0})} &c^\delta(|\boldsymbol{\xi}|)\frac{1}{|\boldsymbol{\xi}|^2}\left[1 - \frac{\alpha(\mathbf{x}) + \alpha(\mathbf{x}+\boldsymbol{\xi})}{2}\right](\xi_i\xi_j\xi_k\xi_l)\Bigg(\xi_q\frac{\partial u_i}{\partial x_k}(\mathbf{x})\frac{\partial^2 u_j}{\partial x_l\partial x_q}(\mathbf{x}) \\
&+\frac{\xi_q\xi_p}{3}\frac{\partial u_i}{\partial x_k}(\mathbf{x})\frac{\partial^3 u_j}{\partial x_l\partial x_q\partial x_p}(\mathbf{z}) + \frac{\xi_m\xi_q}{4}\frac{\partial^2 u_i}{\partial x_k\partial x_m}(\mathbf{x})\frac{\partial^2 u_j}{\partial x_l\partial x_q}(\mathbf{x}) \\
&+\frac{\xi_m\xi_q\xi_p}{6}\frac{\partial^2 u_i}{\partial x_k\partial x_m}(\mathbf{x})\frac{\partial^3 u_j}{\partial x_l\partial x_q\partial x_p}(\mathbf{z}) \\
&+\frac{\xi_m\xi_n\xi_q\xi_p}{36}\frac{\partial^3 u_i}{\partial x_k\partial x_m\partial x_n}(\mathbf{z})\frac{\partial^3 u_j}{\partial x_l\partial x_q\partial x_p}(\mathbf{z})\Bigg)\,\mathrm{d}\boldsymbol{\xi}\Bigg|.
\end{aligned}$$

Splitting $\left(1-\dfrac{\alpha(\mathbf{x})+\alpha(\mathbf{x}+\boldsymbol{\xi})}{2}\right)$ into $\left(1-\dfrac{\alpha(\mathbf{x})}{2}\right)+\left(\dfrac{\alpha(\mathbf{x}+\boldsymbol{\xi})}{2}\right)$ and separating the integrals give us

$$
\begin{aligned}
E \leq & \left|\frac{1}{2}\int_{B_\delta(\mathbf{0})} c^\delta(|\boldsymbol{\xi}|)\frac{1}{|\boldsymbol{\xi}|^2}\left[1-\frac{\alpha(\mathbf{x})}{2}\right](\xi_i\xi_j\xi_k\xi_l)\left(\xi_q\frac{\partial u_i}{\partial x_k}(\mathbf{x})\frac{\partial^2 u_j}{\partial x_l \partial x_q}(\mathbf{x})\right.\right. \\
&\quad +\frac{\xi_q\xi_p}{3}\frac{\partial u_i}{\partial x_k}(\mathbf{x})\frac{\partial^3 u_j}{\partial x_l\partial x_q\partial x_p}(\mathbf{z})+\frac{\xi_m\xi_q}{4}\frac{\partial^2 u_i}{\partial x_k\partial x_m}(\mathbf{x})\frac{\partial^2 u_j}{\partial x_l\partial x_q}(\mathbf{x}) \\
&\quad +\frac{\xi_m\xi_q\xi_p}{6}\frac{\partial^2 u_i}{\partial x_k\partial x_m}(\mathbf{x})\frac{\partial^3 u_j}{\partial x_l\partial x_q\partial x_p}(\mathbf{z}) \\
&\quad \left.\left.+\frac{\xi_m\xi_n\xi_q\xi_p}{36}\frac{\partial^3 u_i}{\partial x_k\partial x_m\partial x_n}(\mathbf{z})\frac{\partial^3 u_j}{\partial x_l\partial x_q\partial x_p}(\mathbf{z})\right)\mathrm{d}\boldsymbol{\xi}\right| \\
& +\left|\frac{1}{2}\int_{B_\delta(\mathbf{0})} c^\delta(|\boldsymbol{\xi}|)\frac{1}{|\boldsymbol{\xi}|^2}\left[\frac{\alpha(\mathbf{x}+\boldsymbol{\xi})}{2}\right](\xi_i\xi_j\xi_k\xi_l)\left(\xi_q\frac{\partial u_i}{\partial x_k}(\mathbf{x})\frac{\partial^2 u_j}{\partial x_l \partial x_q}(\mathbf{x})\right.\right. \\
&\quad +\frac{\xi_q\xi_p}{3}\frac{\partial u_i}{\partial x_k}(\mathbf{x})\frac{\partial^3 u_j}{\partial x_l\partial x_q\partial x_p}(\mathbf{z})+\frac{\xi_m\xi_q}{4}\frac{\partial^2 u_i}{\partial x_k\partial x_m}(\mathbf{x})\frac{\partial^2 u_j}{\partial x_l\partial x_q}(\mathbf{x}) \\
&\quad +\frac{\xi_m\xi_q\xi_p}{6}\frac{\partial^2 u_i}{\partial x_k\partial x_m}(\mathbf{x})\frac{\partial^3 u_j}{\partial x_l\partial x_q\partial x_p}(\mathbf{z}) \\
&\quad \left.\left.+\frac{\xi_m\xi_n\xi_q\xi_p}{36}\frac{\partial^3 u_i}{\partial x_k\partial x_m\partial x_n}(\mathbf{z})\frac{\partial^3 u_j}{\partial x_l\partial x_q\partial x_p}(\mathbf{z})\right)\mathrm{d}\boldsymbol{\xi}\right|
\end{aligned}
$$

Define E_1 to be term with $\left(1-\dfrac{\alpha(\mathbf{x})}{2}\right)$ and E_2 to be the term with $\left(\dfrac{\alpha(\mathbf{x}+\boldsymbol{\xi})}{2}\right)$. We will consider these terms separately for clarity. If we first consider $E_1(\mathbf{u},\mathbf{x})$ and bring the absolute value into the integral

$$
\begin{aligned}
E_1 \leq & \frac{1}{2}\int_{B_\delta(\mathbf{0})} c^\delta(|\boldsymbol{\xi}|)\frac{1}{|\boldsymbol{\xi}|^2}\left[1-\frac{\alpha(\mathbf{x})}{2}\right]\left|\xi_i\xi_j\xi_k\xi_l\right|\left|\xi_q\frac{\partial u_i}{\partial x_k}(\mathbf{x})\frac{\partial^2 u_j}{\partial x_l \partial x_q}(\mathbf{x})\right. \\
&\quad +\frac{\xi_q\xi_p}{3}\frac{\partial u_i}{\partial x_k}(\mathbf{x})\frac{\partial^3 u_j}{\partial x_l\partial x_q\partial x_p}(\mathbf{z})+\frac{\xi_m\xi_q}{4}\frac{\partial^2 u_i}{\partial x_k\partial x_m}(\mathbf{x})\frac{\partial^2 u_j}{\partial x_l\partial x_q}(\mathbf{x}) \\
&\quad +\frac{\xi_m\xi_q\xi_p}{6}\frac{\partial^2 u_i}{\partial x_k\partial x_m}(\mathbf{x})\frac{\partial^3 u_j}{\partial x_l\partial x_q\partial x_p}(\mathbf{z}) \\
&\quad \left.+\frac{\xi_m\xi_n\xi_q\xi_p}{36}\frac{\partial^3 u_i}{\partial x_k\partial x_m\partial x_n}(\mathbf{z})\frac{\partial^3 u_j}{\partial x_l\partial x_q\partial x_p}(\mathbf{z})\right|\mathrm{d}\boldsymbol{\xi}.
\end{aligned}
$$

Apply the triangle inequality,

$$
\begin{aligned}
E_1 \leq & \frac{1}{2}\int_{B_\delta(\mathbf{0})} c^\delta(|\boldsymbol{\xi}|)\frac{1}{|\boldsymbol{\xi}|^2}\left[1-\frac{\alpha(\mathbf{x})}{2}\right]\left|\xi_i\xi_j\xi_k\xi_l\right|\left|\xi_q\frac{\partial u_i}{\partial x_k}(\mathbf{x})\frac{\partial^2 u_j}{\partial x_l\partial x_q}(\mathbf{x})\right|\mathrm{d}\boldsymbol{\xi} \\
& + \frac{1}{6}\int_{B_\delta(\mathbf{0})} c^\delta(|\boldsymbol{\xi}|)\frac{1}{|\boldsymbol{\xi}|^2}\left[1-\frac{\alpha(\mathbf{x})}{2}\right]\left|\xi_i\xi_j\xi_k\xi_l\right|\left|\xi_q\xi_p\frac{\partial u_i}{\partial x_k}(\mathbf{x})\frac{\partial^3 u_j}{\partial x_l\partial x_q\partial x_p}(\mathbf{z})\right|\mathrm{d}\boldsymbol{\xi} \\
& + \frac{1}{8}\int_{B_\delta(\mathbf{0})} c^\delta(|\boldsymbol{\xi}|)\frac{1}{|\boldsymbol{\xi}|^2}\left[1-\frac{\alpha(\mathbf{x})}{2}\right]\left|\xi_i\xi_j\xi_k\xi_l\right|\left|\xi_m\xi_q\frac{\partial^2 u_i}{\partial x_k\partial x_m}(\mathbf{x})\frac{\partial^2 u_j}{\partial x_l\partial x_q}(\mathbf{x})\right|\mathrm{d}\boldsymbol{\xi} \\
& + \frac{1}{12}\int_{B_\delta(\mathbf{0})} c^\delta(|\boldsymbol{\xi}|)\frac{1}{|\boldsymbol{\xi}|^2}\left[1-\frac{\alpha(\mathbf{x})}{2}\right]\left|\xi_i\xi_j\xi_k\xi_l\right|\left|\xi_m\xi_q\xi_p\frac{\partial^2 u_i}{\partial x_k\partial x_m}(\mathbf{x})\frac{\partial^3 u_j}{\partial x_l\partial x_q\partial x_p}(\mathbf{z})\right|\mathrm{d}\boldsymbol{\xi} \\
& + \frac{1}{72}\int_{B_\delta(\mathbf{0})} c^\delta(|\boldsymbol{\xi}|)\frac{1}{|\boldsymbol{\xi}|^2}\left[1-\frac{\alpha(\mathbf{x})}{2}\right]\left|\xi_i\xi_j\xi_k\xi_l\right| \\
& \qquad \times\left|\xi_m\xi_n\xi_q\xi_p\frac{\partial^3 u_i}{\partial x_k\partial x_m\partial x_n}(\mathbf{z})\frac{\partial^3 u_j}{\partial x_l\partial x_q\partial x_p}(\mathbf{z})\right|\mathrm{d}\boldsymbol{\xi}.
\end{aligned}
$$

Bounding each $|\xi_t|$ by $|\boldsymbol{\xi}|$ and summing (because above we are using Einstein's notation)

$$
\begin{aligned}
E_1 \leq & \frac{N^5}{2}\int_{B_\delta(\mathbf{0})} c^\delta(|\boldsymbol{\xi}|)\frac{1}{|\boldsymbol{\xi}|^2}\left[1-\frac{\alpha(\mathbf{x})}{2}\right]|\boldsymbol{\xi}|^5\left|\frac{\partial u_i}{\partial x_k}(\mathbf{x})\frac{\partial^2 u_j}{\partial x_l\partial x_q}(\mathbf{x})\right|\mathrm{d}\boldsymbol{\xi} \\
& + \frac{N^6}{6}\int_{B_\delta(\mathbf{0})} c^\delta(|\boldsymbol{\xi}|)\frac{1}{|\boldsymbol{\xi}|^2}\left[1-\frac{\alpha(\mathbf{x})}{2}\right]|\boldsymbol{\xi}|^6\left|\frac{\partial u_i}{\partial x_k}(\mathbf{x})\frac{\partial^3 u_j}{\partial x_l\partial x_q\partial x_p}(\mathbf{z})\right|\mathrm{d}\boldsymbol{\xi} \\
& + \frac{N^6}{8}\int_{B_\delta(\mathbf{0})} c^\delta(|\boldsymbol{\xi}|)\frac{1}{|\boldsymbol{\xi}|^2}\left[1-\frac{\alpha(\mathbf{x})}{2}\right]|\boldsymbol{\xi}|^6\left|\frac{\partial^2 u_i}{\partial x_k\partial x_m}(\mathbf{x})\frac{\partial^2 u_j}{\partial x_l\partial x_q}(\mathbf{x})\right|\mathrm{d}\boldsymbol{\xi} \\
& + \frac{N^7}{12}\int_{B_\delta(\mathbf{0})} c^\delta(|\boldsymbol{\xi}|)\frac{1}{|\boldsymbol{\xi}|^2}\left[1-\frac{\alpha(\mathbf{x})}{2}\right]|\boldsymbol{\xi}|^7\left|\frac{\partial^2 u_i}{\partial x_k\partial x_m}(\mathbf{x})\frac{\partial^3 u_j}{\partial x_l\partial x_q\partial x_p}(\mathbf{z})\right|\mathrm{d}\boldsymbol{\xi} \\
& + \frac{N^8}{72}\int_{B_\delta(\mathbf{0})} c^\delta(|\boldsymbol{\xi}|)\frac{1}{|\boldsymbol{\xi}|^2}\left[1-\frac{\alpha(\mathbf{x})}{2}\right]|\boldsymbol{\xi}|^8\left|\frac{\partial^3 u_i}{\partial x_k\partial x_m\partial x_n}(\mathbf{z})\frac{\partial^3 u_j}{\partial x_l\partial x_q\partial x_p}(\mathbf{z})\right|\mathrm{d}\boldsymbol{\xi}.
\end{aligned}
$$

For $a,b,c,d = 1,\ldots,N$ let

$$
A(\mathbf{x}) := \max_{a,b}\left|\frac{\partial u_a(\mathbf{x})}{\partial x_b}\right| \qquad B(\mathbf{x}) := \max_{a,b,c}\left|\frac{\partial^2 u_a(\mathbf{x})}{\partial x_b\partial x_c}\right| \qquad C(\mathbf{x}) := \max_{\mathbf{z}\in B_\delta(\mathbf{x})}\left\{\max_{a,b,c,d}\left|\frac{\partial^3 u_a(\mathbf{z})}{\partial x_b\partial x_c\partial x_d}\right|\right\}.
$$

Using these bounds

$$
\begin{aligned}
E_1 \leq & \frac{N^5}{2}\left[1-\frac{\alpha(\mathbf{x})}{2}\right] A(\mathbf{x})B(\mathbf{x}) \int_{B_\delta(\mathbf{0})} c^\delta(|\boldsymbol{\xi}|)\left|\boldsymbol{\xi}\right|^3 \mathrm{d}\boldsymbol{\xi} \\
& + \frac{N^6}{6}\left[1-\frac{\alpha(\mathbf{x})}{2}\right] A(\mathbf{x})C(\mathbf{x}) \int_{B_\delta(\mathbf{0})} c^\delta(|\boldsymbol{\xi}|)\left|\boldsymbol{\xi}\right|^4 \mathrm{d}\boldsymbol{\xi} \\
& + \frac{N^6}{8}\left[1-\frac{\alpha(\mathbf{x})}{2}\right] B(\mathbf{x})B(\mathbf{x}) \int_{B_\delta(\mathbf{0})} c^\delta(|\boldsymbol{\xi}|)\left|\boldsymbol{\xi}\right|^4 \mathrm{d}\boldsymbol{\xi} \\
& + \frac{N^7}{12}\left[1-\frac{\alpha(\mathbf{x})}{2}\right] B(\mathbf{x})C(\mathbf{x}) \int_{B_\delta(\mathbf{0})} c^\delta(|\boldsymbol{\xi}|)\left|\boldsymbol{\xi}\right|^5 \mathrm{d}\boldsymbol{\xi} \\
& + \frac{N^8}{72}\left[1-\frac{\alpha(\mathbf{x})}{2}\right] C(\mathbf{x})C(\mathbf{x}) \int_{B_\delta(\mathbf{0})} c^\delta(|\boldsymbol{\xi}|)\left|\boldsymbol{\xi}\right|^6 \mathrm{d}\boldsymbol{\xi}
\end{aligned}
$$

Bounding any power of $|\boldsymbol{\xi}|$ that is higher than 2 by δ and integrating with respect to $\boldsymbol{\xi}$, end up with

$$
\begin{aligned}
E_1 \leq & \frac{N^5}{2}\left[1-\frac{\alpha(\mathbf{x})}{2}\right] A(\mathbf{x})B(\mathbf{x})\delta E^0 \quad + \frac{N^6}{6}\left[1-\frac{\alpha(\mathbf{x})}{2}\right] A(\mathbf{x})C(\mathbf{x})\delta^2 E^0 \\
& + \frac{N^6}{8}\left[1-\frac{\alpha(\mathbf{x})}{2}\right] B(\mathbf{x})B(\mathbf{x})\delta^2 E^0 \quad + \frac{N^7}{12}\left[1-\frac{\alpha(\mathbf{x})}{2}\right] B(\mathbf{x})C(\mathbf{x})\delta^3 E^0 \\
& + \frac{N^8}{72}\left[1-\frac{\alpha(\mathbf{x})}{2}\right] C(\mathbf{x})C(\mathbf{x})\delta^4 E^0.
\end{aligned}
$$

Now consider E_2, use the fact integration with respect to $\boldsymbol{\xi}$ is taking place over the symmetric domain $B_\delta(\mathbf{0})$ to rewrite

$$
\frac{\alpha(\mathbf{x}+\boldsymbol{\xi})}{2} = \frac{1}{2}\left(\frac{\alpha(\mathbf{x}+\boldsymbol{\xi}) - \alpha(\mathbf{x}-\boldsymbol{\xi})}{2}\right)
$$

within the integral. Then we bring the absolute value inside the integral, apply the triangle inequality, bound each $|\xi_t|$ with $|\boldsymbol{\xi}|$, and bound the partial derivatives (as was done with E_1)

to obtain

$$
\begin{aligned}
E_2 \leq & \frac{N^5}{2} A(\mathbf{x}) B(\mathbf{x}) \int_{B_\delta(\mathbf{0})} c^\delta(|\boldsymbol{\xi}|) |\boldsymbol{\xi}|^3 \left(\frac{\alpha(\mathbf{x}+\boldsymbol{\xi}) - \alpha(\mathbf{x}-\boldsymbol{\xi})}{4} \right) \mathrm{d}\boldsymbol{\xi} \\
& + \frac{N^6}{6} A(\mathbf{x}) C(\mathbf{x}) \int_{B_\delta(\mathbf{0})} c^\delta(|\boldsymbol{\xi}|) |\boldsymbol{\xi}|^4 \left(\frac{\alpha(\mathbf{x}+\boldsymbol{\xi}) - \alpha(\mathbf{x}-\boldsymbol{\xi})}{4} \right) \mathrm{d}\boldsymbol{\xi} \\
& + \frac{N^6}{8} B(\mathbf{x}) B(\mathbf{x}) \int_{B_\delta(\mathbf{0})} c^\delta(|\boldsymbol{\xi}|) |\boldsymbol{\xi}|^4 \left(\frac{\alpha(\mathbf{x}+\boldsymbol{\xi}) - \alpha(\mathbf{x}-\boldsymbol{\xi})}{4} \right) \mathrm{d}\boldsymbol{\xi} \\
& + \frac{N^7}{12} B(\mathbf{x}) C(\mathbf{x}) \int_{B_\delta(\mathbf{0})} c^\delta(|\boldsymbol{\xi}|) |\boldsymbol{\xi}|^5 \left(\frac{\alpha(\mathbf{x}+\boldsymbol{\xi}) - \alpha(\mathbf{x}-\boldsymbol{\xi})}{4} \right) \mathrm{d}\boldsymbol{\xi} \\
& + \frac{N^8}{72} C(\mathbf{x}) C(\mathbf{x}) \int_{B_\delta(\mathbf{0})} c^\delta(|\boldsymbol{\xi}|) |\boldsymbol{\xi}|^6 \left(\frac{\alpha(\mathbf{x}+\boldsymbol{\xi}) - \alpha(\mathbf{x}-\boldsymbol{\xi})}{4} \right) \mathrm{d}\boldsymbol{\xi}.
\end{aligned}
$$

Now define

$$
\overline{\alpha}(\mathbf{x}) = \sup_{\boldsymbol{\xi} \in B_\delta(\mathbf{x})} \alpha(\mathbf{x}+\boldsymbol{\xi}), \qquad \underline{\alpha}(\mathbf{x}) = \inf_{\boldsymbol{\xi} \in B_\delta(\mathbf{x})} \alpha(\mathbf{x}+\boldsymbol{\xi}).
$$

Since $|\boldsymbol{\xi}| \leq \delta$ we have that,

$$
\begin{aligned}
E_2(\mathbf{u}, \mathbf{x}) \leq & \frac{N^5 \delta E^0}{8} A(\mathbf{x}) B(\mathbf{x}) \left(\overline{\alpha}(\mathbf{x}) - \underline{\alpha}(\mathbf{x}) \right) \\
& + \frac{N^6 \delta^2 E^0}{24} A(\mathbf{x}) C(\mathbf{x}) \left(\overline{\alpha}(\mathbf{x}) - \underline{\alpha}(\mathbf{x}) \right) \\
& + \frac{N^6 \delta^3 E^0}{32} B(\mathbf{x}) B(\mathbf{x}) \left(\overline{\alpha}(\mathbf{x}) - \underline{\alpha}(\mathbf{x}) \right) \\
& + \frac{N^7 \delta^3 E^0}{48} B(\mathbf{x}) C(\mathbf{x}) \left(\overline{\alpha}(\mathbf{x}) - \underline{\alpha}(\mathbf{x}) \right) \\
& + \frac{N^8 \delta^4 E^0}{288} C(\mathbf{x}) C(\mathbf{x}) \left(\overline{\alpha}(\mathbf{x}) - \underline{\alpha}(\mathbf{x}) \right).
\end{aligned}
$$

Therefore, the difference E is bounded by a finite quantity dependent on both α,δ, N, and E^0.

Further observe that when $x \in \Omega_{CE}$ we have that $\overline{\alpha}(\mathbf{x}) = \underline{\alpha}(\mathbf{x}) = \alpha(\mathbf{x}) = 0$. Therefore, the error associated with all $x \in \Omega_{CE}$ is independent of the choice of α and thus is dependent on the Taylor Expansion of $\mathbf{u}$ alone. It is also clear that as $\delta \to 0$ we also have that $E \to 0$.

□

Since W_{PD}^{δ} converges to W_{CE} as δ vanishes, this is another way of proving that the blended strain energy density converges to the classical strain energy density. Using a similar technique the above proposition can also be proved for twice differentiable $\mathbf{u}$, therefore this idea of convergence is as strong as the previous one.

Chapter 4

Energy-Based Blending in 1-Dimension

For clarity, we will analyze the blended model in one dimension as we did with the two models it was built from.

4.1 Analysis with fixed δ

In one dimension the strain energy density given in equation 3.4 simplifies to

$$\begin{aligned} W_B^\delta(u,x) =& \frac{1}{2}\int_{B_\delta(x)} c^\delta(|p-x|)\left(1-\frac{\alpha(p)+\alpha(x)}{2}\right)[(p-x)u'(x)]^2\mathrm{d}p \\ &+\frac{1}{2}\int_{B_\delta(x)} c^\delta(|p-x|)\left(\frac{\alpha(p)+\alpha(x)}{2}\right)[u(p)-u(x)]^2\mathrm{d}p. \end{aligned} \tag{4.1}$$

This is illustrated in Figure 4.1.

The following Proposition is the one-dimensional version of Proposition 3.1.

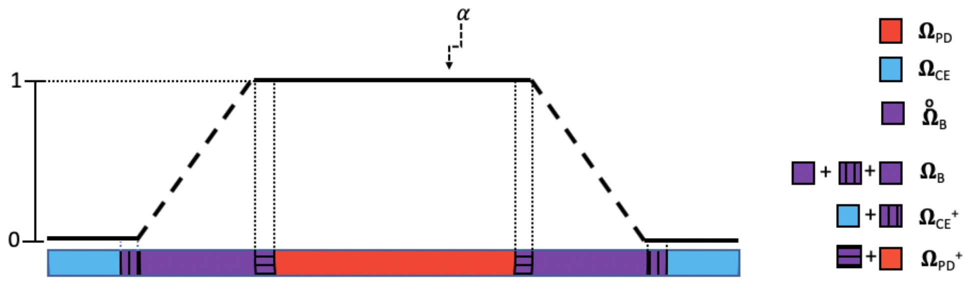

Figure 4.1: The one-dimensional analogue to Figure 3.1 with the blending function α included

Proposition 4.1. *For a differentiable u, the blended strain energy density converges to the classical strain energy density as δ approaches 0, ie*

$$\lim_{\delta\to 0} W_B^\delta(u,x) = \frac{1}{2}E^0\Big[u'(x)\Big]^2.$$

Proof. Rewriting $W_B^\delta(u,x)$ in a different form we have

$$\begin{aligned} W_B^\delta(u,x) &= \frac{1}{2}\int_{B_\delta(x)} c^\delta(|p-x|)\Big[(p-x)u'(x)\Big]^2 \mathrm{d}p \\ &\quad -\frac{1}{2}\int_{B_\delta(x)} c^\delta(|p-x|)\left(\frac{\alpha(p)+\alpha(x)}{2}\right)\Big[(p-x)u'(x)\Big]^2 \mathrm{d}p \\ &\quad +\frac{1}{2}\int_{B_\delta(x)} c^\delta(|p-x|)\left(\frac{\alpha(p)+\alpha(x)}{2}\right)\Big[u(p)-u(x)\Big]^2 \mathrm{d}p. \end{aligned}$$

Since the first term is equal to $\frac{1}{2}E^0\big(u'(x)\big)^2$, we need to show

$$\lim_{\delta\to 0}\left|\frac{1}{2}\int_{B_\delta(x)} c^\delta(|p-x|)\left(\frac{\alpha(p)+\alpha(x)}{2}\right)\left(\big[u(p)-u(x)\big]^2-\big[(p-x)u'(x)\big]^2\right)\mathrm{d}p\right| = 0.$$

Since u is assumed to be differentiable, Taylor's Theorem states that there exits a function h such that

$$u(p) = u(x) + (p-x)u'(x) + (p-x)h(p), \quad \text{where } \lim_{p\to x} h(p) = 0$$

Therefore,

$$
\begin{aligned}
&|(W_B^\delta - W_{CE}{}^\delta)(u,x)| \\
&\qquad \leq \left| \frac{1}{2} \int_{B_\delta(x)} c^\delta(|p-x|) \left(\frac{\alpha(p)+\alpha(x)}{2} \right) \left(\Big[u(p) - u(x) \Big]^2 - \Big[(p-x)u'(x) \Big]^2 \right) \mathrm{d}p \right| \\
&\qquad = \left| \frac{1}{2} \int_{B_\delta(x)} c^\delta(|p-x|) \left(\frac{\alpha(p)+\alpha(x)}{2} \right) (p-x)^2 \Big(2u'(x)h(p) + \big(h(p)\big)^2 \Big) \mathrm{d}p \right| \\
&\qquad \leq \left| \frac{1}{2} \int_{B_\delta(x)} c^\delta(|p-x|)(p-x)^2 \Big(2u'(x)h(p) + \big(h(p)\big)^2 \Big) \mathrm{d}p \right|
\end{aligned}
$$

Since $supp(c^\delta) \subseteq B_\delta(x)$, as δ vanishes effectively $p \to x$ and therefore

$$
\lim_{\delta \to 0} \left| W_B^\delta(u,x) - W_{CE}^\delta(u,x) \right| = 0.
$$

□

This result agrees with our intuitive understanding of how these models should work: As $\delta \to 0$ the model should be accurately be described by a local model.

Since our mathematical model agrees with our intuition as δ decreases, we will fix a δ and take a deeper analytical look at this blended model, $W_B^\delta(u,x)$ and associated spaces. Since δ is fixed we will drop the superscript δ of all functions except c^δ.

Define the **total strain energy** as

$$
W_B(u) := \int_\Omega W_B(u,x)\mathrm{d}x
$$

Let the following condition be referred to as the **blending distance condition**:

$$
\left\{ \text{Each connected component of } \mathring{\Omega}_B \text{ has positive measure} \right\} \tag{4.2}
$$

Proposition 4.2. *If the blending distance condition 4.2 is satisfied, then $W_B(u) = 0$ implies u is constant almost everywhere.*

Proof. Assume $0 = W_B(u)$. Since

$$\begin{aligned} W_B(u) =& \frac{1}{2}\int_\Omega \Big[u'(x)\Big]^2 \int_{B_\delta(x)} c^\delta(|p-x|)(p-x)^2\Big(1-\frac{\alpha(p)+\alpha(x)}{2}\Big)\mathrm{d}p\mathrm{d}x \\ &+ \frac{1}{2}\int_\Omega\int_{B_\delta(x)} c^\delta(|p-x|)\Big(\frac{\alpha(p)+\alpha(x)}{2}\Big)\Big[u(p)-u(x)\Big]^2\mathrm{d}p\mathrm{d}x \end{aligned}$$

and both of these terms are nonnegative by definition, we have that

$$0 = \int_\Omega \Big[u'(x)\Big]^2 \int_{B_\delta(x)} c^\delta(|p-x|)(p-x)^2\Big(1-\frac{\alpha(p)+\alpha(x)}{2}\Big)\mathrm{d}p\mathrm{d}x \text{ (local)} \tag{4.3}$$

$$0 = \int_\Omega\int_{B_\delta(x)} c^\delta(|p-x|)\Big(\frac{\alpha(p)+\alpha(x)}{2}\Big)\Big[u(p)-u(x)\Big]^2\mathrm{d}p\mathrm{d}x \text{ (nonlocal).} \tag{4.4}$$

By assumption c^δ is positive in $B_\delta(x)$, and

$$\begin{aligned} 1-\frac{\alpha(p)+\alpha(x)}{2} &= 0 \text{ iff } x,p\in\Omega^+_{PD} \\ \frac{\alpha(p)+\alpha(x)}{2} &= 0 \text{ iff } x,p\in\Omega^+_{CE}. \end{aligned}$$

Therefore, it follows that

$$\int_{B_\delta(x)} c^\delta(|p-x|)(p-x)^2\Big(1-\frac{\alpha(p)+\alpha(x)}{2}\Big)\mathrm{d}p > 0,\ \text{ when } x\in\big(\Omega\setminus\Omega_{PD}\big) \tag{4.5}$$

and

$$c^\delta(|p-x|)\Big(\frac{\alpha(p)+\alpha(x)}{2}\Big) > 0,\ \text{ when } x\in\big(\Omega\setminus\Omega_{CE}\big) \text{ and } p\in B_\delta(x). \tag{4.6}$$

Combining equations 4.3 and 4.5, we get that $u'(x) = 0$ on $\big(\Omega\setminus\Omega_{PD}\big)$. Thus, u is a constant a.e.. on each connected component of $\big(\Omega\setminus\Omega_{PD}\big)$. Similarly combining equations 4.4 and 4.6 we get that u is constant a.e.. on $\big(\Omega\setminus\Omega_{CE}\big)$. By assumption $\big(\Omega^+_{CE}\cap\Omega^+_{PD}\big) = \emptyset$, therefore

$$|\big(\Omega\setminus\Omega_{PD}\big)\cap\big(\Omega\setminus\Omega_{CE}\big)| = |\Omega_B| > 0.$$

The overlap of these regions implies that u must be constant a.e.. on Ω. $\square$

Let

$$S(\Omega) := \left\{ u \in L^2(\Omega) : W_B(u) := \int_\Omega W_B(u,x)\mathrm{d}x < \infty \right\}. \tag{4.7}$$

This function space is the analogue of the spaces $H^1(\Omega)$ for the classical problem and $\mathbb{S}(\Omega^*)$ for the peridynamic problem and therefore will be known as the **energy space**. Just as we did in Chapters 1 and 2, we will establish some desirable properties of this function space.

Proposition 4.3. *$S(\Omega)$ is a real vector space.*

Proof. Let $u, v \in S(\Omega)$ and $a \in \mathbb{R}$. Because scalars can be brought out of integrals it is easy to show that $S(\Omega)$ is closed under scalar multiplication. Observe

$$\begin{aligned}
W_B(au) =& \frac{1}{2}\int_\Omega [(au)'(x)]^2 \int_{B_\delta(x)} c^\delta(|p-x|)\left(1 - \frac{\alpha(p)+\alpha(x)}{2}\right)(p-x)^2 \mathrm{d}p\mathrm{d}x \\
&+ \frac{1}{2}\int_\Omega \int_{B_\delta(x)} c^\delta(|p-x|)\left(\frac{\alpha(p)+\alpha(x)}{2}\right)[(au)(p)-(au)(x)]^2 \mathrm{d}p\mathrm{d}x \\
\\
=& a^2 \frac{1}{2}\int_\Omega [u'(x)]^2 \int_{B_\delta(x)} c^\delta(|p-x|)\left(1 - \frac{\alpha(p)+\alpha(x)}{2}\right)(p-x)^2 \mathrm{d}p\mathrm{d}x \\
&+ a^2\frac{1}{2}\int_\Omega \int_{B_\delta(x)} c^\delta(|p-x|)\left(\frac{\alpha(p)+\alpha(x)}{2}\right)[(u(p)-u(x))]^2 \mathrm{d}p\mathrm{d}x \\
\\
=& a^2 W_B(u) < \infty.
\end{aligned}$$

Using the fact that the derivative of a sum of functions is the sum of the derivatives of the functions, we have that

$$
\begin{aligned}
W_B(u+v) =&\frac{1}{2}\int_\Omega [u'(x)+v'(x)]^2 \int_{B_\delta(x)} c^\delta(|p-x|)\left(1-\frac{\alpha(p)+\alpha(x)}{2}\right)(p-x)^2 \mathrm{d}p\mathrm{d}x \\
&+\frac{1}{2}\int_\Omega\int_{B_\delta(x)} c^\delta(|p-x|)\left(\frac{\alpha(p)+\alpha(x)}{2}\right)[(u(p)-u(x))+(v(p)-v(x))]^2 \mathrm{d}p\mathrm{d}x
\end{aligned}
$$

After squaring the terms that require squaring, and applying the fact that $ab \leq \frac{a^2}{2}+\frac{b^2}{2}$, it follows that

$$
\begin{aligned}
W_B(u+v) \leq &\int_\Omega [u'(x)]^2 \int_{B_\delta(x)} c^\delta(|p-x|)\left(1-\frac{\alpha(p)+\alpha(x)}{2}\right)(p-x)^2 \mathrm{d}p\mathrm{d}x \\
&+\int_\Omega\int_{B_\delta(x)} c^\delta(|p-x|)\left(\frac{\alpha(p)+\alpha(x)}{2}\right)[(u(p)-u(x))]^2 \mathrm{d}p\mathrm{d}x \\
&+\int_\Omega [v'(x)]^2 \int_{B_\delta(x)} c^\delta(|p-x|)\left(1-\frac{\alpha(p)+\alpha(x)}{2}\right)(p-x)^2 \mathrm{d}p\mathrm{d}x \\
&+\int_\Omega\int_{B_\delta(x)} c^\delta(|p-x|)\left(\frac{\alpha(p)+\alpha(x)}{2}\right)[(v(p)-v(x)]^2 \mathrm{d}p\mathrm{d}x
\end{aligned}
$$

$$
=2W_B(u)+2W_B(v)<\infty.
$$

□

Just as in Chapter 1 and 2, we will establish an appropriate norm on the space $S(\Omega)$.

Proposition 4.4. *The Gâteaux derivative of the blended energy is given by*

$$
\begin{aligned}
&\int_\Omega \Big[u'(x)v'(x)\Big] \int_{B_\delta(x)} c^\delta(|p-x|)\left(1-\frac{\alpha(p)+\alpha(x)}{2}\right)(p-x)^2 \mathrm{d}p\mathrm{d}x \\
&+\int_\Omega\int_{B_\delta(x)} c^\delta(|p-x|)\left(\frac{\alpha(p)+\alpha(x)}{2}\right)\Big[u(p)-u(x)\Big]\Big[v(p)-v(x)\Big] \mathrm{d}p\mathrm{d}x.
\end{aligned}
$$

Proof. Recall that the Gâteaux derivative is defined as

$$
A=\lim_{\epsilon\to 0}\frac{1}{\epsilon}[W_B(u+\epsilon v)-W_B(u)].
$$

Therefore,

$$\begin{aligned} A =\lim_{\epsilon\to 0}\Bigg\{ &\frac{1}{2\epsilon}\int_\Omega \Big[\big(u+\epsilon v\big)'(x)\Big]^2 \int_{B_\delta(x)} c^\delta(|p-x|)\left(1-\frac{\alpha(p)+\alpha(x)}{2}\right)(p-x)^2 \mathrm{d}p\mathrm{d}x \\ &-\frac{1}{2\epsilon}\int_\Omega \Big[u'(x)\Big]^2 \int_{B_\delta(x)} c^\delta(|p-x|)\left(1-\frac{\alpha(p)+\alpha(x)}{2}\right)(p-x)^2 \mathrm{d}p\mathrm{d}x \\ &+\frac{1}{2\epsilon}\int_\Omega\int_{B_\delta(x)} c^\delta(|p-x|)\left(\frac{\alpha(p)+\alpha(x)}{2}\right)\Big[\big(u+\epsilon v\big)(p)-\big(u+\epsilon v\big)(x)\Big]^2 \mathrm{d}p\mathrm{d}x \\ &-\frac{1}{2\epsilon}\int_\Omega\int_{B_\delta(x)} c^\delta(|p-x|)\left(\frac{\alpha(p)+\alpha(x)}{2}\right)\Big[u(p)-u(x)\Big]^2 \mathrm{d}p\mathrm{d}x \qquad \Bigg\}. \end{aligned}$$

Squaring the appropriate expressions and subtracting like terms we have

$$\begin{aligned} A =\lim_{\epsilon\to 0}\Bigg\{ &\frac{1}{2\epsilon}\int_\Omega \Big[2\epsilon u'(x)v'(x)\Big] \int_{B_\delta(x)} c^\delta(|p-x|)\left(1-\frac{\alpha(p)+\alpha(x)}{2}\right)(p-x)^2 \mathrm{d}p\mathrm{d}x \\ &+\frac{1}{2\epsilon}\int_\Omega \Big[\epsilon^2 v'(x)^2\Big] \int_{B_\delta(x)} c^\delta(|p-x|)\left(1-\frac{\alpha(p)+\alpha(x)}{2}\right)(p-x)^2 \mathrm{d}p\mathrm{d}x \\ &+\frac{1}{2\epsilon}\int_\Omega\int_{B_\delta(x)} c^\delta(|p-x|)\left(\frac{\alpha(p)+\alpha(x)}{2}\right)\left(2\epsilon\Big[u(p)-u(x)\Big]\Big[v(p)-v(x)\Big]\right) \mathrm{d}p\mathrm{d}x \\ &+\frac{1}{2\epsilon}\int_\Omega\int_{B_\delta(x)} c^\delta(|p-x|)\left(\frac{\alpha(p)+\alpha(x)}{2}\right)\left(2\epsilon^2\Big[v(p)-v(x)\Big]^2\right) \mathrm{d}p\mathrm{d}x \qquad \Bigg\}. \end{aligned}$$

Simplifying and taking the limit as ϵ vanishes, we are left with

$$\begin{aligned} A = &\int_\Omega \Big[u'(x)v'(x)\Big] \int_{B_\delta(x)} c^\delta(|p-x|)\left(1-\frac{\alpha(p)+\alpha(x)}{2}\right)(p-x)^2 \mathrm{d}p\mathrm{d}x \\ &+\int_\Omega\int_{B_\delta(x)} c^\delta(|p-x|)\left(\frac{\alpha(p)+\alpha(x)}{2}\right)\Big[u(p)-u(x)\Big]\Big[v(p)-v(x)\Big] \mathrm{d}p\mathrm{d}x. \end{aligned}$$

□

Therefore, define the following function on $S(\Omega)\times S(\Omega)$

$$\begin{aligned} (u,v)_{S(\Omega)} = &\int_\Omega \Big[u'(x)v'(x)\Big] \int_{B_\delta(x)} c^\delta(|p-x|)\left(1-\frac{\alpha(p)+\alpha(x)}{2}\right)(p-x)^2 \mathrm{d}p\mathrm{d}x \\ &+\int_\Omega\int_{B_\delta(x)} c^\delta(|p-x|)\left(\frac{\alpha(p)+\alpha(x)}{2}\right)\Big[u(p)-u(x)\Big]\Big[v(p)-v(x)\Big] \mathrm{d}p\mathrm{d}x. \end{aligned} \tag{4.8}$$

Proposition 4.5. $(\cdot,\cdot)_{S(\Omega)}$ *is a symmetric bilinear form on* $S(\Omega)$*.*

Proof. $(u,v)_{S(\Omega)}$ is clearly a symmetric form on $S(\Omega)$. So all we need to show is that it is linear in the first term. Let $u,v,w\in S(\Omega)$ and $a\in\mathbb{R}$.

$$\begin{aligned}(au,v)_{S(\Omega)} =&\int_\Omega [(au)'(x)v'(x)]\int_{B_\delta(x)} c^\delta(|p-x|)\left(1-\frac{\alpha(p)+\alpha(x)}{2}\right)(p-x)^2\mathrm{d}p\mathrm{d}x\\
&+\int_\Omega\int_{B_\delta(x)} c^\delta(|p-x|)\left(\frac{\alpha(p)+\alpha(x)}{2}\right)[(au)(p)-(au)(x)][v(p)-v(x)]\mathrm{d}p\mathrm{d}x\\
=&a\int_\Omega [u'(x)v'(x)]\int_{B_\delta(x)} c^\delta(|p-x|)\left(1-\frac{\alpha(p)+\alpha(x)}{2}\right)(p-x)^2\mathrm{d}p\mathrm{d}x\\
&+a\int_\Omega\int_{B_\delta(x)} c^\delta(|p-x|)\left(\frac{\alpha(p)+\alpha(x)}{2}\right)[u(p)-u(x)][v(p)-v(x)]\mathrm{d}p\mathrm{d}x\\
=&a(u,v)_{S(\Omega)}.\end{aligned}$$

$$\begin{aligned}(u+w,v)_{S(\Omega)} =&\int_\Omega [(u+w)'(x)v'(x)]\int_{B_\delta(x)} c^\delta(|p-x|)\left(1-\frac{\alpha(p)+\alpha(x)}{2}\right)(p-x)^2\mathrm{d}p\mathrm{d}x\\
&+\int_\Omega\int_{B_\delta(x)} c^\delta(|p-x|)\left(\frac{\alpha(p)+\alpha(x)}{2}\right)[(u+w)(p)-(u+w)(x)][v(p)-v(x)]\mathrm{d}p\mathrm{d}x\\
=&\int_\Omega [u'(x)v'(x)]\int_{B_\delta(x)} c^\delta(|p-x|)\left(1-\frac{\alpha(p)+\alpha(x)}{2}\right)(p-x)^2\mathrm{d}p\mathrm{d}x\\
&+\int_\Omega\int_{B_\delta(x)} c^\delta(|p-x|)\left(\frac{\alpha(p)+\alpha(x)}{2}\right)[u(p)-u(x)][v(p)-v(x)]\mathrm{d}p\mathrm{d}x\\
&+\int_\Omega [w'(x)v'(x)]\int_{B_\delta(x)} c^\delta(|p-x|)\left(1-\frac{\alpha(p)+\alpha(x)}{2}\right)(p-x)^2\mathrm{d}p\mathrm{d}x\\
&+\int_\Omega\int_{B_\delta(x)} c^\delta(|p-x|)\left(\frac{\alpha(p)+\alpha(x)}{2}\right)[w(p)-w(x)][v(p)-v(x)]\mathrm{d}p\mathrm{d}x\\
=&(u,v)_{S(\Omega)}+(w,v)_{S(\Omega)}.\end{aligned}$$

Therefore, $(\cdot,\cdot)_{S(\Omega)}$ is a symmetric bilinear form on $S(\Omega)$. □

Proposition 4.6. *Assuming the blending distance condition 4.2 is satisfied,* $(\cdot,\cdot)_{S(\Omega)}$ *is positive semi-definite.*

Proof. The positive semi-definite property follows from

$$W_B(u) = \frac{1}{2}(u,u)_{S(\Omega)}$$

and that $W_B(u) = 0$ implies u is constant as shown in the proof of Proposition 4.2. $\square$

We will refer to $(\cdot,\cdot)_{S(\Omega)}$ as the **energy bilinear form**. Inspired by our work in the earlier chapters, we define

$$((u,v))_{S(\Omega)} = (u,v)_{L^2(\Omega)} + (u,v)_{S(\Omega)}.$$

Proposition 4.7. *Assuming the blending distance condition 4.2 is satisfied, $((\cdot,\cdot))_{S(\Omega)}$ is an inner product on $S(\Omega)$.*

Proof. To be an inner product $((\cdot,\cdot))_S$ needs to be symmetric, linear and positive definite. Since $(\cdot,\cdot)_{L^2(\Omega)}$ is an inner product on $L^2(\Omega)$ and $S(\Omega) \subset L^2(\Omega)$, it is clear that $(\cdot,\cdot)_{L^2(\Omega)}$ has these three properties. We have also just shown that $(\cdot,\cdot)_{S(\Omega)}$ is both symmetric and linear. Although $(\cdot,\cdot)_{S(\Omega)}$ is only positive semi-definite, since it is added to a positive definite bilinear form $(\cdot,\cdot)_{L^2(\Omega)}$, we have that $((\cdot,\cdot))_{S(\Omega)}$ is positive definite. Therefore, we have shown that $((\cdot,\cdot))_{S(\Omega)}$ is an inner product on $S(\Omega)$. $\square$

Since $((\cdot,\cdot))_{S(\Omega)}$ is an inner product, we can define

$$||u||_{S(\Omega)} = \sqrt{((u,u))_{S(\Omega)}} = \sqrt{(u,u)_{L^2(\Omega)} + (u,u)_{S(\Omega)}}.$$

to be a **norm** on the space $S(\Omega)$. Since $S(\Omega)$ is a vector space we have that $(S(\Omega), ||\cdot||_{S(\Omega)})$ is a **normed vector space**.

Theorem 4.8. *Assuming the blending distance condition 4.2 is satisfied. $\big(S(\Omega), ||\cdot||_{S(\Omega)}\big)$ is a complete normed space.*

Proof. Let u_n be a sequence of functions in $S(\Omega)$, that is Cauchy with respect to $||\cdot||_{S(\Omega)}$. Therefore, given ϵ there exists a $N > 0$ such that

$$\big|\big|u_n - u_m\big|\big|^2_{S(\Omega)} < \frac{\epsilon}{2},\ \forall\ n, m > N.$$

By the definition of $||\cdot||_{S(\Omega)}$, we know that u_n is Cauchy with respect to both $||\cdot||^2_{L^2(\Omega)}$ and $|\cdot|^2_{S(\Omega)}$. Since $\{u_n\}_{n=1}^{\infty} \subset S(\Omega) \subset L^2(\Omega)$ is a Cauchy sequence in a complete space $L^2(\Omega)$, we know that there is a unique element $u \in L^2(\Omega)$ such that $u_n \to u$ in $L^2(\Omega)$.

Ultimately, we would like so show to show that $u \in S(\Omega)$ and $u_n \to u$ with respect to the norm $||\cdot||_{S(\Omega)}$ as well. To do so, we first will show that u has a weak derivative in the region $\big(\Omega \setminus \Omega_{PD}\big)$.

Let $K_t \subset \big(\Omega \setminus \Omega_{PD}\big)$ such that for all $x \in K_t$ we have $d\big(x, \partial\Omega_{PD}\big) > \frac{1}{t}$. For any $t > 0$ we have that $K_t \subsetneq \big(\Omega \setminus \Omega_{PD}\big)$ and for each $x \in K_t$ we have that

$$\Psi(x) := \int_{B_\delta(x)} c^\delta(|p-x|)(p-x)^2 \left(1 - \frac{\alpha(p) + \alpha(x)}{2}\right) \mathrm{d}p > 0.$$

So there exists a $C_t > 0$ such that for all $n, m > N$,

$$\begin{aligned}
\int_{K_t} C_t(u_n' - u_m')^2 \mathrm{d}x < & \int_{K_t} \Psi(x)(u_n' - u_m')^2 \mathrm{d}x \\
\leq & \int_{\Omega} \Psi(x)(u_n' - u_m')^2 \mathrm{d}x \\
\leq & |u_n - u_m|^2_{S(\Omega)} \\
\leq & \frac{\epsilon}{2}
\end{aligned}$$

Therefore, the sequence u_n' is Cauchy with respect to $L^2(K_t)$. Since $L^2(K_t)$ is a complete space, there exists a $g_t \in L^2(K_t)$ such that $\big|\big|u_n' - g_t\big|\big|_{L^2(K_t)} \to 0$ as $n \to 0$. On K_t for all $\varphi \in C_c^\infty(K_t)$ we have

$$\begin{aligned}
\left|\int_{K_t} u_n'\varphi \mathrm{d}x - \int_{K_t} g_t\varphi \mathrm{d}x\right| \leq & \int_{K_t} \big|u_n' - g_t\big|\ |\varphi| \mathrm{d}x \\
\leq & \big|\big|u_n' - g_t\big|\big|_{L^2(K_t)} \big|\big|\varphi\big|\big|_{L^2(K_t)}.
\end{aligned}$$

Since $C_c^\infty(K_t) \subset L^2(\Omega)$ we have $\lim_{n\to\infty} \int_{K_t} u_n' \varphi \mathrm{d}x = \int_{K_t} g_t \varphi \mathrm{d}x$. By a similar argument, we can show that $\lim_{n\to\infty} \int_{K_t} u_n \varphi' \mathrm{d}x = \int_{K_t} u\varphi' \mathrm{d}x$.

Therefore, we have

$$-\int_{K_t} u\varphi' \mathrm{d}x = -\lim_{n\to\infty} \int_{K_t} u_n \varphi' \mathrm{d}x = \lim_{n\to\infty} \int_{K_t} u_n' \varphi \mathrm{d}x = \int_{K_t} g_t \varphi \mathrm{d}x,$$

which means that g_t is the weak derivative of u, (i.e $g_t = u'$), a.e.. on K_t.

For $t_1 > t_2$, $K_{t_1} \subset K_{t_2}$ and by the uniqueness of limits we have that $g_{t_2}\big|_{K_{t_1}} = g_{t_1}$. For each $x \in \big(\Omega \setminus \Omega_{PD}\big)$ we have that $x \in K_s$ for some s. Therefore, we define $g(x) = g_s(x)$ and we can say,

$$-\int_{\Omega} u\varphi' \mathrm{d}x = -\lim_{n\to\infty} \int_{\Omega} u_n \varphi' \mathrm{d}x = \lim_{n\to\infty} \int_{\Omega} u_n' \varphi \mathrm{d}x = \int_{\Omega} g\varphi \mathrm{d}x$$

so $g = u'$ *a.e.*. on $\big(\Omega \setminus \Omega_{PD}\big)$.

Now that we have shown that $|u|_{S(\Omega)}$ is well defined we need to show that $\big|u_m - u\big|_{S(\Omega)} \to 0$ as $m \to \infty$. In order to show convergence, we will consider the local part and the nonlocal part of the energy separately and show that both

$$\int_{\Omega} \int_{B_\delta(x)} c^\delta(|p-x|)(p-x)^2 \left[1 - \frac{\alpha(p)+\alpha(x)}{2}\right] \mathrm{d}p \ \ (u_m'(x) - u'(x))^2 \mathrm{d}x \leq \frac{\epsilon}{2}$$
$$\int_{\Omega} \int_{B_\delta(x)} c^\delta(|p-x|) \left[\frac{\alpha(p)+\alpha(x)}{2}\right] [(u_m - u)(p) - (u_m - u)(x)]^2 \mathrm{d}p\mathrm{d}x \leq \frac{\epsilon}{2}.$$

Since u_n is a Cauchy sequence in $||\cdot||_{S(\Omega)}$, there is a large enough N such that for all $n, m > N$

$$||u_m - u_n||_{S(\Omega)}^2 \leq \frac{\epsilon}{2}.$$

Since we have shown that $u_n' \to u'$ on $\big(\Omega \setminus \Omega_{PD}\big)$, by Fatou's Lemma we have that

$$
\begin{aligned}
&\int_\Omega \int_{B_\delta(x)} c^\delta(|p-x|)(p-x)^2 \left[1 - \frac{\alpha(p)+\alpha(x)}{2}\right] \mathrm{d}p \ \left(u_m' - u'\right)^2 \mathrm{d}x \\
&\qquad = \int_\Omega \int_{B_\delta(x)} c^\delta(|p-x|)(p-x)^2 \left[1 - \frac{\alpha(p)+\alpha(x)}{2}\right] \mathrm{d}p \ \liminf_{n\to\infty} \left(u_m' - u_n'\right)^2 \mathrm{d}x \\
&\qquad \le \liminf_{n\to\infty} \int_\Omega \int_{B_\delta(x)} c^\delta(|p-x|)(p-x)^2 \left[1 - \frac{\alpha(p)+\alpha(x)}{2}\right] \mathrm{d}p \ \left(u_m' - u_n'\right)^2 \mathrm{d}x \\
&\qquad = \liminf_{n\to\infty} \left|u_m - u_n\right|^2_{S(\Omega)} \\
&\qquad \le \frac{\epsilon}{2}.
\end{aligned}
$$

Now we want to show the analogous thing for the nonlocal part of the norm. To do this, we introduce a modified operator with a truncated kernel, $c_\tau^\delta(z) := \chi_{z>\tau}(z) c^\delta(z)$ where $\tau > 0$. It is important to note that $c_\tau^\delta(z) \to c^\delta(z)$ pointwise as $\tau \to 0$. Therefore, we have that,

$$
\begin{aligned}
&\int_\Omega \int_{B_\delta(x)} c_\tau^\delta(p-x) \left(\frac{\alpha(p)+\alpha(x)}{2}\right) \Big[u_m(p) - u_n(p) - u_m(x) + u_n(x)\Big]^2 \mathrm{d}p\mathrm{d}x \\
&\qquad \le \int_\Omega \int_{B_\delta(x)} c^\delta(|p-x|) \left(\frac{\alpha(p)+\alpha(x)}{2}\right) \Big[u_m(p) - u_n(p) - u_m(x) + u_n(x)\Big]^2 \mathrm{d}p\mathrm{d}x \\
&\qquad \le \epsilon/2 \quad \forall \tau > 0, n, m > N.
\end{aligned}
$$

For fixed m and $\forall\ x, p$

$$
\begin{aligned}
&\lim_{n\to\infty} c_\tau^\delta(p-x) \left(\frac{\alpha(p)+\alpha(x)}{2}\right) \Big[u_m(p) - u_n(p) - u_m(x) + u_n(x)\Big]^2 \\
&\qquad = c_\tau^\delta(p-x) \left(\frac{\alpha(p)+\alpha(x)}{2}\right) \Big[u_m(p) - u(p) - u_m(x) + u(x)\Big]^2.
\end{aligned}
$$

Therefore, by the Lebesgue dominated convergence theorem, for all $\tau > 0$ and for all $m \ge N$

$$
\begin{aligned}
&\lim_{n\to\infty} \int_\Omega \int_{B_\delta(x)} c_\tau^\delta(p-x) \left(\frac{\alpha(p)+\alpha(x)}{2}\right) \Big[u_m(p) - u_n(p) - u_m(x) + u_n(x)\Big]^2 \mathrm{d}p\mathrm{d}x \\
&\qquad = \int_\Omega \int_{B_\delta(x)} c_\tau^\delta(p-x) \left(\frac{\alpha(p)+\alpha(x)}{2}\right) \Big[u_m(p) - u(p) - u_m(x) + u(x)\Big]^2 \mathrm{d}p\mathrm{d}x.
\end{aligned}
$$

Thus, for $\tau > 0$ and for $m \geq N$,

$$\begin{aligned}
&\int_\Omega \int_{B_\delta(x)} c_\tau^\delta(p-x)\left(\frac{\alpha(p)+\alpha(x)}{2}\right)\Big[u_m(p)-u(p)-u_m(x)+u(x)\Big]^2 \mathrm{d}p\mathrm{d}x \\
&\quad \leq \liminf_{n\to\infty} \int_\Omega \int_{B_\delta(x)} c^\delta(|p-x|)\left(\frac{\alpha(p)+\alpha(x)}{2}\right)\Big[u_m(p)-u_n(p)-u_m(x)+u_n(x)\Big]^2 \mathrm{d}p\mathrm{d}x \\
&\quad \leq \frac{\epsilon}{2}.
\end{aligned}$$

Now applying Fatou's Lemma over τ, we obtain that

$$\int_\Omega \int_{B_\delta(x)} c^\delta(|p-x|)\left(\frac{\alpha(p)+\alpha(x)}{2}\right)\Big[u_m(p)-u(p)-u_m(x)+u(x)\Big]^2 \mathrm{d}p\mathrm{d}x \leq \frac{\epsilon}{2} \quad \forall m > N.$$

Thus for any $\epsilon > 0$ there exists an N large enough that $|u_m - u|^2_{S(\Omega)} < \epsilon$ for $m > N$. Note that the convergence in $|\cdot|_{S(\Omega)}$ implies that $W_B(u)$ is finite and therefore $u \in S(\Omega)$. Thus, we have shown that $S(\Omega)$ is complete with respect to the chosen norm $||\cdot||_{S(\Omega)}$. . □

Now we want to show how $S(\Omega)$ relates to the known Hilbert Spaces $L^2(\Omega)$ and $H^1(\Omega)$. It is clear by its definition that $S(\Omega) \subset L^2(\Omega)$, but we can further show

Proposition 4.9. *Assuming the blending distance condition 4.2 is satisfied, $S(\Omega)$ embeds continuously into $L^2(\Omega)$.*

Proof. Let $u \in S(\Omega)$. Since $|\cdot|_{S(\Omega)}$ is a semi-norm on $S(\Omega)$ it follows that $|u|_{S(\Omega)} \geq 0$. Therefore,

$$\begin{aligned}
||u||_{L^2(\Omega)} &= \sqrt{||u||^2_{L^2(\Omega)}} \\
&\leq \sqrt{||u||^2_{L^2(\Omega)} + |u|^2_{S(\Omega)}} \\
&= ||u||_S
\end{aligned}$$

Therefore, $S(\Omega)$ continuously embeds into $L^2(\Omega)$. □

Proposition 4.10. *Assuming the blending distance condition 4.2 is satisfied, if $u \in S(\Omega)$, then $u\big|_{(\Omega\setminus\Omega_{PD})} \in H^1\big(\Omega \setminus \Omega_{PD}\big)$.*

Proof. Let $u \in S(\Omega)$. By definition, u has a weak derivative on $\big(\Omega \setminus \Omega_{PD}\big)$. By 4.5, we know there exists a $C > 0$

$$\begin{aligned}
\int_{\left(\Omega\setminus\Omega_{PD}\right)} C[u'(x)]^2 \mathrm{d}x &\leq \int_{\left(\Omega\setminus\Omega_{PD}\right)} \int_{B_\delta(x)} c^\delta(|p-x|)(p-x)^2 \left[1 - \frac{\alpha(p)+\alpha(x)}{2}\right] \mathrm{d}p \left[u'(x)\right]^2 \mathrm{d}x \\
&\leq \int_\Omega \int_{B_\delta(x)} c^\delta(|p-x|)(p-x)^2 \left[1 - \frac{\alpha(p)+\alpha(x)}{2}\right] \mathrm{d}p \left[u'(x)\right]^2 \mathrm{d}x \\
&\leq |u|^2_{S(\Omega)} \\
&< \infty.
\end{aligned}$$

Therefore, $u \in H^1\big(\Omega \setminus \Omega_{PD}\big)$. ∎

Proposition 4.11. *Assuming the blending distance condition 4.2 is satisfied, if* $|\Omega| < \infty$*,* $H^1(\Omega)$ *embeds continuously into* $S(\Omega)$*.*

Proof. Let $u \in H^1(\Omega)$. There is a $\bar{u} \in C(\bar{\Omega})$ that agrees with u on Ω by 1.8. Recall,

$$\begin{aligned}
|u|^2_{S(\Omega)} = &\int_\Omega \int_{B_\delta(x)} c^\delta(|p-x|)(p-x)^2 \left[1 - \frac{\alpha(p)+\alpha(x)}{2}\right] \mathrm{d}p[u'(x)]^2 \mathrm{d}x \\
&+ \int_\Omega \int_{B_\delta(x)} c^\delta(|p-x|) \left(\frac{\alpha(p)+\alpha(x)}{2}\right) [u(p)-u(x)]^2 \mathrm{d}p \mathrm{d}x
\end{aligned}$$

For convenience, define

$$|u|^2_L = \int_\Omega \int_{B_\delta(x)} c^\delta(|p-x|)(p-x)^2 \left[1 - \frac{\alpha(p)+\alpha(x)}{2}\right] \mathrm{d}p[u'(x)]^2 \mathrm{d}x$$

and

$$|u|^2_{NL} = \int_\Omega \int_{B_\delta(x)} c^\delta(|p-x|) \left(\frac{\alpha(p)+\alpha(x)}{2}\right) [u(p)-u(x)]^2 \mathrm{d}p \mathrm{d}x.$$

We know that $0 \leq \alpha(x) \leq 1$ for all $x \in \Omega$, and therefore it follows that for all $x \in \Omega$ and $p \in B_\delta(x)$, we have that

$$0 \leq \left[1 - \frac{\alpha(p)+\alpha(x)}{2}\right] \leq 1 \qquad \text{and} \qquad 0 \leq \left(\frac{\alpha(p)+\alpha(x)}{2}\right) \leq 1$$

Since $u \in H^1(\Omega)$ we know that u' is defined on all of Ω. Therefore,

$$|u|_L^2 \leq \int_\Omega \int_{B_\delta(x)} c^\delta(|p-x|)(p-x)^2 \, [1] \, \mathrm{d}p[u'(x)]^2 \mathrm{d}x.$$

Knowing that $\int_{B_\delta(x)} c^\delta(|p-x|)(p-x)^2 \mathrm{d}p = E^0$ we now have that

$$|u|_L^2 \leq E^0 \int_\Omega [u'(x)]^2 \mathrm{d}x = E^0 |u|_{H^1(\Omega)}^2.$$

Since $\left(\frac{\alpha(p)+\alpha(x)}{2}\right) = 0$ if and only if both p and x are elements of Ω_{PD}^+, therefore if p were allowed to be outside of Ω (this could happen when x is less than δ from the boundary of Ω), this term would be zero as $x \in \Omega_{CE}$. Thus, it follows that

$$|u|_{NL}^2 = \int_\Omega \int_\Omega c^\delta(|p-x|) \left(\frac{\alpha(p)+\alpha(x)}{2} \right) [u(p)-u(x)]^2 \mathrm{d}p \mathrm{d}x.$$

Therefore,

$$|u|_{NL}^2 \leq \int_\Omega \int_\Omega c^\delta(|p-x|)[u(p)-u(x)]^2 \mathrm{d}p \mathrm{d}x.$$

But by the integral mean value theorem, we know that

$$u(p) - u(x) = \int_x^p u'(t) \mathrm{d}t.$$

Through a parameterization $t(s) = x + s(p-x)$ it follows that

$$u(p) - u(x) = (p-x) \int_0^1 u'(x + s(p-x)) \mathrm{d}s.$$

Through an application of Hölder's inequality we get that

$$|u(p) - u(x)|^2 \leq (p-x)^2 \int_0^1 |u'(x + s(p-x))|^2 \mathrm{d}s.$$

Since $u \in H^1(\Omega)$, we know that it can be extended to a function $\tilde{u} \in H^1(\mathbb{R})$ such that $u = \tilde{u}$ on Ω and both

$$||\tilde{u}||_{L^2(\mathbb{R})} \leq C||u||_{L^2(\Omega)}$$
$$||\tilde{u}||_{H^1(\mathbb{R})} \leq C||u||_{H^1(\Omega)}$$

and C only depends on $|\Omega|$. This implies that

$$|\tilde{u}|_{H^1(\mathbb{R})} \leq C|u|_{H^1(\Omega)}$$

Therefore,

$$\begin{aligned} |u(p) - u(x)|^2 &\leq (p-x)^2 \int_0^1 |u'(x + s(p-x))|^2 \mathrm{d}s \\ &\leq (p-x)^2 |\tilde{u}|^2_{H^1(\mathbb{R})} \\ &\leq C^2 (p-x)^2 |u|^2_{H^1(\Omega)}. \end{aligned}$$

Thus, it follows that

$$|u|^2_{NL} \leq \int_\Omega \int_\Omega c^\delta(|p-x|) C^2 (p-x)^2 |u|^2_{H^1(\Omega)}.$$

Through integration with respect to both x and p we find that

$$|u|^2_{NL} \leq C^2 E^0 |\Omega| \quad |u|^2_{H^1(\Omega)}.$$

Putting this together we find that

$$\begin{aligned} |u|^2_{S(\Omega)} &= |u|^2_L + |u|^2_{NL} \\ &\leq E^0 |u|^2_{H^1(\Omega)} + C^2 E^0 |\Omega| \quad |u|^2_{H^1(\Omega)} \\ &\leq \max\left(E^0, C^2 E^0 |\Omega|\right) |u|^2_{H^1(\Omega)}. \end{aligned}$$

Since $||\cdot||^2_{S(\Omega)} = ||\cdot||^2_{L^2(\Omega)} + |\cdot|^2_{S(\Omega)}$, it follows that

$$\begin{aligned} |u|^2_{S(\Omega)} + ||u||^2_{L^2(\Omega)} &\leq \max\left(E^0, C^2E^0|\Omega|\right)|u|^2_{H^1(\Omega)} + ||u||^2_{L^2(\Omega)} \\ &\leq \max\left(E^0, C^2E^0|\Omega|, 1\right)||u||^2_{H^1(\Omega)}. \end{aligned}$$

□

Corollary 4.12. *Assuming the blending distance condition 4.2 is satisfied. For each $u \in S(\Omega)$, there is a $\tilde{u} \in S(\Omega)$, that can be continuously extended to the boundary.*

The following lemmas will prove useful in proving Theorem 4.16.

Lemma 4.13. *Assuming that c^δ satisfies the conditions given in equations 3.1 and u_n is a bounded sequence in $L^2(\Omega)$ such that*

$$\int_\Omega \int_{B_\delta(x)} c^\delta(|p-x|)(p-x)^2\left(1 - \frac{\alpha(p)+\alpha(x)}{2}\right)\mathrm{d}p\left[u_n'(x)\right]^2\mathrm{d}x \to 0 \text{ as } n \to \infty$$

Then there exists a subsequence $u_{n_{k_m}}$ that converges strongly to a constant function in $L^2\left(\Omega^+_{CE}\right)$ as m increases.

Proof. Every bounded sequence in a Hilbert space has a weakly convergent subsequence, i.e. there exists a u such that

$$\lim_{k\to\infty}\left(u_{n_k}, v\right)_{L^2(\Omega)} = \left(u, v\right)_{L^2(\Omega)}.$$

For all $x \in \Omega^+_{CE}$ we know $\alpha(x) = 0$, therefore for all $p \in \Omega$,

$$1 \geq \left(1 - \frac{\alpha(p)+\alpha(x)}{2}\right) \geq \left(1 - \frac{1-0}{2}\right) = \frac{1}{2}$$

Recalling equations 3.1 we have that

$$\frac{E^0}{2} \leq \int_\Omega c^\delta(|p-x|)(p-x)^2\left(1 - \frac{\alpha(p)+\alpha(x)}{2}\right)\mathrm{d}p \leq E^0.$$

Therefore it follows that,

$$\begin{aligned}
\int_{\Omega_{CE}^+} \big(u_{n_k}'(x)\big)^2 \mathrm{d}x &= \frac{2}{E^0} \int_{\Omega_{CE}^+} \frac{E^0}{2} \big(u_{n_k}'(x)\big)^2 \mathrm{d}x \\
&\leq \frac{2}{E^0} \int_{\Omega_{CE}^+} \int_{B_\delta(x)} c^\delta(|p-x|)(p-x)^2 \bigg(1 - \frac{\alpha(p)+\alpha(x)}{2}\bigg) \mathrm{d}p \big(u_{n_k}'(x)\big)^2 \mathrm{d}x \\
&\leq \frac{2}{E^0} \int_{\Omega} \int_{B_\delta(x)} c^\delta(|p-x|)(p-x)^2 \bigg(1 - \frac{\alpha(p)+\alpha(x)}{2}\bigg) \mathrm{d}p \big(u_{n_k}'(x)\big)^2 \mathrm{d}x \\
&\leq \frac{2}{E^0} \big|u_{n_k}\big|_{S(\Omega)}^2 \to 0
\end{aligned}$$

as $k \to \infty$. Thus, we have shown that u_{n_k}' is a bounded sequence in $L^2\big(\Omega_{CE}^+\big)$. By assumption u_{n_k} is a bounded sequence in $L^2\big(\Omega\big)$ and therefore is a bounded sequence in $L^2\big(\Omega_{CE}^+\big)$. This implies that u_{n_k} is a bounded sequence in $H^1\big(\Omega_{CE}^+\big)$.

Since u_{n_k} is a bounded sequence in $H^1\big(\Omega_{CE}^+\big)$, we have that there exists a $\tilde{u} \in H^1\big(\Omega_{CE}^+\big)$ and a subsequence $u_{n_{k_m}}$ such that

$$\begin{aligned}
\lim_{m\to\infty} \big|u_{n_{k_m}} - \tilde{u}\big|_{L^2\left(\Omega_{CE}^+\right)} &= 0 \\
\lim_{m\to\infty} \big(u_{n_{k_m}}', v\big)_{L^2(\Omega_{CE}^+)} &= \big(\tilde{u}', v\big)_{L^2\left(\Omega_{CE}^+\right)}.
\end{aligned}$$

By Theorem 4.10.7 in [21], we have

$$\big|\big|\tilde{u}'\big|\big|_{L^2\left(\Omega_{CE}^+\right)} \leq \liminf_{m} \big|\big|u_{n_{k_m}}'\big|\big|_{L^2\left(\Omega_{CE}^+\right)} = 0.$$

Therefore $||\tilde{u}'||_{L^2\left(\Omega_{CE}^+\right)} = 0$, which implies that $\tilde{u}' = 0$ a.e. on Ω_{CE}^+. Thus on any connected components of Ω_{CE}^+ $\tilde{u}$ is a constant a.e.. By the uniqueness of limits, we have that $u = \tilde{u}$ a.e. on Ω_{CE}^+. Thus, the weak limit found at the beginning of the proof u is a constant a.e. on the connected components of Ω_{CE}^+ and that $u_{n_{k_m}}$ converges strongly to u in $L^2\big(\Omega_{CE}^+\big)$. □

Lemma 4.14. *Assuming c^δ satisfies the conditions given in equations 3.1 and u_n is a bounded sequence in $L^2(\Omega)$ such that*

$$\lim_{n\to\infty} \int_{\Omega} \int_{B_\delta(x)} c^\delta(|p-x|)(p-x)^2 \left(\frac{\alpha(p)-\alpha(x)}{2}\right) \big[u_n(p) - u_n(x)\big]^2 \mathrm{d}p\mathrm{d}x = 0,$$

then there exists a $u \in L^2(\Omega)$ such that

$$\lim_{k\to\infty} \big(u_{n_k}, v\big)_{L^2(\Omega)} = \big(u, v\big)_{L^2(\Omega)}$$

and that u is a constant on $\big(\Omega \setminus \Omega_{CE}\big)$.

Proof. Every bounded sequence in a Hilbert Space has a weakly convergent subsequence, ie there exists a u such that

$$\lim_{k\to\infty} \big(u_{n_k}, v\big)_{L^2(\Omega)} = \big(u, v\big)_{L^2(\Omega)}.$$

Now we need to show that this u is constant on $\big(\Omega \setminus \Omega_{CE}\big)$. Define $\mathcal{L}$ a map on $L^2(\Omega)$ as

$$\begin{aligned}\big(\mathcal{L}v\big)(x) &= -\int_{B_\delta(x)} c^\delta(|p-x|)(p-x)^2 \left(\frac{\alpha(p)+\alpha(x)}{2}\right) \big[v(p)-v(x)\big]\mathrm{d}p \\ &= -\int_{\Omega} c^\delta(|p-x|)(p-x)^2 \left(\frac{\alpha(p)+\alpha(x)}{2}\right) \big[v(p)-v(x)\big]\mathrm{d}p\end{aligned}$$

Let $\phi \in C_c^\infty(\Omega)$ and define a functional

$$J_n(\phi) = \int_\Omega \big(\mathcal{L}\phi\big)(x)u_n(x)\mathrm{d}x$$

Using the fact that $a = \dfrac{a}{2} + \dfrac{a}{2}$, we can see that

$$\begin{aligned}J_n(\phi) &= -\int_\Omega\int_\Omega c^\delta(|p-x|)(p-x)^2\left(\frac{\alpha(p)+\alpha(x)}{2}\right)\Big[\phi(p)-\phi(x)\Big]\mathrm{d}p\Big[u_n(x)\Big]\mathrm{d}x \\ &= -\frac{1}{2}\int_\Omega\int_\Omega c^\delta(|p-x|)(p-x)^2\left(\frac{\alpha(p)+\alpha(x)}{2}\right)\Big[\phi(p)-\phi(x)\Big]\mathrm{d}p\Big[u_n(x)\Big]\mathrm{d}x \\ &\quad -\frac{1}{2}\int_\Omega\int_\Omega c^\delta(|p-x|)(p-x)^2\left(\frac{\alpha(p)+\alpha(x)}{2}\right)\Big[\phi(p)-\phi(x)\Big]\mathrm{d}p\Big[u_n(x)\Big]\mathrm{d}x.\end{aligned}$$

Switching the roles of x and p in the second term,

$$\begin{aligned}J_n(\phi) &= -\frac{1}{2}\int_\Omega\int_\Omega c^\delta(|p-x|)(p-x)^2\left(\frac{\alpha(p)+\alpha(x)}{2}\right)\Big[\phi(p)-\phi(x)\Big]\mathrm{d}p\Big[u_n(x)\Big]\mathrm{d}x \\ &\quad -\frac{1}{2}\int_\Omega\int_\Omega c^\delta(|x-p|)(x-p)^2\left(\frac{\alpha(x)+\alpha(p)}{2}\right)\Big[\phi(x)-\phi(p)\Big]\mathrm{d}x\Big[u_n(p)\Big]\mathrm{d}p.\end{aligned}$$

Factoring a -1 out of the second term,

$$\begin{aligned}J_n(\phi) =& -\frac{1}{2}\int_\Omega\int_\Omega c^\delta(|p-x|)(p-x)^2\left(\frac{\alpha(p)+\alpha(x)}{2}\right)\Big[\phi(p)-\phi(x)\Big]\mathrm{d}p\Big[u_n(x)\Big]\mathrm{d}x\\ &+\frac{1}{2}\int_\Omega\int_\Omega c^\delta(|p-x|)(p-x)^2\left(\frac{\alpha(p)+\alpha(x)}{2}\right)\Big[\phi(p)-\phi(x)\Big]\mathrm{d}x\Big[u_n(p)\Big]\mathrm{d}p.\end{aligned}$$

Applying Fubini's Theorem

$$\begin{aligned}J_n(\phi) =& -\frac{1}{2}\int_\Omega\int_\Omega c^\delta(|p-x|)(p-x)^2\left(\frac{\alpha(p)+\alpha(x)}{2}\right)\Big[\phi(p)-\phi(x)\Big]\mathrm{d}p\Big[u_n(x)\Big]\mathrm{d}x\\ &+\frac{1}{2}\int_\Omega\int_\Omega c^\delta(|p-x|)(p-x)^2\left(\frac{\alpha(p)+\alpha(x)}{2}\right)\Big[\phi(p)-\phi(x)\Big]\Big[u_n(p)\Big]\mathrm{d}p\mathrm{d}x\\ =&\frac{1}{2}\int_\Omega\int_\Omega c^\delta(|p-x|)(p-x)^2\left(\frac{\alpha(p)+\alpha(x)}{2}\right)\Big[\phi(p)-\phi(x)\Big]\Big[u_n(p)-u_n(x)\Big]\mathrm{d}p\mathrm{d}x.\end{aligned}$$

Applying similar steps in the reverse order give us

$$\begin{aligned}J_n(\phi) =& -\int_\Omega\int_\Omega c^\delta(|p-x|)(p-x)^2\left(\frac{\alpha(p)+\alpha(x)}{2}\right)\Big[u_n(p)-u_n(x)\Big]\mathrm{d}p\Big[\phi(x)\Big]\mathrm{d}x\\ =&\int_\Omega\big(\mathcal{L}u_n\big)(x)\phi(x)\mathrm{d}x.\end{aligned}$$

The use of Fubini-Tonelli is justified by the following chain of inequalities

$$\begin{aligned}\big|J_n(\phi)\big| &= \left|\int_\Omega\big(\mathcal{L}u_n\big)(x)\phi(x)\mathrm{d}x\right|\\ &\leq \int_\Omega\Big|\big(\mathcal{L}u_n\big)(x)\phi(x)\Big|\mathrm{d}x\\ &= \int_\Omega\int_\Omega\left(\left[c^\delta(|p-x|)(p-x)^2\left(\frac{\alpha(p)+\alpha(x)}{2}\right)\right]^{\frac{1}{2}}\right)^2\big|u_n(p)-u_n(x)\big|\big|\phi(x)\big|\mathrm{d}p\mathrm{d}x\\ &\overset{\text{Hölder's}}{\leq} \left(\int_\Omega\int_\Omega\left[c^\delta(|p-x|)(p-x)^2\left(\frac{\alpha(p)+\alpha(x)}{2}\right)\right]\big|u_n(p)-u_n(x)\big|^2\mathrm{d}p\mathrm{d}x\right)^{\frac{1}{2}}\\ &\leq \left(\int_\Omega\int_\Omega\left[c^\delta(|p-x|)(p-x)^2\left(\frac{\alpha(p)+\alpha(x)}{2}\right)\right]\big|u_n(p)-u_n(x)\big|^2\mathrm{d}p\mathrm{d}x\right)^{\frac{1}{2}}\\ &\quad\times (E^0)^{\frac{1}{2}}||\phi||_{L^2(\Omega)}.\end{aligned}$$

By assumption we know that

$$\left(\int_\Omega\int_{B_\delta(x)}\left[c^\delta(|p-x|)(p-x)^2\left(\frac{\alpha(p)+\alpha(x)}{2}\right)\right]\big|u_n(p)-u_n(x)\big|^2\mathrm{d}p\mathrm{d}x\right)^{\frac{1}{2}}\to 0 \text{ as } n\to\infty.$$

Because when $d(x,\partial\Omega)<\delta$ we have that $\alpha(p)=\alpha(x)=0$, it follows that

$$\left(\int_\Omega\int_\Omega\left[c^\delta(|p-x|)(p-x)^2\left(\frac{\alpha(p)+\alpha(x)}{2}\right)\right]\big|u_n(p)-u_n(x)\big|^2\mathrm{d}p\mathrm{d}x\right)^{\frac{1}{2}}\to 0 \text{ as } n\to\infty.$$

Therefore, for all $\phi\in C_c^\infty(\Omega)$

$$|J_n(\phi)|\to 0 \text{ as } n\to\infty$$

We will show that $\big(\mathcal{L}\phi\big)\in L^2(\Omega)$. Let

$$A=\left(\int_\Omega\Big[\mathcal{L}\phi\Big]^2\mathrm{d}x\right)^{\frac{1}{2}}$$

Since the absolute value of a quantity is always greater than or equal to the quantity,

$$\begin{aligned}A=&\left(\int_\Omega\left[\int_{B_\delta(x)}c^\delta(|p-x|)(p-x)^2\left(\frac{\alpha(p)+\alpha(x)}{2}\right)\big[\phi(p)-\phi(x)\big]\mathrm{d}p\right]^2\mathrm{d}x\right)^{\frac{1}{2}}\\ \le&\left(\int_\Omega\left[\int_{B_\delta(x)}c^\delta(|p-x|)(p-x)^2\left(\frac{\alpha(p)+\alpha(x)}{2}\right)\big|\phi(p)-\phi(x)\big|\mathrm{d}p\right]^2\mathrm{d}x\right)^{\frac{1}{2}}\end{aligned}$$

Applying the triangle inequality and bounding α by 1,

$$\begin{aligned}A\le&\left(\int_\Omega\left[\int_{B_\delta(x)}c^\delta(|p-x|)(p-x)^2\left(\frac{\alpha(p)+\alpha(x)}{2}\right)\Big(\big|\phi(p)\big|+\big|\phi(x)\big|\Big)\mathrm{d}p\right]^2\mathrm{d}x\right)^{\frac{1}{2}}\\ \le&\left(\int_\Omega\Big(||\phi||_{L^\infty(\Omega)}E^0+|\phi(x)|E^0\Big)^2\mathrm{d}x\right)^{\frac{1}{2}}\\ \le&(1+\sqrt{2})||\phi||_{L^\infty(\Omega)}E^0\big|\Omega\big|^{\frac{1}{2}}+E^0||\phi||_{L^2(\Omega)}\\ <&\infty.\end{aligned}$$

Since $\big(\mathcal{L}\phi\big) \in L^2(\Omega)$ and u is a weak limit of u_n in $L^2(\Omega)$ we have

$$\Big(\big(\mathcal{L}\phi\big), u_n\Big)_{L^2(\Omega)} \to \Big(\big(\mathcal{L}\phi\big), u\Big)_{L^2(\Omega)}.$$

This means that

$$0 = \lim_{n\to\infty} J_n(\phi) = \int_\Omega \big(\mathcal{L}\phi\big)(x)u(x)\mathrm{d}x.$$

Since we know that

$$\int_\Omega \big(\mathcal{L}\phi\big)(x)u(x)\mathrm{d}x = \int_\Omega \big(\mathcal{L}u\big)(x)\phi(x)\mathrm{d}x$$

for any $\phi \in C_c^\infty(\Omega)$, we get that $\big(\mathcal{L}u\big)(x) = 0$ a.e. in Ω. On $\big(\Omega \setminus \Omega_{CE}^+\big)$ we know that $\alpha(x) > 0$, therefore a covering argument shows u is constant a.e. on $\big(\Omega \setminus \Omega_{CE}\big)$. $\square$

The following lemma is taken from Step 2 of Corollary 1 in [38].

Lemma 4.15. *If u_n is a sequence that weakly converges to 0 in $L^2(\Omega)$ on $\big(\Omega \setminus \Omega_{CE}\big)$ such that*

$$\lim_{n\to\infty} \int_\Omega \int_{B_\delta(x)} c^\delta(|p-x|)(p-x)^2 \left(\frac{\alpha(p)+\alpha(x)}{2}\right) \big[u_n(p) - u_n(x)\big]^2 \mathrm{d}p\mathrm{d}x = 0,$$

Then $u_n \to 0$ strongly in $L^2\big(\Omega \setminus \Omega_{CE}\big)$.

Proof. Define the following operator

$$\big(\mathcal{L}v\big)(x) = -\int_{\left(\Omega\setminus\Omega_{CE}\right)} c^\delta(|p-x|)(p-x)^2\big[v(p) - v(x)\big]\mathrm{d}p. \tag{4.9}$$

We can write $\mathcal{L}$ as the sum of two operators

$$\big(\mathcal{L}v\big)(x) = \big(K * \bar{v}\big)(x) + a(x)v(x), \text{ (where } \bar{v} = v(x) \text{ if } x \in \big(\Omega \setminus \Omega_{CE}\big), 0 \text{ otherwise)}$$

where

$$\big(K * \bar{v}\big)(x) = -\int_{\mathbb{R}} c^\delta(|p-x|)(p-x)^2\bar{v}(p)\mathrm{d}p \qquad \text{and}$$

$$a(x) = \int_{\left(\Omega\setminus\Omega_{CE}\right)} c^\delta(|p-x|)(p-x)^2 \mathrm{d}p.$$

Since the convolution operator is a compact operator and $u_n \rightharpoonup u$ in $L^2(\mathbb{R})$, it follows that $\left(K * \bar{u}_n\right) \to 0$ strongly in $L^2(\mathbb{R})$. By the assumption on c^δ and the absolute continuity of the integral, $a(x)$ is a positive continuous function on $\left(\Omega \setminus \Omega_{CE}\right)$. Therefore, there exists a constant c such that $0 < c \leq a(x)$ for all $x \in \left(\Omega \setminus \Omega_{CE}\right)$. Therefore, we obtain that

$$c \lim_{n\to 0} \int_{\left(\Omega\setminus\Omega_{CE}\right)} (u_n)^2 \mathrm{d}x \leq \lim_{n\to 0} \left[\left(K * \bar{u}_n\right)(x) + a(x)u_n(x)\right] = \lim_{n\to 0}\left(\left(\mathcal{L}u_n\right), u_n\right)_{L^2(\Omega)} = 0.$$

$\square$

By Proposition 4.10, it makes sense to discuss the trace of u for each $u \in S(\Omega)$. Therefore, define the following set

$$S_0(\Omega) = \left\{u \in S(\Omega) : tr(u) = 0\right\}. \tag{4.10}$$

It follows that $S_0(\Omega)$ is a linear subspace that is closed with respect to the norm $||\cdot||_{S(\Omega)}$.

On this set, $S_0(\Omega)$, we will consider the following theorem:

Theorem 4.16 (Strong Poincaré Inequality)**.** *Assuming that c^δ satisfies 3.1 and $\left(\Omega^+_{CE} \cap \Omega^+_{PD}\right) = \emptyset$. There exists a $\mathcal{C} > 0$, that may depend on δ, such that*

$$\begin{aligned}||u||^2_{L^2(\Omega)} \leq &\mathcal{C}\left(\int_\Omega\int_{B_\delta(x)} c^\delta(|p-x|)(p-x)^2\left(1-\frac{\alpha(p)+\alpha(x)}{2}\right)\mathrm{d}p\left[u'(x)\right]^2\mathrm{d}x\right.\\ &\left.+\int_\Omega\int_{B_\delta(x)} c^\delta(|p-x|)(p-x)^2\left(\frac{\alpha(p)+\alpha(x)}{2}\right)\left[u(p)-u(x)\right]^2\mathrm{d}p\mathrm{d}x\right)\end{aligned}$$

for all $u \in S_0(\Omega)$.

Proof. For contradiction assume that there exists sequence u_n such that $||u_n||_{L^2(\Omega)} = 1$ for all n, but

$$\begin{aligned}\Bigg(\int_\Omega \int_{B_\delta(x)} c^\delta(|p-x|)(p-x)^2 \left(1 - \frac{\alpha(p)+\alpha(x)}{2}\right) \mathrm{d}p \Big[u_n'(x)\Big]^2 \mathrm{d}x \\ + \int_\Omega \int_{B_\delta(x)} c^\delta(|p-x|)(p-x)^2 \left(\frac{\alpha(p)+\alpha(x)}{2}\right) \Big[u_n(p) - u_n(x)\Big]^2 \mathrm{d}p\mathrm{d}x\Bigg) \to 0\end{aligned} \tag{4.11}$$

as $n \to \infty$.

Since u_n is a bounded sequence in $L^2(\Omega)$ there exists a subsequence u_{n_k} and an element $u \in L^2(\Omega)$ such that

$$\lim_{k\to\infty} (u_{n_k}, v)_{L^2(\Omega)} = (u, v)_{L^2(\Omega)} \ \forall v \in L^2(\Omega).$$

By assumption 4.11 and the non-negativity of the two terms, we have that

$$\left(\int_\Omega \int_{B_\delta(x)} c^\delta(|p-x|)(p-x)^2 \left(1 - \frac{\alpha(p)+\alpha(x)}{2}\right) \mathrm{d}p \Big[u_{n_k}'(x)\Big]^2 \mathrm{d}x\right) \to 0$$

$$\left(\int_\Omega \int_{B_\delta(x)} c^\delta(|p-x|)(p-x)^2 \left(\frac{\alpha(p)+\alpha(x)}{2}\right) \Big[u_{n_k}(p) - u_{n_k}(x)\Big]^2 \mathrm{d}p\mathrm{d}x\right) \to 0.$$

By Lemma 4.13 we have that u, the weak limit of u_{n_k} in $L^2(\Omega)$, is constant almost everywhere on Ω_{CE}^+ and that there is a subsequence $u_{n_{k_m}}$ that converges strongly to u in $L^2(\Omega_{CE}^+)$. Since $u_n \in S_0(\Omega)$, we further get that $u(x) = 0$ on Ω_{CE}^+. By Lemma 4.14, we have that u is constant a.e. in $\big(\Omega \setminus \Omega_{CE}\big)$. Since $\Big|\big(\Omega \setminus \Omega_{CE}\big) \cap \Omega_{CE}^+\Big| > 0$ we have that u is zero almost everywhere on Ω. By Lemma 4.15 we have that that $u_{n_{k_m}}$ converges to 0 strongly in $L^2\big(\Omega \setminus \Omega_{CE}\big)$. Therefore we have shown that $\big|\big|u_{n_{k_m}}\big|\big|_{L^2(\Omega)} \to 0$ as m increases, but this is a contradiction to our assumption that $||u_n||_{L^2(\Omega)} = 1$ for all n. □

This strong Poincaré inequality allows us to prove the following desirable result on the function space $S_0(\Omega)$:

Corollary 4.17 (Weak Blended Poincaré Inequality)**.** *Assuming that c^δ satisfies 3.1 and $\left(\Omega^+_{CE} \cap \Omega^+_{PD}\right) = \emptyset$. There exists a $\mathscr{C} > 0$ (that may depend on δ) such that*

$$||u||^2_{L^2(\Omega)} \leq \mathscr{C}\Bigg(\int_\Omega \int_{B_\delta(x)} c^\delta(|p-x|)(p-x)^2 \left(1 - \frac{\alpha(p)+\alpha(x)}{2}\right) \mathrm{d}p \left[u'(x)\right]^2 \mathrm{d}x \\ + \int_\Omega \int_{B_\delta(x)} c^\delta(|p-x|) \left(\frac{\alpha(p)+\alpha(x)}{2}\right) \left[u(p)-u(x)\right]^2 \mathrm{d}p\mathrm{d}x \Bigg) \tag{4.12}$$

for all $u \in S_0(\Omega)$.

Proof. By Theorem 4.16 for all $u \in S_0(\Omega)$, we have that

$$||u||^2_{L^2(\Omega)} \leq \mathcal{C} \left(\int_\Omega \int_{B_\delta(x)} c^\delta(|p-x|)(p-x)^2 \left[1 - \frac{\alpha(p)+\alpha(x)}{2}\right] \mathrm{d}p[u'(x)]^2 \mathrm{d}x \right. \\ \left. + \int_\Omega \int_{B_\delta(x)} c^\delta(|p-x|)(p-x)^2 \left[\frac{\alpha(p)+\alpha(x)}{2}\right] [u(p)-u(x)]^2 \mathrm{d}p\mathrm{d}x \right).$$

Since $|p-x| < diam(\Omega)$, we know that our desired result will hold. But, since $c^\delta(|p-x|)$ is only nonzero when $|p-x| < \delta$, we actually have a stronger result:

$$\leq \mathcal{C} \left(\int_\Omega \int_{B_\delta(x)} c^\delta(|p-x|)(p-x)^2 \left[1 - \frac{\alpha(p)+\alpha(x)}{2}\right] \mathrm{d}p[u'(x)]^2 \mathrm{d}x \right. \\ \left. + \delta^2 \int_\Omega \int_{B_\delta(x)} c^\delta(|p-x|) \left[\frac{\alpha(p)+\alpha(x)}{2}\right] [u(p)-u(x)]^2 \mathrm{d}p\mathrm{d}x \right) \\ \leq \mathcal{C}|u_n|^2_{S(\Omega)}.$$

Letting $\mathscr{C} = \max(\mathcal{C}, \mathcal{C}\delta^2)$, we obtain the desired result. □

Now that we have proved the weak Poincaré inequality on the subspace $S_0(\Omega)$, we can prove the following result.

Proposition 4.18. *On $S_0(\Omega)$ $||\cdot||_{S_0(\Omega)}$ and $|\cdot|_{S_0(\Omega)}$ are equivalent norms.*

Proof. First we know that for all $u \in S_0(\Omega)$

$$|u|^2_{S_0(\Omega)} \leq |u|^2_{L^2(\Omega)} + |u|^2_{S_0(\Omega)} = ||u||^2_{S_0(\Omega)}.$$

By the weak Poincaré inequality it follows that

$$||u||^2_{L^2(\Omega)} \leq C|u|^2_{S_0(\Omega)}$$

Therefore, we have that

$$|u|^2_{S_0(\Omega)} \leq ||u||^2_{S_0(\Omega)} = |u|^2_{L^2(\Omega)} + |u|^2_{S_0(\Omega)} \leq (C+1)|u|^2_{S_0(\Omega)}.$$

Thus

$$|u|_{S_0(\Omega)} \leq ||u||_{S_0(\Omega)} \leq \sqrt{(C+1)}|u|_{S_0(\Omega)},$$

which means that on the space $S_0(\Omega)$ these two norms are equivalent. □

It follows that $S_0(\Omega)$ is a linear space that is closed with respect to the seminorm $|\cdot|_{S(\Omega)}$. Therefore, it follows that (assuming $\left(\Omega^+_{CE} \cap \Omega^+_{PD}\right) = \emptyset$) $(S_0(\Omega), |\cdot|_{S(\Omega)})$ is a **Hilbert Space** and that if $u \in S_0(\Omega)$ and $|u|_{S(\Omega)} = 0$, then $u = 0$. $S_0(\Omega)$ is the blended analogue to $H^1_0(\Omega)$ and $\mathbb{S}_0(\Omega^*)$ in Chapters 1 and 2 respectively. Therefore, analogously we say the **weak formulation** corresponding to the homogeneous Dirichlet-type BVP is given by: find a $u \in S_0(\Omega)$ such that

$$\big(u, v\big)_{S(\Omega)} = \int_\Omega f(x)v(x)\mathrm{d}x \tag{4.13}$$

for all $v \in S_0(\Omega)$ and where $(\cdot, \cdot)_{S(\Omega)}$ is defined by equation 4.8.

By Hölder's inequality $(\cdot, \cdot)_S$ is a bounded linear operator on $S_0(\Omega)$. Therefore, we can apply Lax-Millgram Theorem to get the weak formulation of the energy-based blended problem.

Theorem 4.19. *If f is an element of $L^2(\Omega)$, then there exists a unique $u \in S_0(\Omega)$ such that*

$$(u, v)_S = (f, v)_2 \quad \forall v \in S_0(\Omega).$$

4.2 Strong formulation of the homogeneous Dirichlet-type BVP

Now that we have a weak solution to the weak formulation of the problem, we will derive the corresponding strong formulation of this problem. Although the strong formulation is not needed for the mathematical analysis of the problem, as showing existence and uniqueness of weak solutions was the goal, the strong formulation of the problem will be useful in both completing the analogy between the three discussed models and in manufacturing solutions for testing of the finite element method code. Recalling that, for both the local and nonlocal models, integration by parts was used to derive the weak formulations as well as the energy bilinear forms, therefore integration by parts will be used on the blended energy bilinear form to derive a strong formulation of the blended model. In this case, because we have both a local and a nonlocal term in our bilinear form, we will need to use both local and nonlocal integration by parts. Start with the weak formulation of the problem:
Given $f \in L^2(\Omega)$, find $u \in S_0(\Omega)$ such that

$$(u, v)_S = \int_\Omega f(x)v(x)\mathrm{d}x \tag{4.14}$$

for all $v \in S_0(\Omega)$, where

$$\begin{aligned}(u, v)_S = &\int_\Omega [u'(x)v'(x)] \int_{B_\delta(x)} c^\delta(|p-x|)(p-x)^2 \left(1 - \frac{\alpha(p)+\alpha(x)}{2}\right) \mathrm{d}p\mathrm{d}x \\ &+ \int_\Omega \int_{B_\delta(x)} c^\delta(|p-x|) \left(\frac{\alpha(p)+\alpha(x)}{2}\right) [u(p)-u(x)][v(p)-v(x)]\mathrm{d}p\mathrm{d}x.\end{aligned}$$

For clarity, in the application of integration by parts, the local and nonlocal terms will be considered separately. First consider,

$$\int_\Omega [u'(x)v'(x)] \int_{B_\delta(x)} c^\delta(|p-x|)(p-x)^2 \left(1 - \frac{\alpha(p)+\alpha(x)}{2}\right) \mathrm{d}p\mathrm{d}x.$$

The goal is to move the derivative off of v, and for simplicity, we will denote

$$\Phi(x) = \int_{B_\delta(x)} c^\delta(|p-x|)(p-x)^2 \left(1 - \frac{\alpha(p)+\alpha(x)}{2}\right) \mathrm{d}p.$$

Through an application of integration by parts and then the chain rule we have

$$\begin{aligned}\int_\Omega \Phi(x)u'(x)v'(x)\mathrm{d}x =& \Phi(x)u'(x)v(x)\Big|_{\partial\Omega} - \int_\Omega \frac{\partial}{\partial x}(\Phi(x)u'(x))\ v(x)\mathrm{d}x \\ =& \Phi(x)u'(x)v(x)\Big|_{\partial\Omega} - \int_\Omega (\Phi'(x)u'(x) + \Phi(x)u''(x))\ v(x)\mathrm{d}x\end{aligned}$$

By assumption $v \in S_0(\Omega)$, therefore $\Phi(x)u'(x)v(x)|_{\partial\Omega} = 0$. As with the strong form of the previous problems discussed, to state the strong formulation of the problem, we need to require that u is twice differentiable. In an ideal situation, we would be able to take the derivative of the product $\Phi u'$. Therefore, assuming we can take the derivative we can better understand what requirements on α will be necessary for the strong form. Despite the fact that the local region occurs near the boundary, this blended model will have surface effects. Surface effects are forces that come from interactions between material points and points outside of the material. Since we do not want to look at the surface effects, we will determine the explicit form of the force by considering the model away from the boundary .

For $x \in \Omega$ such that $d(x, \partial\Omega) > \delta$ (i.e $x \in \mathring{\Omega}$), we have

$$\begin{aligned}\Phi'(x) =& \frac{d}{dx}\int_{B_\delta(x)} c^\delta(|p-x|)(p-x)^2 \left(1 - \frac{\alpha(p)+\alpha(x)}{2}\right) \mathrm{d}p \\ =& \frac{d}{dx}\int_{B_\delta(0)} c^\delta(\xi)(\xi)^2 \left(1 - \frac{\alpha(x+\xi)+\alpha(x)}{2}\right) \mathrm{d}\xi \\ =& \int_{B_\delta(0)} c^\delta(\xi)(\xi)^2 \frac{d}{dx}\left(1 - \frac{\alpha(x+\xi)+\alpha(x)}{2}\right) \mathrm{d}\xi \\ =& -\int_{B_\delta(0)} c^\delta(\xi)(\xi)^2 \left(\frac{\alpha'(x+\xi)+\alpha'(x)}{2}\right) \mathrm{d}\xi.\end{aligned}$$

It is precisely because we are away from the boundary, that we are allowed to do the change of variables $\xi = p - x$. This change of variables, allows us to see that since everything else is independent of x, we can just take the derivative of the term involving α.

As you can see in order to state the strong formulation of the problem we will need to assume that u is twice differentiable in the appropriate part of the domain, and also that α is (weakly) differentiable on Ω^*.

Now we will apply nonlocal integration by parts to the nonlocal term of the bilinear form

$$\begin{aligned}\int_\Omega \int_{B_\delta(x)} c^\delta(|p-x|)\left(\frac{\alpha(p)+\alpha(x)}{2}\right)[u(p)-u(x)][v(p)-v(x)]\mathrm{d}p\mathrm{d}x \\ = -2\int_\Omega \int_{B_\delta(x)} c^\delta(|p-x|)\left(\frac{\alpha(p)+\alpha(x)}{2}\right)[u(p)-u(x)][v(x)]\mathrm{d}p\mathrm{d}x\end{aligned}$$

Noting that because the entire nonlocal piece of the bilinear form is finite Fubini's is justified. Since we are working with $u, v \in S_0(\Omega)$, we know that we are dealing with homogenous Dirichlet-type boundary conditions (this was the reason we could get rid of the boundary term from the local integration by parts). Now we can state the strong formulation of the problem:

Definition 4.20. *Assume that c^δ satisfies 3.1and $\left(\Omega^+_{CE} \cap \Omega^+_{PD}\right) = \emptyset$. Further assume that the blending function α is differentiable, and given $f \in L^2(\Omega)$. There exists u that is twice differentiable on $\Omega \setminus \Omega_{PD}$, such that*

$$\begin{cases} -(\Phi'(x)u'(x) + \Phi(x)u''(x)) & \\ \quad -2\displaystyle\int_{B_\delta(x)} c^\delta(|p-x|)\left(\frac{\alpha(p)+\alpha(x)}{2}\right)[u(p)-u(x)]\mathrm{d}p = f, & x \in \Omega \\ \qquad\qquad u(x) = 0, & x \in \partial\Omega. \end{cases} \tag{4.15}$$

where

$$\Phi(x) = \int_{B_\delta(x)} c^\delta(|p-x|)(p-x)^2\left(1-\frac{\alpha(p)+\alpha(x)}{2}\right)\mathrm{d}p.$$

.

4.3 The nonhomogeneous Dirichlet-type blended BVP

In Chapters 1 and 2 the nonhomogeneous boundary valued problems or BVP (2.2 and 1.1) were given and the weak formulation of the problems were shown to be 1.17 and 2.10. In Chapter 4 the homogeneous BVP 4.15 was derived from the weak formulation 4.14. In order to analogously discuss the implementation of each of these three methods, the nonhomogeneous BVP and it associated weak formulation must be stated for the blended model. Consider the nonhomogeneous BVP for the blended model,

$$\begin{cases} -\left\{[\Phi'(x)u'(x) + \Phi(x)u''(x)] + 2\int_{B_\delta(x)} c^\delta(|p-x|)\left(\frac{\alpha(p)+\alpha(x)}{2}\right)[u(p)-u(x)]\mathrm{d}p\right\} \\ \qquad\qquad = f(x), \qquad\qquad\qquad\qquad x \in \Omega \\ u(a) = g_a, u(b) = g_b \end{cases} \tag{4.16}$$

where

$$\Phi(x) = \int_{B_\delta(x)} c^\delta(|p-x|)(p-x)^2\left(1 - \frac{\alpha(p)+\alpha(x)}{2}\right)\mathrm{d}p.$$

Let g be defined as it was for the classical model: see equation 1.2. If $w(x) := u(x) - g(x)$, observe

$$\begin{aligned} &-(\Phi'(x)w'(x) + \Phi(x)w''(x)) - 2\int_{B_\delta(x)} c^\delta(|p-x|)\left(\frac{\alpha(p)+\alpha(x)}{2}\right)[w(p)-w(x)]\mathrm{d}p \\ &\quad = -\left(\Phi'(x)u'(x) + \Phi(x)u''(x)\right) - 2\int_{B_\delta(x)} c^\delta(|p-x|)\left(\frac{\alpha(p)+\alpha(x)}{2}\right)[u(p)-u(x)]\mathrm{d}p \\ &\qquad + (\Phi'(x)g'(x) + \Phi(x)g''(x)) + 2\int_{B_\delta(x)} c^\delta(|p-x|)\left(\frac{\alpha(p)+\alpha(x)}{2}\right)[g(p)-g(x)]\mathrm{d}p \\ &\quad = f(x) + \Phi'(x)g'(x) + 2\int_{B_\delta(x)} c^\delta(|p-x|)\left(\frac{\alpha(p)+\alpha(x)}{2}\right)[g(p)-g(x)]\mathrm{d}p \\ &\quad = f(x) + \Phi'(x)\left(\frac{g_b-g_a}{b-a}\right) + \left(\frac{g_b-g_a}{b-a}\right)\int_{B_\delta(x)} c^\delta(|p-x|)\Big(\alpha(p)+\alpha(x)\Big)[p-x]\mathrm{d}p \end{aligned} \tag{4.17}$$

Since

$$\begin{aligned}\Phi(x) =& \int_{B_\delta(x)} c^\delta(|p-x|)(p-x)^2 \left(1 - \frac{\alpha(p)+\alpha(x)}{2}\right) \mathrm{d}p \\ =& \left(1 - \frac{\alpha(x)}{2}\right) \int_{B_\delta(x)} c^\delta(|p-x|)(p-x)^2 \mathrm{d}p - \int_{B_\delta(x)} c^\delta(|p-x|)(p-x)^2 \left(\frac{\alpha(p)}{2}\right) \mathrm{d}p \\ =& \left(1 - \frac{\alpha(x)}{2}\right) E^0 - \int_{B_\delta(0)} c^\delta(|\xi|)\xi^2 \left(\frac{\alpha(x+\xi)}{2}\right) \mathrm{d}\xi,\end{aligned} \tag{4.18}$$

it is clear that

$$\Phi'(x) = -\left(\frac{\alpha'(x)}{2}\right) E^0 - \int_{B_\delta(0)} c^\delta(|\xi|)\xi^2 \left(\frac{\alpha'(x+\xi)}{2}\right) \mathrm{d}\xi. \tag{4.19}$$

Therefore, w satisfies the homogeneous BVP

$$\begin{cases} -(\Phi'(x)w'(x) + \Phi(x)w''(x)) - 2\displaystyle\int_{B_\delta(x)} c^\delta(|p-x|) \left(\frac{\alpha(p)+\alpha(x)}{2}\right) [w(p)-w(x)]\mathrm{d}p \\ \qquad\qquad\qquad\qquad\qquad\qquad = F_B(x), \qquad\qquad x \in \Omega \\ w(a) = 0, w(b) = 0 \end{cases} \tag{4.20}$$

and the associated weak formulation is given by

$$(w, v)_S = \int_\Omega F_B(x)v(x)\mathrm{d}x, \tag{4.21}$$

where

$$\begin{aligned}F_B(x) = f(x) - &\left[\left(\frac{\alpha'(x)}{2}\right) E^0 + \int_{B_\delta(0)} c^\delta(|\xi|)\xi^2 \left(\frac{\alpha'(x+\xi)}{2}\right) \mathrm{d}\xi\right] \left(\frac{g_b - g_a}{b-a}\right) \\ &+ \left(\frac{g_b - g_a}{b-a}\right) \int_{B_\delta(x)} c^\delta(|p-x|) \Big(\alpha(p)\Big) [p-x]\mathrm{d}p.\end{aligned} \tag{4.22}$$

Chapter 5

Ghost Force Analysis

5.1 Definition

One way in which the quality of a coupling method is evaluated is through an investigation of the ghost forces that arise from the coupling. The ghost force is the nonzero force required in the strong formulation of the problem to get a linear displacement $u(x) = Ax + B$ as the solution where $A, B \in \mathbb{R}$. In the classical (local) problem given by equation 1.1, the force required to get a linear displacement is 0. This can be seen by applying the local differential operator $-\Delta$ to the desired u,

$$-\Delta u(x) = -\frac{d^2}{dx^2}(Ax + B) = 0. \tag{5.1}$$

Similarly, if you apply the peridynamic operator from equation 2.2 to the desired displacement

$$
\begin{aligned}
-\int_{B_\delta(x)} c^\delta(|p-x|)[u(p)-u(x)]\mathrm{d}p &= -\int_{B_\delta(x)} c^\delta(|p-x|)[Ap+B-Ax-B]\mathrm{d}p \\
&= \int_{B_\delta(x)} c^\delta(|p-x|)[A(p-x)]\mathrm{d}p \\
&= -A\int_{B_\delta(0)} c^\delta(|\xi|)\xi\mathrm{d}\xi \quad \text{(an odd function)} \\
&= 0.
\end{aligned}
\tag{5.2}
$$

Now consider the nonhomogeneous BVP given by 4.16. First notice that the integro-differential operator

$$
\mathscr{L}u := -(\Phi'(x)u'(x) + \Phi(x)u''(x)) - 2\int_{B_\delta(x)} c^\delta(|p-x|)\left(\frac{\alpha(p)+\alpha(x)}{2}\right)[u(p)-u(x)]\mathrm{d}p
$$

is the same one that was given in the homogeneous BVP 4.15. Observe that since

$$
\begin{aligned}
\Phi(x) = &\int_{B_\delta(x)} c^\delta(|p-x|)(p-x)^2\left(1-\frac{\alpha(p)+\alpha(x)}{2}\right)\mathrm{d}p \\
=&\left(1-\frac{\alpha(x)}{2}\right)\int_{B_\delta(x)} c^\delta(|p-x|)(p-x)^2\mathrm{d}p - \int_{B_\delta(x)} c^\delta(|p-x|)(p-x)^2\left(\frac{\alpha(p)}{2}\right)\mathrm{d}p \\
=&\left(1-\frac{\alpha(x)}{2}\right)E^0 - \int_{B_\delta(0)} c^\delta(|\xi|)\xi^2\left(\frac{\alpha(x+\xi)}{2}\right)\mathrm{d}\xi,
\end{aligned}
\tag{5.3}
$$

it is clear that when α is a continuous function,

$$
\Phi'(x) = -\left(\frac{\alpha'(x)}{2}\right)E^0 - \int_{B_\delta(0)} c^\delta(|\xi|)\xi^2\left(\frac{\alpha'(x+\xi)}{2}\right)\mathrm{d}\xi. \tag{5.4}
$$

Applying this integro-differential operator $\mathscr{L}$ to the linear displacement $u(x) = Ax + B$ as we did for both the classical and peridynamic cases, it becomes clear that in the strong form of the blended model the force required is

$$
\begin{aligned}
F_g(x) =& \left[\left(\frac{\alpha'(x)}{2}\right)E^0 + \int_{B_\delta(0)} c^\delta(|\xi|)\xi^2\left(\frac{\alpha'(x+\xi)}{2}\right)\mathrm{d}\xi\right]A \\
& - 2A\int_{B_\delta(0)} c^\delta(|\xi|)\xi\left(\frac{\alpha(x+\xi)+\alpha(x)}{2}\right)\mathrm{d}\xi \\
=& \frac{AE^0}{2}\Big(\alpha'(x)\Big) + \frac{A}{2}\int_{B_\delta(0)} c^\delta(|\xi|)\xi^2\Big(\alpha'(x+\xi)\Big)\mathrm{d}\xi \\
& - A\int_{B_\delta(0)} c^\delta(|\xi|)\xi\Big(\alpha(x+\xi)+\alpha(x)\Big)\mathrm{d}\xi.
\end{aligned}
\tag{5.5}
$$

The force given in 5.5 denoted F_g will be called the **ghost force**. First notice that for all $x \in \Omega_{CE}$, the ghost force vanishes. The ghost force vanishes in this region because for all $x \in \Omega_{CE}$ it is clear that

$$\alpha'(x+\xi) = 0 \text{ and } \alpha(x+\xi) = 0$$

for all $\xi \in B_\delta(0)$. Similarly, for $x \in \Omega_{PD}$ the ghost force vanishes. Therefore, the ghost force can only have nonzero value when $x \in \Omega_B$, which agrees with our intuition of the blended model.

Since the ghost force at each point $x \in \Omega_B$ is dependent on the blending function α, further analysis must be done on how the smoothness of α and the length of the blending region affect the ghost force.

5.2 Analysis

In order to analyze these properties, consider the following simplification of the model by centering the blending region on $x = 0$ and let $2b$ be the length of the first component $\mathring{\Omega}_B$. For clarity this simplification is illustrated in Figure 5.1. Although in previous sections $\mathring{\Omega}_B$ referred to two disjoint regions as shown in Figure 4.1, for simplicity of notation in the ***rest*** of this section (5.2), $\mathring{\Omega}_B$ will refer to the interval $[-b, b]$. The exploration and analysis of the ghost force was done in **Mathematica** so that no information would be lost in the

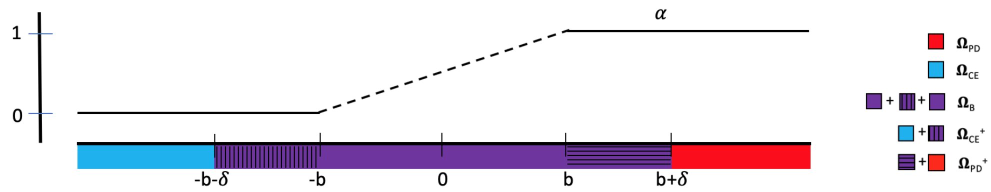

Figure 5.1: Simplification of the model domain

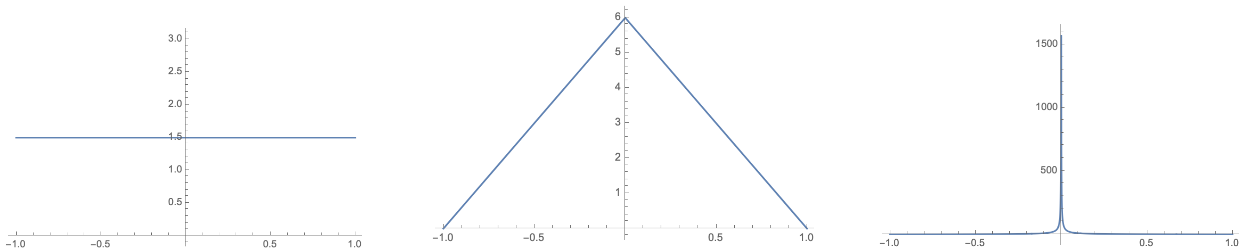

(a) $c_0(z) = \frac{3}{2} \forall z \in (-1, 1)$ (b) $c_1(z) = -6|z| + 6 \forall z \in (-1, 1)$ (c) $c_2(z) = \frac{1}{|z|} \forall z \in (-1, 1)$

Figure 5.2: Unscaled kernel functions explicitly considered for this analysis.

discretization of the ghost force, (i.e. exact integration was used). Although the kernel is only assumed to satisfy the properties outlined by equation 3.1, in order to explore the effects of changing b and the smoothness of α, assume that c is a nonnegative, nonincreasing radial function with support $B_1(0)$ such that

$$\int_{B_1(0)} c(|z|) z^2 \mathrm{d}z = 1. \tag{5.6}$$

Therefore, let c^δ be the following scaling of c

$$c^\delta(z) = \frac{E^0}{\delta^3} c\left(\frac{z}{\delta}\right). \tag{5.7}$$

It can easily be shown that such a c^δ satisfies the requirements given in equation 3.1. Defining c^δ as a particular scaling of c, allows us to explicitly consider different types of kernels. Specifically in this exploration, the effects of changing b and the smoothness of the blending function will be considered for three different c functions. These three functions are defined and illustrated in Figure 5.2. For each of these kernels consider four different blending functions:

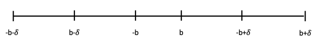

(a) $0 < |\mathring{\Omega}_B| < \delta$

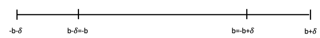

(b) $|\mathring{\Omega}_B| = \delta$

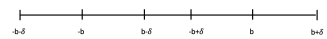

(c) $\delta < |\mathring{\Omega}_B| < 2\delta$

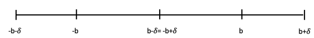

(d) $2\delta = |\mathring{\Omega}_B|$

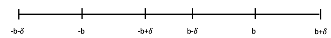

(e) $2\delta < |\mathring{\Omega}_B|$

Figure 5.3: Possible ratios of $|\mathring{\Omega}_B|$ to δ.

1. a continuous blending function that is *linear* on $\mathring{\Omega}_B$ (referred to as $\boldsymbol{\alpha_1}$)

2. a continuously differentiable function that is *cubic* on $\mathring{\Omega}_B$ (referred to as $\boldsymbol{\alpha_3}$)

3. a twice continuously differentiable function that is *quintic* on $\mathring{\Omega}_B$ (referred to as $\boldsymbol{\alpha_5}$)

4. a three times continuously differentiable function that is *septic* on on $\mathring{\Omega}_B$ (referred to as $\boldsymbol{\alpha_7}$)

Fix $\delta = 0.5$.
Through varying the smoothness of the blending function and keeping the length of the region $\mathring{\Omega}_B$ we can explore how this smoothness of ultimately affects the ghost force.
Alternatively through varying length of the region $\mathring{\Omega}_B$ and fixing the smoothness of the blending function, we will explore how the length of $|\mathring{\Omega}_B|$ affects the ghost forces. Specifically we will consider $|\mathring{\Omega}_B| = 2b = 0.1, 0.3, 0.5, 0.7, 0.9, 1, 1.3, 1.5,$ and 1.7.
These specific choices for $|\mathring{\Omega}_B|$ consider the possible five cases of how $|\mathring{\Omega}_B|$ relates to δ. These cases are illustrated in Figure 5.3. We will do the above mentioned the analysis for all three of functions c_i given in Figure 5.2. The data generated through this exploration will help us to establish patterns on how choices of both the smoothness and the length of $\mathring{\Omega}_B$ affect the ghost forces.

5.2.1 Effects of varying $|\mathring{\Omega}_B|$

To explore the effects of changing $|\mathring{\Omega}_B|$, fix a unscaled kernel c_i and a smoothness of blending function α_k and vary $|\mathring{\Omega}_B|$. Fixing the smoothness of the blending function to be the continuous piecewise linear blending function, α_1, and plotting the ghost force (5.5) generates the following three figures (Figure 5.4, 5.5 and 5.6) corresponding to the three unscaled kernels.

Fixing the smoothness of the blending function to be the continuously differentiable piecewise cubic blending function, α_3, and plotting the ghost force (5.5) generates the following three figures (Figure 5.7, 5.8 and 5.9) corresponding to the three unscaled kernels.

Fixing the smoothness of the blending function to be the twice continuously differentiable piecewise quintic blending function, α_5, and plotting the ghost force (5.5) generates the following three figures (Figure 5.10, 5.11 and 5.12) corresponding to the three unscaled kernels.

Fixing the smoothness of the blending function to be the three times continuously differentiable piecewise septic blending function, α_7, and plotting the ghost force (5.5) generates the following three figures (Figure 5.13, 5.14 and 5.15) corresponding to the three unscaled kernels

In each of the Figures 5.4, 5.5, 5.6, 5.7, 5.8, 5.9,5.10, 5.11, 5.12, 5.13, 5.14, and 5.15 it can be visually observed that the maximum value that $F_g(x)$ takes decreases as the length of $\mathring{\Omega}_B$ increases. Therefore, without even doing further calculations our hypothesis would be that regardless of the choice of unscaled kernel c_i or smoothness of the blending function a_i, the maximum value that $F_g(x)$ takes decreases as the length of $\mathring{\Omega}_B$ increases. From these plots, one might suggest that the 'size' of the ghost force decreases as the length of $\mathring{\Omega}_B$ increases.

To confirm this hypothesis from the visual observation, we calculate the L^1-norms of each plotted ghost force. These values are tabulated in Tables 5.1a, 5.2a, and 5.3a. Since we

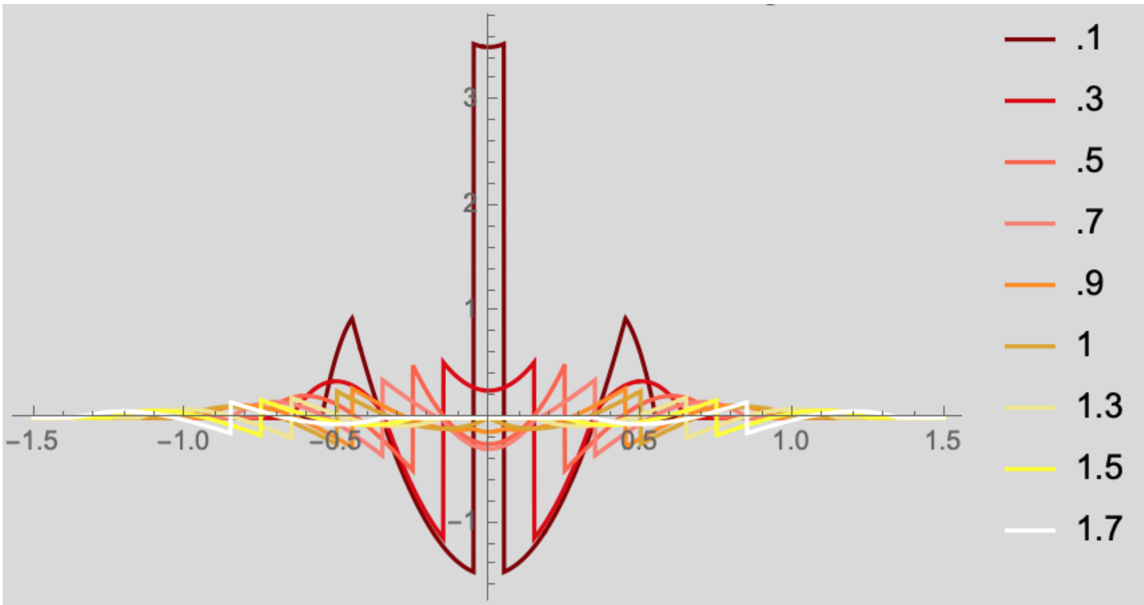

(a) All specified lengths

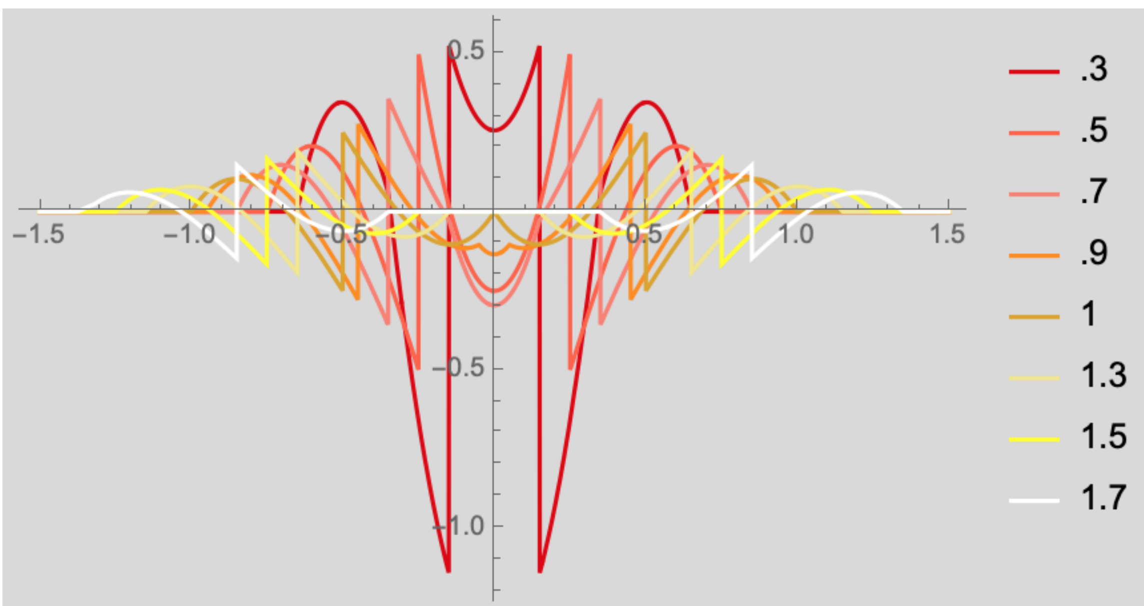

(b) $|\mathring{\Omega}_B| = .1$ removed for visual clarity

Figure 5.4: Fix c_0 and α_1.

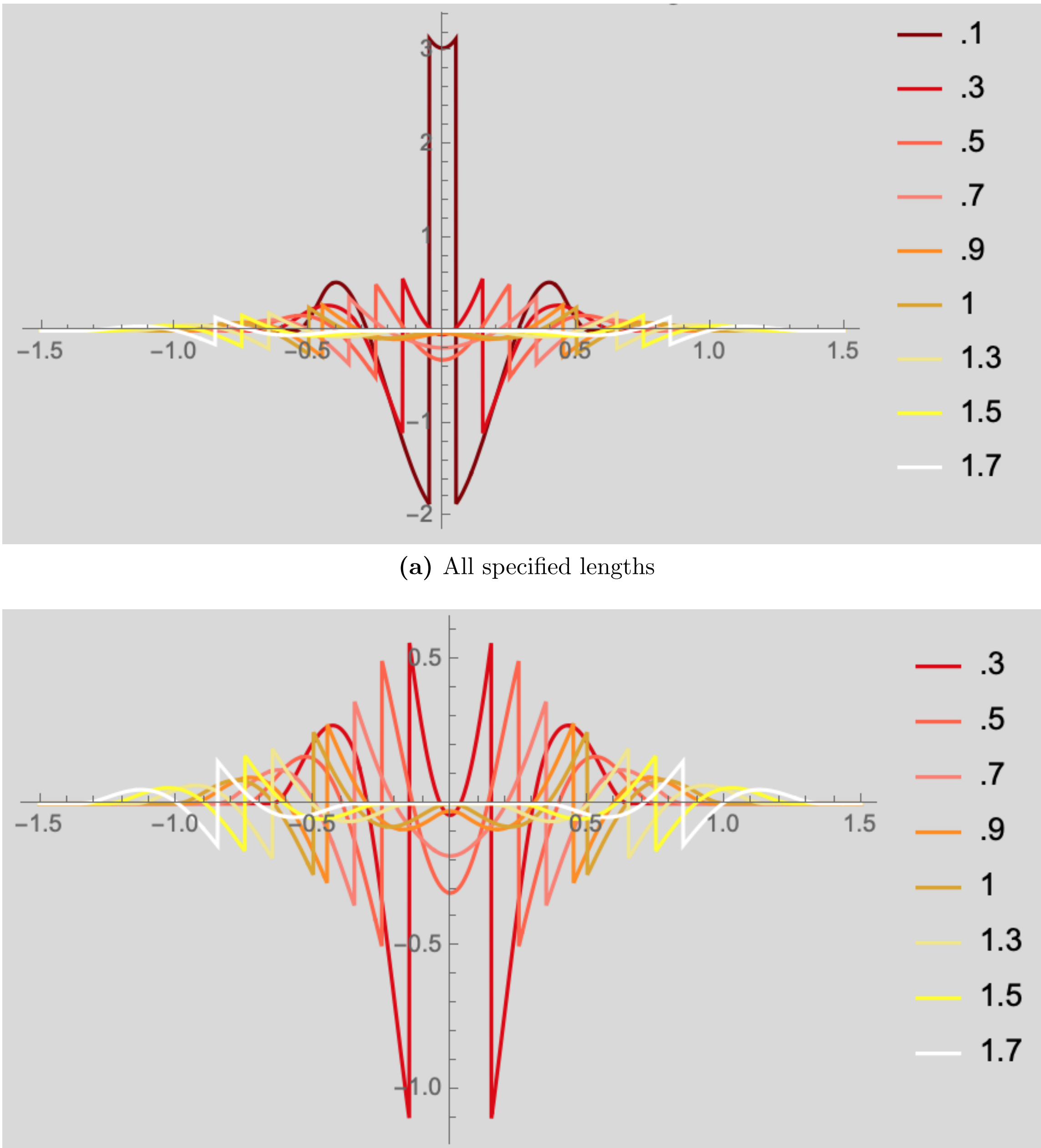

(a) All specified lengths

(b) $|\mathring{\Omega}_B| = .1$ removed for visual clarity

Figure 5.5: Fix c_1 and α_1.

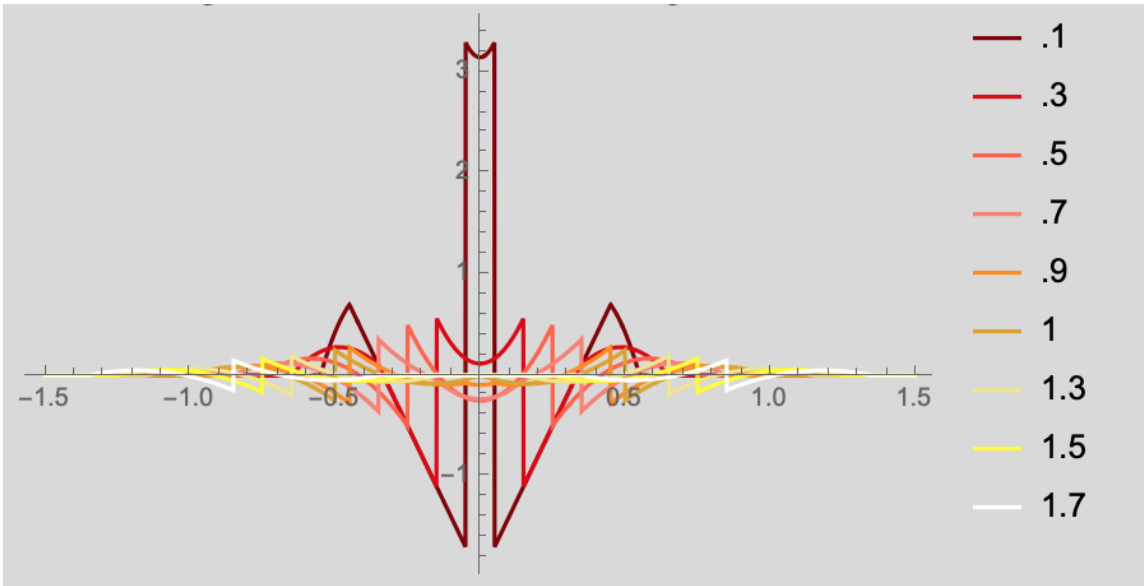

(a) All specified lengths

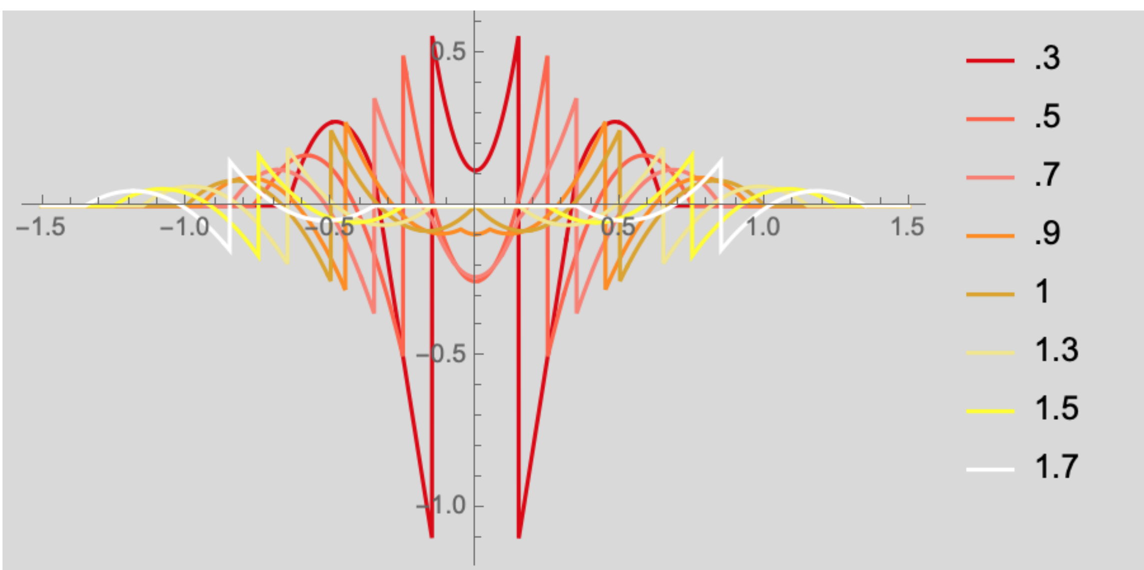

(b) $|\mathring{\Omega}_B| = .1$ removed for visual clarity

Figure 5.6: Fix c_2 and α_1.

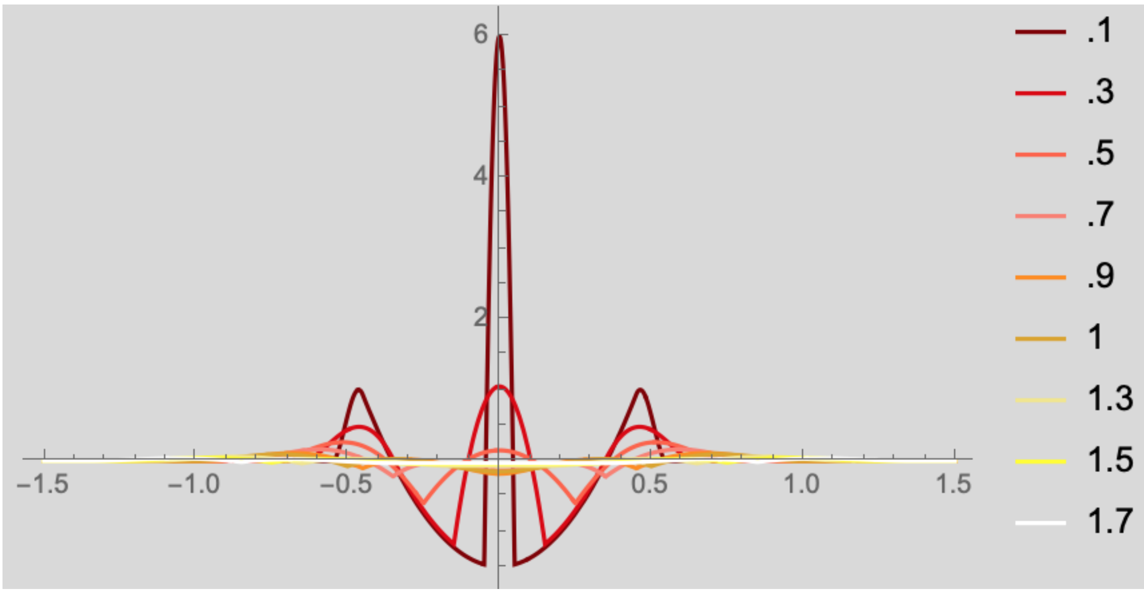

(a) All specified lengths

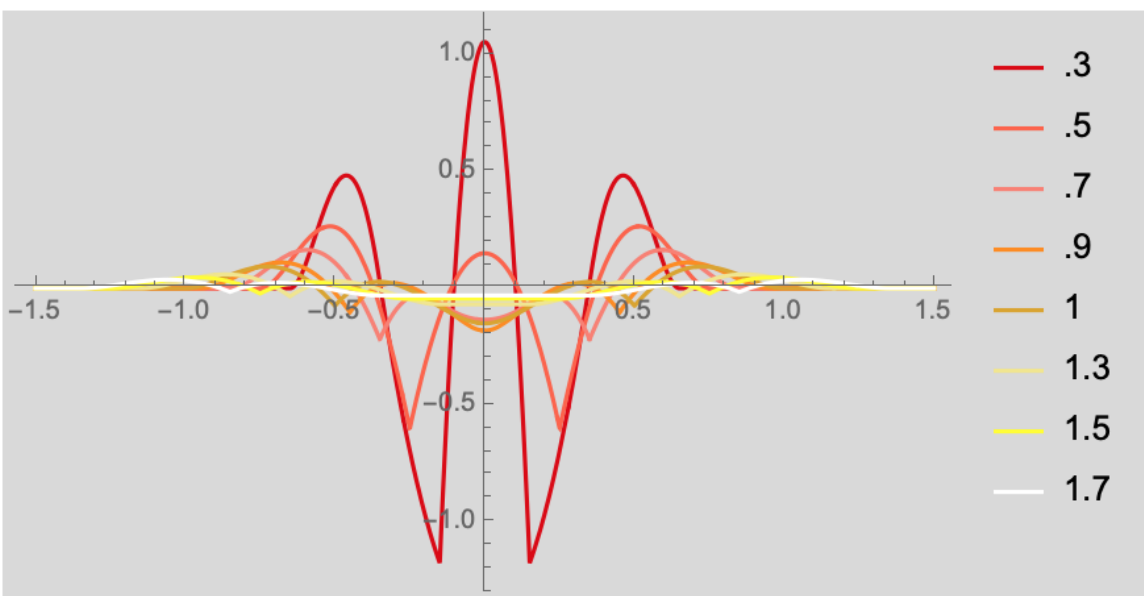

(b) $|\mathring{\Omega}_B| = .1$ removed for visual clarity

Figure 5.7: Fix c_0 and α_3.

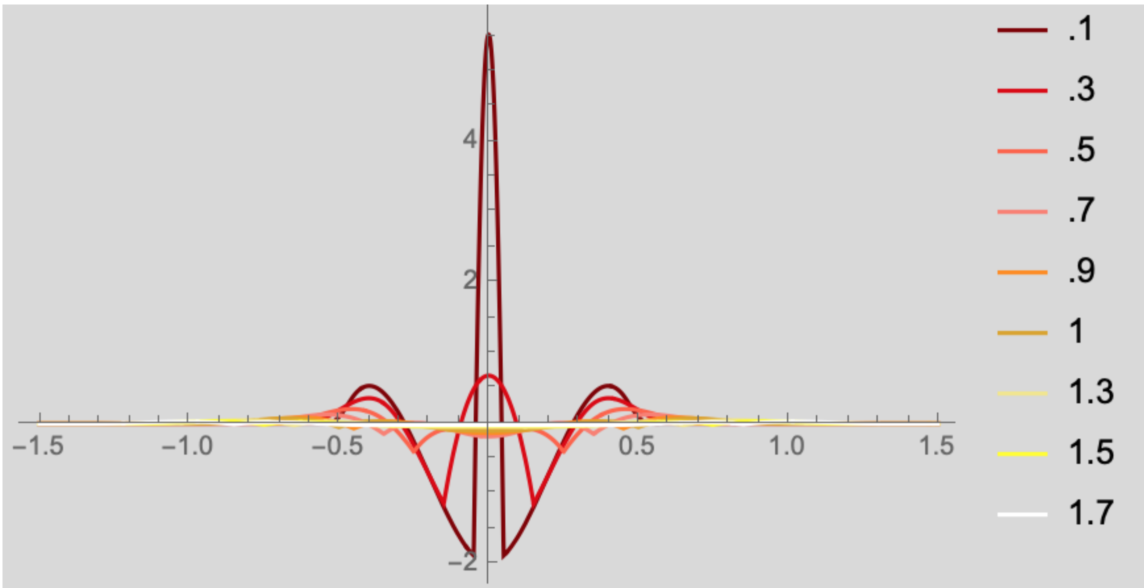

(a) All specified lengths

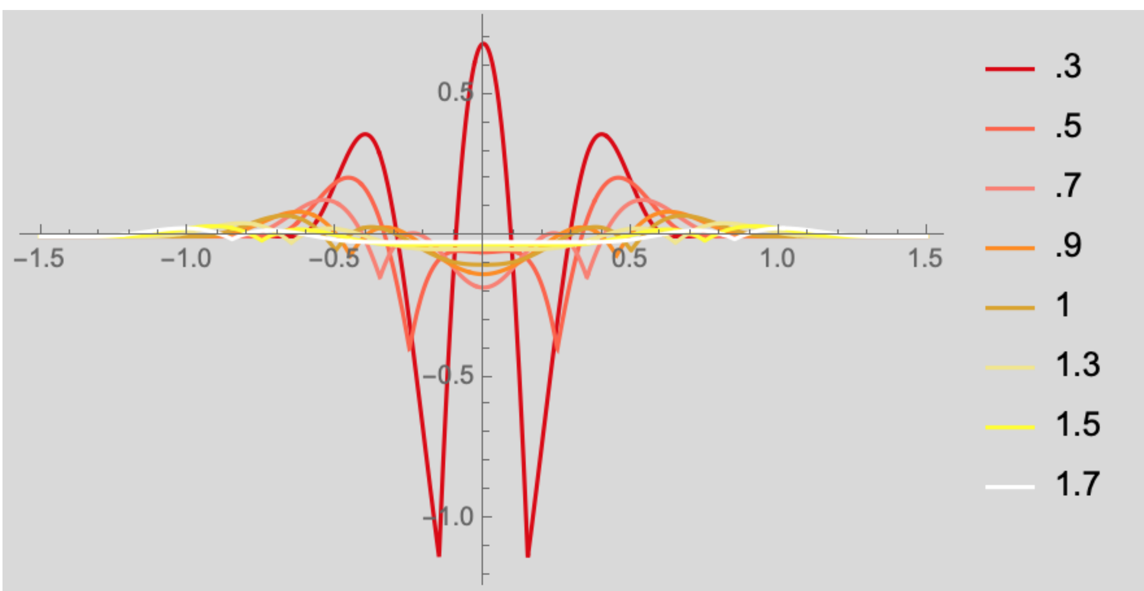

(b) $|\mathring{\Omega}_B| = .1$ removed for visual clarity

Figure 5.8: Fix c_1 and α_3.

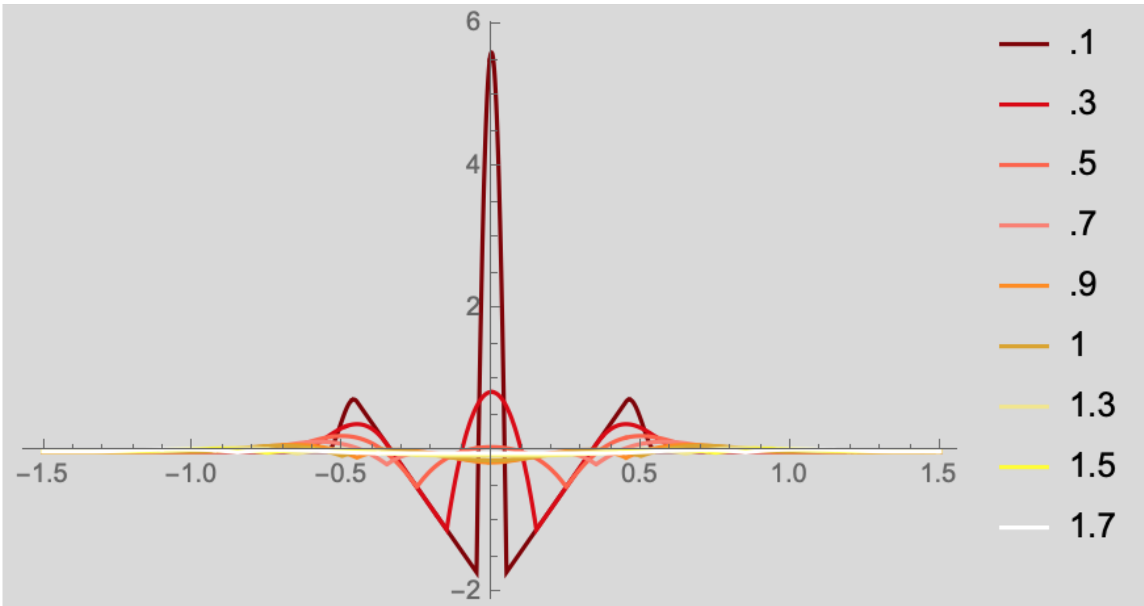

(a) All specified lengths

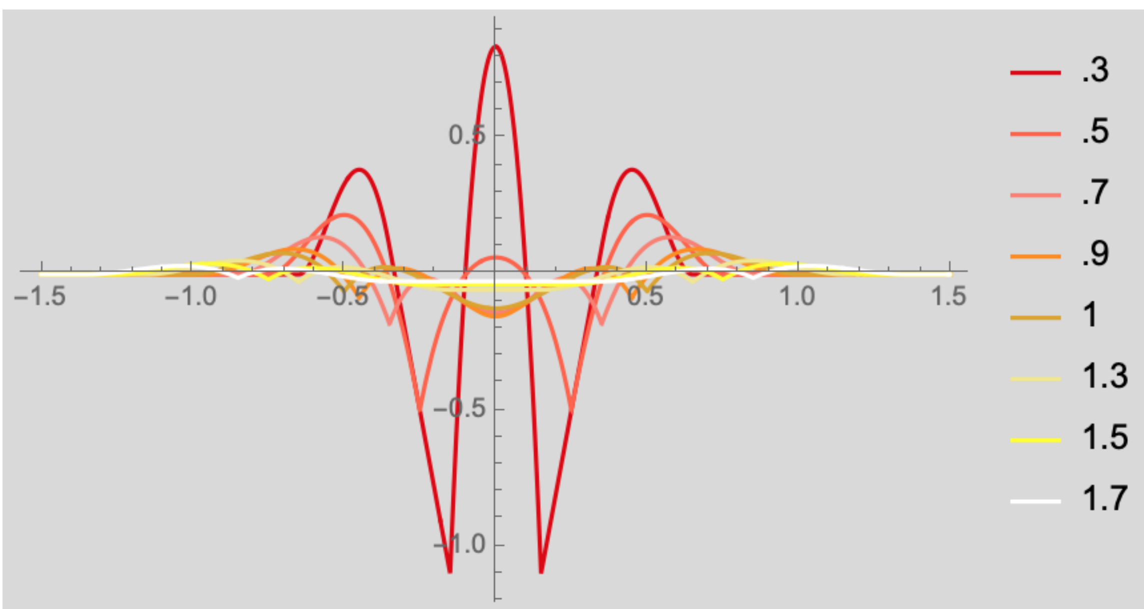

(b) $|\mathring{\Omega}_B| = .1$ removed for visual clarity

Figure 5.9: Fix c_2 and α_3.

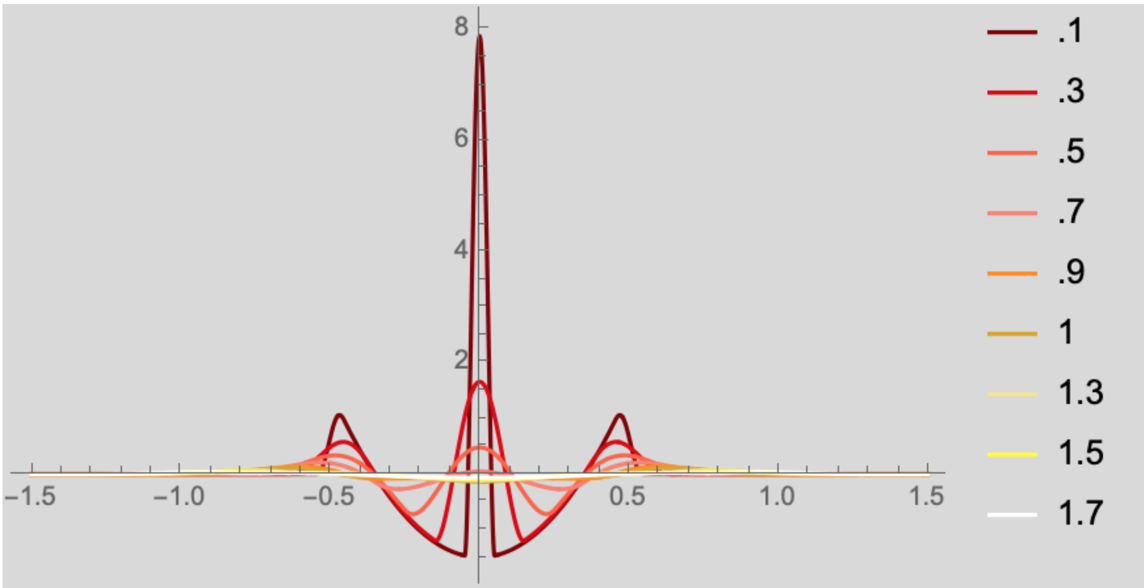

(a) All specified lengths

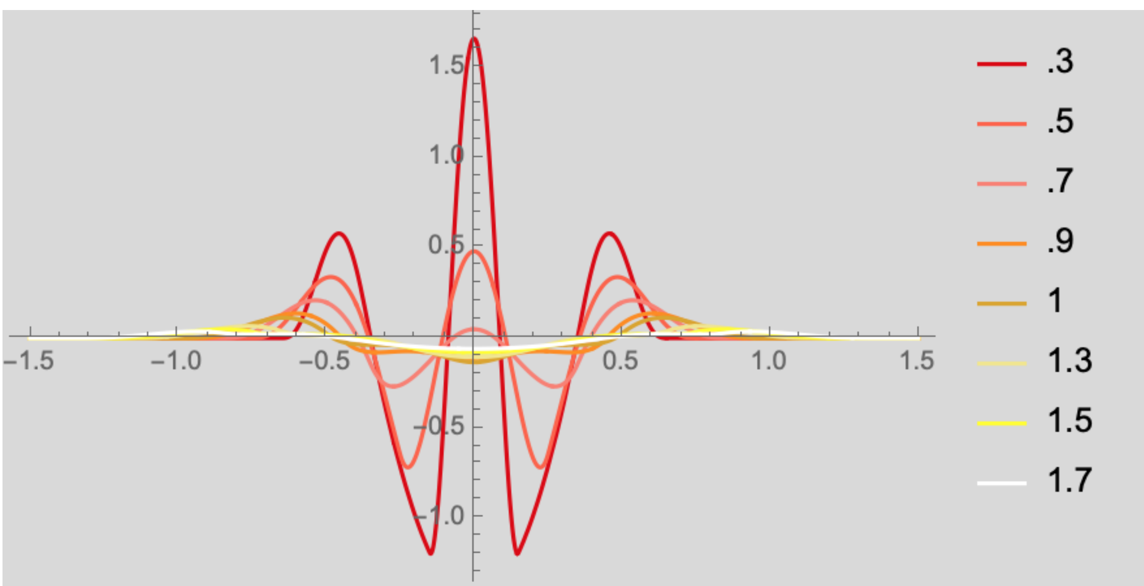

(b) $|\mathring{\Omega}_B| = .1$ removed for visual clarity

Figure 5.10: Fix c_0 and α_5.

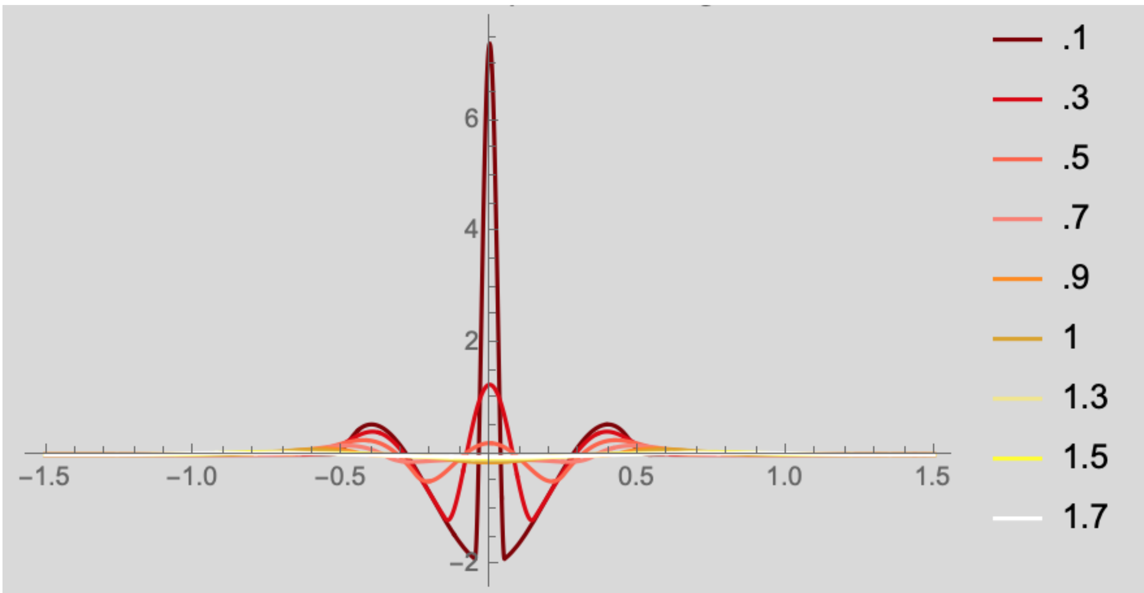

(a) All specified lengths

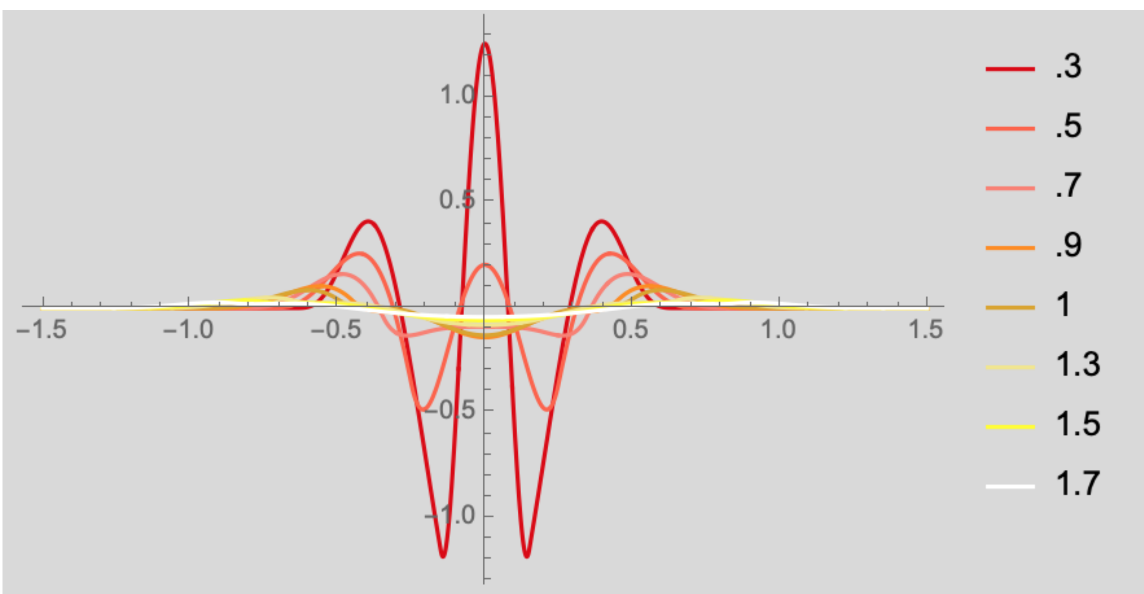

(b) $|\mathring{\Omega}_B| = .1$ removed for visual clarity

Figure 5.11: Fix c_1 and α_5.

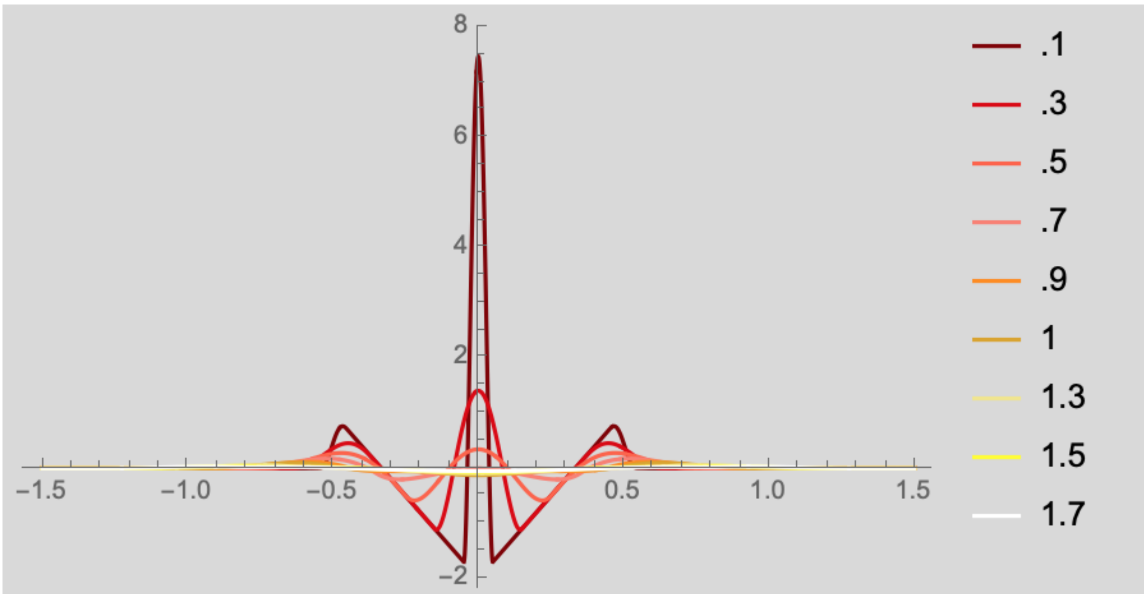

(a) All specified lengths

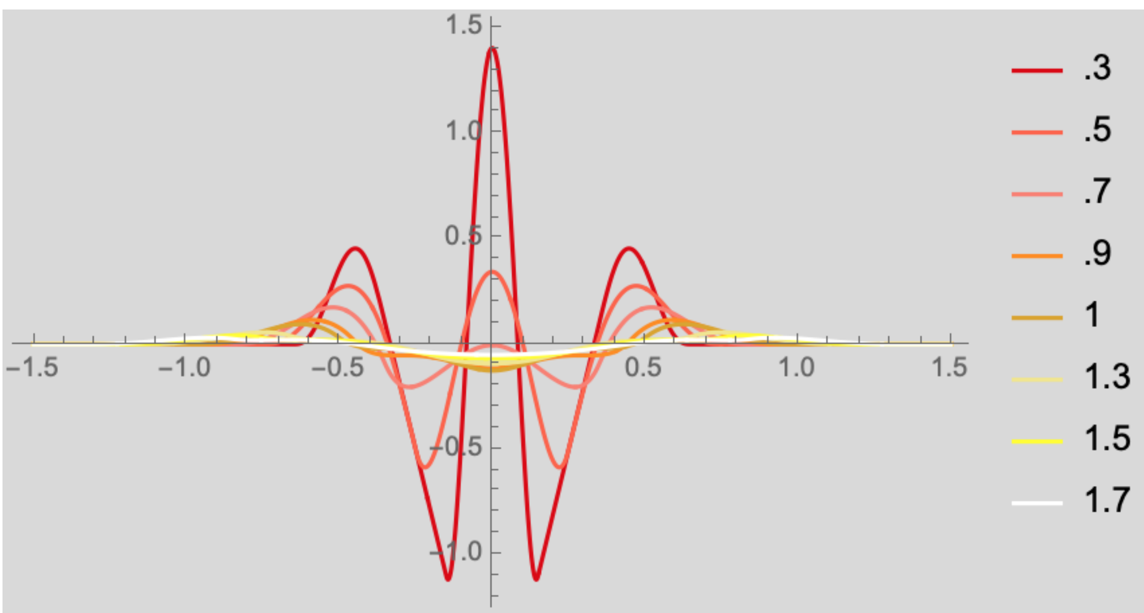

(b) $|\mathring{\Omega}_B| = .1$ removed for visual clarity

Figure 5.12: Fix c_2 and α_5.

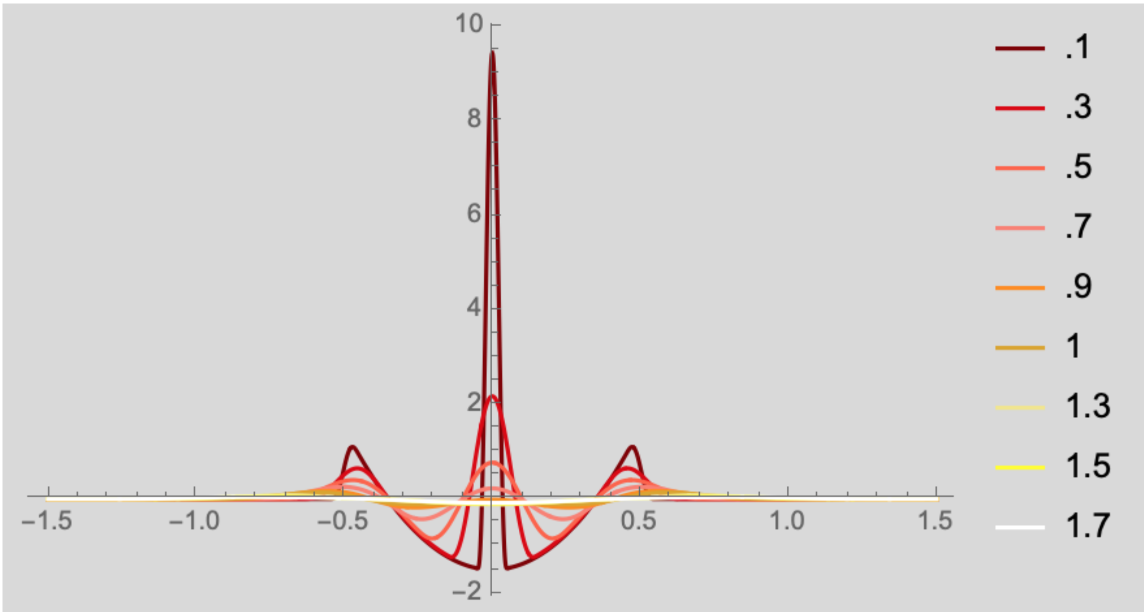

(a) All specified lengths

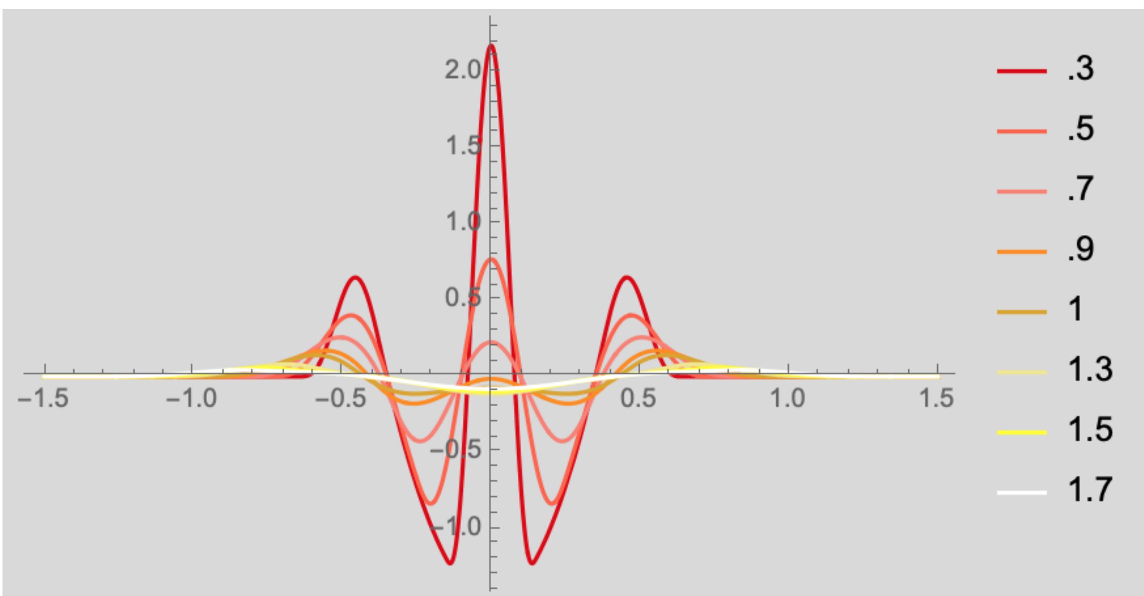

(b) $|\mathring{\Omega}_B| = .1$ removed for visual clarity

Figure 5.13: Fix c_0 and α_7.

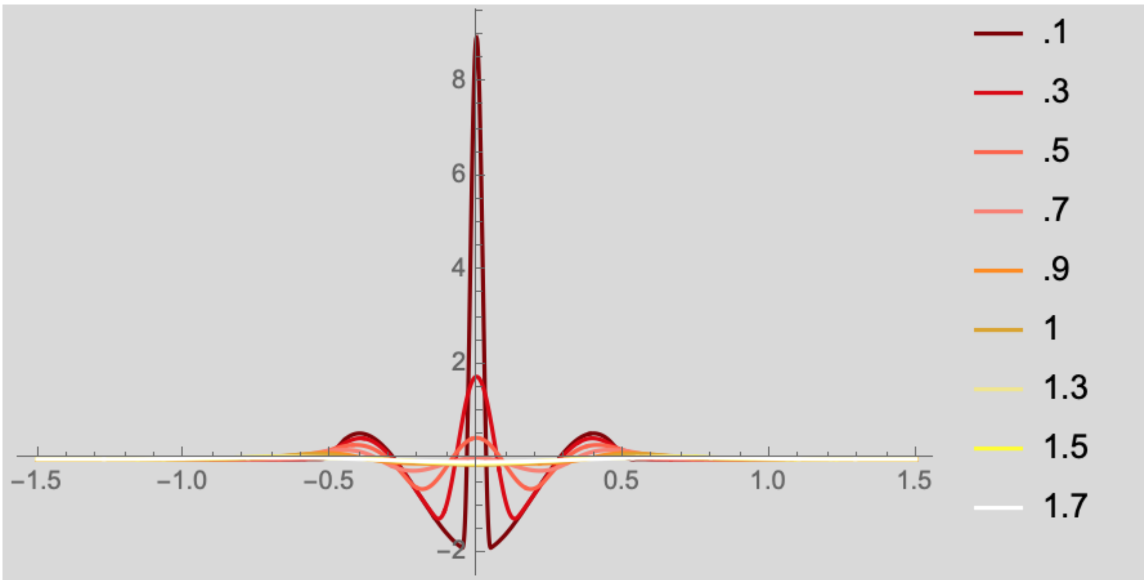

(a) All specified lengths

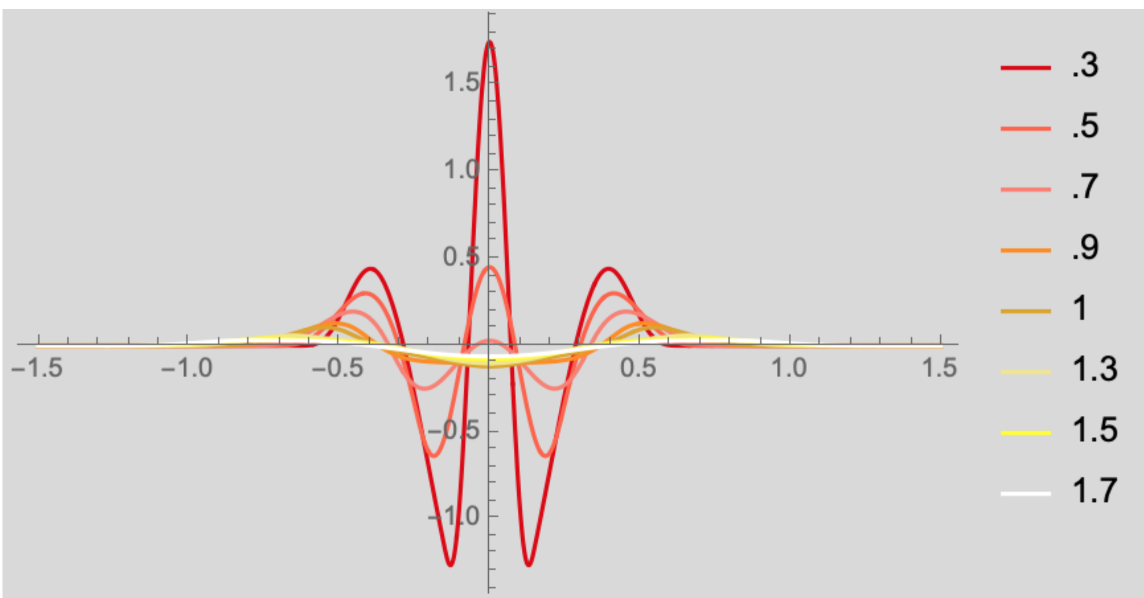

(b) $|\mathring{\Omega}_B| = .1$ removed for visual clarity

Figure 5.14: Fix c_1 and α_7.

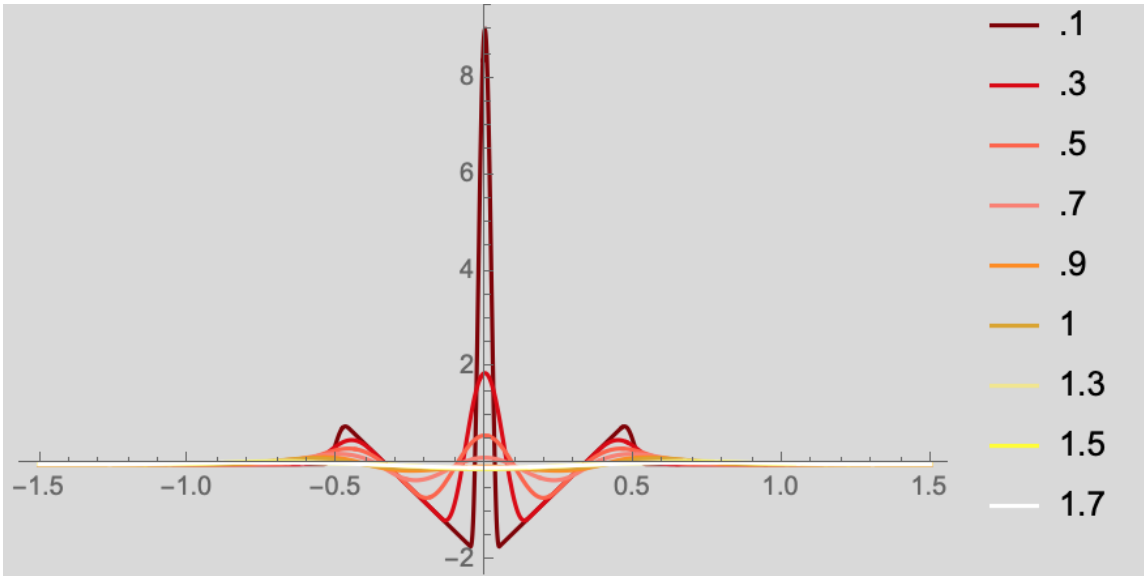

(a) All specified lengths

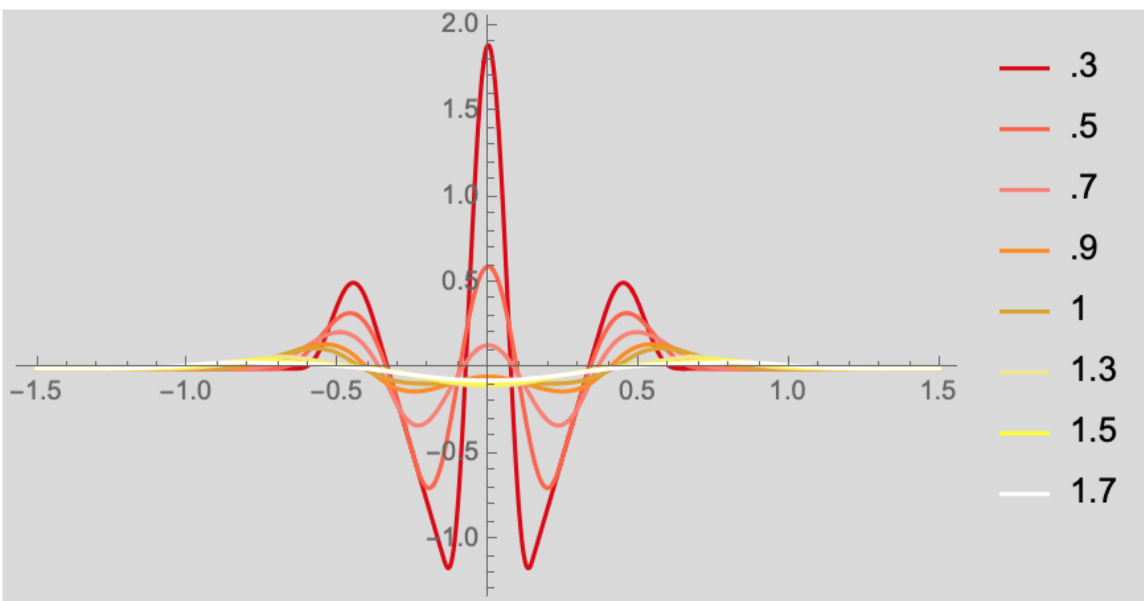

(b) $|\mathring{\Omega}_B| = .1$ removed for visual clarity

Figure 5.15: Fix c_2 and α_7.

require that the force is an element of $L^2(\Omega)$ in the statement of Theorem 4.19 in order to obtain a unique solution to the weak problem, we also tabulate the L^2-norm of the each plotted ghost force in Tables 5.1b, 5.2b, and 5.3b. Observe that in addition to the nine lengths previously discussed, $||F_g||_{L^1}$ and $||F_g||_{L^2}^2$ are also calculated for $|\mathring{\Omega}_B| = 20$ and $|\mathring{\Omega}_B| = 30$ explicitly.

A clear pattern emerges from examining Tables 5.1a, 5.2a, and 5.3a: For a fixed c_i and α_k as $|\mathring{\Omega}_B|$ increases $||F_g||_{L^1}$ decreases. Observe that the same pattern emerges from examining Tables 5.1b, 5.2b, 5.3b: For a fixed c_i and α_k as $|\mathring{\Omega}_B|$ increases $||F_g||_{L^2}^2$ decreases.

5.2.2 Effects of varying the smoothness of α

Using Tables 5.1a, 5.2a, 5.3a, 5.1b, 5.2b and 5.3b, but looking across the tables horizontally rather than vertically as was done in the previous analysis, the effect of varying the smoothness can be explored. Table 5.4, record which smoothness is ideal for the given length and the selected unscaled kernel.

From Table 5.4 it can be inferred that the optimal choice of blending function α_k depends not only on the unscaled kernel, c_i, but also on the distance $|\mathring{\Omega}_B|$. This finding is in stark contrast to the finding in [34] where it is claimed that the ghost force decreases as the smoothness of the blending function increases. Obviously, for even just the three basic unscaled kernels, more choices of distances $|\mathring{\Omega}_B|$ would need to be considered to determine the specific range of distances for which each α_k is the optimum smoothness. Based on the results in these two tables, it *appears* that

- when the ratio of $|\mathring{\Omega}_B|$ to δ is very small the piecewise linear blending function α_1 is the optimal choice
- when the ratio of $|\mathring{\Omega}_B|$ to δ is large the piecewise quintic blending function α_5 is the optimal choice

Table 5.1: $||\mathcal{F}_g||^k_{L^k}$ with c_0

(a) $k = 1$

	α_1	α_3	α_5	α_7
$\mathring{\Omega}_B = 0.1$	1.041	1.12379	1.15337	1.17646
$\mathring{\Omega}_B = 0.3$	0.496863	0.628384	0.730202	0.797581
$\mathring{\Omega}_B = 0.5$	0.270263	0.278209	0.408589	0.499646
$\mathring{\Omega}_B = 0.7$	0.248626	0.158371	0.206697	0.286663
$\mathring{\Omega}_B = 0.9$	0.193376	0.119284	0.140640	0.16915
$\mathring{\Omega}_B = 1.0$	0.174038	0.108277	0.119534	0.146041
$\mathring{\Omega}_B = 1.3$	0.133875	0.082035	0.088043	0.102528
$\mathring{\Omega}_B = 1.5$	0.116025	0.068738	0.078446	0.089589
$\mathring{\Omega}_B = 1.7$	0.102375	0.058116	0.686421	0.797281
$\mathring{\Omega}_B = 20$	0.008702	0.000714	0.000720	0.000936
$\mathring{\Omega}_B = 30$	0.005801	0.000323	0.000320	0.000417

(b) $k = 2$

	α_1	α_3	α_5	α_7
$\mathring{\Omega}_B = 0.1$	1.986200	2.497810	3.077360	3.590000
$\mathring{\Omega}_B = 0.3$	0.280178	0.445680	0.642303	0.817740
$\mathring{\Omega}_B = 0.5$	0.067857	0.079870	0.170579	0.264674
$\mathring{\Omega}_B = 0.7$	0.051041	0.019507	0.037513	0.074846
$\mathring{\Omega}_B = 0.9$	0.027053	0.011887	0.013298	0.022297
$\mathring{\Omega}_B = 1.0$	0.021429	0.009192	0.010209	0.014496
$\mathring{\Omega}_B = 1.3$	0.012680	0.004074	0.005620	0.007273
$\mathring{\Omega}_B = 1.5$	0.009524	0.002473	0.003749	0.005236
$\mathring{\Omega}_B = 1.7$	0.007415	0.001569	0.002499	0.003748
$\mathring{\Omega}_B = 20$	5.4E-5	9.5E-8	3.3E-8	5.4E-8
$\mathring{\Omega}_B = 30$	2.3E-5	1.9E-8	4.4E-9	7.2E-9

Table 5.2: $||\mathcal{F}_g||^k_{L^k}$ with c_1

(a) $k = 1$

	α_1	α_3	α_5	α_7
$\mathring{\Omega}_B = 0.1$	0.927877	0.955229	0.994614	1.024320
$\mathring{\Omega}_B = 0.3$	0.326674	0.430081	0.531470	0.600805
$\mathring{\Omega}_B = 0.5$	0.246525	0.174789	0.253368	0.328394
$\mathring{\Omega}_B = 0.7$	0.191278	0.117404	0.143082	0.171212
$\mathring{\Omega}_B = 0.9$	0.148772	0.092939	0.098960	0.120926
$\mathring{\Omega}_B = 1.0$	0.133895	0.083285	0.086365	0.105069
$\mathring{\Omega}_B = 1.3$	0.102996	0.060762	0.070324	0.080593
$\mathring{\Omega}_B = 1.5$	0.089263	0.050018	0.059863	0.070046
$\mathring{\Omega}_B = 1.7$	0.078762	0.041732	0.060684	0.060458
$\mathring{\Omega}_B = 20$	0.006694	0.000478	0.000480	0.000625
$\mathring{\Omega}_B = 30$	0.004463	0.000216	0.000214	0.000278

(b) $k = 2$

	α_1	α_3	α_5	α_7
$\mathring{\Omega}_B = 0.1$	1.620610	2.197240	2.672760	3.177240
$\mathring{\Omega}_B = 0.3$	0.159661	0.242850	0.393639	0.539568
$\mathring{\Omega}_B = 0.5$	0.063095	0.032284	0.070546	0.123777
$\mathring{\Omega}_B = 0.7$	0.033240	0.013011	0.016248	0.028769
$\mathring{\Omega}_B = 0.9$	0.018636	0.007294	0.008557	0.011218
$\mathring{\Omega}_B = 1.0$	0.015079	0.005326	0.006842	0.008669
$\mathring{\Omega}_B = 1.3$	0.008923	0.002194	0.0033422	0.004837
$\mathring{\Omega}_B = 1.5$	0.006702	0.001305	0.002142	0.003272
$\mathring{\Omega}_B = 1.7$	0.005218	0.000818	0.001364	0.002202
$\mathring{\Omega}_B = 20$	3.7E-5	4.6E-8	1.5E-8	2.5E-8
$\mathring{\Omega}_B = 30$	1.7E-5	9.4E-9	2.0E-9	3.2E-9

Table 5.3: $||\mathcal{F}_g||_{L^k}^k$ with c_2

(a) $k = 1$

	α_1	α_3	α_5	α_7
$\mathring{\Omega}_B = 0.1$	0.963333	0.983843	1.018100	1.04477
$\mathring{\Omega}_B = 0.3$	0.403333	0.504409	0.596259	0.658939
$\mathring{\Omega}_B = 0.5$	0.244373	0.213618	0.320766	0.397409
$\mathring{\Omega}_B = 0.7$	0.211640	0.133962	0.165959	0.223321
$\mathring{\Omega}_B = 0.9$	0.164609	0.102655	0.117976	0.141882
$\mathring{\Omega}_B = 1.0$	0.148148	0.092966	0.100332	0.122785
$\mathring{\Omega}_B = 1.3$	0.113960	0.069813	0.077367	0.088772
$\mathring{\Omega}_B = 1.5$	0.098765	0.058253	0.067929	0.078081
$\mathring{\Omega}_B = 1.7$	0.087146	0.049101	0.058840	0.068912
$\mathring{\Omega}_B = 20$	0.007407	0.000596	0.000600	0.000780
$\mathring{\Omega}_B = 30$	0.004938	0.000269	0.000367	0.000347

(b) $k = 2$

	α_1	α_3	α_5	α_7
$\mathring{\Omega}_B = 0.1$	1.648470	2.117437	2.671610	6.168130
$\mathring{\Omega}_B = 0.3$	0.201933	0.300857	0.452169	0.595095
$\mathring{\Omega}_B = 0.5$	0.058333	0.050000	0.106685	0.170449
$\mathring{\Omega}_B = 0.7$	0.038825	0.014377	0.023796	0.046011
$\mathring{\Omega}_B = 0.9$	0.020872	0.008778	0.009799	0.014884
$\mathring{\Omega}_B = 1.0$	0.016667	0.006696	0.007761	0.010366
$\mathring{\Omega}_B = 1.3$	0.009861	0.002919	0.004230	0.005600
$\mathring{\Omega}_B = 1.5$	0.007407	0.001764	0.002778	0.003986
$\mathring{\Omega}_B = 1.7$	0.005767	0.001116	0.001830	0.0028081
$\mathring{\Omega}_B = 20$	4.2E-5	6.7E-8	2.3E-8	3.8E-8
$\mathring{\Omega}_B = 30$	1.9E-5	1.3E-8	3.1E-9	5.0E-9

Table 5.4: Which α_k gives the smallest $||\mathcal{F}_g||_H^2$ for each c_i?

(a) $H = L^1$

	c_0	c_1	c_2
$\mathring{\Omega}_B = 0.1$	α_1	α_1	α_1
$\mathring{\Omega}_B = 0.3$	α_1	α_1	α_1
$\mathring{\Omega}_B = 0.5$	α_1	α_3	α_3
$\mathring{\Omega}_B = 0.7$	α_3	α_3	α_3
$\mathring{\Omega}_B = 0.9$	α_3	α_3	α_3
$\mathring{\Omega}_B = 1.0$	α_3	α_3	α_3
$\mathring{\Omega}_B = 1.3$	α_3	α_3	α_3
$\mathring{\Omega}_B = 1.5$	α_3	α_3	α_3
$\mathring{\Omega}_B = 1.7$	α_3	α_3	α_3
$\mathring{\Omega}_B = 20$	α_3	α_5	α_3
$\mathring{\Omega}_B = 30$	α_5	α_5	α_3

(b) $H = L^2$

	c_0	c_1	c_2
$\mathring{\Omega}_B = 0.1$	α_1	α_1	α_1
$\mathring{\Omega}_B = 0.3$	α_1	α_1	α_1
$\mathring{\Omega}_B = 0.5$	α_1	α_3	α_3
$\mathring{\Omega}_B = 0.7$	α_3	α_3	α_3
$\mathring{\Omega}_B = 0.9$	α_3	α_3	α_3
$\mathring{\Omega}_B = 1.0$	α_3	α_3	α_3
$\mathring{\Omega}_B = 1.3$	α_3	α_3	α_3
$\mathring{\Omega}_B = 1.5$	α_3	α_3	α_3
$\mathring{\Omega}_B = 1.7$	α_3	α_3	α_3
$\mathring{\Omega}_B = 20$	α_5	α_5	α_5
$\mathring{\Omega}_B = 30$	α_5	α_5	α_5

- when the ratio of $|\mathring{\Omega}_B|$ to δ is between those the piecewise cubic blending function α_3 is the optimal choice

We **hypothesize** that if larger and larger ratios were selected, then eventually the piecewise septic polynomial would be come optimal. Continuing this pattern, at some point the piecewise $9th$-degree polynomial blending function would become optimal.

That being said, when implementing the energy-based blending method, it is important to recall that the entries, A_{ij}, of the stiffness matrix which correspond to either basis element φ_i or φ_j having support that intersects the blending region Ω_B all must be calculated individually. Therefore, especially when dealing with implementing this model on a uniform mesh (as was done in Chapter 6), choosing a very large blending region could significantly slow down the computations.

For these reasons, it would seem that when selecting the length of the blending region it would be desirable to restrict this length in order to ensure that

$$1 \leq \frac{|\mathring{\Omega}_B|}{\delta} \leq 4. \tag{5.8}$$

With this range in the length of the blending function you would be able to keep your blending region small enough to not excessively slow the construction of the stiffness matrixs, but allow you a large enough blending region to decrease the effects of the ghost force. With this range of lengths of the region $\mathring{\Omega}_B$ selecting the piecewise cubic blending function when implementing this blended model would be optimal.

Chapter 6

Obtaining Approximate Solutions via the Finite Element Method

6.1 The general finite element method

Let Ω be a closed, bounded and connected domain. Assume that $\mathscr{H}(\Omega) \subset L^2(\Omega)$ on which $a(\cdot,\cdot)$ is a symmetric semi-inner product. Let $((\cdot,\cdot))_{\mathscr{H}(\Omega)} = (\cdot,\cdot)_{L^2(\Omega)} + a(\cdot,\cdot)$, then $((\cdot,\cdot))_{\mathscr{H}(\Omega)}$ is clearly an inner product on $\mathscr{H}(\Omega)$. If the space $\big(\mathscr{H}(\Omega), ||\cdot||_{\mathscr{H}(\Omega)}\big)$ is a Hilbert space, the Cauchy-Schwarz inequality

$$\left|\big((u,v)\big)_{\mathscr{H}(\Omega)}\right| \leq ||u||_{\mathscr{H}(\Omega)}||v||_{\mathscr{H}(\Omega)}$$

follows. Therefore, further assume that $\big(\mathscr{H}(\Omega), ||\cdot||_{\mathscr{H}(\Omega)}\big)$ is Hilbert. Let $H(\Omega)$ be a closed subspace of $\mathscr{H}(\Omega)$ such that $H(\Omega) \cap \{\text{constant functions on } \Omega\} = 0$, then $\big(H(\Omega), |\cdot|_{\mathscr{H}(\Omega)}\big)$ is also a Hilbert space, where $|u|_{a(\Omega)} := a(u,u)$.

If it can be shown that there exists $\mathcal{C}_1 \in \mathbb{R}$ such that

$$\text{(Poincaré inequality) } ||u||^2_{L^2(\Omega)} \leq \mathcal{C}_1 |u|^2_{\mathscr{H}(\Omega)} \tag{6.1}$$

for all $u, v \in H(\Omega)$ and V_h is a finite dimensional subspace of $H(\Omega)$ with basis $\{\varphi_1, \cdots, \varphi_N\}$ the following results hold. Naturally, any element $u \in V_h$ can be uniquely represented as

$$u_h(x) = \sum_{i=1}^{N} \eta_i \varphi_i(x) \tag{6.2}$$

for $\eta_i \in \mathbb{R}$.

Proposition 6.1. *The $N \times N$ square matrix A given by*

$$a_{ij} = a\big(\varphi_j, \varphi_i\big) \quad \textit{for } 1 \leq i, j \leq N$$

*is symmetric positive definite (SPD). This matrix is known as the **stiffness matrix***

Proof. A is clearly symmetric as

$$a\big(\varphi_j, \varphi_i\big) = a_{ij} = a_{ji} = a\big(\varphi_i, \varphi_j\big)$$

Let $\boldsymbol{\eta} \in \mathbb{R}^N$ be arbitrary. Define

$$u(x) = \sum_{i=1}^{N} \eta_i \varphi_i(x).$$

Then,

$$\begin{aligned}
\boldsymbol{\eta}^T A \boldsymbol{\eta} &= \sum_{i=1}^{N} \eta_i \Bigg(\sum_{j=1}^{N} a_{ij} \eta_j \Bigg) \\
&= \sum_{i=1}^{N} \sum_{j=1}^{N} \eta_i a_{ij} \eta_j \\
&= \sum_{i=1}^{N} \sum_{j=1}^{N} a(\eta_j \varphi_j, \eta_i \varphi_i) \\
&= a(u, u) \\
&\geq \frac{1}{\mathcal{C}_1} ||u||^2_{L^2(\Omega)}.
\end{aligned}$$

Notice that the Poincaré inequality was used to obtain the last inequality. Thus, A is SPD. □

Proposition 6.2. *The Galerkin approximation problem has a unique solution. The Galerkin approximation problem is stated as: Given an $F \in L^2(\Omega)$, find a $u_h \in V_h$ such that*

$$a\big(u_h, v\big) = \big(F, v\big)_{L^2(\Omega)} \quad \forall\ v \in V_h.$$

Proof. Suppose that $u_h \in V_h$ solves the Galerkin approximation problem. Since $u_h \in V_h$, there exists unique η_i such that

$$u_h(x) = \sum_{i=1}^{N} \eta_i \varphi_i(x).$$

Therefore,

$$\begin{aligned}
& a(u_h, v) = (F, v)_{L^2(\Omega)}\ \forall\ v \in V_h \\
\iff \quad & a(u_h, \varphi_i) = (F, \varphi_i)_{L^2(\Omega)} \quad i = 1, \cdots, N \\
\iff \quad & a\Bigg(\sum_{j=1}^{N} \eta_j \varphi_j, \varphi_i\Bigg) = (F, \varphi_i)_{L^2(\Omega)} \quad i, j = 1, \cdots, N \\
\iff \quad & \sum_{j=1}^{N} \eta_j\ a(\varphi_j, \varphi_i) = (F, \varphi_i)_{L^2(\Omega)} \quad i, j = 1, \cdots, N
\end{aligned}$$

Define

$$\begin{aligned}
\boldsymbol{\eta} &= [\eta_j]_{j=1}^{N} \\
\boldsymbol{\mathcal{F}} &= [(F, \varphi_i)_{L^2(\Omega)}]_{i=1}^{N}.
\end{aligned}$$

Then the Galerkin approximation problem holds iff $A\boldsymbol{\eta} = \boldsymbol{\mathcal{F}}$. Since A is SPD, this matrix problem has a unique solution. □

Lemma 6.3 (Céa's Lemma)**.** *For a given $F \in L^2(\Omega)$, suppose $u \in H(\Omega)$ solves*

$$a\big(u, v\big) = \big(F, v\big)_{L^2(\Omega)} \quad \forall\ v \in H(\Omega).$$

and $u_h \in V_h$ solves the Galerkin approximation problem, then

$$||u-u_h||_{\mathscr{H}(\Omega)} \leq \min_{v\in V_h} ||u-v||_{\mathscr{H}(\Omega)}$$

Proof. Since $V_h \subset H(\Omega)$

$$a\big(u,v\big) = \big(F,v\big)_{L^2(\Omega)} \ \ \forall\ v \in H$$

implies that

$$a\big(u,v\big) = \big(F,v\big)_{L^2(\Omega)} \ \ \forall\ v \in V_h.$$

By Galerkin orthogonality,

$$a\big(u-u_h,v\big) = 0 \ \ \forall\ v \in V_h.$$

Since $v - u_h \in V_h$ for all $v \in V_h$, it is clear that

$$a(u-u_h, v-u_h) = 0.$$

Subtracting this form of zero from the above equality, it follows

$$a(u-u_h, u-u_h) = a(u-u_h, u-v) \ \ \forall v \in V_h$$

Using the Cauchy-Schwarz inequality, an inequality we get for free with the Hilbert space $\mathscr{H}(\Omega)$, we have

$$\big|a(u-u_h, u-v)\big| \leq |u-u_h|_{a(\Omega)}|u-v|_{a(\Omega)}.$$

Therefore,

$$|u-u_h|^2_{a(\Omega)} \leq |u-u_h|_{a(\Omega)}|u-v|_{a(\Omega)}$$

which implies that

$$|u-u_h|_{a(\Omega)} \leq |u-v|_{a(\Omega)}\ \forall v \in V_h,$$

Or equivalently stated

$$|u-u_h|_{a(\Omega)} \leq \inf_{v\in V_h} |u-v|_{a(\Omega)}.$$

Since V_h is a closed subspace of $\mathscr{H}$, the infimum is obtained by some element in V. Therefore,

$$|u - u_h|_{a(\Omega)} \leq \min_{v \in V_h} |u - v|_{a(\Omega)}.$$

$\square$

Theorem 6.4 (Best Approximation Theorem)**.** *Let V_h be the finite dimensional subspace of $H(\Omega)$ spanned by the selected basis elements. For a given $f \in L^2(\Omega)$, suppose $u \in \mathscr{H}(\Omega)$ solves*

$$a\big(u, v\big) = \big(f, v\big)_{L^2(\Omega)} \quad \forall\ v \in \mathscr{H}(\Omega).$$

and $u_h \in V_h$ solves the Galerkin approximation problem

$$a\big(u_h, v\big) = \big(f, v\big)_{L^2(\Omega)} \quad \forall\ v \in V_h.$$

Then u_h is the best approximation of u by an element of V_h.

Proof. Since $u_h \in V_h$ by the results of Cea's Lemma (6.3),

$$|u - u_h|_{a(\Omega)} \leq \min_{v \in V_h} |u - v|_{a(\Omega)} \leq |u - u_h|_{a(\Omega)}.$$

Therefore, we can conclude that u_h is the best approximation of u in V_h or

$$|u - u_h|_{a(\Omega)} = \min_{v \in V_h} |u - v|_{a(\Omega)}.$$

$\square$

6.2 Implementation of FEM for the BVPs 1.1, 2.2 and 4.16

Although we have discussed existence and uniqueness of solutions to the nonhomogeneous weak formulations of the BVPs, it can be difficult to explicitly express those solutions due to the complicated nature of the energy spaces to which solutions belong. Observing that dimensions of the energy space for each of the three models is infinite, we will use the finite element method (FEM) to approximate solutions to these problems by elements belonging some finite dimensional subspace. Specifically, these approximate solutions can be expressed explicitly.

When considering the nonhomogeneous Dirichlet-type BVPs given in equations 1.1, 2.2 and 4.16, the three analogous spaces to $\mathscr{H}(\Omega)$ discussed in Section 6.1 are

$$\begin{aligned}
&\mathscr{H}_1 := H^1(\Omega)\\
&\mathscr{H}_2 := \mathbb{S}(\Omega^*) \text{ as defined in equation 2.5}\\
&\mathscr{H}_3 := S(\Omega) \text{ as defined in equation 4.7.}
\end{aligned} \tag{6.3}$$

Recall from the analysis in Chapters 1, 2, and 4, the spaces associated to the homogeneous Dirichlet-type BVP are

$$\begin{aligned}
&\mathcal{H}_1 := H_0^1(\Omega)\\
&\mathcal{H}_2 := \mathbb{S}_0(\Omega^*) \text{ as defined in equation 2.8}\\
&\mathcal{H}_3 := S_0(\Omega) \text{ as defined in equation 4.10,}
\end{aligned} \tag{6.4}$$

thus these are the spaces analogous to $H(\Omega)$ in Section 6.1. The corresponding weak formulations of these three BVPs can be stated as:

Find w in the appropriate space $\mathcal{H}_k$, where

$$a_k(w, v) = \int_\Omega F_k(x)v(x)\mathrm{d}x \tag{6.5}$$

where

$$\begin{aligned}
a_1(w,v) &= \int_\Omega w'(x)v'(x)\mathrm{d}x \\
a_2(w,v) &= \int_{\Omega^*}\int_{\Omega^*} c^\delta(|p-x|)\big[w(p)-w(x)\big]\big[v(p)-v(x)\big]\mathrm{d}p\mathrm{d}x \\
a_3(w,v) &= \int_\Omega\int_{B_\delta(x)} c^\delta(|p-x|)(p-x)^2\left(1-\frac{\alpha(p)+\alpha(x)}{2}\right)\mathrm{d}pu'(x)v'(x)\mathrm{d}x \\
&\quad + \int_\Omega\int_\Omega c^\delta(|p-x|)\left(\frac{\alpha(p)+\alpha(x)}{2}\right)\big[w(p)-w(x)\big]\big[v(p)-v(x)\big]\mathrm{d}p\mathrm{d}x \\
F_1(x) &= f(x) \\
F_2(x) &= f(x) + 2\int_{\Omega^*} c^\delta(p-x)[\tilde{g}(p)-\tilde{g}(x)]\mathrm{d}p \\
F_3(x) &= F_B(x) \text{ as in equation 4.22}
\end{aligned} \tag{6.6}$$

for all $v \in \mathcal{H}_k$.

Because we wish to compare the three models for solutions on which they should all agree in Chapter 8, we restrict our attention to the space $H_0^1(\Omega)$ which is a subset of H_i for i=1,2,3. Note that $H_0^1(\Omega) \subset \mathcal{H}_2$ if it is assumed that elements are extended by 0 on Γ. For simplicity let $\Omega = (0,1)$, $\Gamma = [-\delta, 0] \cup [1, 1+\delta]$ and $\Omega^* = [-\delta, 1+\delta]$. In order to select a $N-$dimensional subspace V_h of the subspace $H_0^1(\Omega)$, partition the space Ω in the following way:

$$0 = x_0 < x_1 < x_2 < \cdots < x_{N-1} < x_N < x_{N+1} = 1. \tag{6.7}$$

For the both the peridynamic model and the blended model partition Γ:

$$\begin{aligned}
-\delta = x_{-k_1} < x_{-k+1} < \cdots < x_{-1} < x_0 = 0 \\
1 = x_{N+1} < x_{N+2} < \cdots < x_{N+k} < x_{N+k_2+1} = 1+\delta.
\end{aligned} \tag{6.8}$$

For simplicity, the blended model suggests that the four endpoints of $\mathring{\Omega}_B$ also occur on nodes of our partition. Although nonuniform partitions can be selected, for each model there are particular requirements that the partition must satisfy. To avoid unnecessary complications, we use a uniform partition: ie

$$h = x_i - x_{i-1}$$

for all $i = -k_1, \ldots, N + k_2 + 1$.

Notice, that in order for the entire partition of Ω^* to be uniform, it must be assumed that h divides δ as well as 1. Thus, $k_1 = k_2 = \delta/h =: k$ and $N = 1/h - 1$. The full partition of Ω^* is given by

$$x_{-k} < x_{-k+1} < \cdots < x_{-1} < x_0 < x_1 < \cdots x_N < x_{N+1} < x_{N+2} < \cdots < x_{N+1+k} \tag{6.9}$$

where $x_{-k} = -\delta$, x_0=0, $x_{N+1} = 1$ and $x_{N+k+1} = 1+\delta$. Since all three solutions w are assumed to vanish on the "boundary" ($\partial\Omega$ for the classical model and the blended model and Γ for the PD model), and once an appropriate h has been selected, define the $N-$dimensional space

$$V_h = \left\{ v \in C(\Omega) : v\big|_{e_i} \in \mathcal{P}^1\big(e_i\big) \text{ for } i = 0, \ldots, N \text{ and } v(0) = v(1) = 0 \right\} \tag{6.10}$$

where $e_i = [x_i, x_{i+1}]$ and $\mathcal{P}^1(e_i)$ is the set of affine functions defined on e_i. A useful basis for this space is given by

$$\varphi_i(x) = \begin{cases} \dfrac{x - x_{i-1}}{h_{i-1}}, & x_{i-1} \le x \le x_i \\ \dfrac{x_{i+1} - x}{h_i}, & x_i \le x \le x_{i+1} \\ 0, & \text{else.} \end{cases} \tag{6.11}$$

for $i = 1, \ldots, N$. Equation 6.5 can now be stated as a matrix equation

$$A^k \boldsymbol{\lambda} = \boldsymbol{\mathcal{F}}_k \tag{6.12}$$

where $A^k \in M(N \times N)$ is given by

$$A^k_{ij} = a_k(\varphi_i, \varphi_j)$$

and $\boldsymbol{\mathcal{F}}_k \in \mathbb{R}^N$ is given by

$$\boldsymbol{\mathcal{F}}_{k,i} = \int_\Omega F_k(x)\varphi_i(x)\mathrm{d}x.$$

Since the same basis elements are being used for all three models and the forces F_1, F_2 and F_3 (defined in 6.6) all include the given function $f(x)$ we now calculate the entries of the vector, $\boldsymbol{\rho}$ given by

$$\rho_i = \int_\Omega f(x)\varphi_i(x)\mathrm{d}x. \tag{6.13}$$

Since f is a given function in the BVPs, the vector $\boldsymbol{\rho}$ can be explicitly calculated in the following way. Since we know that $supp(\varphi_i) = [x_{i-1}, x_{i+1}]$, it is easy to see that

$$\rho_i = \int_\Omega f(x)\varphi_i(x)\mathrm{d}x = \int_{x_{i-1}}^{x_{i+1}} f(x)\varphi_i(x)\mathrm{d}x$$

Since φ_i is piecewise linear we consider

$$\rho_i = \int_{x_{i-1}}^{x_i} f(x)\varphi_i(x)\mathrm{d}x + \int_{x_i}^{x_{i+1}} f(x)\varphi_i(x)\mathrm{d}x.$$

For smooth f this calculation can quickly be done in most software, but the rougher that f is the longer direct integration will take the computer. To reduce computational time, we will use the Gauss-Legendre quadrature rule to approximate these integrals.

A **quadrature rule** is an approximation of a definite integral by a sum of weighted function values

$$\int_a^b S(x)\mathrm{d}x \approx \sum_{p=1}^{N_p} w_p S(x_p),$$

where the collection of points $\{x_p\}$ are known as abscissa and $\{w_p\}$ are known as weights. This leaves us with $2(N_p)$ free parameters, thus a quadrature rule has the potential of being exact for polynomials degree $2(N_p) - 1$. One such quadrature rule is the Gauss-Legendre quadrature rule. The Gauss-Legendre quadrature rule first requires that one finds the $(N_p)-$th degree Legendre polynomial. The Legendre polynomials are defined recursively as

$$P_{k+1}(x) = \frac{2k+1}{k+1} x P_k(x) - \frac{k}{k+1} P_{k-1}(x)$$

assuming that $P_0(x) = 1$ and $P_1(x) = x$. The N_p abscissa are the N_p roots of $P_{N_p}(x)$. The weights are determined by

$$w_i = \int_{-1}^{1} \left(\prod_{k=1, k \neq i}^{N_p} \frac{x - x_i}{x_k - x_i} \right) \mathrm{d}x.$$

Fortunately, for specific N_p these weights and the abscissas have been calculated and tabulated. It is also important to note that all of the zeros of the Legendre polynomials occur on the interval $[-1, 1]$. In practice, we generate the weights and abscissa on a 'standardized' interval such as $[-1, 1]$ and use linear transformations to map these to the appropriate locations in the interval over which we are integrating. Therefore, if we were interested in integrating over the element $e_m = [x_m, x_{m+1}]$ and if $\{w_p\}$ are the weights and $\{\hat{x}_p\}$ are the abscissa for integration over the interval $[-1, 1]$, we use the transformation

$$T(\hat{x}, m) = x_m + \frac{1+t}{2} h.$$

If convenient such a transformation can be used to select a different standard interval $[a, b]$ form which we start. Thus, integration over element e_m is done as follows

$$\int_{x_m}^{x_{m+1}} f(x)\varphi_i(x)\mathrm{d}x \approx \sum_{p=1}^{N_p} w_p f\big(T(\hat{x}_p, m)\big)\varphi_i\big(T(\hat{x}_p, m)\big) * \frac{h}{2}.$$

Using this quadrature rule (or others like it) can vastly increase the efficiency of the computation, but there is an error associated with this process.

Note: We have not yet calculated the forcing vector $\boldsymbol{\mathcal{F}_i}$, rather we have just calculated the portion of this vector $\boldsymbol{\rho}$ that is common to all three models.

Note: Using a partition of Ω^* that is uniform does simplify the implementation that will be discussed significantly. Therefore, if you would like to use a nonuniform mesh, details on the requirements for such a mesh can be found in [7].

Next the stiffness matrix A^k will be calculated. Although there are computing systems, such as Mathematica, that can calculate the matrix entries A_{ij} directly, it is often desirable to discretize the equation of the matrix elements, as we did for the vector $\boldsymbol{\rho}$, in order to speed up computational time. The discussion of this discretization will be handled for each of the models individually.

6.2.1 Stiffness matrix A for the classical model

Recall from equation 6.6 that

$$a_1(\varphi_i, \varphi_j) := \int_\Omega \varphi_i'(x)\varphi_j'(x)\mathrm{d}x.$$

Through the definition of φ_i, in equation 6.11, it is clear that the weak derivative

$$\varphi_i'(x) = \begin{cases} 1/h, & x_{i-1} < x < x_i \\ -1/h, & x_i < x < x_{i+1} \\ 0, & \text{else.} \end{cases}$$

Therefore, $A_{ij} \neq 0$ only when $i = j \pm 1$. Thus, A is a tridiagonal matrix with entries that can be simply calculated by hand. Along the main diagonal the matrix entries will be $2/h$ and along the two off diagonals the matrix entries will be $-1/h$.

Note: If using a nonuniform partition of Ω, A will still be a tridiagonal matrix with $A^1_{ii} = 1/h_{i-1} + 1/h_i$ and $A_{i,i+1} = -1/h_i$.

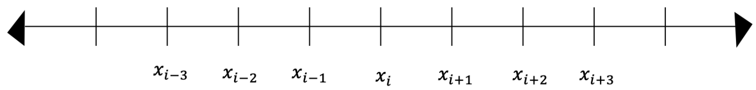

Figure 6.1: The one-dimensional uniform mesh.

6.2.2 Stiffness matrix A for the PD model

Recall from equation 6.6 that

$$a_2(\varphi_i, \varphi_j) := \int_{\Omega^*} \int_{\Omega^*} c^\delta(|p - x|)\big(\varphi_i(p) - \varphi_i(x)\big)\big(\varphi_j(p) - \varphi_j(x)\big)\mathrm{d}p\mathrm{d}x. \tag{6.14}$$

Although theoretically the FEM is very straightforward, implementing this method for nonlocal models can be challenging. Therefore, a process for implementing this model will be discussed in general. In order to help the reader follow the process a number of figures will be included. First, consider the one-dimensional uniform mesh generated by the partition of Ω^* given by equations 6.7 and 6.8 which is illustrated by Figure 6.1. In order to generate the stiffness matrix A^2 corresponding to the PD model, we would like to apply a quadrature rule, as was done in calculating the vector F. Knowing that Ω^* has been subdivided into elements $e_m = [x_m, x_{m+1}]$ for any function $s(x,p)$, we know that

$$\int_\Omega \int_\Omega s(x,p)\mathrm{d}p\mathrm{d}x = \sum_{m=-k}^{N+k+1} \sum_{n=-k}^{N+k+1} \int_{e_m} \int_{e_n} s(x,p)\mathrm{d}p\mathrm{d}x. \tag{6.15}$$

The decision to consider the integration element by element, suggests working with the two-dimensional grid (illustrated in Figure 6.2) generated by crossing the one-dimensional grid with itself. Although this grid seems like the natural two-dimensional mesh to consider, properties of the PD kernel function, c^δ, will require that some of these square elements, which will be denoted $e_m \times e_n$, must be further subdivided into triangular elements. Specifically, the dependence of c^δ on only the distance between p and x, suggests that all square elements that lie on the line $p = x$ be subdivided along that line. The assumption that material points can only interact if they are with in δ of each other, a fact encoded in the support of

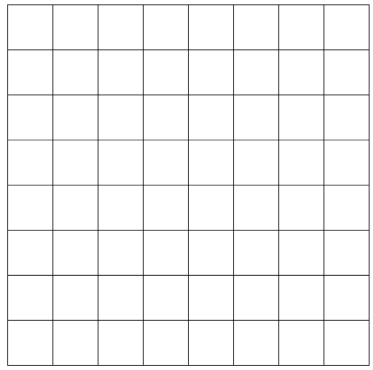

Figure 6.2: The 2-dimensional uniform grid.

c^δ, suggests that any square elements that lie on the lines $p = x + \delta$ and $p = x - \delta$ also be subdivided. Therefore, consider the two-dimensional mesh illustrated by Figure 6.3. Now that we have generated both the one-dimensional and its associated two dimensional mesh, the process of discretizing the integrals in A_{ij} can begin. Discretizing the integrals will reduce the computational cost of solving the system. Since the two-dimensional mesh contains both squares and right-triangles, appropriate quadrature rules on standard elements of this shape must be discussed. Apply the chosen quadrature rule to generate the abscissa and weights for a standard interval, square and triangle given in Figure 6.4 (*Note:* Above the Gauss-Legendre quadrature rule was selected, if a different method is selected for consistency also use it to calculate the elements of F_i). If Q_i is a quadrature point of the interval $Q_i = (\hat{x}_i, w_i)$, where $\hat{x}$ is a location on the interval and w_i is the weight assigned to that point. If Q_i is a quadrature point of the square or the triangle $Q_i = (\hat{x}_i, \hat{y}_i, w_i)$ where $(\hat{x}_i, \hat{y}_i)$ is the location in the square or triangle respectively and w_i is the assigned weight. Recall that $i, j = 1, \dots, N$ but that $m, n = -k, -k+1, \dots, -1, 0, 1, \dots, N+k, N+k+1$. To calculate

$$A_{ij}^{mn} := \int_{e_m} \int_{e_n} c^\delta(|p - x|)\big(\varphi_i(p) - \varphi_i(x)\big)\big(\varphi_j(p) - \varphi_j(x)\big)\mathrm{d}p\mathrm{d}x \tag{6.16}$$

we need to determine whether the elements material points in e_m interact with the material points in e_n. Material points that are within δ of each other interact, therefore only the elements of the two dimensional mesh (in Figure 6.3) that lie between the lines $p = x + \delta$ and $p = x - \delta$ contribute to the value (this idea is illustrated in 6.5). Any given square element,

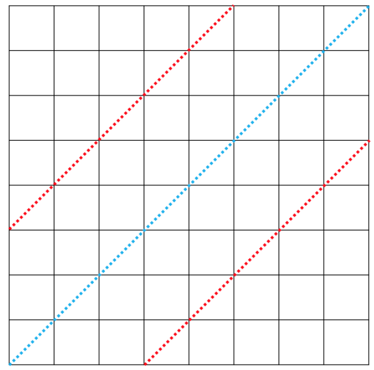

Figure 6.3: The two-dimensional mesh of $\Omega \times \Omega$ associated with the one-dimensional mesh given in Figure 6.1.

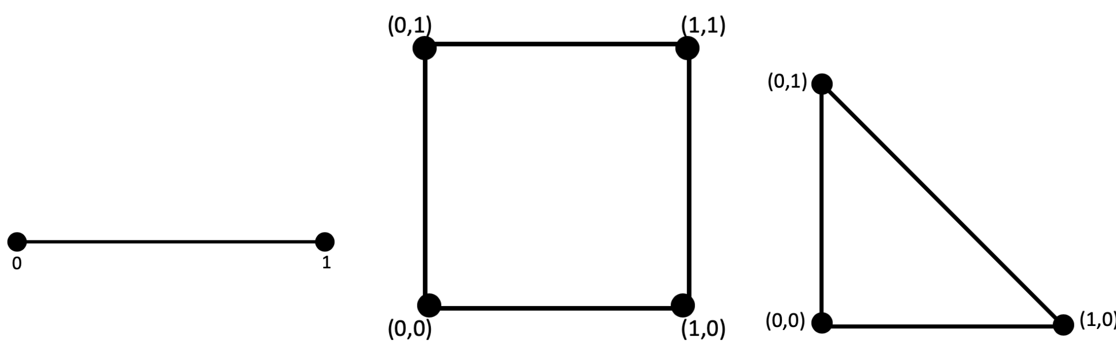

(a) Interval **(b)** Square **(c)** Triangle

Figure 6.4: Standard elements on which the chosen quadrature rule is used to generate the weights and abscissa for the desired number of quadrature points.

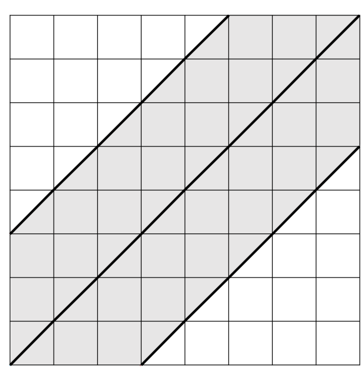

Figure 6.5: The shaded region represents elements of the two-dimensional grid that have the potential to contribute value to any term A^2_{ij}.

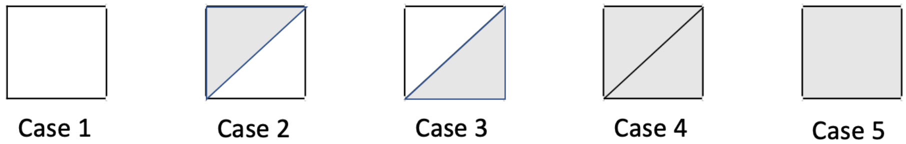

Figure 6.6: The five cases to consider for each square $e_m \times e_n$.

$e_m \times e_n$, can fall into one of five categories shown in Figure 6.6. Assume $T : [0,1]^2 \times \mathbb{Z}^2 \to \mathbb{R}^2$ is a transformation from the appropriate standard element (square or triangle) onto the shaded region of element $e_m \times e_n$. If we define

$$\gamma_A(x,\ p,\ i,\ j) = c^\delta(|p-x|)\big(\varphi_i(p) - \varphi_i(x)\big)\big(\varphi_j(p) - \varphi_j(x)\big), \tag{6.17}$$

and assume that we are using an N_p-point quadrature rule, then

$$A_{ij}^{mn} = \sum_{l=1}^{N_p} w_l * \gamma_A\Big(T\big(\hat{x}_l,\ \hat{y}_l,\ m,\ n\big),\ i,\ j\Big). \tag{6.18}$$

If $e_m \times e_n$ belongs to Case 1, then we know that $A_{ij}^{mn} = 0$. If $e_m \times e_n$ belongs to Case 2, map the abscissa of each quadrature points of the standard triangle to the triangle that via

$$T_2(\hat{x},\ \hat{y},\ m,\ n) = (-h\hat{x} + x_m + h,\ h\hat{p} + x_n). \tag{6.19}$$

If $e_m \times e_n$ belongs to Case 3, use

$$T_3(\hat{x},\ \hat{y},\ m,\ n) = (h\hat{x} + x_m,\ -h\hat{p} + x_n + h) \tag{6.20}$$

If $e_m \times e_n$ belongs to Case 4, we need to consider both triangular elements of our mesh separately. Therefore, we use the transformation

$$T_4(\hat{x},\ \hat{y},\ m,\ n) = \Big(T_2 + T_3\Big)(\hat{x},\ \hat{y},\ m,\ n) \tag{6.21}$$

Finally, if $e_m \times e_n$ belongs to Case 5, use the transformation

$$T_5(\hat{x},\ \hat{y},\ m,\ n) = (h\hat{x} + x_m,\ h\hat{p} + x_n). \tag{6.22}$$

When constructing $\mathbf{A}$, you should also use the following facts

- $A_{ij} = 0$ if $|i - j| > \frac{\delta}{h} + 1$
- $A_{ij} = A_{ji}$

to better optimize your code. These two facts are true because our partition (given in equation 6.9) is uniform.

Note: With a nonuniform mesh (satisfying any required properties) the elements that intersect with the lines $y = x$ and $y = x \pm \delta$ will still need to be subdivided. Therefore, if a nonuniform mesh was approached this way, any rectangular element $e_m \times e_n$ would fall into one of the 29 cases illustrated in Figure 6.7.

6.2.3 Stiffness matrix A for the blended model

Recall from equation 6.6 that

$$\begin{aligned}a_3(\varphi_i, \varphi_j) :=& \int_\Omega \int_{B_\delta(x)} c^\delta(|p-x|)\left(1 - \frac{\alpha(p)+\alpha(x)}{2}\right)\mathrm{d}p\left[\varphi_i'(x)\varphi_j'(x)\right]\mathrm{d}x \\ &+ \int_\Omega \int_{B_\delta(x)} c^\delta(|p-x|)\left(\frac{\alpha(p)+\alpha(x)}{2}\right)\left[\varphi_i(p)-\varphi_i(x)\right]\left[\varphi_j(p)-\varphi_j(x)\right]\mathrm{d}p\mathrm{d}x.\end{aligned}$$

Once the matrix is generated it will be a block matrix. While there are multiple ways to construct this matrix, since this model is a blending of two distinct models, it will be useful to consider the local part of the model and the nonlocal part of the model separately.

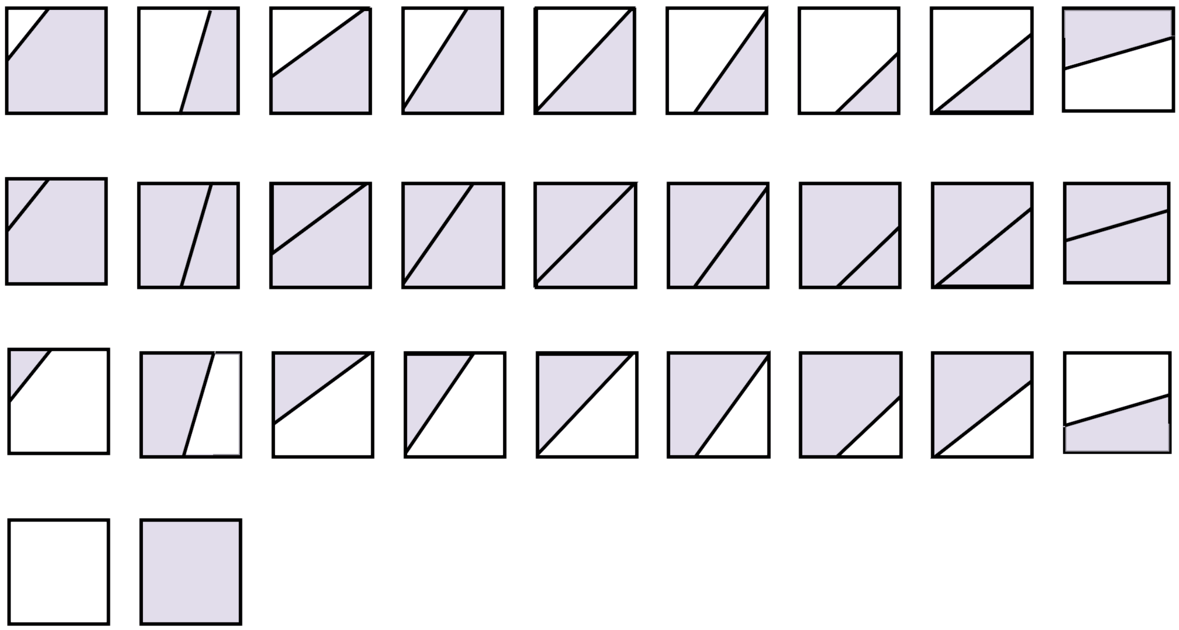

Figure 6.7: 29 possible cases for the element $e_m \times e_n$ when a nonuniform 1-D mesh is selected.

Therefore, define

$$\begin{aligned} a_L(\varphi_i, \varphi_j) &:= \int_\Omega \int_{B_\delta(x)} c^\delta(|p-x|)\left(1 - \frac{\alpha(p)+\alpha(x)}{2}\right)\mathrm{d}p\big[\varphi_i'(x)\varphi_j'(x)\big]\mathrm{d}x \\ a_{NL}(\varphi_i, \varphi_j) &:= \int_\Omega \int_{B_\delta(x)} c^\delta(|p-x|)\left(\frac{\alpha(p)+\alpha(x)}{2}\right)\big[\varphi_i(p)-\varphi_i(x)\big]\big[\varphi_j(p)-\varphi_j(x)\big]\mathrm{d}p\mathrm{d}x. \end{aligned} \tag{6.23}$$

Due to the double integration in the definition of a_L and a_{NL}, this one-dimensional problem must be thought of as a two-dimensional problem, where the square mesh elements that can possibly contribute nonzero values are shown in Figure 6.5 and can fall into one of the five cases shown in Figure 6.6.

To evaluate the elements of the matrix associated to a_L, called A_L, first define

$$\gamma_L(x,p,i,j) = c^\delta(|p-x|)\big(p-x\big)^2\left(1 - \frac{\alpha(p)+\alpha(x)}{2}\right)\varphi_i'(x)\varphi_j'(x). \tag{6.24}$$

and evaluate $\displaystyle\int_{\Omega}\int_{B_\delta(x)} \gamma_L(x,p,i,j)\mathrm{d}p\mathrm{d}x$ square element by square element as we did in the peridynamic case. To evaluate the elements of the matrix associated to a_{NL}, called A_{NL}, define

$$\gamma_{NL}(x,p,i,j) = c^\delta(|p-x|)\left(\frac{\alpha(p)+\alpha(x)}{2}\right)\big(\varphi_i(p)-\varphi_i(x)\big)\big(\varphi_j(p)-\varphi_j(x)\big). \tag{6.25}$$

and evaluate $\displaystyle\int_{\Omega}\int_{B_\delta(x)} \gamma_L(x,p,i,j)\mathrm{d}p\mathrm{d}x$ square element by square element as we did in the peridynamic case.

Since the five cases in which $e_m \times e_n$ can fall are the same as the ones in the peridynamic model, the same transformations T_2, T_3, T_4, T_5 are used. Therefore, for $j = i, i \pm 1$

$$(A_L)_{ij} = \sum_{m,n} (A_L)_{ij}^{mn} = \sum_{m,n}\left[\sum_{l=1}^{N_p} w_l * \gamma_L\Big(T\big(\hat{x}_l, \hat{y}_l, m, n\big), i, j\Big)\right]. \tag{6.26}$$

Therefore, for $j = i, i\pm 1, i\pm 2, \cdots, i \pm (k+1)$

$$(A_{NL})_{ij} = \sum_{m,n} (A_{NL})_{ij}^{mn} = \sum_{m,n}\left[\sum_{l=1}^{N_p} w_l * \gamma_L\Big(T\big(\hat{x}_l, \hat{y}_l, m, n\big), i, j\Big)\right], \tag{6.27}$$

where $k = \delta/h$.

Note: The speed of this calculation can be increased by further considering properties associated with the model. When the support of both φ_i and φ_j are fully contained in Ω_{CE},

$$\begin{aligned} &(A_L)_{ij} = 2/h \text{ when } j = i \\ &(A_L)_{ij} = -1/h \text{ when } j = i \pm 1 \\ &(A_{NL})_{ij} = 0. \end{aligned} \tag{6.28}$$

A_L is a tridiagonal block matrix in which the first block and the last block will have the same structure as the local stiffness matrix discussed above and the middle block will be all zeros. This is illustrated in Figure 6.8.

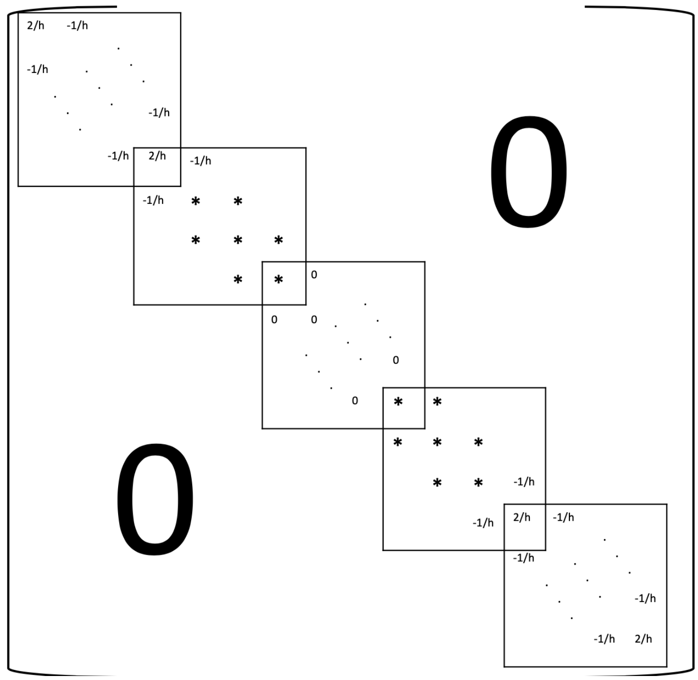

Figure 6.8: Block structure of the matrix A_L.

Similarly, when the supports of φ_i and φ_j are fully contained in Ω_{PD},

$$
\begin{aligned}
&(A_L)_{ij} = 0 \\
&(A_{NL})_{ij} = (A_{NL})_{d,d} \text{ when } j = i \\
&(A_{NL})_{ij} = (A_{NL})_{d,d+1} \text{ when } j = i \pm 1 \\
&(A_{NL})_{ij} = (A_{NL})_{d,d+2} \text{ when } j = i \pm 2 \\
&\qquad\qquad \vdots \\
&(A_{NL})_{ij} = (A_{NL})_{d,d+k+1} \text{ when } j = i \pm (k+1)
\end{aligned}
\tag{6.29}
$$

where φ_d is a fixed basis element with support fully contained in Ω_{PD}. A_{NL} will be a $[2*(\delta/h+1)+1]$ diagonal block matrix, where the first and last block are zero blocks, and the third block is the same structure as the purely peridynamic stiffness matrix. This is illustrated in Figure 6.9. Adding A_L and A_{NL} together we get the stiffness matrix A associated with the blended model.

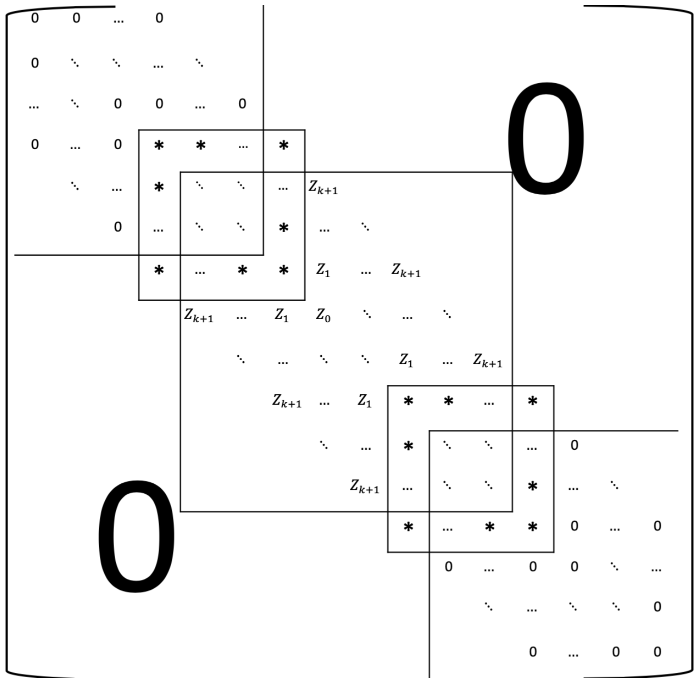

Figure 6.9: Block structure of the matrix A_{NL}.

6.2.4 Forcing vector $\boldsymbol{\mathcal{F}}$ for the classical model

In the classical model $F_1(x) = f(x)$. Therefore,

$$\boldsymbol{\mathcal{F}}_1 = \boldsymbol{\rho} \tag{6.30}$$

which was already calculated.

6.2.5 Forcing vector $\boldsymbol{\mathcal{F}}$ for the PD model

In the PD model $F_2(x) \neq f(x)$. Rather

$$\left(\boldsymbol{\mathcal{F}}_2\right)_i = \rho_i + 2\int_\Omega \varphi_i(x) \int_{\Omega^*} c^\delta(|p-x|)\left[\tilde{g}(p) - \tilde{g}(x)\right] \mathrm{d}p \mathrm{d}x. \tag{6.31}$$

In order to calculate $\left(\boldsymbol{\mathcal{F}}_2\right)_i - \rho_i$, once again think of the integration for each square element $e_m \times e_n \subset \left(\Omega \times (\Omega^*)\right)$. It is important to note that for this calculation $m = 1, \ldots, N$, whereas $n = -k, \ldots, N + k + 1$.

6.2.6 Forcing vector $\boldsymbol{\mathcal{F}}$ for the blended model

In the blended model $F_3(x) \neq f(x)$. Rather,

$$\begin{aligned}\left(\boldsymbol{\mathcal{F}}_{\mathbf{3}}\right)_i =& \rho_i - \left(g_1 - g_0\right) \int_\Omega \varphi_i'(x) \left[\left(\frac{\alpha'(x)}{2}\right) E^0\right] \mathrm{d}x \\ &- \left(g_1 - g_0\right) \int_\Omega \varphi_i'(x) \int_{B_\delta(0)} c^\delta(|\xi|)\xi^2 \left(\frac{\alpha'(x+\xi)}{2}\right) \mathrm{d}\xi \Bigg] \mathrm{d}x \\ &+ \left(g_1 - g_0\right) \int_\Omega \varphi_i(x) \int_{B_\delta(x)} c^\delta(|p - x|)\left(\alpha(p) + \alpha(x)\right)\left(p - x\right) \mathrm{d}p\mathrm{d}x.\end{aligned} \tag{6.32}$$

The part of $(\boldsymbol{\mathcal{F}}_3)_i$ expressed by

$$- \left(g_1 - g_0\right) \int_\Omega \varphi_i'(x) \left[\left(\frac{\alpha'(x)}{2}\right) E^0\right] \mathrm{d}x \tag{6.33}$$

is only single integration, and therefore can be calculated for each interval element, as was done in the calculation of $\boldsymbol{\rho}$. The part of $(\boldsymbol{\mathcal{F}}_3)_i$ expressed by

$$\begin{aligned}&-\left(g_1 - g_0\right) \int_\Omega \varphi_i'(x) \left[\int_{B_\delta(0)} c^\delta(|\xi|)\xi^2 \left(\frac{\alpha'(x+\xi)}{2}\right) \mathrm{d}\xi\right] \mathrm{d}x \\ &\qquad + \left(g_1 - g_0\right) \int_\Omega \varphi_i(x) \left[\int_{B_\delta(x)} c^\delta(|p - x|)\left(\alpha(p) + \alpha(x)\right)\left(p - x\right) \mathrm{d}p\right] \mathrm{d}x\end{aligned} \tag{6.34}$$

involves double integration, and thusly must be calculated for each square element $e_m \times e_n$, where $m = 1, \ldots, N$ and $n = -k, \ldots, N + k + 1$.

6.2.7 Putting it all together

Now that the appropriate stiffness matrices A and forcing vectors $\boldsymbol{\mathcal{F}}$ have been defined, any program that has matrix capabilities can be used to solve the matrix equation 6.12 can be solved for the vector $\boldsymbol{\lambda}$. Using equation 6.2, $w_h(x)$ is now explicitly express for $x \in \Omega$. The approximate solution u_h of the BVPs 1.1, 2.2 and 4.16 can be explicitly stated as $u_h(x) = w_h(x) + G(x)$ where

$$G(x) = \begin{cases} g(x), & \text{defined in equation 1.2 for the classical problem and the blended problem} \\ \tilde{g}(x), & \text{defined in equation 2.3 for the peridynamic problem} \end{cases} \tag{6.35}$$

for all $x \in \Omega$, for the classical problem and the blended problem, and $x \in \Omega^*$, for the PD problem.

Chapter 7

Error Analysis

Now that we have worked through the idea of FEM and the implementation of the FEM for these three BVPs, we would like to determine what facts can be theoretically established for each of the models. Ultimately, we would like to establish an error estimate under each model for solution's on which the models theoretically should agree. Particularly, if the 'true' solution to the homogeneous boundary valued problem is an element of $H^2(\Omega)$, how close is our approximated solution with respect to the various norms under consideration.

First, we begin with the following assumptions which will hold throughout this Chapter:
Let $u \in H^2(\Omega)$ and let V_h is the finite dimensional subspace spanned by the piecewise linear basis elements defined in equation 6.11. Let

$$\big(\Pi u\big)(x) = \sum_{i=1}^{N} u(x_i)\varphi_i(x).$$

Πu is known as the **Lagrange interpolant** of u in V_h. Specifically, it is the element of V_h that agrees with the true solution on the interior nodes, $\{x_i\}_{i=1}^{N}$.

7.1 Classical model

Lemma 7.1. *Let $u \in H^2(\Omega) \cap H_0^1(\Omega)$. If*

$$E(x) := u(x) - \big(\Pi u\big)(x),$$

then

$$||E'||_{L^2(\Omega)} \leq h||u''||_{L^2(\Omega)}.$$

Proof. Since $u \in H^2(\Omega)$ and $\Pi u \in V_h$, it follows that $E_{|e_j} \in H^2(e_j)$, where $e_j = [x_j, x_{j+1}]$ for $i = 0, \cdots, N$. This is due to the fact that elements in V_h are piecewise linear on these elements. Now let $x \in \Omega$, we know that $x \in e_i$ for some $i = 0, \cdots, N$. It is clear that $E(x_i) = E(x_{i+1}) = 0$. By Corollary 1.10, there is a continuously differentiable representative $\overline{E}$ of $E_{|e_j}$ that agrees with E on the nodes x_i and x_{i+1}. Therefore, there exists a point $\xi \in e_i$ such that $\overline{E}'(\xi) = 0$. Thus, it follows that

$$\overline{E}'(x) = \overline{E}'(x) - \overline{E}'(\xi) = \int_{\xi}^{x} E''(t)\mathrm{d}t.$$

Since Πu is linear when restricted to e_I, we know that

$$E''(t) = u''(t).$$

Taking the absolute value of both sides, we find that

$$\big|\overline{E}'(x)\big| = \bigg|\int_{\xi}^{x} u''(t)\mathrm{d}t\bigg|.$$

Since $[\xi, x] \subseteq e_i$,

$$\big|\overline{E}'(x)\big| \leq \bigg|\int_{e_i} u''(t)\mathrm{d}t\bigg|.$$

By bringing the absolute value under the integration, and applying Hölder's inequality, we know that

$$\big|\overline{E}'(x)\big| \leq h^{1/2}||u''||_{L^2(e_i)}. \tag{7.1}$$

Squaring both sides and integrating over e_i we arrive at

$$||E'||^2_{L^2(e_i)} \leq h||u''||^2_{L^2(e_i)} \int_{e_i} 1\mathrm{d}t = h^2||u''||^2_{L^2(e_i)}$$

Since $\sum_{i=0}^{N} ||E||^2_{L^2(e_j)} = ||E||^2_{L^2(\Omega)}$, we have this inequality over all of Ω. Through taking the square root of both sides we subsequently arrive at the desired inequality. □

Corollary 7.2. *It follows that*

$$|E|_{a_1(\Omega)} \leq h||u''||_{L^2(\Omega)}$$

for a_1 is defined in equation 6.6.

Proof. This is by definition as $|E|_{a_1(\Omega)} := ||E'||_{L^2(\Omega)}$. □

Theorem 7.3. *Let $u \in H^2(\Omega)$. If*

$$E(x) := u(x) - \big(\Pi u\big)(x),$$

then

$$||E||_{L^2(\Omega)} \leq h^2||u''||_{L^2(\Omega)}$$

Proof. First, we will prove that

$$||E||_{L^2(\Omega)} \leq h||E'||_{L^2(\Omega)}.$$

Let $x \in \Omega$. This implies that there is some i such that $x \in e_i$, where $e_i = [x_i, x_{i+1}]$ for $i = 0, \cdots, N$. Since Πu agrees with u at the nodes of the partition, it is clear that E is zero at each nodal value. Therefore, it follows that

$$E(x) = E(x) - E(x_i).$$

Since $u \in H^2(\Omega) \cap H_0^1(\Omega)$ and $\Pi u \in H_0^1(\Omega)$, it follows that $E \in H_0^1(\Omega)$. Therefore, by the Fundamental Theorem of Calculus, we know that

$$E(x) - E(x_i) = \int_{x_i}^{x} E'(t)\mathrm{d}t.$$

Thus,

$$\big|E(x)\big| = \left|\int_{x_i}^{x} E'(t)\mathrm{d}t\right|.$$

Due to the fact that $x \in e_i$, it is clear that

$$\int_{x_i}^{x} |E'(t)|\mathrm{d}t \leq \int_{e_i} |E'(t)|\mathrm{d}t.$$

Therefore, it follows that

$$\big|E(x)\big| = \int_{e_i} |E'(t)|\mathrm{d}t \leq \int_{e_i} \big|E'(t)\big|\mathrm{d}t$$

Applying Hölder's inequality on the righthand side of this expression we find that

$$\int_{e_i} \big|E'(t)\big|\mathrm{d}t \leq h^{1/2}||E'||_{L^2(e_i)}.$$

Therefore, we have shown that

$$\big|E(x)\big| \leq h^{1/2}||E'||_{L^2(e_i)}.$$

Beginning with this inequality we can say that

$$\int_{e_i} |E(x)|^2\mathrm{d}x \leq \int_{e_i} \big|h^{1/2}||E'||_{L^2(e_i)}\big|^2\mathrm{d}x.$$

This means that

$$\begin{aligned} ||E||_{L^2(e_i)}^2 &\leq h||E'||_{L^2(e_i)}^2 h \\ &= h^2||E'||_{L^2(e_i)}^2 \end{aligned}$$

Since $\sum_{i=0}^{N} ||E||^2_{L^2(e_j)} = ||E||^2_{L^2(\Omega)}$, it follows that

$$||E||^2_{L^2(\Omega)} \leq h^2 ||E'||^2_{L^2(\Omega)}$$

Applying the results of Lemma 7.1, and square rooting both sides, we arrive at the desired inequality.

$\square$

Corollary 7.4. *It follows that*

$$||E||_{H^1(\Omega)} \leq Ch||u''||_{L^2(\Omega)}$$
$$\textit{and } ||E||_{H^1(\Omega)} \leq Ch||u||_{H^2(\Omega)}.$$

Proof. Adding $||E'||^2_{L^2(\Omega)}$ to both sides of the the proven inequality

$$||E||^2_{L^2(\Omega)} \leq h^4 ||u''||^2_{L^2(\Omega)}$$

we have

$$||E||^2_{L^2(\Omega)} + ||E'||^2_{L^2(\Omega)} \leq ||E'||^2_{L^2(\Omega)} + h^4 ||u''||^2_{L^2(\Omega)}.$$

Applying the inequality from Lemma 7.1 on the righthand side of the above inequality, we have

$$||E||^2_{L^2(\Omega)} + ||E'||^2_{L^2(\Omega)} \leq h^2 ||u''||^2_{L^2(\Omega)} + h^4 ||u''||^2_{L^2(\Omega)}.$$

Therefore it follows,

$$||E||^2_{L^2(\Omega)} + ||E'||^2_{L^2(\Omega)} \leq h^2(1 + h^2) ||u''||^2_{L^2(\Omega)}.$$

Since norms are nonnegative adding $h^2(1+h^2)||u||^2_{L^2(\Omega)}$, and $h^2(1+h^2)||u'||_{L^2(\Omega)}$ to the right hand side does not change the inequality. Therefore,

$$||E||_{H^1(\Omega)} \leq Ch||u||_{H^2(\Omega)}$$

where $C = \sqrt{1 + h^2}$. $\square$

Theorem 7.5. *Let V_h be the finite dimensional subspace of $H_0^1(\Omega)$ spanned by the basis elements defined in equation 6.11. For a given $f \in L^2(\Omega)$, suppose $w \in H_2(\Omega) \cap H_0^1(\Omega)$ solves*

$$a_1\big(w, v\big) = \big(f, v\big)_{L^2(\Omega)} \quad \forall\ v \in \mathcal{H}(\Omega).$$

and $w_h \in V$ solves the Galerkin approximation problem

$$a_1\big(w_h, v\big) = \big(f, v\big)_{L^2(\Omega)} \quad \forall\ v \in V_h.$$

then

$$||w - w_h||_{L^2(\Omega)} \leq h^2 ||w''||_{L^2(\Omega)}$$
$$|w - w_h|_{H^1(\Omega)} \leq Ch||w''||_{L^2(\Omega)}$$

Proof. Since $\big(\Pi w\big) \in V_h$ and $w \in H^2(\Omega) \cap H_0^1(\Omega)$, by Theorems 6.4 and 7.3 we know that

$$||w - w_h||_{L^2(\Omega))} \leq \big|\big|w - (\Pi w)\big|\big|_{L^2(\Omega)} \leq h^2 ||w''||_{L^2(\Omega)}$$
$$|w - w_h|_{H^1(\Omega)} \leq \big|w - (\Pi w)\big|_{H^1(\Omega)} \leq Ch||w''||_{L^2(\Omega)}.$$

$\square$

7.2 PD model

In the proof of the following proposition, we will use the same technique as the analogous classical result.

Proposition 7.6. *Let $u \in H^2(\Omega^*) \cap \mathbb{S}_0(\Omega^*)$. If*

$$E(x) := u(x) - \big(\Pi u\big)(x),$$

then

$$|E|_{a_2(\Omega^*)} \leq h^{\frac{1}{2}}||u''||_{L^2(\Omega^*)}$$

Proof. For each $t \in \Omega^*$, there exists an $i \in \mathbb{Z}$ such that $t \in e_i$. Since E is zero on the nodes of the mesh, there exists a $\xi \in e_i$ such that $E'(\xi) = 0$. Therefore, $E'(t) = E'(t) + E'(\xi)$. Since $E_{|e_i} \in H^2(e_i)$, it follows that

$$E'(t) = \int_{\xi}^{t} E''(z)\mathrm{d}z \leq \int_{e_i} u''(z)\mathrm{d}z.$$

Through an application of Hölder's inequality, we have that

$$|E'(t)| \leq h^{\frac{1}{2}}||u''||_{L^2(e_i)}.$$

Now that this fact has been established for all $t \in \Omega^*$, we will use this fact to prove the claim.

We know that $E \in H^1(\Omega)$ and that $E = 0$ on Γ, therefore for any $x, p \in \Omega^*$

$$E(p) - E(x) = \int_{x}^{p} E'(t)\mathrm{d}t \leq \left| \int_{x}^{p} E'(t)\mathrm{d}t \right| \leq \int_{x}^{p} |E'(t)|\mathrm{d}t$$

Thus, we have that

$$E(p) - E(x) \leq \int_{x}^{p} h^{\frac{1}{2}}||u''||_{L^2(\Omega)}\mathrm{d}t.$$

From this and an application of Hölder's inequality, we have

$$\Big(E(p) - E(x)\Big)^2 \leq h||u''||^2_{L^2(\Omega)}\bigg(\int_{x}^{p} \mathrm{d}t\bigg)^2 = h||u''||^2_{L^2(\Omega)^2}(p-x)^2$$

Since $c^{\delta}(|p-x|) \geq 0$ for all $x, p \in \mathbb{R}$, it follows that

$$c^{\delta}(|p-x|)\Big(E(p) - E(x)\Big)^2 h||u''||_{L^2(\Omega)^2}(p-x)^2 c^{\delta}(|p-x|).$$

Therefore,

$$|E|^2_{a_2(\Omega^*)} = \int_{\Omega^*}\int_{\Omega^*} c^\delta(|p-x|)\Big(E(p)-E(x)\Big)^2 \mathrm{d}p\mathrm{d}x \leq \big(h||u''||^2_{L^2(\Omega)}\big)E^0|\Omega^*|.$$

Which means that

$$|E|_{a_2(\Omega^*)} \leq h^{\frac{1}{2}}\mathcal{C}||u''||_{L^2(\Omega)}$$

as desired. □

Theorem 7.7. *Let V_h be the finite dimensional subspace of $H^1_0(\Omega^*) \subseteq \mathbb{S}_0(\Omega^*)$ spanned by the basis elements defined in equation 6.11. For a given $f \in L^2(\Omega)$, suppose $w \in H^2(\Omega^*) \cap \mathbb{S}_0(\Omega^*)$ solves*

$$a_2\big(w,v\big) = \big(f,v\big)_{L^2(\Omega^*)} \quad \forall\ v \in V_h.$$

and $w_h \in V_h$ solves the Galerkin approximation problem

$$a_2\big(w_h,v\big) = \big(f,v\big)_{L^2(\Omega^*)} \quad \forall\ v \in V_h.$$

then

$$|w - w_h|_{a_2(\Omega^*)} \leq Ch^{\frac{1}{2}}||w''||_{L^2(\Omega^*)}$$

Proof. By the Best Approximation Theorem (6.4) we know that

$$|w-w_h|_{a_2(\Omega^*)} = \min_{v \in V_h} |w-v|_{a_2(\Omega^*)}.$$

Since $\Pi w \in V_h$ and $w \in H^2(\Omega^*) \cap \mathbb{S}_0(\Omega^*)$, it follows that

$$|w-w_h|_{a_2(\Omega^*)} \leq |w - \Pi w|_{a_2(\Omega^*)} \leq Ch||w''||_{L^2(\Omega^*)}.$$

□

Theorem 7.8. *Let V_h be the finite dimensional subspace of $H^1_0(\Omega^*) \subseteq \mathbb{S}_0(\Omega^*)$ spanned by the basis elements defined in equation 6.11. For a given $f \in L^2(\Omega)$, suppose $w \in H^2(\Omega^*) \cap \mathbb{S}_0(\Omega^*)$*

solves

$$a_2\big(w,v\big) = \big(f,v\big)_{L^2(\Omega^*)} \quad \forall\ v \in V_h.$$

and $w_h \in V_h$ *solves the Galerkin approximation problem*

$$a_2\big(w_h,v\big) = \big(f,v\big)_{L^2(\Omega^*)} \quad \forall\ v \in V_h.$$

then

$$||w - w_h||_{L^2(\Omega^*)} \leq Ch^{\frac{1}{2}}||w''||_{L^2(\Omega^*)}$$

Proof. This follows form the nonlocal Poincaré inequality. □

We will now use the embedding of $H_0^1(\Omega)$ into $\mathbb{S}_0(\Omega^*)$ to prove a stronger result on set $\Big(H_0^1(\Omega) \cap H^2(\Omega^*)\Big) \subset \Big(H^2(\Omega^*) \cap \mathbb{S}_0(\Omega^*)\Big)$.

Theorem 7.9. *Let* $u \in H^2(\Omega^*) \cap H_0^1(\Omega)$. *If*

$$E(x) := u(x) - \big(\Pi u\big)(x),$$

then

$$|E|_{a_2(\Omega^*)} \leq Ch||u''||_{L^2(\Omega^*)}$$

Proof. Since $u \in H^2(\Omega^*) \cap \mathbb{S}_0(\Omega^*)$ and $\Pi u \in V_h \subseteq H_0^1(\Omega^*)$, it follows that $E \in H^1(\Omega)$. Therefore, by Remark 2.10, we have that

$$|E|_{\mathbb{S}(\Omega^*)} \leq \big(E^0|\Omega|\big)^{\frac{1}{2}}|E|_{H^1(\Omega)}.$$

Therefore, by Corollary 7.2 we have

$$|E|_{\mathbb{S}(\Omega^*)} \leq Ch||u''||_{L^2(\Omega)}$$

as desired. $\square$

Theorem 7.10. *Let V_h be the finite dimensional subspace of $H_0^1(\Omega^*) \subseteq H_0^1(\Omega^*)$ spanned by the basis elements defined in equation 6.11. For a given $f \in L^2(\Omega)$, suppose $w \in H^2(\Omega^*) \cap \mathbb{S}_0(\Omega^*)$ solves*

$$a_2\big(w, v\big) = \big(f, v\big)_{L^2(\Omega^*)} \quad \forall\ v \in V_h.$$

and $w_h \in V_h$ solves the Galerkin approximation problem

$$a_2\big(w_h, v\big) = \big(f, v\big)_{L^2(\Omega^*)} \quad \forall\ v \in V_h.$$

then

$$|w - w_h|_{a_2(\Omega^*)} \leq Ch||w''||_{L^2(\Omega^*)}$$
$$||w - w_h||_{L^2(\Omega^*)} \leq \mathcal{C}h||w''||_{L^2(\Omega^*)}$$

Proof. By the Best Approximation Theorem (6.4) we know that

$$|w - w_h|_{a_2(\Omega^*)} = \min_{v \in V_h} |w - v|_{a_2(\Omega^*)}.$$

Since $\Pi w \in V_h$ and $w \in H^2(\Omega^*) \cap H_0^1(\Omega)$, it follows that

$$|w - w_h|_{a_2(\Omega^*)} \leq |w - \Pi w|_{a_2(\Omega^*)} \leq Ch||w''||_{L^2(\Omega^*)}.$$

Once again, the result

$$||w - w_h||_{L^2(\Omega^*)} \leq Ch||w''||_{L^2(\Omega^*)}$$

follows from an application of the Poincaré inequality. $\square$

7.3 Blended model

Theorem 7.11. *Let $u \in H^2(\Omega) \cap S_0(\Omega)$. If*

$$E(x) := u(x) - \big(\Pi u\big)(x),$$

then

$$|E|_{a_3(\Omega)} \leq Ch^{\frac{1}{2}} ||u''||_{L^2(\Omega)}$$

Proof. Consider

$$\begin{aligned}|E|^2_{a_3(\Omega)} = &\int_\Omega \int_\Omega c^\delta(p-x)(p-x)^2 \left(1 - \frac{\alpha(p)+\alpha(x)}{2}\right) \mathrm{d}p \big(E'(x)\big)^2 \mathrm{d}x \\ &+ \int_\Omega \int_\Omega c^\delta(p-x)(p-x)^2 \left(\frac{\alpha(p)+\alpha(x)}{2}\right) \big(E(p)-E(x)\big)^2 \mathrm{d}p\mathrm{d}x\end{aligned}$$

For all $z \in \Omega$, we have that $0 \leq \alpha(z) \leq 1$ it is clear that

$$\begin{aligned}\left(1 - \frac{\alpha(p)+\alpha(x)}{2}\right) &\leq 1 \\ \left(\frac{\alpha(p)+\alpha(x)}{2}\right) &\leq 1\end{aligned}$$

therefore

$$\begin{aligned}|E|^2_{a_3(\Omega)} = &\int_\Omega \int_\Omega c^\delta(p-x)(p-x)^2 \mathrm{d}p \big(E'(x)\big)^2 \mathrm{d}x \\ &+ \int_\Omega \int_\Omega c^\delta(p-x)(p-x)^2 \big(E(p)-E(x)\big)^2 \mathrm{d}p\mathrm{d}x\end{aligned}$$

By equation 7.1 in Lemma 7.1 and the process used in the proof of Theorem 7.9, we find that

$$\begin{aligned}|E|^2_{a_3(\Omega)} \leq &\int_\Omega \int_\Omega c^\delta(p-x)(p-x)^2 \mathrm{d}p \big(h^{1/2}||u''||_{L^2(\Omega)}\big)^2 \mathrm{d}x \\ &+ \int_\Omega \int_\Omega c^\delta(p-x)(p-x)^2 \big(h^{1/2}||u''||_{L^2(\Omega)}\big)^2 \mathrm{d}p\mathrm{d}x\end{aligned}$$

Therefore,

$$
\begin{aligned}
|E|^2_{a_3(\Omega)} &\leq 2h||u''||^2_{L^2(\Omega)} \int_\Omega \int_\Omega c^\delta(p-x)(p-x)^2 \mathrm{d}p\mathrm{d}x \\
&\leq 2h||u''||^2_{L^2(\Omega)} \int_\Omega \int_{\mathbb{R}} c^\delta(z)(z^2)^2 \mathrm{d}z\mathrm{d}x \\
&= (2hE^0)||u''||^2_{L^2(\Omega)} \int_\Omega \mathrm{d}x \\
&= (2E^0\big|\Omega\big|)h||u''||^2_{L^2(\Omega)}.
\end{aligned}
$$

□

Theorem 7.12. *Let V_h be the finite dimensional subspace of $H^1_0(\Omega) \subseteq S_0(\Omega)$ spanned by the basis elements defined in equation 6.11. For a given $f \in L^2(\Omega)$, suppose $w \in H^2(\Omega) \cap S_0(\Omega)$ solves*

$$a_3\big(w, v\big) = \big(f, v\big)_{L^2(\Omega)} \quad \forall\ v \in V_h.$$

and $w_h \in V_h$ solves the Galerkin approximation problem

$$a_3\big(w_h, v\big) = \big(f, v\big)_{L^2(\Omega)} \quad \forall\ v \in V_h.$$

Then

$$|w - w_h|_{a_3(\Omega)} \leq Ch^{\frac{1}{2}}||w''||_{L^2(\Omega)}||w - w_h||_{L^2(\Omega)} \leq \mathcal{C}h^{\frac{1}{2}}||w''||_{L^2(\Omega)}$$

Proof. By the Best Approximation Theorem (6.4) we know that

$$|w - w_h|_{a_3(\Omega)} = \min_{v \in V_h} |w - v|_{a_3(\Omega)}.$$

Since $\Pi w \in V_h$ and $w \in H^2(\Omega) \cap S_0(\Omega)$, it follows that

$$|w - w_h|_{a_3(\Omega)} \leq |w - \Pi w|_{a_3(\Omega)} \leq Ch^{\frac{1}{2}}||w''||_{L^2(\Omega)}.$$

Once again, the result

$$||w - w_h||_{L^2(\Omega^*)} \leq \mathcal{C}h^{\frac{1}{2}}||w''||_{L^2(\Omega^*)}$$

follows from an application of the Poincaré inequality. $\square$

Once again, if we consider the space $\Big(H^2(\Omega)\cap H_0^1(\Omega)\Big) \subset \Big(H^2(\Omega)\cap S_0(\Omega)\Big)$ we can prove a stronger result.

Theorem 7.13. *Let $u \in H^2(\Omega)\cap H_0^1(\Omega)$. If*

$$E(x) := u(x) - \big(\Pi u\big)(x),$$

then

$$|E|_{a_3(\Omega)} \leq Ch||u''||_{L^2(\Omega)}$$

Proof. Since $u \in H^2(\Omega)\cap S_0(\Omega)$ and $\Pi u \in V_h \subseteq H_0^1(\Omega)$, it follows that $E \in H^1(\Omega)$. Therefore, by Proposition 4.11, we have that

$$|E|_{S(\Omega)} \leq \max\big(E^0, E^0C^2|\Omega|\big)^{\frac{1}{2}}|E|_{H^1(\Omega)}.$$

Therefore, it follows that

$$|E|_{S(\Omega)} \leq \mathcal{C}h||u''||_{L^2(\Omega)}$$

as desired. $\square$

Theorem 7.14. *Let V_h be the finite dimensional subspace of $H_0^1(\Omega) \subseteq S_0(\Omega)$ spanned by the basis elements defined in equation 6.11. For a given $f \in L^2(\Omega)$, suppose $w \in H^2(\Omega)\cap H_0^1(\Omega)$ solves*

$$a_3\big(w,v\big) = \big(f,v\big)_{L^2(\Omega)} \quad \forall\ v \in V_h.$$

and $w_h \in V_h$ solves the Galerkin approximation problem

$$a_3\big(w_h,v\big) = \big(f,v\big)_{L^2(\Omega)} \quad \forall\ v \in V_h.$$

Then

$$|w - w_h|_{a_3(\Omega)} \leq Ch||w''||_{L^2(\Omega)}$$
$$||w - w_h||_{L^2(\Omega)} \leq \mathcal{C}h||w''||_{L^2(\Omega)}$$

This proof is emitted as it is analogous to the previous proofs.

Chapter 8

Comparing the Computational Results to the Error Analysis in Chapter 7

Based on discussions in Chapters 5, 6, and 7, we will start with manufactured solution u which is a polynomial with degree higher than 2. Using the operators associated with the strong nonhomogeneous BVPs (given by equations 1.1, 2.2, and 4.16), we calculate the model specific force required to generate the desired solution. Rewrite the nonhomogeneous BVP as a homogeneous boundary valued problem by subtracting the model specific boundary function G (defined in 6.35). Follow the implementation of the models discussed in Chapter 6. Then solve the homogeneous BVP for its approximate solution and add back the appropriate model specific boundary function, G, to obtain the approximate solution to the nonhomogeneous BVP. Since we have manufactured the appropriate force, $\mathcal{F}_k$ (as defined in equation 6.6, to generate our desired exact solution u, we can now compare the approximate solution generated by each model to the exact solution with respect to the various norms discussed in Chapter 7.

For the following comparisons, we have used the kernel generated by unscaled kernel c_1 (defined in Figure 5.2) in both the PD and blended models with $\delta = 1/20$. This selection was made for simplicity in implementation and because this kernel can accurately be represented using the continuous piecewise linear basis elements we chose in Chapter 6. For the blended model, we have selected

$$\begin{aligned} \Omega_{CE} &= (0, 0.25) \cup (0.75, 1) \\ \Omega_B &= (0.25, 0.4) \cup (0.6, 0.75) \\ \Omega_{PD} &= (0.4, 0.6) \end{aligned}$$

Based on the analysis done on the ghost force in Chapter 5, we will consider the continuously differentiable piecewise cubic blending function, α_3

$$\alpha_3(x) = \begin{cases} 0, & x \in (0, 0.3) \\ 540 - 5040x + 15600x^2 - 16000x^3, & x \in [0.3, 0.35] \\ 1, & x \in (0.35, 0.65) \\ -4900 + 21840x - 32400x^2 + 16000x^3, & x \in [0.65, 0.7] \\ 0, & x \in (0.7, 1). \end{cases} \tag{8.1}$$

Let $u_{h,1}$, $u_{h,2}$, and $u_{h,3}$ be the approximate solutions obtain through solving the classical, PD, and blended models with FEM respectively. From the error analysis that was done in Chapter 7, for smooth enough u we know that

$$\begin{aligned} ||u - u_{h,1}||_{L^2(\Omega)} &\le Ch^2||u''||_{L^2(\Omega)} \\ |u - u_{h,1}|_{H^1(\Omega)} &\le Ch||u''||_{L^2(\Omega)} \\ |u - u_{h,2}|_{a_2(\Omega^*)} &\le Ch^{\frac{1}{2}}||u''||_{L^2(\Omega)} \\ |u - u_{h,3}|_{a_3(\Omega)} &\le Ch^{\frac{1}{2}}||u''||_{L^2(\Omega)}. \end{aligned}$$

With respect to each of the above mentioned norms, the power of h is the lower bound for the rate of convergence with respect to this norm. To determine if our implementation of the model agrees with these theoretical results we compute the convergence rates using the formula

$$\text{rate} \approx \ln\left(\frac{\text{error}(h_2)}{\text{error}(h_1)}\right) \div \ln\left(\frac{h_2}{h_1}\right). \tag{8.2}$$

8.1 Analysis

The above steps will be done and tabulated for the exact solutions on Ω

$$\begin{aligned} u_1(x) &= 5x^2 - 5x \\ u_2(x) &= x^3 - 1.5x^2 + 0.5x. \end{aligned} \tag{8.3}$$

Note that u_1 and u_2 not just $H^2(\Omega)$ functions, but they are C^∞ solutions. Because these functions are smoother than we require for the theoretical analysis, it is possible that their rate of convergence is higher than the predicted value.

8.1.1 Classical model

In Tables 8.1a and 8.2a the calculated (through direct integration) errors $||u - u_h||_{L^2(\Omega)}$ and $||u - u_h||_{H^1(\Omega)}$ (rounded to nearest millionth) are tabulated using for the two cases: $u = u_1$ and $u = u_2$ defined in equation 8.3. In Tables 8.1b and 8.2b the approximate rates of convergence for the two exact solutions $u = u_1$ and $u = u_2$.

As you can see from Table 8.1b, the approximate solution, $u_{h,1}$, converges to the true quadratic solution with respect to L^2 with the expected approximate rate of 2. From Table 8.1b the approximate solution, $u_{h,1}$, converges to the true quadratic solution with respect to H^1 with the expected approximate rate of 1. As you can see from Table 8.2b, the approximate solution, $u_{h,1}$, converges to the true cubic solution with respect to L^2 with the expected approximate rate of 2. From Table 8.2b the approximate solution, $u_{h,1}$, converges to the true cubic solution with respect to H^1 with the expected approximate rate of 1.

Table 8.1: The approximate errors and rates of convergence for the **classical** model when the exact solution is $u = u_1$ the **quadratic** solution.

(a) Errors

	$\|\|u - u_{h,1}\|\|_{L^2(\Omega)}$	$\|\|u - u_{h,1}\|\|_{H^1(\Omega)}$
$h = 1/20$	0.002224	0.140700
$h = 1/40$	0.000563	0.071263
$h = 1/60$	0.000251	0.047711
$h = 1/80$	0.000142	0.035858
$h = 1/100$	0.000091	0.028723
$h = 1/120$	0.000063	0.023956
$h = 1/140$	0.000046	0.020546
$h = 1/160$	0.000036	0.017986

(b) Approximate rate

	L^2-rate	H^1-rate
$1/20 : 1/40$	1.98126	0.981298
$1/40 : 1/60$	1.98951	0.989548
$1/60 : 1/80$	1.99265	0.992672
$1/80 : 1/100$	1.99433	0.994347
$1/100 : 1/120$	1.99539	0.995395
$1/120 : 1/140$	1.99611	0.996114
$1/140 : 1/160$	1.99663	0.996639

Table 8.2: The approximate errors and rates of convergence for the **classical** model when the exact solution is $u = u_2$ the **cubic** solution.

(a) Errors

	$\|\|u - u_h\|\|_{L^2(\Omega)}$	$\|\|u - u_h\|\|_{H^1(\Omega)}$
$h = 1/20$	0.000367	0.023222
$h = 1/40$	0.000095	0.012043
$h = 1/60$	0.000043	0.008129
$h = 1/80$	0.000024	0.006134
$h = 1/100$	0.000016	0.004926
$h = 1/120$	0.000011	0.004115
$h = 1/140$	0.000008	0.003533
$h = 1/160$	0.000006	0.003096

(b) Approximate rate

	L^2-rate	H^1-rate
$1/20 : 1/40$	1.94690	0.947263
$1/40 : 1/60$	1.96945	0.969561
$1/60 : 1/80$	1.98784	0.978460
$1/80 : 1/100$	1.98327	0.983303
$1/100 : 1/120$	1.98634	0.986359
$1/120 : 1/140$	1.98845	0.988466
$1/140 : 1/160$	1.99000	0.990008

8.1.2 PD model

In Tables 8.3a and 8.4a the calculated errors $||u-u_{h,2}||_{L^2(\Omega)}$, $||u-u_{h,2}||_{H^1(\Omega)}$, and $|u-u_{h_2}|_{a_2(\Omega^*)}$ (rounded to nearest millionth) are tabulated using for the manufactured solutions: $u = u_1$ and $u = u_2$ defined in equation 8.3. In Tables 8.3b and 8.4b the approximate rates of convergence for the two exact solutions $u = u_1$ and $u = u_2$.

Note 8.1. *Although we do not have any theoretical results showing the minimum convergence rate with respect to the H^1, we include the H^1 errors and convergence rates to allow the reader to compare them to the rate achieved in by the classical model.*

As you can see from Table 8.3b, the approximate solution, $u_{h,2}$, converges to the true quadratic solution with respect to L^2 with the a rate of two, better than the theoretical minimum rate 1. From Table 8.3b the approximate solution, $u_{h,2}$, converges to the true quadratic solution with respect to H^1 with the an approximate rate of 1. From Table 8.3b the approximate solution, $u_{h,2}$, converges to the true quadratic solution with respect to a_2 semi-norm with an approximate rate of 2, higher than the theoretical minimum rate of 1.

As you can see from Table 8.4b, the approximate solution, $u_{h,2}$, converges to the true cubic solution with respect to L^2 with the a rate of two, better than the theoretical minimum rate of 1. From Table 8.3b the approximate solution, $u_{h,2}$, converges to the true cubic solution with respect to H^1 with an approximate rate of 1. From Table 8.4b the approximate solution, $u_{h,2}$, converges to the true cubic solution with respect to a_2 seminorm with an approximate rate of 2, which is higher than the theoretical minimum in this case which is 1.

8.1.3 Blended model

the calculated errors $||u-u_{h,3}||_{L^2(\Omega)}$, $||u-u_{h,3}||_{H^1(\Omega)}$, and $|u-u_{h,3}|_{a_3(\Omega^*)}$ (rounded to nearest millionth) are tabulated using for the manufactured solutions: $u = u_1$ and $u = u_2$ defined

Table 8.3: The approximate errors and rates of convergence for the **PD** model when the exact solution is $u = u_1$ the **quadratic** solution.

(a) Errors

	$\|\|u - u_{h,2}\|\|_{L^2(\Omega^*)}$	$\|\|u - u_{h,2}\|\|_{H^1(\Omega^*)}$	$\|u - u_{h,2}\|_{a_2(\Omega^*)}$
$h = 1/20$	0.001455	0.140773	0.058742
$h = 1/40$	0.000301	0.071319	0.015156
$h = 1/60$	0.000121	0.047747	0.006803
$h = 1/80$	0.000065	0.035882	0.003845
$h = 1/100$	0.000040	0.028739	0.002468
$h = 1/120$	0.000027	0.023967	0.001717
$h = 1/140$	0.000020	0.020555	0.001263
$h = 1/160$	0.000015	0.017993	0.000968

(b) Approximate rate

	L^2-rate	H^1-rate	a_2-rate
$1/20 : 1/40$	2.27219	0.981006	1.95459
$1/40 : 1/60$	2.24561	0.989599	1.97544
$1/60 : 1/80$	2.18484	0.993041	1.98343
$1/80 : 1/100$	2.13769	0.994734	1.98743
$1/100 : 1/120$	2.10469	0.995777	1.98988
$1/120 : 1/140$	2.08165	0.996474	1.99153
$1/140 : 1/160$	2.06520	0.996975	1.99272

Table 8.4: The approximate errors and rates of convergence for the **PD** model when the exact solution is $u = u_2$ the **cubic** solution.

(a) Errors

	$\|\|u - u_{h,2}\|\|_{L^2(\Omega^*)}$	$\|\|u - u_{h,2}\|\|_{H^1(\Omega^*)}$	$\|u - u_{h,2}\|_{a_2(\Omega^*)}$
$h = 1/20$	0.000243	0.023268	0.008523
$h = 1/40$	0.000051	0.012074	0.002332
$h = 1/60$	0.000021	0.008148	0.001067
$h = 1/80$	0.000011	0.006147	0.000608
$h = 1/100$	0.000007	0.004395	0.000393
$h = 1/120$	0.000005	0.004121	0.000274
$h = 1/140$	0.000003	0.003538	0.000202
$h = 1/160$	0.000003	0.003100	0.000155

(b) Approximate rate

	L^2-rate	H^1-rate	a_2-rate
$1/20 : 1/40$	2.24143	0.946382	1.89655
$1/40 : 1/60$	2.22517	0.969967	1.92865
$1/60 : 1/80$	2.17221	0.979765	1.95181
$1/80 : 1/100$	2.12953	0.984604	1.96333
$1/100 : 1/120$	2.09930	0.987607	1.97042
$1/120 : 1/140$	2.07803	0.989642	1.97520
$1/140 : 1/160$	2.06275	0.991079	1.97864

in equation 8.3. In Tables 8.3b and 8.4b the approximate rates of convergence for the two exact solutions $u = u_1$ and $u = u_2$.

Note 8.2. *Although we do not have any theoretical results showing the minimum convergence rate with respect to the H^1, we include the H^1 errors and convergence rates to allow the reader to compare them to the rate achieved in by the classical model.*

As you can see from Table 8.5b, the approximate solution, $u_{h,3}$, converges to the true quadratic solution with respect to L^2 with the a rate of 2, better than the theoretically predicted rate of 1. From Table 8.5b the approximate solution, $u_{h,3}$, converges to the true quadratic solution with respect to H^1 with an approximate rate of 1. From Table 8.3b the approximate solution, $u_{h,3}$, converges to the true quadratic solution with respect to a_3 seminorm with the expected approximate rate of 1.

As you can see from Table 8.6b, the approximate solution, $u_{h,3}$, converges to the true cubic solution with respect to L^2 with the a rate of 2, better than the theoretically predicted rate of 1. From Table 8.6b the approximate solution, $u_{h,3}$, converges to the true cubic solution with respect to H^1 with an approximate rate of 1. From Table 8.3b the approximate solution, $u_{h,3}$, converges to the true cubuc solution with respect to a_3 seminorm with the expected approximate rate of 1.

8.1.4 Comparison to different choices of the blending function

It was shown in Section 5.2, when the length of the connected regions of $\mathring{\Omega}_B$ are equal to the δ and the unscaled kernel c_1 is used, the blending function α_3 is the optimal choice of blending function to minimize the ghost force $F_B(x)$ with respect to both the L^1 and L^2-norms. Therefore, these assumptions were used to create tables in Section 8.1.3. In Tables 8.7 and 8.8 the errors and approximate rates of convergence are tabulated for the piecewise linear blending function α_1 for the two exact solutions $u = u_1$ and $u = u_2$ respectively.

Table 8.5: The approximate errors and rates of convergence for the $\boldsymbol{\alpha_3}$ **blended** model when the exact solution is $u = u_1$ the **quadratic** solution.

(a) Errors

	$\|\|u - u_h\|\|_{L^2(\Omega)}$	$\|\|u - u_h\|\|_{H^1(\Omega)}$	$\|u - u_h\|_{a_3(\Omega)}$
$h = 1/20$	0.001825	0.140936	0.106048
$h = 1/40$	0.000463	0.071306	0.052864
$h = 1/60$	0.000297	0.047724	0.035485
$h = 1/80$	0.000117	0.035864	0.026739
$h = 1/100$	0.000075	0.028726	0.021459
$h = 1/120$	0.000052	0.023958	0.017924
$h = 1/140$	0.000038	0.020547	0.015390
$h = 1/160$	0.000029	0.017987	0.013484

(b) Approximate rate

	L^2-rate	H^1-rate	a_3-rate
1/20 : 1/40	1.97897	0.982914	1.004370
1/40 : 1/60	1.98437	0.990327	0.983122
1/60 : 1/80	1.98887	0.993088	0.983686
1/80 : 1/100	1.99143	0.994606	0.985659
1/100 : 1/120	1.99304	0.995571	0.987451
1/120 : 1/140	1.99415	0.996241	0.988917
1/140 : 1/160	1.99496	0.996734	0.990105

Table 8.6: The approximate errors and rates of convergence for the $\boldsymbol{\alpha_3}$ **blended** model when the exact solution is $u = u_2$ the **cubic** solution.

(a) Errors

	$\|\|u - u_h\|\|_{L^2(\Omega)}$	$\|\|u - u_h\|\|_{H^1(\Omega)}$	$\|u - u_h\|_{a_3(\Omega)}$
$h = 1/20$	0.000360	0.023239	0.018164
$h = 1/40$	0.000093	0.012046	0.009879
$h = 1/60$	0.000042	0.008129	0.006780
$h = 1/80$	0.000024	0.006135	0.005160
$h = 1/100$	0.000015	0.004826	0.004164
$h = 1/120$	0.000011	0.004115	0.003490
$h = 1/140$	0.000008	0.003534	0.003004
$h = 1/160$	0.000006	0.003096	0.002636

(b) Approximate rate

	L^2-rate	H^1-rate	a_3-rate
1/20 : 1/40	1.95084	0.947963	0.878667
1/40 : 1/60	1.97120	0.969884	0.928247
1/60 : 1/80	1.97903	0.978626	0.94949
1/80 : 1/100	1.98346	0.983405	0.961024
1/100 : 1/120	1.98633	0.986428	0.968262
1/120 : 1/140	1.98336	0.988515	0.973229
1/140 : 1/160	1.98986	0.990045	0.976850

This specific α was selected since α_1 preformed the second best to α_3 in the described situation.

$$\alpha_1(x) = \begin{cases} 0, & x \in (0, 0.3) \\ -6 + 20x, & x \in [0.3, 0.35] \\ 1, & x \in (0.35, 0.65) \\ 14 - 20x & x \in [0.65, 0.7] \\ 0, & x \in (0.7, 1) \end{cases} \tag{8.4}$$

First we observe that in Tables 8.7b and 8.8b, the approximate rate of convergence with respect to the L^2- norm, the H^1-norm and the a_3-semi-norm are as they were with the previous choice of α_k 2, 1, and 1. Furthermore, if Tables 8.5a and 8.7a (8.6a and 8.8a) are compared we can see that they are basically the same. This similarity is due to the fact that these polynomials are manufactured solutions.

8.1.5 Additional manufactured solutions to the blended problem

Using the piecewise cubic blending function α_3 the convergence rate of the blended model is further explored. This is done through manufacturing more complicated solutions than the polynomial solutions discussed earlier. Our theoretical error analysis showed that for any solution $u \in H^2(\Omega) \cap S_0(\Omega)$ the convergence rate with respect to the $|\cdot|_{S(\Omega)}$ norm should be at least $\frac{1}{2}$. To test this we calculate the necessary force required to manufacture the solution

$$u(x) = \exp[\sin(2\pi x)] - 1 \tag{8.5}$$

from the blended model. As with the polynomial manufactured solutions, we calculate the L^2, H^1 and S error between the exact solution and the approximate solution.

Table 8.7: The approximate errors and rates of convergence for the $\boldsymbol{\alpha_1}$ **blended** model when the exact solution is $u = u_1$ the **quadratic** solution.

(a) Errors

	$\|\|u - u_{h,3}\|\|_{L^2(\Omega)}$	$\|\|u - u_{h,3}\|\|_{H^1(\Omega)}$	$\|u - u_{h,3}\|_{a_3(\Omega)}$
$h = 1/20$	0.001835	0.140891	0.106101
$h = 1/40$	0.000433	0.071304	0.052867
$h = 1/60$	0.000207	0.047725	0.035485
$h = 1/80$	0.000117	0.035865	0.026739
$h = 1/100$	0.000075	0.028765	0.021459
$h = 1/120$	0.000052	0.023958	0.017924
$h = 1/140$	0.000038	0.020547	0.015390
$h = 1/160$	0.000029	0.012987	0.013484

(b) Approximate rate

	L^2-rate	H^1-rate	a_3-rate
1/20 : 1/40	1.98623	0.982530	1.005000
1/40 : 1/60	1.98650	0.990199	0.983255
1/60 : 1/80	1.98996	0.993080	0.983721
1/80 : 1/100	1.99210	0.994617	0.985667
1/100 : 1/120	1.99350	0.995588	0.987452
1/120 : 1/140	1.99448	0.996258	0.988917
1/140 : 1/160	1.99520	0.996750	0.990104

Table 8.8: The approximate errors and rates of convergence for the $\boldsymbol{\alpha_1}$ **blended** model when the exact solution is $u = u_2$ the **cubic** solution.

(a) Errors

	$\|\|u - u_h\|\|_{L^2(\Omega)}$	$\|\|u - u_h\|\|_{H^1(\Omega)}$	$\|u - u_{h,3}\|_{a_3(\Omega)}$
$h = 1/20$	0.000357	0.023236	0.018167
$h = 1/40$	0.000093	0.012046	0.009877
$h = 1/60$	0.000042	0.008129	0.006779
$h = 1/80$	0.000024	0.006135	0.005158
$h = 1/100$	0.000015	0.004926	0.004163
$h = 1/120$	0.000011	0.004115	0.003489
$h = 1/140$	0.000008	0.003534	0.003003
$h = 1/160$	0.000006	0.003096	0.002636

(b) Approximate rate

	L^2-rate	H^1-rate	a_3-rate
1/20 : 1/40	1.94494	0.947787	0.879117
1/40 : 1/60	1.96827	0.969844	0.928344
1/60 : 1/80	1.97744	0.978624	0.949521
1/80 : 1/100	1.98248	0.983406	0.961037
1/100 : 1/120	1.98567	0.986432	0.968267
1/120 : 1/140	1.98788	0.988520	0.973231
1/140 : 1/160	1.98950	0.990049	0.976849

Table 8.9: The approximate errors and rates of convergence for the $\boldsymbol{\alpha_3}$ **blended** model when the exact solution is given by equation 8.5.

(a) Errors

	$\|\|u - u_h\|\|_{L^2(\Omega)}$	$\|\|u - u_h\|\|_{H^1(\Omega)}$	$\|u - u_h\|_{a_3(\Omega)}$
$h = 1/20$	0.009188	0.640276	0.560937
$h = 1/40$	0.002310	0.323269	0.280124
$h = 1/60$	0.001029	0.216190	0.187400
$h = 1/80$	0.000580	0.162399	0.140877
$h = 1/100$	0.000371	0.130043	0.112877
$h = 1/120$	0.000258	0.108438	0.094168
$h = 1/140$	0.000190	0.092989	0.080782
$h = 1/160$	0.000145	0.081393	0.070729

(b) Approximate rate

	L^2-rate	H^1-rate	a_3-rate
1/20 : 1/40	1.99191	0.985961	1.00177
1/40 : 1/60	1.99437	0.992255	0.991421
1/60 : 1/80	1.99496	0.994511	0.991933
1/80 : 1/100	1.99571	0.995745	0.993010
1/100 : 1/120	1.99632	0.996523	0.993937
1/120 : 1/140	1.99680	0.997060	0.994678
1/140 : 1/160	1.99717	0.997453	0.995268

Table 8.10: The approximate errors for the $\boldsymbol{\alpha_3}$ **blended** model when the exact solution is given by equation 8.6.

(a) Errors

	$\|\|u-u_h\|\|_{L^2(\Omega)}$	$\|\|u-u_h\|\|_{H^1(\Omega)}$	$\|u-u_h\|_{a_3(\Omega)}$
$h=1/20$	1.286E-14	4.542E-14	4.043E-14
$h=1/40$	2.153E-14	8.566E-14	7.665E-14
$h=1/60$	1.522E-13	5.169E-13	4.602E-13
$h=1/80$	1.779E-13	6.354E-13	5.664E-13
$h=1/100$	5.658E-13	1.953E-12	1.770E-12
$h=1/120$	1.634E-13	6.260E-13	5.313E-13
$h=1/140$	1.446E-12	4.986E-12	4.516E-12
$h=1/160$	7.279E-14	4.699E-13	2.413E-13

As seen in Table 8.9, the convergence rate is 2 with respect to the L^2 norm and 1 with respect to both the S and the H^1 norms. These are the same rates of convergence shown for the polynomial solutions.

Although our theory only covers solutions in $H^2(\Omega)\cap S_0(\Omega)$ and $H^2(\Omega)\cap H_0^1(\Omega)$, we calculate the force needed to manufacture the solution

$$u(x) = \begin{cases} 2(x-0.5)+1, & 0 \le x \le 0.5 \\ -2(x-0.5)+1, & 0.5 \le x \le 1. \end{cases} \tag{8.6}$$

The errors are presented in Table 8.10. The errors with respect to all three norms are negligible, as expected, since this solution is in each of the finite element subspaces V_h.

Now consider a piecewise linear solution

$$u(x) = \begin{cases} 2(x-\frac{99}{200})+1, & 0 \le x \le \frac{99}{200} \\ -2(x-\frac{99}{200})+1, & \frac{99}{200} \le x \le 1. \end{cases} \tag{8.7}$$

Although this solution is piecewise linear, it is not an element of any of the considered finite element subspaces, therefore we can not expect the error to be negligible, but we still expect that the error will decrease as the size of h decreases. The error and convergence rates are given in Table 8.11.

Next consider,

$$u(x) = \begin{cases} 25x^2, & 0 \leq x \leq 0.5 \\ 25(x-1)^2, & 0.5 \leq x \leq 1. \end{cases} \tag{8.8}$$

Like the previous two solutions this function is not smooth enough to belong to $H^2(\Omega) \cap S_0(\Omega)$, but due to the location of the cusp, we do expect that the FEM should approximate the solution fairly well. The error and convergence rates are given in Table 8.12. We see that we are getting the same rate of convergence in this case as we did for solutions on which we had established some theory. Therefore, we believe that there is a wider class of functions on which this theoretical analysis can be applied.

Finally, we consider a solution that involves a jump

$$u(x) = \begin{cases} 2, & 0 \leq x \leq 0.5 \\ 4, & 0.5 \leq x \leq 1. \end{cases} \tag{8.9}$$

This function is not even H^1, therefore it can not be expected to converge with respect to the H^1 norm. The errors and convergence rates are presented in Table 8.13 and agree with our expectations.

Table 8.11: The approximate errors and rates of convergence for the $\boldsymbol{\alpha_3}$ **blended** model when the exact solution is given by equation 8.7.

(a) Errors

	$\|\|u - u_h\|\|_{L^2(\Omega)}$	$\|\|u - u_h\|\|_{H^1(\Omega)}$	$\|u - u_h\|_{a_3(\Omega)}$
$h = 1/20$	0.002714	0.355314	0.101008
$h = 1/40$	0.004805	0.247411	0.069926
$h = 1/60$	0.003849	0.213486	0.058027
$h = 1/80$	0.000569	0.239817	0.040634
$h = 1/100$	0.001521	0.208722	0.030609
$h = 1/120$	0.000306	0.195529	0.025163
$h = 1/140$	0.000728	0.141327	0.021389
$h = 1/160$	0.000318	0.125305	0.016544

(b) Approximate rate

	L^2-rate	H^1-rate	a_3-rate
$1/20 : 1/40$	-0.824289	0.522184	0.530582
$1/40 : 1/60$	0.547194	0.363733	0.460200
$1/60 : 1/80$	6.647880	-0.404291	1.238270
$1/80 : 1/100$	-4.41148	0.622358	1.269620
$1/100 : 1/120$	8.79179	0.358118	1.074660
$1/120 : 1/140$	-5.62042	2.106410	1.053930
$1/140 : 1/160$	6.214000	0.900559	1.923590

Table 8.12: The approximate errors and rates of convergence for the $\boldsymbol{\alpha_3}$ **blended** model when the exact solution is given by equation 8.8.

(a) Errors

	$\|\|u-u_h\|\|_{L^2(\Omega)}$	$\|\|u-u_h\|\|_{H^1(\Omega)}$	$\|u-u_h\|_{a_3(\Omega)}$
$h=1/20$	0.009085	0.704694	0.530244
$h=1/40$	0.002315	0.356529	0.264319
$h=1/60$	0.001036	0.238620	0.177423
$h=1/80$	0.000584	0.179321	0.133692
$h=1/100$	0.000375	0.143630	0.107297
$h=1/120$	0.000261	0.119788	0.089619
$h=1/140$	0.000192	0.102735	0.076948
$h=1/160$	0.000147	0.089933	0.064718

(b) Approximate rate

	L^2-rate	H^1-rate	a_3-rate
$1/20:1/40$	1.97246	0.982974	1.004380
$1/40:1/60$	1.98410	0.990327	0.983122
$1/60:1/80$	1.98883	0.993088	0.983686
$1/80:1/100$	1.99142	0.994696	0.985659
$1/100:1/120$	1.99297	0.995571	0.984510
$1/120:1/140$	1.99419	0.996241	0.988917
$1/140:1/160$	1.99501	0.996734	0.990105

Table 8.13: The approximate errors and rates of convergence for the $\boldsymbol{\alpha_3}$ **blended** model when the exact solution is given by equation 8.9.

(a) Errors

	$\|\|u - u_h\|\|_{L^2(\Omega)}$	$\|\|u - u_h\|\|_{H^1(\Omega)}$	$\|u - u_h\|_{a_3(\Omega)}$
$h = 1/20$	0.173561	6.889770	10.80734
$h = 1/40$	0.120192	11.39182	8.367272
$h = 1/60$	0.098097	14.22589	6.912009
$h = 1/80$	0.084953	16.48024	6.050634
$h = 1/100$	0.075984	18.47869	5.459009
$h = 1/120$	0.069363	20.26908	5.024273
$h = 1/140$	0.064217	21.91523	4.687992
$h = 1/160$	0.060070	23.44441	4.418533

(b) Approximate rate

	L^2-rate	H^1-rate	a_3-rate
$1/20 : 1/40$	0.530102	-0.725471	0.369182
$1/40 : 1/60$	0.500986	-0.547932	0.471231
$1/60 : 1/80$	0.500061	-0.511323	0.462654
$1/80 : 1/100$	0.500034	-0.512928	0.461119
$1/100 : 1/120$	0.500008	-0.507224	0.455166
$1/120 : 1/140$	0.500005	-0.506554	0.449408
$1/140 : 1/160$	0.500002	-0.505136	0.443314

Chapter 9

Analysis for Energy-based Blending in N-Dimensions

Given an external force $\mathbf{b} \in L^2(\Omega; \mathbb{R}^d)$ acting on the body, we would like to minimize the blended potential strain energy

$$E(\mathbf{u}) = \int_\Omega W_B^\delta(\mathbf{u})(\mathbf{x})d\mathbf{x} - \int_\Omega \mathbf{b} \cdot \mathbf{u} d\mathbf{x}$$

over an admissible class of functions satisfying a boundary condition. First, let us introduce the energy space

$$\mathcal{S} = \{\mathbf{u} \in L^2(\Omega; \mathbb{R}^n) : \mathbf{u} \text{ is weakly differentiable in } \Omega \setminus \Omega_{PD}, \text{ and } \int_\Omega W_B^\delta(\mathbf{u})(\mathbf{x})d\mathbf{x} < \infty\}.$$

It is not difficult to see that the function $|\mathbf{u}|_S^2 := \int_\Omega W_B^\delta(\mathbf{u})(\mathbf{x})d\mathbf{x}$ defines a seminorm on the energy space. The following proposition describes the zero set of this seminorm.

Proposition 9.1. *Suppose that* $\left(\Omega_{CE}^+ \cap \Omega_{PD}^+\right) = \emptyset$*. Then if* $|\mathbf{u}|_S = 0$*, then* $\mathbf{u}$ *is an infinitesimal rigid displacement. That is* $\mathbf{u}(\mathbf{x}) = \mathbb{Q}\mathbf{x}+\mathbf{q}$*, and* $\mathbb{Q}$ *is a constant skew symmetric matrix.*

Proof. We begin by rewriting the potential energy from 3.4 as

$$\int_\Omega W_B^\delta(\mathbf{u},\mathbf{x})d\mathbf{x} = \int_\Omega \int_{B_\delta(0)} \Phi(\mathbf{x},\mathbf{z}) \left| \nabla \mathbf{u}(\mathbf{x}) \frac{\mathbf{z}}{|\mathbf{z}|} \cdot \mathbf{z} \right|^2 \mathrm{d}\mathbf{z} d\mathbf{x}$$
$$+ \int_\Omega \int_\Omega \Psi(\mathbf{x},\mathbf{p}) \left| \big(\mathbf{u}(\mathbf{p}) - \mathbf{u}(\mathbf{x})\big) \cdot \frac{\mathbf{p}-\mathbf{x}}{|\mathbf{p}-\mathbf{x}|} \right|^2 \mathrm{d}\mathbf{p} d\mathbf{x}$$

where

$$\Phi(\mathbf{x},\mathbf{z}) = \frac{1}{2} c^\delta(|\mathbf{z}|) \left(1 - \frac{\alpha(\mathbf{x}+\mathbf{z}) + \alpha(\mathbf{x})}{2}\right) \quad \text{and} \quad \Psi(\mathbf{x},\mathbf{p}) = \frac{1}{2} c^\delta(|\mathbf{p}-\mathbf{x}|) \left(\frac{\alpha(\mathbf{p}) + \alpha(\mathbf{x})}{2}\right)$$

Both functions Φ and Ψ are nonnegative. Moreover, $\Phi(\mathbf{x},\mathbf{z}) = 0$ when $(\mathbf{x},\mathbf{z}) \in \Omega_{PD} \times B_\delta(0)$ and $\Psi(\mathbf{x},\mathbf{p}) = 0$ when $\mathbf{p},\mathbf{x} \in \Omega_{CE}^+$. Notice also that

$$\Phi(\mathbf{x},\mathbf{z}) > 0, \quad \text{for all } (\mathbf{x},\mathbf{z}) \in (\Omega \setminus \Omega_{PD}^+) \times B_\delta(0)$$

and $\Psi(\mathbf{x},\mathbf{p}) > 0$ when $(\mathbf{x},\mathbf{p}) \in (\Omega \setminus \Omega_{CE}^+) \times (\Omega \setminus \Omega_{CE}^+)$. Now if $W_B^\delta(\mathbf{u}) = 0$, then both terms on the right hand side must be zero. This in turn implies that

$$|\mathcal{E}(\mathbf{u}(\mathbf{x}))|^2 + |\mathrm{div}\mathbf{u}(\mathbf{x})|^2 = 0, \quad \text{for all } \mathbf{x} \text{ such that } (\mathbf{x},\mathbf{z}) \in \mathrm{supp}(\Phi).$$

In particular for almost all $\mathbf{x} \in \Omega \setminus \Omega_{PD}^+$, $2|\mathcal{E}(\mathbf{u}(\mathbf{x}))|^2 + |\mathrm{div}\mathbf{u}(\mathbf{x})|^2 = 0$, and therefore $\mathbf{u}$ is an infinitesimal rigid displacement in $\Omega \setminus \Omega_{PD}^+$. Similarly, we also have

$$\int_{(\Omega\setminus\Omega_{CE}^+)} \int_{(\Omega\setminus\Omega_{CE}^+)} c^\delta(|\mathbf{p}-\mathbf{x}|) \left| \big(\mathbf{u}(\mathbf{p}) - \mathbf{u}(\mathbf{x})\big) \cdot \frac{\mathbf{p}-\mathbf{x}}{|\mathbf{p}-\mathbf{x}|} \right|^2 \mathrm{d}\mathbf{p} d\mathbf{x} = 0,$$

and as a consequence, using the characterization in [37], we have $\mathbf{u}$ is an infinitesimal rigid displacement in $\Omega \setminus \Omega_{CE}^+$. By assumption the sets $\Omega \setminus \Omega_{CE}^+$ and $\Omega \setminus \Omega_{PD}^+$ have overlaps, and therefore $\mathbf{u}$ is the same infinitesimal rigid displacement in both of these sets.

∎

We remark that by construction and the definition of Φ, for any $\mathbf{x} \in \Omega \setminus \Omega_{PD}$ such that $\text{dist}(\mathbf{x}, \Omega_{PD}) > 0$, we have that

$$0 < \int_{B_\delta(0)} \Phi(\mathbf{x}, \mathbf{z}) \left| \mathbb{A} \frac{\mathbf{z}}{|\mathbf{z}|} \cdot \mathbf{z} \right|^2 d\mathbf{z} < \infty, \quad \text{for all nonzero } d \times d \text{ symmetric matrices } \mathbb{A}\ .$$

Moreover, we have the following lemma.

Lemma 9.2. *Suppose that $\tau > 0$ is small and $K_\tau \subset \Omega \setminus \Omega_{PD}$ such that dist$(K_\tau, \Omega_{PD}) > \tau$. Then there exists a constant $C = C(\tau, \delta) > 0$ such that*

$$\int_{B_\delta(0)} c^\delta(\mathbf{z}) \left| \mathbb{A} \frac{\mathbf{z}}{|\mathbf{z}|} \cdot \mathbf{z} \right|^2 d\mathbf{z} \le C \int_{B_\delta(0)} \Phi(\mathbf{x}, \mathbf{z}) \left| \mathbb{A} \frac{\mathbf{z}}{|\mathbf{z}|} \cdot \mathbf{z} \right|^2 d\mathbf{z}$$

for all $x \in K_\tau$, and all nonzero $d \times d$ symmetric matrices $\mathbb{A}$.

Proof. By dividing both sides by the Fröbineous norm of the matrix,$\|\mathbb{A}\|$, it suffices to prove the lemma for symmetric matrices $\mathbb{A}$ with norm 1. To that end, suppose the conclusion of the lemma is not true. Then for each n, there exist $\mathbf{x}_n \in K_\tau$ and a symmetric matrix $\mathbb{A}_n$ with norm 1 such that

$$\int_{B_\delta(0)} c^{\delta(}\mathbf{z}) \left| \mathbb{A}_n \frac{\mathbf{z}}{|\mathbf{z}|} \cdot \mathbf{z} \right|^2 d\mathbf{z} > n \int_{B_\delta(0)} \Phi(\mathbf{x}_n, \mathbf{z}) \left| \mathbb{A}_n \frac{\mathbf{z}}{|\mathbf{z}|} \cdot \mathbf{z} \right|^2 d\mathbf{z} \tag{9.1}$$

Now since both sequences $\{\mathbf{x}_n\}$ and $\{\mathbb{A}_n\}$ are bounded, up to a subsequence, they converge to $\mathbf{x}$ and $\mathbb{A}$ respectively. It follows that $\mathbf{x}$ is a positive distance away from Ω_{PD} and $\mathbb{A}$ is a symmetric matrix with norm 1. Therefore after noticing $\Phi(\mathbf{x}_n, \mathbf{z}) \to \Phi(\mathbf{x}, \mathbf{z})$ as $n \to \infty$ we have by bounded convergence theorem we have that

$$\lim_{n\to\infty} \int_{B_\delta(0)} c^\delta(\mathbf{z}) \left| \mathbb{A}_n \frac{\mathbf{z}}{|\mathbf{z}|} \cdot \mathbf{z} \right|^2 d\mathbf{z} = \int_{B_\delta(0)} c^\delta(\mathbf{z}) \left| \mathbb{A} \frac{\mathbf{z}}{|\mathbf{z}|} \cdot \mathbf{z} \right|^2 d\mathbf{z} < \infty,$$

and

$$\lim_{n\to\infty} \int_{B_\delta(0)} \Phi(\mathbf{x}_n, \mathbf{z}) \left| \mathbb{A}_n \frac{\mathbf{z}}{|\mathbf{z}|} \cdot \mathbf{z} \right|^2 d\mathbf{z} = \int_{B_\delta(0)} \Phi(\mathbf{x}, \mathbf{z}) \left| \mathbb{A} \frac{\mathbf{z}}{|\mathbf{z}|} \cdot \mathbf{z} \right|^2 d\mathbf{z} > 0.$$

However, if we take the limit on both sides of (9.1), we see that $\int_{B_\delta(0)} c^{\delta(}\mathbf{z}) \left|\mathbb{A}\frac{\mathbf{z}}{|\mathbf{z}|}\cdot\mathbf{z}\right|^2 d\mathbf{z} = \infty$, which is a contradiction. $\square$

On $\mathcal{S}(\Omega)$, we define the norm

$$\|\mathbf{u}\|_S = \sqrt{\|\mathbf{u}\|_{L^2}^2 + |\mathbf{u}|_s^2}.$$

It is not difficult to show that $\|\cdot\|_S$ is indeed a norm on $\mathcal{S}(\Omega)$. In fact we have the following

Theorem 9.3. *$\big(\mathcal{S}(\Omega), ||\cdot||_S\big)$ is a Hilbert space.*

Proof. Let $\mathbf{u}_n$ be a Cauchy sequence in $\mathcal{S}(\Omega)$. That is for a given ϵ there exists a $N > 0$ such that

$$\big|\big|\mathbf{u}_n - \mathbf{u}_m\big|\big|_S^2 < \frac{\epsilon}{2},\ \forall\ n, m > N.$$

This implies by the definition of $||\cdot||_S$, $\mathbf{u}_n$ is Cauchy with respect in $||\cdot||_{L^2}$ and therefore there is $\mathbf{u} \in L^2(\Omega)$ such that $\mathbf{u}_n \to \mathbf{u}$ strongly in L^2.

In fact, we will show that $\mathbf{u} \in S(\Omega)$ and $\mathbf{u}_n \to \mathbf{u}$ with respect to the norm $||\cdot||_S$ as well. To that end, we first will show that $\mathbf{u}$ has a weak derivative in the region $\big(\Omega \setminus \Omega_{PD}\big)$.

For $\tau > 0$ small, let $K_\tau \subset \big(\Omega \setminus \Omega_{PD}\big)$ such that $\mathrm{dist}\big(K_\tau, \partial\Omega_{PD}\big) > \tau$. Then by Lemma 9.2, there exists a constant $C > 0$ such that

$$\begin{aligned}
&\int_{K_\tau}\int_{B_\delta(\mathbf{0})} c^\delta(\mathbf{z})|\mathbf{z}|^2 \left|(\nabla\mathbf{u}_n(\mathbf{x}) - \nabla\mathbf{u}_m(\mathbf{x}))\frac{\mathbf{z}}{|\mathbf{z}|}\cdot\frac{\mathbf{z}}{|\mathbf{z}|}\right|^2 d\mathbf{z}d\mathbf{x}\\
&\qquad\le C\int_{K_\tau}\int_{B_\delta(\mathbf{0})} \Phi(\mathbf{x},\mathbf{z}) \left|(\nabla\mathbf{u}_n(\mathbf{x}) - \nabla\mathbf{u}_m(\mathbf{x}))\frac{\mathbf{z}}{|\mathbf{z}|}\cdot\frac{\mathbf{z}}{|\mathbf{z}|}\right|^2 d\mathbf{z}d\mathbf{x}\\
&\qquad\le C\int_{\Omega}\int_{B_\delta(\mathbf{0})} \Phi(\mathbf{x},\mathbf{z}) \left|(\nabla\mathbf{u}_n(\mathbf{x}) - \nabla\mathbf{u}_m(\mathbf{x}))\frac{\mathbf{z}}{|\mathbf{z}|}\cdot\frac{\mathbf{z}}{|\mathbf{z}|}\right|^2 d\mathbf{z}d\mathbf{x}\\
&\qquad\le C|\mathbf{u}_n - \mathbf{u}_m|_S^2
\end{aligned}$$

It then follows that for any $\epsilon > 0$, there exists N large such that for all $n, m > N$ we have

$$\int_{K_\tau}\int_{B_\delta(\mathbf{0})} c^\delta(\mathbf{z})|\mathbf{z}|^2 \left|(\nabla\mathbf{u}_n(\mathbf{x}) - \nabla\mathbf{u}_m(\mathbf{x}))\frac{\mathbf{z}}{|\mathbf{z}|}\cdot\frac{\mathbf{z}}{|\mathbf{z}|}\right|^2 d\mathbf{z}d\mathbf{x} < \frac{\epsilon}{2}.$$

For each $\mathbf{x} \in K_\tau$, the integrand on the left can be calculated as

$$\int_{B_\delta(\mathbf{0})} c^\delta(\mathbf{z})|\mathbf{z}|^2 \left|(\nabla \mathbf{u}_n(\mathbf{x}) - \nabla \mathbf{u}_m(\mathbf{x}))\frac{\mathbf{z}}{|\mathbf{z}|} \cdot \frac{\mathbf{z}}{|\mathbf{z}|}\right|^2 d\mathbf{z} = \frac{E^0}{2}\left\{2|\mathcal{E}(\mathbf{u}_n - \mathbf{u}_m)|^2 + |\mathrm{div}(\mathbf{u}_n - \mathbf{u}_m)|^2\right\}$$

This implies that the sequence $\mathbf{u}_n|_{K_\tau}$ is a Cauchy sequence in the norm $\|\mathbf{v}\|_{L^2(K_\tau)} + \|\mathcal{E}\mathbf{v}\|_{L^2(K_\tau)}$. By Korn's inequality, this norm is equivalent to the $H^1(K_\tau)$ norm. Therefore, the sequence $\{\mathbf{u}_n\}$ is Cauchy in $H^1(K_\tau)$ and therefore converges. But since $\mathbf{u}_n \to \mathbf{u}$ in $L^2(\Omega)$, by uniqueness the limit of $\mathbf{u}_n$ in $H^1(K_\tau)$ must be $\mathbf{u}$. By letting $\tau \to 0$, we see that $\mathbf{u}$ is weakly differentiable on $\Omega \setminus \Omega_{PD}$ and $\mathbf{u}_n \to \mathbf{u}$ in $H^1_{loc}(\Omega \setminus \Omega_{PD})$. In particular, we have that as $n \to \infty$,

$$\mathbf{u}_n \to \mathbf{u}, \quad a.e. \text{ in } \Omega \text{ and },\quad \nabla \mathbf{u}_n \to \nabla \mathbf{u} \quad \text{a.e. in } \Omega \setminus \Omega_{PD}.$$

We can now apply Fatou's lemma to conclude that

$$\begin{aligned}
\int_\Omega W_B^\delta(\mathbf{u},\mathbf{x})d\mathbf{x} &= \int_{\Omega\setminus\Omega_{PD}}\int_{B_\delta(\mathbf{0})} \Phi(\mathbf{x},\mathbf{z})|\nabla\mathbf{u}(\mathbf{x})\frac{\mathbf{z}}{|\mathbf{z}|}\cdot\mathbf{z}|^2 d\mathbf{z}d\mathbf{x}\\
&+ \int_\Omega\int_\Omega \Psi(\mathbf{x},\mathbf{p})|(\mathbf{u}(\mathbf{p}) - \mathbf{u}(\mathbf{x}))\cdot\frac{\mathbf{p}-\mathbf{x}}{|\mathbf{p}-\mathbf{x}|}|d\mathbf{p}d\mathbf{x}\\
&\le \liminf_{n\to\infty}\left[\int_{\Omega\setminus\Omega_{PD}}\int_{B_\delta(\mathbf{0})} \Phi(\mathbf{x},\mathbf{z})|\nabla\mathbf{u}_n(\mathbf{x})\frac{\mathbf{z}}{|\mathbf{z}|}\cdot\mathbf{z}|^2 d\mathbf{z}d\mathbf{x}\right.\\
&\left.+ \int_\Omega\int_\Omega \Psi(\mathbf{x},\mathbf{p})|(\mathbf{u}_n(\mathbf{p}) - \mathbf{u}_n(\mathbf{x}))\cdot\frac{\mathbf{p}-\mathbf{x}}{|\mathbf{p}-\mathbf{x}|}|d\mathbf{p}d\mathbf{x}\right]\\
&\le C < \infty.
\end{aligned}$$

where the boundedness in the last inequality follows from the fact that $\mathbf{u}_n$ is a Cauchy sequence in $\mathcal{S}(\Omega)$. We thus conclude that $\mathbf{u} \in \mathcal{S}(\Omega)$.

Now what remains to show is $|\mathbf{u} - \mathbf{u}_m|_S \to 0$ as $m \to \infty$. To that end, for any $\epsilon > 0$, there exists N large such that for all $n, m \ge N$ we have

$$\begin{aligned}
\frac{\epsilon}{2} &> \int_\Omega W_B^\delta(\mathbf{u}_m - \mathbf{u}_n,\mathbf{x})d\mathbf{x}\\
&= \int_{\Omega\setminus\Omega_{PD}}\int_{B_\delta(\mathbf{0})} \Phi(\mathbf{x},\mathbf{z})|(\nabla\mathbf{u}_m(\mathbf{x}) - \nabla\mathbf{u}_n(\mathbf{x}))\frac{\mathbf{z}}{|\mathbf{z}|}\cdot\mathbf{z}|^2 d\mathbf{z}d\mathbf{x}\\
&+ \int_\Omega\int_\Omega \Psi(\mathbf{x},\mathbf{p})|(\mathbf{u}_m(\mathbf{p}) - \mathbf{u}_n(\mathbf{p})) - (\mathbf{u}_m(\mathbf{x}) - \mathbf{u}_n(\mathbf{x}))\cdot\frac{\mathbf{p}-\mathbf{x}}{|\mathbf{p}-\mathbf{x}|}|d\mathbf{p}d\mathbf{x}
\end{aligned}$$

To obtain the desired estimate we fix $m \geq N$ and take the limit as $n \to \infty$ in the above inequality. It then follows from applying Fatou's lemma that

$$
\begin{aligned}
\frac{\epsilon}{2} \geq & \liminf_{n\to\infty} \int_{\Omega\setminus\Omega_{PD}} \int_{B_\delta(\mathbf{0})} \Phi(\mathbf{x},\mathbf{z}) |(\nabla \mathbf{u}_m(\mathbf{x}) - \nabla \mathbf{u}_n(\mathbf{x})) \frac{\mathbf{z}}{|\mathbf{z}|} \cdot \mathbf{z}|^2 d\mathbf{z} d\mathbf{x} \\
& + \int_\Omega \int_\Omega \Psi(\mathbf{x},\mathbf{p}) |(\mathbf{u}_m(\mathbf{p}) - \mathbf{u}_n(\mathbf{p})) - (\mathbf{u}_m(\mathbf{x}) - \mathbf{u}_n(\mathbf{x})) \cdot \frac{\mathbf{p}-\mathbf{x}}{|\mathbf{p}-\mathbf{x}|} | d\mathbf{p} d\mathbf{x} \\
& = \int_{\Omega\setminus\Omega_{PD}} \int_{B_\delta(\mathbf{0})} \Phi(\mathbf{x},\mathbf{z}) |(\nabla \mathbf{u}_m(\mathbf{x}) - \nabla \mathbf{u}(\mathbf{x})) \frac{\mathbf{z}}{|\mathbf{z}|} \cdot \mathbf{z}|^2 d\mathbf{z} d\mathbf{x} \\
& + \int_\Omega \int_\Omega \Psi(\mathbf{x},\mathbf{p}) |(\mathbf{u}_m(\mathbf{p}) - \mathbf{u}(\mathbf{p})) - (\mathbf{u}_m(\mathbf{x}) - \mathbf{u}(\mathbf{x})) \cdot \frac{\mathbf{p}-\mathbf{x}}{|\mathbf{p}-\mathbf{x}|} | d\mathbf{p} d\mathbf{x} \\
& = \int_\Omega W_B^\delta(\mathbf{u}_m - \mathbf{u}, \mathbf{x}) d\mathbf{x}
\end{aligned}
$$

That concludes the proof. □

Part III

Conclusions

Dissertation Summary

In **Chapter 1**, equation 1.1 introduces a classic Dirichlet-type BVP. In order find solutions to this BVP, it first is converted to a homogeneous Dirichlet-type BVP, given by equation 1.3. Then using integration by parts, a weak formulation of this homogeneous Dirichlet-type BVP is stated in equation 1.4. Recognizing that this weak formulation of the BVP relates to the energy of the system, rather than the force, we focus on the energy space $H^1(\Omega)$. This space is exactly the space of L^2 functions for which the strain energy

$$W_{CE}(u) = \int_{\Omega} \big(u'(x)\big)^2 \mathrm{d}x$$

is finite. This energy space is shown to be a Hilbert space (Theorem 1.6) that embeds continuously into $L^2(\Omega)$ (Theorem 1.7). Then a particular subspace of this energy space $H_0^1(\Omega)$ is also studied. This subspace corresponds to elements of the energy space that can be thought of as vanishing on the boundary of Ω. On this subspace, we prove the Poincaré inequality (Theorem 1.13) which in turn allows us to existence and uniqueness of solutions to the weak formulation of the BVP as stated in Theorem 1.20.

In **Chapter 2**, equation 2.2 introduces the analogous bond-based peridynamic Dirichlet-type BVP. In order find solutions to this BVP, it first is converted to a homogeneous Dirichlet-type BVP, given by equation 2.4. Then using nonlocal integration by parts, the associated weak formulation of this homogeneous Dirichlet-type BVP is derived.. Recognizing that this weak formulation of the BVP relates to the energy of the system, rather than the force, we focus on the energy space $\mathbb{S}(\Omega^*)$. This space is exactly the space of L^2 functions for which the strain energy

$$W_{PD}^{\delta}(u) = \int_{\Omega} \int_{B_\delta(x)} c^{\delta}(|p-x|)(u(p)-u(x))^2 \mathrm{d}p\mathrm{d}x$$

is finite. This energy space is shown to be a Hilbert space (Theorem 2.4) that embeds continuously into $L^2(\Omega)$ (Remark 2.5). Then a particular subspace of this energy space $\mathbb{S}_0(\Omega^*)$ is also studied. This subspace corresponds to elements of the energy space that can be thought of as vanishing on the boundary layer of Ω or Γ. On this subspace, we prove the Poincaré inequality (Corollary 2.8) which in turn allows us to existence and uniqueness of solutions to the weak formulation of the BVP as stated in Theorem 2.17. It is of note, that in order to prove the PD Poincaré inequality analogous to the original, we actually prove a stronger result first, which is stated in Theorem 2.6.

In **Chapter 3**, we couple the classical energy and the peridynamic energy to create an energy-based blended model. The motivation for this model, it trying to capture a spatial discontinuity in the deformation that occurs away from the boundary, in a more computationally cost effective manner. The initial motivation involves a homogeneous elastic material, under a particular strain in which we can predict where the spatial discontinuity of the deformation will occur.

In **Chapter 4** the one-dimensional simplification of this blended model is studied. In this chapter, all of the analogous properties to those discussed in chapters 1 and 2 are established. An important difference in this chapter is that for this one-dimensional blended model, we are starting with the blended energy,

$$\begin{aligned} W_B^{\delta}(u) =& \frac{1}{2} \int_{\Omega} \int_{B_\delta(x)} c^{\delta}(|p-x|) \left(1 - \frac{\alpha(p)+\alpha(x)}{2}\right) [(p-x)u'(x)]^2 \mathrm{d}p\mathrm{d}x \\ &+ \frac{1}{2} \int_{\Omega} \int_{\Omega} c^{\delta}(|p-x|) \left(\frac{\alpha(p)+\alpha(x)}{2}\right) [u(p)-u(x)]^2 \mathrm{d}p\mathrm{d}x. \end{aligned}$$

Therefore, we begin by establishing properties of the energy space $S(\Omega)$. First, we establish that the energy space is a Hilbert space (Theorem 9.3). Then we establish how $S(\Omega)$ relates to the well known function spaces $H^1(\Omega)$ and $L^2(\Omega)$ (Propositions 4.9 4.10, and 4.11). Focusing on $S_0(\Omega)$, the subspace of the energy space that corresponds to the deformation vanishing on the boundary, we prove a strong Poincaré type inequality in Theorem 4.16 by making use of Lemmas 4.13, 4.14, and 4.15. As done in chapter 2, this allows us to prove a weak Poincaré inequality (Corollary 4.17 that is analogous to the one in chapter 1. This Poincaré inequality allows us to establish existence and uniqueness of solutions to the weak BVP as stated in Theorem 4.19. Finally, in order to complete the analogy with the first two chapters, we use integration by parts to state the associated strong formulation of the homogeneous Dirichlet-type BVP in equation 4.15.

In **Chapter 5**, we use this strong formulation to manufacture the force required to obtain a linear solution and name this force the ghost force. Then, we study how the choices made during the selection of the blending function α can affect the size of this force. We confirm a result of [34]through direct calculations (done in Mathematica) that increasing the distance over which the blending occurs will decrease the size of this ghost force with respect to both the L^1 and L^2 norms. Through a careful study of this ghost force, we find, contrary to the results predicted in [34], that smoothening the blending function α will not always decrease the size of the ghost force. In actuality, we found that the optimal smoothness for the blending function depends on the ratio of the length of the blending region to the material horizon, δ. Based on these results, and the fact that increasing the blending distance will likely increase the computational cost of modeling, we recommend fixing the blending region to be between 1 and 4 times the horizon of the material, and using the cubic blending function.

In **Chapter 6**, we discuss the implementation of the CE, PD and blended models through the use of the FEM. In this chapter, we restrict our attention to a "α-aligned" uniform mesh (i.e. one in which the nodes of the mesh must fall on the end points of the interval Ω as well as the "corners" of the blending function α). We discuss how for both the PD and the blended models, it is necessary to partition the interval Ω^* rather than just Ω to allow for δ-length interactions between material points. We also discuss how thinking of this as a two-dimensional problem on $\Omega^* \times \Omega^*$ will allow us to use a quadrature rule to approximate the elements of the PD and blended stiffness matrices. This discussion is important, especially for people that are new to nonlocal modeling, as it details the issues that need to be considered.

In **Chapter 7**, theoretical bounds on the error between the true solution and the approximate solution to all three models are calculated. In **Chapter 8**, using our discussed implementation of the three models, we compare the errors of manufactured solutions and approximate rate of convergence with respect to each model to those predicted by the theoretical analysis from chapter 7. In particular, we consider the manufactured solutions:

$$u(x) = 5x^2 - 5x + 3$$

$$u(x) = x^3 - 1.5x^2 + 0.5x + 2$$

$$u(x) = \exp[\sin(2\pi x)] - 1$$

$$u(x) = \begin{cases} 2(x-0.5)+1, & 0 \leq x \leq 0.5 \\ -2(x-0.5)+1, & 0.5 \leq x \leq 1. \end{cases}$$

$$u(x) = \begin{cases} 2(x-\frac{99}{200})+1, & 0 \leq x \leq \frac{99}{200} \\ -2(x-\frac{99}{200})+1, & \frac{99}{200} \leq x \leq 1 \end{cases}$$

$$u(x) = \begin{cases} 25x^2, & 0 \leq x \leq 0.5 \\ 25(x-1)^2, & 0.5 \leq x \leq 1 \end{cases}$$

$$u(x) = \begin{cases} 2, & 0 \leq x \leq 0.5 \\ 4, & 0.5 \leq x \leq 1. \end{cases}$$

We show that we get the expected rate of convergence in the classical model, with respect to the L^2 norm. For the PD model, we in fact get a higher rate of convergence than expected with respect to the PD norm. And that we get the expected rate of convergence with the blended model, with respect to its norm. Additionally, we show that for smooth enough solutions, we get that the rate of convergence of blending approximated solutions to the true solution is comparable with respect to both the L^2 and H^1 norms as would be expected by use of the classical model.

In **Chapter 9**, many of the analogous properties of the energy space that were discussed in the one-dimensional models of chapters 1, 2, and 4 are established for the N-dimensional model.

In **Appendix A**, there is a short discussion of form for which Neumann-type boundary conditions for these three one-dimensional models take.

Discussion of Results

The results in chapters 1 and 2 are known results and are included so that any reader of this dissertation can draw appropriate analogies between these proofs and the proofs included in chapter 4 without having to either seek out these proofs or recreate them. The results presented in chapter 4, lend credence to the idea of using this model, by showing mathematically that this model and its associated energy space has the same types of properties that we have been able to establish for classical PDEs. Essentially, this chapter establishes that the mathematical concept of this model is valid and therefore it makes sense to begin thinking about the situations in which its use can be advantageous. Conversion of this weak (energy-based) model into the appropriate strong (force-based) model is the first step in exploring the physical situations where this model can be employed. This is due to the fact that experimentation on materials is often done through the application of various types of loading forces, and therefore it is essential to have a firm understanding of how the force relates to the energy as proposed.

This idea lead to the discussion of ghost forces, as presented in chapter 5. Since both the classical model and the peridynamic model are accepted and can be shown to be in agreement forces that produce smooth solutions, it is important to understand how this energy-based blending relates. Intuitively, this blended model should agree with the classical and peridynamic models in these situations. The most basic smooth deformation is a linear deformation, and therefore this is how the ghost force is defined. Ideally, this ghost force would be zero, as it does not correspond to a physical force that can be applied to the material. Mathematically speaking, this ghost force could just be added to the physical forces, but that will not correspond to a physical experiment. Since the ghost force is nonzero, we want to discover what adjustments can be made to the model in order to minimize this ghost force which will allow us to explore how physical forces deform the material. By choosing the appropriate length of the blending region and smoothness of blending function, we can show that this model will approximately agree with it two predecessors. This will be useful if this model is used as a predictive model for material failure. The results of this chapter are very important as they provide guidance now how to select an appropriate blending function. Additionally, our finding that the optimal smoothness of the blending function depends on the ratio of the length of the blending region to the interaction distance, δ, is in contradiction to the expected results presented in [34]. This difference is due to our consideration ratio could play an important role.

In chapter 6, the discussion of using the FEM to implement both the PD and blended models emphasizes the complicated nature of models involving nonlocal interactions. Although many papers reference the use of FEM to implement peridynamics, for someone new to this area these complications are not obvious. Additionally, it can be recognized that this implementation is not an ideal implementation of either method, but it meant as a stepping off point for comparison. In particular, it could be more beneficial to include piecewise constant basis elements in Ω_{PD} as well for the blended model. This would allow for discontinuity in the deformation and could ultimately produce a better approximation. This also would allow for more complicated kernels, that the piecewise linear one that has been studied the most. Although not considered in detail, the use of a nonuniform mesh or an adaptive mesh could be particularly useful in the implementation of this model.

The theoretical discussion of error and convergence rate in chapter 7 is significant, because we can show that the refinement of the mesh, at least for smooth solutions, will lead to the convergence of the approximate solution to the true solution. Although theoretically, we have only shown this for smooth enough solutions, it does give us hope that this convergence will happen to all solutions in $S_0(\Omega)$. The computations done in chapter 8 further give evidence that this may be the case. In particular, we have shown that for smooth functions even with this simple implementation, we are obtaining the predicted convergence rates. We also have evidence to say that for these smooth solution this convergence still occurs with respect to the L^2 and H^1 norms. The additional manufactured solutions, suggest that this convergence will hold for a much larger class of solutions that $H^2(\Omega) \cap S_0(\Omega)$. These results suggest that this model can adequately handle piecewise solutions and discontinuous solutions.

Since it is rare for a physical situation to described as a one-dimensional problem, the work in chapter 9 suggests, that with work, this model can be employed to describe physical situations. We believe that with appropriate assumptions, it will be possible to show that the N-dimensional Poincaré inequality will be able to be extended, which would allow for existence and uniqueness of solutions in higher dimensional space.

Although this model was originally proposed for its use on homogeneous elastic material, the work that was done in this dissertation has lead us to believe that it can be useful in composite materials as well. Specifically, in materials where there are different subregions of the material that are more homogeneous. Using peridynamics or other nonlocal models, we know that in order to state the BVP, we need to have knowledge of the deformation of the material on a boundary layer and not just the boundary itself. Therefore, another potential use of this model, is to determine appropriate boundary layer conditions for the pure peridynamic model.

Future Work

Theoretically:

It would be beneficial to determine if $C_0^\infty(\Omega)$ is a dense subspace of the $S_0(\Omega)$ and if we can show the density of the piecewise linear approximation space.

Since much of the work in this dissertation has been focused on the one-dimensional case with the hope of understanding any complications that arise for this particular coupling, one obvious area for future work is to extend the results to two- and three-dimensional space. In particular, extending the analytical results such as the Poincaré inequality would be very valuable. Additionally, a study and exploration of the ghost forces and implementation FEM for N-dimensional space is another valuable direction to take this work. After these time-independent questions have been answered, it would be very interesting to begin considering how time-dependency would effect these arguments.

It could be very interesting to consider the same type of energy-based blending of other nonlocal models, such as state-based peridynamics, with classical PDEs. Additionally, exploring these types of blending on nonlinear classical elasticity and nonlinear peridynamics could yield interesting results.

Computationally:

As mentioned before, using different types of mesh, such as adaptive or nonuniform, or more complicated basis elements could lead to a more computationally affective model. In particular, the selection of basis element that would be able to capture discontinuity are important in capturing the possible discontinuity of the solution. Additionally, these basis element could allow consideration for a larger variety of PD kernels as well.

Bibliography

[1] Aguiar, A. R. and Fosdick, R. (2014). A constitutive model for a linearly elastic peridynamic body. *Mathematics and Mechanics of Solids*, 19(5):502–523. 4

[2] Agwai, A., Guven, I., and Madenci, E. (2011). Predicting crack propagation with peridynamics: a comparative study. *International journal of fracture*, 171(1):65. 3

[3] Askari, E., Bobaru, F., Lehoucq, R., Parks, M., Silling, S., and Weckner, O. (2008). Peridynamics for multiscale materials modeling. In *Journal of Physics: Conference Series*, volume 125, page 012078. IOP Publishing. 3

[4] Askari, E., Xu, J., and Silling, S. (2006). Peridynamic analysis of damage and failure in composites. In *44th AIAA aerospace sciences meeting and exhibit*, page 88. 3

[5] Azdoud, Y., Han, F., and Lubineau, G. (2013). A morphing framework to couple non-local and local anisotropic continua. *International Journal of Solids and Structures*, 50(9):1332–1341. 4

[6] Bobaru, F. and Zhang, G. (2015). Why do cracks branch? a peridynamic investigation of dynamic brittle fracture. *International Journal of Fracture*, 196(1-2):59–98. 3

[7] Brenner, S. and Scott, R. (2007). *The mathematical theory of finite element methods*, volume 15. Springer Science & Business Media. 13, 116

[8] Brezis, H. (2010). *Functional analysis, Sobolev spaces and partial differential equations*. Springer Science & Business Media. 6, 12, 30

[9] Chadwick, P. (2012). *Continuum mechanics: concise theory and problems*. Courier Corporation. 2

[10] Chen, X. and Gunzburger, M. (2011). Continuous and discontinuous finite element methods for a peridynamics model of mechanics. *Computer Methods in Applied Mechanics and Engineering*, 200(9-12):1237–1250. 4

[11] D'Elia, M., Perego, M., Bochev, P., and Littlewood, D. (2016). A coupling strategy for nonlocal and local diffusion models with mixed volume constraints and boundary conditions. *Computers & Mathematics with Applications*, 71(11):2218–2230. 4

[12] Du, Q., Gunzburger, M., Lehoucq, R., and Zhou, K. (2013a). Analysis of the volume-constrained peridynamic navier equation of linear elasticity. *Journal of Elasticity*, 113(2):193–217. 4

[13] Du, Q., Ju, L., Tian, L., and Zhou, K. (2013b). A posteriori error analysis of finite element method for linear nonlocal diffusion and peridynamic models. *Mathematics of computation*, 82(284):1889–1922. 4

[14] Du, Q., Li, X. H., Lu, J., and Tian, X. (2018). A quasi-nonlocal coupling method for nonlocal and local diffusion models. *SIAM Journal on Numerical Analysis*, 56(3):1386–1404. 4

[15] Du, Q. and Lipton, R. (2014). Peridynamics, fracture, and nonlocal continuum models. *SIAM News*, 47(3). 3

[16] Du, Q. and Zhou, K. (2011). Mathematical analysis for the peridynamic nonlocal continuum theory. *ESAIM: Mathematical Modelling and Numerical Analysis*, 45(2):217–234. 4

[17] Emmrich, E. and Weckner, O. (2007). The peridynamic equation and its spatial discretisation. *Mathematical Modelling and Analysis*, 12(1):17–27. 3

[18] Emmrich, E., Weckner, O., et al. (2007). On the well-posedness of the linear peridynamic model and its convergence towards the navier equation of linear elasticity. *Communications in Mathematical Sciences*, 5(4):851–864. 3

[19] Eringen, A. C. (2002). *Nonlocal continuum field theories*. Springer Science & Business Media. 3

[20] Evans, L. (2010). *Partial Differential Equations*, volume 19. American Mathematical Society. 6

[21] Friedman, A. (1982). *Foundations of modern analysis*. Courier Corporation. 68

[22] Gelfand, I. M., Silverman, R. A., et al. (2000). *Calculus of variations*. Courier Corporation. 6

[23] Gunzburger, M. and Lehoucq, R. B. (2010). A nonlocal vector calculus with application to nonlocal boundary value problems. *Multiscale Modeling & Simulation*, 8(5):1581–1598. 4, 22

[24] Gurtin, M. E. (1982). *An introduction to continuum mechanics*, volume 158. Academic press. 2

[25] Ha, Y. D. and Bobaru, F. (2010). Studies of dynamic crack propagation and crack branching with peridynamics. *International Journal of Fracture*, 162(1-2):229–244. 3

[26] Han, F. and Lubineau, G. (2012). Coupling of nonlocal and local continuum models by the arlequin approach. *International Journal for Numerical Methods in Engineering*, 89(6):671–685. 4

[27] Jost, J. (2006). *Postmodern analysis*. Springer Science & Business Media. 6

[28] Kilic, B. and Madenci, E. (2010). Coupling of peridynamic theory and the finite element method. *Journal of mechanics of materials and structures*, 5(5):707–733. 4

[29] Kröner, E. (1967). Elasticity theory of materials with long range cohesive forces. *International Journal of Solids and Structures*, 3(5):731–742. 3

[30] KUNIN, I. (1982). Elastic media with microstructure i: One-dimensional models. *Springer Series in Solid-State Sciences*, 26. 3

[31] KUNIN, I. (1983). Elastic media with microstructure ii:three-dimensioal models. *Springer Series in Solid-State Sciences*, 44. 3

[32] Lai, W. M., Rubin, D. H., Krempl, E., and Rubin, D. (2009). *Introduction to continuum mechanics*. Butterworth-Heinemann. 2

[33] Li, X. H. and Lu, J. (2017). Quasi-nonlocal coupling of nonlocal diffusions. *SIAM Journal on Numerical Analysis*, 55(5):2394–2415. 4

[34] Lubineau, G., Azdoud, Y., Han, F., Rey, C., and Askari, A. (2012). A morphing strategy to couple non-local to local continuum mechanics. *Journal of the Mechanics and Physics of Solids*, 60(6):1088–1102. vii, 4, 38, 100, 170, 174

[35] MacCluer, B. (2008). *Elementary functional analysis*, volume 253. Springer Science & Business Media. 6

[36] Macek, R. W. and Silling, S. A. (2007). Peridynamics via finite element analysis. *Finite Elements in Analysis and Design*, 43(15):1169–1178. 4

[37] Mengesha, T. (2012). Nonlocal korn-type characterization of sobolev vector fields. *Communications in Contemporary Mathematics*, 14(04):1250028. 162

[38] Mengesha, T. and Du, Q. (2013). Analysis of a scalar peridynamic model with a sign changing kernel. *Discrete Contin. Dynam. Systems B*, 18:1415–1437. 3, 19, 23, 25, 27, 31, 72

[39] Mengesha, T. and Du, Q. (2014). The bond-based peridynamic system with dirichlet-type volume constraint. *Proceedings of the Royal Society of Edinburgh Section A: Mathematics*, 144(1):161–186. 3

[40] Mengesha, T. and Du, Q. (2015). On the variational limit of a class of nonlocal functionals related to peridynamics. *Nonlinearity*, 28(11):3999. 3

[41] Mengesha, T. and Du, Q. (2016). Characterization of function spaces of vector fields and an application in nonlinear peridynamics. *Nonlinear Analysis*, 140:82–111. 3

[42] Rogula, D. (1982). Introduction to nonlocal theory of material media. In *Nonlocal theory of material media*, pages 123–222. Springer. 3

[43] Seleson, P., Beneddine, S., and Prudhomme, S. (2013). A force-based coupling scheme for peridynamics and classical elasticity. *Computational Materials Science*, 66:34–49. 4

[44] Seleson, P., Ha, Y. D., and Beneddine, S. (2015). Concurrent coupling of bond-based peridynamics and the navier equation of classical elasticity by blending. *International Journal for Multiscale Computational Engineering*, 13(2). 4, 44

[45] Seleson, P., Parks, M. L., and Gunzburger, M. (2014). Peridynamic state-based models and the embedded-atom model. *Communications in Computational Physics*, 15(1):179?205. 3

[46] Seleson, P., Parks, M. L., Gunzburger, M., and Lehoucq, R. B. (2009). Peridynamics as an upscaling of molecular dynamics. *Multiscale Modeling & Simulation*, 8(1):204–227. 3

[47] Silling, S. A. (2000). Reformulation of elasticity theory for discontinuities and long-range forces. *Journal of the Mechanics and Physics of Solids*, 48(1):175–209. 3, 19

[48] Silling, S. A. (2010). Linearized theory of peridynamic states. *Journal of Elasticity*, 99(1):85–111. 3

[49] Silling, S. A., Epton, M., Weckner, O., Xu, J., and Askari, E. (2007). Peridynamic states and constitutive modeling. *Journal of Elasticity*, 88(2):151–184. 3

[50] Xu, F., Gunzburger, M., Burkardt, J., and Du, Q. (2016). A multiscale implementation based on adaptive mesh refinement for the nonlocal peridynamics model in one dimension. *Multiscale Modeling & Simulation*, 14(1):398–429. 3, 4

[51] Xu, J., Askari, A., Weckner, O., and Silling, S. (2008). Peridynamic analysis of impact damage in composite laminates. *Journal of Aerospace Engineering*, 21.3:187–194. 3

[52] Zhou, K. and Du, Q. (2010). Mathematical and numerical analysis of linear peridynamic models with nonlocal boundary conditions. *SIAM Journal on Numerical Analysis*, 48(5):1759–1780. 4

[53] Zhu, Q.-z. and Ni, T. (2017). Peridynamic formulations enriched with bond rotation effects. *International Journal of Engineering Science*, 121:118–129. 3

Appendices

A Neumann-type boundary conditions in one-dimension

A.1 Classical model

The *natural* boundary condition in classical PDEs naturally arises from determining the weak formulation of the problem from the strong fomulation:

1. Multiply by a test function
2. Integrate over the domain on which the differential equation is defined
3. Apply integration by parts.

Starting with the differential equation in the BVP

$$\begin{cases} -\nabla u''(x) = f(x), & x \in \Omega \\ \text{TBD}, & x \text{ on } \partial\Omega, \end{cases}$$

multiply by a test function in $v \in L^2(\Omega)$ and integrate over Ω. The subspace of $L^2(\Omega)$ to which v belongs will also be determined during this process.

$$-\int_{\Omega} (u''(x))v(x)\mathrm{d}x = \int_{\Omega} f(x)v(x)\mathrm{d}x$$

Applying integration by parts reveals that

$$-v(x)u'(x)_{|\partial\Omega} + \int_{\Omega} u'(x)v'(x)\mathrm{d}x = \int_{\Omega} f(x)v(x)\mathrm{d}x.$$

If one had a homogeneous Dirichlet-type boundary condition the term $v(x)u'(x)_{|\partial\Omega} = 0$ as v would have been selected to vanish on the boundary. Therefore, to get an analogous result with the homogeneous natural type boundary condition, we assume that

$$u'(x)_{|\partial\Omega} = 0.$$

We call the condition

$$u'(x)_{|\partial\Omega} = N(x)$$

a **natural/Neumann-type** boundary condition. In a homogenous Neumann-type BVP, the test function v would be chosen from $\{v \in L^2(\Omega) | v'(x) = 0 \forall x \in \partial\Omega\}$.

A.2 PD model

Although the Neumann type boundary conditions are clearly defined for the classical model and therefore for the blended model presented in this dissertation, there is some debate on the form of the Neumann type boundary conditions for the PD model. In this section, Natural and Neumann type conditions are derived in an analogous way to the classical model.

The *natural* boundary condition in classical PDEs naturally arises from determining the weak formulation of the problem from the strong fomulation:

1. Multiply by a test function
2. Integrate over the domain on which the differential equation is defined
3. Apply integration by parts.

Following the analogous process with the PD model, a natural boundary condition is derived. Start with the integro-differential equation that would be in the strong formulation of such a problem.

$$\begin{cases} -2\displaystyle\int_{B_\delta(x)} c^\delta(p-x)[u(p)-u(x)]\mathrm{d}p = f(x), & x \in \Omega \\ \text{TBD}, & x \in \Gamma. \end{cases}$$

With the goal of determining the form of a natural boundary condition, multiply the integro-differential equation by a test function v belonging to some subspace of $L^2(\Omega^*)$ and integrate over Ω the region where this equation holds. The subspace of $L^2(\Omega^*)$ to which v belongs will also be determined during this process. After multiplying by the test function and integrating over Ω, the equation becomes

$$-2\int_{\Omega} v(x)\int_{B_\delta(x)} c^\delta(p-x)[u(p)-u(x)]\mathrm{d}p\mathrm{d}x = \int_{\Omega} f(x)v(x)\mathrm{d}x.$$

Since c^δ has compact support $B_\delta(0)$, the interior integration can be extended to be over the region $\left(\Omega^*\right)$.

$$-2\int_{\Omega} v(x)\int_{\Omega^*} c^\delta(p-x)[u(p)-u(x)]\mathrm{d}p\mathrm{d}x = \int_{\Omega} f(x)v(x)\mathrm{d}x. \tag{2}$$

Recall when converting the homogeneous Dirichlet-type boundary value problem, v belonged to the subset of $L^2\left(\Omega^*\right)$ that vanished on Γ. Here, just as in the natural boundary conditions for the classical case, the test function v can no longer be assumed to be zero on the boundary. Below are two options of how to proceed:

Option One

Proceeding analogously to the classical case, nonlocal integration by parts must be performed. In order to apply nonlocal integration by parts, the two-dimensional integration domain *must* be symmetric. Therefore, separate the lefthand side of the equation into two pieces.

$$\begin{aligned} -2\int_{\Omega} v(x)\int_{\Omega} c^\delta(p-x)[u(p)-u(x)]\mathrm{d}p\mathrm{d}x - 2\int_{\Omega} v(x)\int_{\Gamma} c^\delta(p-x)[u(p)-u(x)]\mathrm{d}p\mathrm{d}x \\ = \int_{\Omega} f(x)v(x)\mathrm{d}x. \end{aligned} \tag{3}$$

Since the first term has a symmetric integration domain in $\mathbb{R}^2$, nonlocal integration by parts can directly be applied to this term. The second term does not have a symmetric integration domain, so as the equation is stated, nonlocal integration by parts cannot be applied to this term. Recall that with homogeneous Dirichlet-type boundary conditions, this second term would be zero due to $v = 0$ on Γ. Therefore, analogously to the classical model, in problem

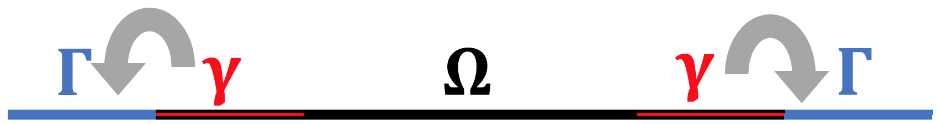

Figure 1: Illustration of **option one** of Neumann-type boundary conditions.

with a homogeneous Neumann-type boundary condition the "boundary" term would vanish, ie

$$0 = \int_{\Omega} v(x) \int_{\Gamma} c^{\delta}(p-x)[u(p)-u(x)]\mathrm{d}p\mathrm{d}x.$$

Since v is an arbitrary test function, if this "boundary" term vanished, it would imply

$$\int_{\Gamma} c^{\delta}(p-x)[u(p)-u(x)]\mathrm{d}p = 0 \ \forall x \in \Omega.$$

Therefore, is

$$\int_{\Gamma} c^{\delta}(p-x)[u(p)-u(x)]\mathrm{d}p = N(x) \ \forall x \in \Omega \tag{4}$$

the analogous PD Neuman-type boundary condition. In order to answer this question, consider what this condition would mean with reference to the nonlocal interactions on the one-dimensional domain $\left(\Omega^{*}\right)$. Recalling that in the PD model, it is assumed that particles that are within δ of each other can interact. Therefore, the proposed natural boundary condition 4 can equivalently be stated as

$$\int_{\Gamma} c^{\delta}(p-x)[u(p)-u(x)]\mathrm{d}p = N(x) \ \forall x \in \gamma, \tag{5}$$

where $\gamma = \{x \in \Omega | d(x, \partial\Omega) \leq \delta\}$. Roughly speaking, this potential boundary condition details how a $\delta-$layer, γ, inside of Ω interacts with the boundary layer Γ.

While this boundary condition naturally arises in the course of doing nonlocal integration by parts, is it analogous to the natural/Neumann boundary condition in partial differential equations? The Neumann boundary condition, in partial differential equations, is a condition on the boundary that shows how the boundary affects the points in the interior of the domain.

Since this boundary condition shows how material points inside of the material affect the boundary layer, this is not quite an analogous boundary condition. For this reason, we call this condition (equation 4) a *natural* boundary condition, but not a *Neumann* boundary condition.

Noting that the energy bilinear form for the classical BVP, given by equation 1.6, is the same for both the Dirichlet- and Neumann-type boundary conditions. Recall that in all three Dirichlet-type BVP discussed in earlier sections, the energy bilinear form comes from the term on which integration by parts was done to arrive at the weak formulation of the problem. Analogously, if the natural boundary condition, given by equation 4, is chosen, then the energy bilinear form for the PD BVP is given by the term on which integration by parts was done. This means that for this BVP,

$$b(u,v) := \int_\Omega \int_\Omega c^\delta(|p-x|)\big(u(p)-u(x)\big)\big(v(p)-v(x)\big)\mathrm{d}p\mathrm{d}x.$$

While this is similar to the energy bilinear form associated to the Dirichlet-type boundary condition (found in equation 2.11), the two-dimensional domain of integration associated to the Dirichlet-type boundary conditions is $\big(\Omega^*\big)^2$ rather than Ω^2. Deciding that having the energy bilinear form associated with the different types of boundary values should probably coincide, we return to equation 2 and decide to consider a different approach.

Option 2

Starting back at

$$-2\int_\Omega v(x)\int_{\Omega^*} c^\delta(p-x)[u(p)-u(x)]\mathrm{d}p\mathrm{d}x = \int_\Omega f(x)v(x)\mathrm{d}x$$

and knowing that we cannot assume that $v=0$ in Γ, we decide to add

$$-2\int_\Gamma v(x)\int_{\Omega^*} c^\delta(p-x)[u(p)-u(x)]\mathrm{d}p\mathrm{d}x$$

to both sides of our equation. This brings us to

$$-2\int_{\Omega} v(x)\int_{\Omega^*} c^{\delta}(p-x)[u(p)-u(x)]\mathrm{d}p\mathrm{d}x - 2\int_{\Gamma} v(x)\int_{\Omega^*} c^{\delta}(p-x)[u(p)-u(x)]\mathrm{d}p\mathrm{d}x$$
$$= \int_{\Omega} f(x)v(x)\mathrm{d}x - 2\int_{\Gamma} v(x)\int_{\Omega^*} c^{\delta}(p-x)[u(p)-u(x)]\mathrm{d}p\mathrm{d}x$$

Combining the two integral terms on the left hand side of this equation we find that

$$-2\int_{\Omega^*} v(x)\int_{\Omega^*} c^{\delta}(p-x)[u(p)-u(x)]\mathrm{d}p\mathrm{d}x$$
$$= \int_{\Omega} f(x)v(x)\mathrm{d}x - 2\int_{\Gamma} v(x)\int_{\Omega^*} c^{\delta}(p-x)[u(p)-u(x)]\mathrm{d}p\mathrm{d}x$$

Since the domain of integration on the lefthand side is symmetric, apply nonlocal integration by parts to that side to obtain

$$\int_{\Omega'}\int_{\Omega'} c^{\delta}(p-x)[u(p)-u(x)][v(p)-v(x)]\mathrm{d}p\mathrm{d}x$$
$$= \int_{\Omega} f(x)v(x)\mathrm{d}x - 2\int_{\Gamma} v(x)\int_{\Omega'} c^{\delta}(p-x)[u(p)-u(x)]\mathrm{d}p\mathrm{d}x$$

Observe that the energy bilinear form we just generated (the lefthand side of this equation) agrees with the energy bilinear form (found in equation 2.11 that was generated in the homogeneous Dirichlet-type BVP. Therefore, we decide that

$$-2\int_{\Gamma} v(x)\int_{\Omega'} c^{\delta}(p-x)[u(p)-u(x)]\mathrm{d}p\mathrm{d}x$$

is the boundary term associated to some natural BVP. Once again recall that to determine the form of the natural boundary condition classically, we considered what would make this boundary term zero.

$$0 = -2\int_{\Gamma} v(x)\int_{\Omega'} c^{\delta}(p-x)[u(p)-u(x)]\mathrm{d}p\mathrm{d}x$$

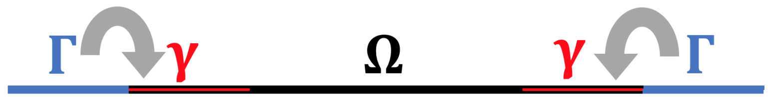

Figure 2: Illustration of **option two** of Neumann-type boundary conditions.

We note that if $v(x) = 0 \forall x \in \Gamma$, this term would be zero and we would be dealing with exact weak formulation we discussed for the Dirichlet problem. This term would also vanish if

$$0 = \int_{\Omega'} c^{\delta}(p-x)[u(p)-u(x)]\mathrm{d}p \;\forall x \in \Gamma.$$

So far this is promising because for both zero Neumann and zero Dirichlet boundary conditions, the BVP simplifies to the same weak formulation of the problem, as it did in classical differential equations. Therefore, we want to decide if the condition

$$N(x) = \int_{\Omega'} c^{\delta}(p-x)[u(p)-u(x)]\mathrm{d}p \;\forall x \in \Gamma. \tag{6}$$

is a more natural analogy to the Neumann condition for differential equations.

Like the classical differential equation Neumann-type condition, this condition expresses how things happening in the 'boundary' are interacting with material points in the domain, Ω.

In the classical case there is really no information on how the boundary layer interacts with itself, but this is consistent with the fact that the classical case is a local problem and the material points are assumed to interact via contact. Since the bond-based peridynamic model assumes that particles within a finite distance δ interact with each other, it could be considered natural that we would need information on how points in Γ interact and influence other points in Γ as well. Therefore, we will call this natural boundary condition a **nonlocal Neumann-type** boundary condition.

A.3 Blended model

Since the blended model, behaves classically near the boundary, the Neumann-type boundary condition is the same as it is for the classical model.

Vita

Kileen A. Berry was born in Lexington, Kentucky. She spent four years living there, before moving with her family to Antwerp, Belgium. After spending four years in Europe, she moved to Richmond Hill, Georgia where she stayed until she was 18. Kileen attended Berry College, where she earned a Bachelor of Science in Physics and Mathematics and graduated summa cum laude in 2012.

In 2013, she began a Ph.D program in Mathematics at the University of Tennessee Knoxville, where she earned a Master of Science Degree in 2015. Kileen continued on to pursue a Ph.D in Mathematics there as well. Kileen was awarded the *Spike Tickle STEM Fellowship* to focus on her research in both 2016 and 2017. She also was selected to participate in the *Department of Energy's Office of Science Graduate Student Research* program which allowed her to spend spring and summer of 2018 working on her research at Oak Ridge National Lab. While at the University of Tennessee, Kileen not only spent time learning and becoming a more proficient mathematician, but she had the opportunity to teach a variety of undergraduate mathematics courses. In 2016 she received a *Teaching for Impact grant* from the Tennessee Learning Center that allowed her to focus on small changes to the College Algebra/Precalculus courses that can be made in order have a high level of impact in terms of student engagement and success. In 2017 she received the *Dorthea and Edgar D. Graduate Student Teaching Award* that recognizes outstanding teaching among graduate teaching associates. Kileen also participated in various outreach programs such as high school mathematics competitions, elementary school field trips, and *ProjectGRAD* during her time at the University of Tennessee Knoxville. ProjectGRAD is a K-16 program that helps students pursue excellence in education and secure a better future. Kileen participated as a summer mathematics instructor for high school students.

Currently, Kileen is living in Ooltewah, Tennessee and is excited to see what the next step of her career will be.